UNIVERSITY OF CALIFORNIA

Los Angeles

Higher-Dimension Operators and Applications in SMEFT and Tidal Gravitational Effects

A dissertation submitted in partial satisfaction

of the requirements for the degree

Doctor of Philosophy in Physics

by

Eric Jonathan Sawyer

2021

ABSTRACT OF THE DISSERTATION

Higher-Dimension Operators and Applications in SMEFT and Tidal Gravitational Effects

by

Eric Jonathan Sawyer

Doctor of Philosophy in Physics

University of California, Los Angeles, 2021

Professor Zvi Bern, Chair

This dissertation explores the effects of higher-dimension operators in scattering amplitudes, and how such amplitudes can be used to gain insight into areas of physics ranging from elementary particle interactions to the tidal responses of black holes and neutron stars. Chapter 1 provides a brief introduction to higher-dimension operators and the Effective Field Theories (EFTs) which are their natural environment. In Chapter 2, we prove a theorem stating that operators which are "longer" in a specific sense cannot renormalize "shorter" operators at low loop levels. This result applies very generally, and can apply at high loop levels given the appropriate operators. We also discuss how the theorem applies to specifically to the Standard Model Effective Field Theory (SMEFT). In Chapter 3, we extend this discussion of renormalization within the SMEFT by calculating a large class of one loop amplitudes of dimension-six SMEFT operators and showing how to use these amplitudes to compute two loop anomalous dimensions. Finally, in Chapter 4 we turn the calculation of amplitudes with higher-dimension operators to the purpose of calculating the effects of tides on the gravitational potential between, for example, orbiting black holes and neutron stars. This work, which includes in principle the leading effect of tidal operators at all loops, has direct relevance for gravitational wave detectors.

The dissertation of Eric Jonathan Sawyer is approved.

Thomas Dumitrescu

Eric D'Hoker

Michael Gutperle

Zvi Bern, Committee Chair

University of California, Los Angeles

2021

For my dad.

Contents

1 Introduction **1**

2 Non-renormalization and operator mixing via on-shell methods **13**

2.1 Introduction 14

2.2 Renormalization and Form Factors 16

2.3 Non-renormalization theorem 18

2.4 Two-loop examples 22

2.5 Conclusions 24

3 Structure of two-loop SMEFT anomalous dimensions via on-shell methods **30**

3.1 Introduction 31

3.2 Setup and formalism 34

3.2.1 Conventions and basic setup 35

3.2.2 Anomalous dimensions from UV divergences 39

3.2.3 Anomalous dimensions directly from unitarity cuts 42

3.2.4 Comments on evanescent operators 50

3.2.5 Anomalous dimensions and non-interference 51

3.3 One-loop amplitudes and anomalous dimensions 52

3.3.1 One-loop amplitudes from generalized unitarity 53

3.3.2 One-loop UV anomalous dimensions 58

3.3.3 Structure of one-loop amplitudes and rational terms 60
3.4 Two-loop zeros in the anomalous dimension matrix 63
3.4.1 Zeros from length selection rules 63
3.4.2 Zeros from vanishing one-loop rational terms 64
3.4.3 Zeros from color selection rules 74
3.4.4 Outlook on additional zeros 77
3.5 Implications for the SMEFT 79
3.5.1 Mapping our theory to the SMEFT 79
3.5.2 Verification of one-loop anomalous dimensions 83
3.5.3 Two-loop implications 83
3.6 Conclusions 84
3.A Integral reduction via gauge-invariant tensors 87
3.B Tree-level and one-loop amplitudes 91
3.B.1 Four-vector amplitudes 93
3.B.2 Four-fermion amplitudes 95
3.B.3 Four-scalar amplitudes 98
3.B.4 Two-fermion, two-vector amplitudes 100
3.B.5 Two-scalar, two-vector amplitudes 103
3.B.6 Two-fermion, two-scalar amplitudes 106

4 Leading Nonlinear Tidal Effects and Scattering Amplitudes 122
4.1 Introduction 123
4.2 Effective actions for tidal effects 127
4.2.1 Effective actions for post-Minkowskian potentials 127
4.2.2 Effective actions for linear and non-linear tidal effects 131
4.3 Leading order E^2 and B^2 tidal effects 141
4.3.1 Constructing integrands 142

4.3.2 Momentum-space analysis 148
4.3.3 Position-space analysis 151
4.3.4 General multipole operators 155
4.3.5 Adding spin 160
4.4 Nonlinear tidal effects 164
4.4.1 Leading order position-space analysis 165
4.4.2 Order by order momentum-space analysis 170
4.5 Effective field theory extensions of GR 175
4.6 Conclusions 180
4.A Appendix: Summary of Explicit Results 182

List of Figures

1.1 Diagram of a binary merger signal 5

2.1 Unitary cuts of one- and two-loop form factors 17
2.2 Examples of forbidden renormalization 25

3.1 Unitary cut of a one-loop form factor 44
3.2 Unitary cuts of a two-loop form factor 46
3.3 Iterated two-particle cuts 48
3.4 Example unitary cuts 54
3.5 Cuts determining example anomalous dimensions 66
3.6 Cuts determining additional anomalous dimensions 69
3.7 Cuts determining additional anomalous dimensions 74
3.8 Examples of anomalous dimensions determined by a single unitary cut . . . 77

4.1 Generalized cut for LO contributions to E^2- or B^2-type tidal operators . . . 141
4.2 Generalized cut for LO contributions to nonlinear tidal operators 164
4.3 The L-loop fan integral 172
4.4 Generalized cuts at NLO for an R^n type tidal operator 174
4.5 Sample simple diagrams for NLO contributions for the R^3 tidal operators . . 174
4.6 More difficult diagrams for NLO contributions for the R^3 tidal operators . . 174
4.7 Cut for a general R^n type operator 176
4.8 Corrections from R^3 and R^4 operators in EFT extensions of GR 178

List of Tables

2.1 Application of the non-renormalization theorem to dimension-five operators . 23

2.2 Application to dimension-six operators 23

2.3 Application to dimension-seven operators 24

3.1 List of dimension-six operators considered 37

3.2 Zeros in the one-loop anomalous dimension matrix 59

3.3 Structure of the full one-loop helicity amplitudes 60

3.4 Structure of the two-loop anomalous dimension matrix $\gamma_{ij}^{(2)}$ 78

3.5 Checks on previously calculated one-loop anomalous dimensions 82

3.6 Predictions for the SMEFT two-loop anomalous-dimension matrix 110

Acknowledgements

I would like to first thank my advisor, Zvi Bern, for his mentorship, his patience and understanding, and his insight. Next, I would like to thank my collaborators, especially Julio Parra-Martinez, for many stimulating discussions and much support, and Chia-Hsien Shen and Radu Roiban, for helping make working in quarantine actually fun. I must also thank the Bhaumik Institute for its support, and for contributing to the stimulating research environment at UCLA. Next, thank you to my committee, Thomas Dumitrescu, Eric D'Hoker, and Michael Gutperle. Of course I thank my friends and colleagues in the Bern group, Julio Parra-Martinez, Chia-Hsien Shen Dimitrios Kosmopoulos, Alex Edison, Andrés Luna Godoy, and Michael Enciso.

Outside of UCLA, I would like to thank my family, especially my mom and my step-dad Dave, without whom my interest in science would have never begun. To Bruce and Sheryl, you have been like a second set of parents to me, and I thank you dearly for all the support you have given me and Sam. Sam, thank you for all the love, compassion, and encouragement you have given me throughout the years—I couldn't have come this far without you.

Finally, I'd like to thank all the healthcare workers and scientists that have sacrificed their time and often their lives over the past year trying to get us finally back to normal. The number of lives saved by your actions is incalculable.

Contribution of authors

Chapter 1, which serves as an introduction, draws from Ref [1-3] in collaboration with the authors detailed below. Chapters 2 and 3 are adapted from Refs. [1] and [2] respectively, in collaboration with Zvi Bern and Julio Parra-Martinez. Chapter 4 is adapted from Ref. [3], with Zvi Bern, Julio Parra-Martinez, Radu Roiban, and Chia-Hsien Shen.

Vita

Institution	Position	Year
Cornell University	B.A., Physics	2009–2013
University of California San Diego	M.S., NanoEngineering	2013–2015
University of California Los Angeles	Graduate Student Researcher	2015–2021

Publications

- Z. Bern, J. Parra-Martinez, and E. Sawyer, "Nonrenormalization and Operator Mixing via On-Shell Methods", Phys. Rev. Lett. 124, 051601 (2020), arXiv:1910.05831 [hep-ph].
- Z. Bern, J. Parra-Martinez, and E. Sawyer, "Structure of two-loop SMEFT anomalous dimensions via on-shell methods", JHEP 2020, 211 (2020), arXiv:2005.12917 [hep-ph].
- Z. Bern, J. Parra-Martinez, R. Roiban, E. Sawyer, and C. H. Shen, "Leading Nonlinear Tidal Effects and Scattering Amplitudes", JHEP 2021, 188 (2021) arXiv:2010.08559 [hep-th].

Chapter 1

Introduction

Our understanding of physics has for centuries developed on the principle that simple rules dominate on the scales we experience in our day to day lives, and as situations approach the more extreme, be it on the scale of particles or on the scale of galaxies, new effects begin to result in corrections to the familiar rules. This intuition that new physics can be conceived as corrections to theories that work well at low energy is the foundational idea behind Effective Field Theories (EFTs). In this context, the normal field theory requirement for renormalizability is discarded, with the assumption that a renormalizable theory ultimately describes physics at high energies. However, knowledge of the high energy theory is unnecessary for understanding the physics at low energies, which can simply be described in terms of a low energy theory plus corrections given by higher-dimension operators. These operators, constructed only out of the fields of the low-energy theory, capture corrections given by the high-energy physics, and are suppressed by a characteristic high-energy scale.

The Standard Model Effective Field Theory (SMEFT) provides an illustrative example. The well-known Standard Model Lagrangian,

$$\begin{aligned}\mathcal{L}^{(4)}_{SM} = &-\frac{1}{4}G^A_{\mu\nu}G^{A\mu\nu} - \frac{1}{4}W^I_{\mu\nu}W^{I\mu\nu} - \frac{1}{4}B_{\mu\nu}B^{\mu\nu} + (D_\mu\varphi)^\dagger(D^\mu\varphi) + m^2\varphi^\dagger\varphi - \frac{1}{2}\lambda(\varphi^\dagger\varphi)^2 \\ &+ i(\bar{l}\not{D}l + \bar{e}\not{D}e + \bar{q}\not{D}q + \bar{u}\not{D}u + \bar{d}\not{D}d) - (\bar{l}\Gamma_e e\varphi + \bar{q}\Gamma_u u\tilde{\varphi} + \bar{q}\Gamma_d d\varphi + \text{h.c.})\end{aligned} \tag{1.1}$$

is fully renormalizable in four dimensions, with all of the terms being of dimension four. The requirement of renormalizability leaves little room for adding additional physics, but in the framework of an effective field theory, we can add additional higher-dimension operators which provide corrections to the Lagrangian, and thus to the physical scattering amplitudes:

$$\mathcal{L} = \mathcal{L}^{(4)} + \frac{1}{\Lambda}\sum_i c_i^{(5)}\mathcal{O}_i^{(5)} + \frac{1}{\Lambda^2}\sum_i c_i^{(6)}\mathcal{O}_i^{(6)} + \mathcal{O}\left(\frac{1}{\Lambda^3}\right), \tag{1.2}$$

where operators with higher mass dimension are suppressed by more powers of the high-energy scale Λ. A comprehensive review of the SMEFT can be found in Ref. [1]

Within this bottom-up approach for building an EFT, no assumption is made about the relative magnitudes of the operator coefficients ($c_i^{(5)}$, $c_i^{(6)}$ etc.). It is thus important to include all possible operators in the Lagrangian for each operator dimension, and thus for each power of Λ^{-1}. This can prove a challenge at higher dimensions, as the number of operators quickly grows out of hand. For example, there is only one valid operator at dimension five for the SMEFT, fifty-nine valid operators at dimension six [2], and 1,029 operators at dimension eight [3], not including the large variety of flavor structures allowed. The benefit of this completeness, however, is that by experimentally searching for the effects of these operators, we can systematically search for new physics without assuming a model for its high-energy realization.

Along with the need to systematically explore the effects of the higher-dimension operators individually, care must be paid to understand the relationships between the operators under the renormalization group flow. Understanding the meaning behind the experimental appearance of certain operators involves performing EFT matching at the high energies relevant to the underlying theory, but experiments can only access data at the relative low energies of particle colliders. The evolution of the theory between the two scales is described

by the renormalization group equation,

$$\left[(\mu\partial_\mu + \beta\,\partial)\,\delta_{ij} + \left(\gamma^{\rm UV} - \gamma^{\rm IR}\right)_{ij}\right] F_j = 0, \tag{1.3}$$

where $F_j[p_1, ..., p_n; q; \mu] = \langle p_1, ..., p_n|\mathcal{O}_j(q)|0\rangle$ is a form factor, and γ_{ij}^{UV} is the anomalous dimension, which can be computed perturbatively and describes the running of the couplings from the high-energy scale down to the energies accessible by experiment.

In the landmark works of Refs. [4], the authors completed a systematic computation of the one-loop anomalous dimension matrix for dimension-six operators in the SMEFT. Besides their importance for interpreting experimental data, these calculations reveal a remarkable structure with the appearance of nontrivial zeros in the anomalous dimension matrix [5]. These zeros implied an unforeseen structure in the SMEFT, as the general naive assumption for EFTs is that every operator that is not forbidden from renormalizing another operator will produce a non-zero anomalous dimension. The one-loop zeros were elegantly explained using helicity selection rules [6], but the question remained whether they would persist at higher loop orders, or whether this was an accident of the simplicity of the one-loop calculations. In Chapters 2 and 3 we show that indeed there is additional structure beyond one loop in the SMEFT anomalous dimension matrix. We make use of an elegant formalism developed by Caron-Huot and Wilhelm in [7], which casts the calculation of the anomalous dimensions in terms of on-shell form factors and amplitudes.

On-shell methods have gained in prominence in a large variety of physical settings, including, for example, collider physics (see e.g. Refs. [8]), ultraviolet properties of (super)gravity (see e.g. Refs. [9]), cosmological observables (see e.g. Refs. [10]), and gravitational wave physics(see e.g. Refs. [11]). This is in large measure due to the ability to construct higher loop integrands and amplitudes out of lower loop objects, and often merely out of tree level amplitudes. This manner of construction avoids the need for Feynmann rules that are simple to state, but which in practice lead to an explosion of terms in the intermediate stages of the

calculation. The SMEFT community has also seen a shift to the inclusion of more on-shell methods, including the classification of interactions in an on-shell framework [12] and the calculation of some anomalous dimensions using on-shell methods [13].

In the context of anomalous dimensions and renormalization-group analyses, unitarity cuts give us direct access to renormalization-scale dependence. After subtracting infrared singularities, the renormalization-scale dependence can be read off from remaining dimensional imbalances in the arguments of logarithms [7]. The direct link between anomalous dimensions at any loop order and unitarity cuts is made explicit in the formulation of Caron-Huot and Wilhelm. In Chapter 2, we use their on-shell formalism, along with an insight about the nature of scaleless integrals, to demonstrate that non-trivial zeros in the anomalous dimension matrix persist at any given order in perturbation theory.

In Chapter 3, we continue this analysis of the dimension-six SMEFT operators by showing the calculation of a number of two-loop anomalous dimension matrix elements. Along the way, we calculate a large class of the full one-loop amplitudes, which are used as building blocks in the two loop calculation. We also verify a number of the one-loop anomalous dimensions calculated in Refs. [4]. We will further show that additional structure can be found in the two-loop anomalous dimensions, including the ability to set certain matrix elements to zero using judicious choices of the renormalization scheme for the one-loop amplitudes.

While we have so far focused on the SMEFT as our example of an EFT with higher dimension operators, another example is the calculation of corrections to gravitational wave signals, as detected by the LIGO and Virgo collaborations [14]. In this context, the physics of the gravitational interaction between black holes or neutron stars binary pairs is viewed as a process that takes place on a number of characteristic scales [15]. The wavelength of the gravitational radiation represents the largest scale, from which the radiation may well be represented as emanating from a point source. Zooming in, the separation between the two bodies represents the next scale, where the bodies themselves are treated as point

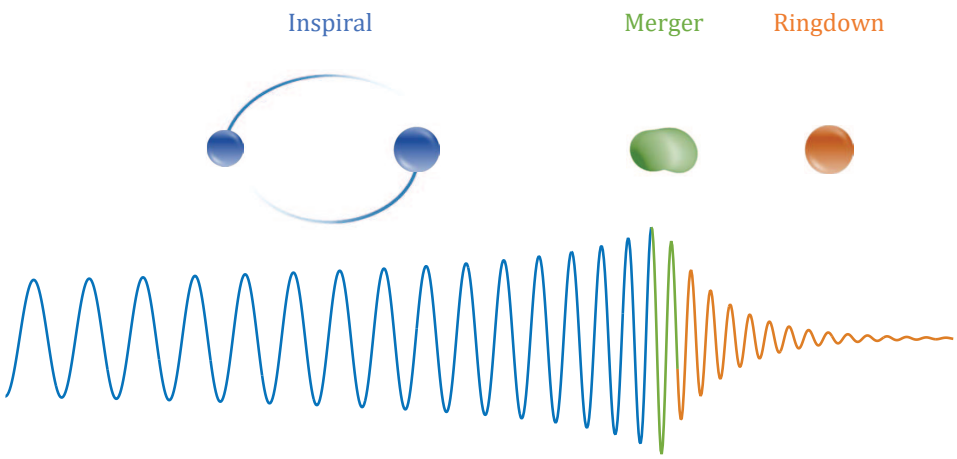

Figure 1.1: Diagram of a binary merger gravitational wave signal. The perturbative methods discussed here are used to analyze the inspiral phase, with higher-order corrections becoming more prominent as the merger phase approaches. Figure reproduced from Ref. [16]

particles. Indeed at this scale the leading contributions to the gravitational wave signal can be calculated quite accurately. However, finite size effects are not included by treating the particles as point sources. In an EFT setting, however, the separation of scales lends the problem naturally to doing just that, but including finite size effects as corrections due to higher-dimensional operators.

These corrections are encoded in their effects on the two-body Hamiltonian,

$$H(\boldsymbol{p},\boldsymbol{r}) = \sqrt{\boldsymbol{p}^2 + m_1^2} + \sqrt{\boldsymbol{p}^2 + m_2^2} + V(\boldsymbol{p},\boldsymbol{r})\,, \tag{1.4}$$

and are extracted systematically, following the general approach introduced in Ref. [17], by matching QFT scattering amplitudes to a non-relativistic EFT. The potential is analyzed perturbatively, either in the Post-Minkowskian (PM: expansion in the gravitational coupling G, all orders in velocity), or in the Post-Neutonian (PN: expansion in the velocity, with $v^2/c^2 \sim G$) schemes. Either scheme produces physically equivalent results in their regions of overlap, and both are used extensively to study the inspiral phase of the binary merger, as illustrated in the diagram of a gravitational wave signal in Figure 1.1. The PM expansion

has the benefit of taking advantage of modern amplitude techniques, including construction from unitary cuts of on-shell tree amplitudes. Recently, friendly competition between those working in either scheme has led to results including the 4PM potential [18] (fourth order in G), the full 4PN potential [19], and partial results up to 6PN [20].

These results effectively treat the objects as scalar particles with no spin or internal structure, but the EFT methods used can also accommodate both these additional complications. In terms of spin, progress has been made by a number of authors, including the calculation of $\text{spin}_1 \cdot \text{spin}_2$ effects up to $\mathcal{O}(G^2)$ [21] in the PM framework. In the PN framework, recent results include the N^{3}LO quadratic in spin static contribution at order G^4 [22], the NLO gravitational quartic-in-spin interaction [23], and the N^{3}LO spin-orbit coupling at order G^4 [24].

These works still treat the objects effectively as point particles without internal structure, however, but recently finite size effects have begun to receive more attention in both the PN [25] and PM [26] frameworks, including the calculation of the leading effects of the first-relevant tidal operators. In Chapter 4 of this thesis, we greatly expand upon previous results on the finite size effects by presenting the two-body Hamiltonian and associated eikonal phase, to leading PM order, for infinitely many tidal deformations described by operators with arbitrary powers of the curvature tensor. We proceed to derive the leading contributions of various infinite classes of R^n-type tidal operators and also comment on their higher-order contributions. Lastly, we discuss the application of our methods to the case of pure R^n extensions of General Relativity.

Bibliography

[1] I. Brivio and M. Trott, "The Standard Model as an Effective Field Theory," Phys. Rept. **793**, 1 (2019) [arXiv:1706.08945 [hep-ph]].

[2] B. Grzadkowski, M. Iskrzynski, M. Misiak and J. Rosiek, "Dimension-Six Terms in the Standard Model Lagrangian," JHEP **1010**, 085 (2010) [arXiv:1008.4884 [hep-ph]].

[3] C. W. Murphy, "Dimension-8 Operators in the Standard Model Effective Field Theory," [arXiv:2005.00059 [hep-ph]].

[4] E. E. Jenkins, A. V. Manohar and M. Trott, "Renormalization Group Evolution of the Standard Model Dimension Six Operators I: Formalism and lambda Dependence," JHEP **1310**, 087 (2013) [arXiv:1308.2627 [hep-ph]];
E. E. Jenkins, A. V. Manohar and M. Trott, "Renormalization Group Evolution of the Standard Model Dimension Six Operators II: Yukawa Dependence," JHEP **1401**, 035 (2014) [arXiv:1310.4838 [hep-ph]];
R. Alonso, E. E. Jenkins, A. V. Manohar and M. Trott, "Renormalization Group Evolution of the Standard Model Dimension Six Operators III: Gauge Coupling Dependence and Phenomenology," JHEP **1404**, 159 (2014) [arXiv:1312.2014 [hep-ph]].

[5] R. Alonso, E. E. Jenkins and A. V. Manohar, "Holomorphy without Supersymmetry in the Standard Model Effective Field Theory," Phys. Lett. B **739**, 95 (2014) [arXiv:1409.0868 [hep-ph]];

J. Elias-Miró, J. R. Espinosa and A. Pomarol, "One-loop non-renormalization results in EFTs," Phys. Lett. B **747**, 272 (2015) [arXiv:1412.7151 [hep-ph]].

[6] C. Cheung and C. H. Shen, "Nonrenormalization Theorems without Supersymmetry," Phys. Rev. Lett. **115**, no. 7, 071601 (2015) [arXiv:1505.01844 [hep-ph]].

[7] S. Caron-Huot and M. Wilhelm, "Renormalization Group Coefficients and the S-matrix," JHEP **1612**, 010 (2016) [arXiv:1607.06448 [hep-th]].

[8] C. Berger, Z. Bern, L. Dixon, F. Febres Cordero, D. Forde, H. Ita, D. Kosower and D. Maitre, "An Automated Implementation of On-Shell Methods for One-Loop Amplitudes," Phys. Rev. D **78**, 036003 (2008) [arXiv:0803.4180 [hep-ph]];
C. Berger, Z. Bern, L. J. Dixon, F. Febres Cordero, D. Forde, T. Gleisberg, H. Ita, D. Kosower and D. Maitre, "Precise Predictions for W + 4 Jet Production at the Large Hadron Collider," Phys. Rev. Lett. **106**, 092001 (2011) [arXiv:1009.2338 [hep-ph]].

[9] J. L. Bourjaily, E. Herrmann, C. Langer, A. J. McLeod and J. Trnka, "All-Multiplicity Non-Planar MHV Amplitudes in sYM at Two Loops," Phys. Rev. Lett. **124**, no.11, 111603 (2020) [arXiv:1911.09106 [hep-th]];
Z. Bern, J. Parra-Martinez and R. Roiban, "Canceling the U(1) Anomaly in the S Matrix of N=4 Supergravity," Phys. Rev. Lett. **121**, no.10, 101604 (2018) [arXiv:1712.03928 [hep-th]];
A. Edison, E. Herrmann, J. Parra-Martinez and J. Trnka, "Gravity Loop Integrands from the Ultraviolet," [arXiv:1909.02003 [hep-th]].

[10] N. Arkani-Hamed, D. Baumann, H. Lee and G. L. Pimentel, "The Cosmological Bootstrap: Inflationary Correlators from Symmetries and Singularities," JHEP **04**, 105 (2020) [arXiv:1811.00024 [hep-th]];
D. Baumann, C. Duaso Pueyo, A. Joyce, H. Lee and G. L. Pimentel, "The Cosmological Bootstrap: Weight-Shifting Operators and Scalar Seeds," [arXiv:1910.14051 [hep-th]];

D. Baumann, C. Duaso Pueyo, A. Joyce, H. Lee and G. L. Pimentel, "The Cosmological Bootstrap: Spinning Correlators from Symmetries and Factorization," [arXiv:2005.04234 [hep-th]].

[11] Z. Bern, C. Cheung, R. Roiban, C. Shen, M. P. Solon and M. Zeng, "Scattering Amplitudes and the Conservative Hamiltonian for Binary Systems at Third Post-Minkowskian Order," Phys. Rev. Lett. **122**, no.20, 201603 (2019) [arXiv:1901.04424 [hep-th]];
J. Parra-Martinez, M. S. Ruf and M. Zeng, "Extremal black hole scattering at $\mathcal{O}(G^3)$: graviton dominance, eikonal exponentiation, and differential equations," [arXiv:2005.04236 [hep-th]].

[12] N. Arkani-Hamed, T. C. Huang and Y. t. Huang, "Scattering Amplitudes For All Masses and Spins," [arXiv:1709.04891 [hep-th]];
Y. Shadmi and Y. Weiss, "Effective Field Theory Amplitudes the On-Shell Way: Scalar and Vector Couplings to Gluons," JHEP **02**, 165 (2019) [arXiv:1809.09644 [hep-ph]];
T. Ma, J. Shu and M. L. Xiao, "Standard Model Effective Field Theory from On-shell Amplitudes," [arXiv:1902.06752 [hep-ph]];
G. Durieux, T. Kitahara, Y. Shadmi and Y. Weiss, "The Electroweak Effective Field Theory from On-Shell Amplitudes," JHEP **01**, 119 (2020) [arXiv:1909.10551 [hep-ph]];
B. Bachu and A. Yelleshpur, "On-Shell Electroweak Sector and the Higgs Mechanism," [arXiv:1912.04334 [hep-th]].

[13] M. Jiang, J. Shu, M. Xiao and Y. Zheng, "New Selection Rules from Angular Momentum Conservation," [arXiv:2001.04481 [hep-ph]].;
N. Craig, M. Jiang, Y. Li and D. Sutherland, "Loops and Trees in Generic EFTs," [arXiv:2001.00017 [hep-ph]].;
J. Elias Miro, J. Ingoldby and M. Riembau, "EFT Anomalous Dimensions from the S-matrix," [arXiv:2005.06983 [hep-ph]]. P. Baratella, C. Fernandez and A. Pomarol, "Renormalization of Higher-Dimensional Operators from On-shell Amplitudes,"

[arXiv:2005.07129 [hep-ph]];
M. Jiang, T. Ma and J. Shu, "Renormalization Group Evolution from On-shell SMEFT," [arXiv:2005.10261 [hep-ph]].

[14] B. P. Abbott *et al.* [LIGO Scientific and Virgo Collaborations], "Observation of gravitational waves from a binary black hole merger," Phys. Rev. Lett. **116**, no. 6, 061102 (2016) [arXiv:1602.03837 [gr-qc]];
B. P. Abbott *et al.* [LIGO Scientific and Virgo Collaborations], "GW170817: Observation of gravitational waves from a binary neutron star inspiral," Phys. Rev. Lett. **119**, no. 16, 161101 (2017) [arXiv:1710.05832 [gr-qc]].

[15] M. Levi, "Effective field theories of post-Newtonian gravity: A comprehensive review," arXiv:1807.01699 [hep-th].

[16] J. M. Antelis and C. Moreno, Eur. Phys. J. Plus **132** (2017) no.1, 10 [arXiv:1610.03567 [astro-ph.IM]].

[17] C. Cheung, I. Z. Rothstein and M. P. Solon, "From scattering amplitudes to classical potentials in the post-Minkowskian expansion," Phys. Rev. Lett. **121**, no. 25, 251101 (2018) [arXiv:1808.02489 [hep-th]].

[18] Z. Bern, J. Parra-Martinez, R. Roiban, M. S. Ruf, C. H. Shen, M. P. Solon and M. Zeng, "Scattering Amplitudes and Conservative Binary Dynamics at $\mathcal{O}(G^4)$," Phys. Rev. Lett. **126** (2021) no.17, 171601 [arXiv:2101.07254 [hep-th]].

[19] T. Damour, P. Jaranowski and G. Schäfer, "Nonlocal-in-time action for the fourth post-Newtonian conservative dynamics of two-body systems," Phys. Rev. D **89**, no. 6, 064058 (2014) [arXiv:1401.4548 [gr-qc]];
T. Damour, P. Jaranowski and G. Schäfer, "Fourth post-Newtonian effective one-body dynamics," Phys. Rev. D **91** (2015) no.8, 084024 doi:10.1103/PhysRevD.91.084024

[arXiv:1502.07245 [gr-qc]].;

L. Bernard, L. Blanchet, A. Bohé, G. Faye and S. Marsat, "Fokker action of nonspinning compact binaries at the fourth post-Newtonian approximation," Phys. Rev. D **93**, no.8, 084037 (2016) [arXiv:1512.02876 [gr-qc]];

L. Bernard, L. Blanchet, A. Bohé, G. Faye and S. Marsat, "Energy and periastron advance of compact binaries on circular orbits at the fourth post-Newtonian order," Phys. Rev. D **95** (2017) no.4, 044026 doi:10.1103/PhysRevD.95.044026 [arXiv:1610.07934 [gr-qc]].;

S. Foffa and R. Sturani, "Conservative dynamics of binary systems to fourth Post-Newtonian order in the EFT approach I: Regularized Lagrangian," Phys. Rev. D **100**, no. 2, 024047 (2019) [arXiv:1903.05113 [gr-qc]];

S. Foffa, R. A. Porto, I. Rothstein and R. Sturani, "Conservative dynamics of binary systems to fourth Post-Newtonian order in the EFT approach II: Renormalized Lagrangian," Phys. Rev. D **100**, no. 2, 024048 (2019) [arXiv:1903.05118 [gr-qc]];

[20] S. Foffa, P. Mastrolia, R. Sturani, C. Sturm and W. J. Torres Bobadilla, "Static two-body potential at fifth post-Newtonian order," Phys. Rev. Lett. **122**, no. 24, 241605 (2019) [arXiv:1902.10571 [gr-qc]];

J. Blümlein, A. Maier and P. Marquard, "Five-Loop static contribution to the gravitational interaction potential of two point masses," Phys. Lett. B **800**, 135100 (2020) [arXiv:1902.11180 [gr-qc]];

J. Blümlein, A. Maier, P. Marquard and G. Schäfer, "Testing binary dynamics in gravity at the sixth post-Newtonian level," arXiv:2003.07145 [gr-qc];

D. Bini, T. Damour and A. Geralico, "Binary dynamics at the fifth and fifth-and-a-half post-Newtonian orders," [arXiv:2003.11891 [gr-qc]];

D. Bini, T. Damour and A. Geralico, "Sixth post-Newtonian local-in-time dynamics of

binary systems," [arXiv:2004.05407 [gr-qc]].

[21] Z. Bern, A. Luna, R. Roiban, C. H. Shen and M. Zeng, "Spinning Black Hole Binary Dynamics, Scattering Amplitudes and Effective Field Theory," [arXiv:2005.03071 [hep-th]].

[22] M. Levi, A. J. Mcleod and M. Von Hippel, "NNNLO gravitational quadratic-in-spin interactions at the quartic order in G," [arXiv:2003.07890 [hep-th]].

[23] M. Levi and F. Teng, "NLO gravitational quartic-in-spin interaction," JHEP **01** (2021), 066 doi:10.1007/JHEP01(2021)066 [arXiv:2008.12280 [hep-th]].

[24] M. Levi, A. J. Mcleod and M. Von Hippel, "N^{3}LO gravitational spin-orbit coupling at order G^4," [arXiv:2003.02827 [hep-th]].

[25] Q. Henry, G. Faye and L. Blanchet, "Tidal effects in the equations of motion of compact binary systems to next-to-next-to-leading post-Newtonian order," Phys. Rev. D **101**, no.6, 064047 (2020) [arXiv:1912.01920 [gr-qc]];

Q. Henry, G. Faye and L. Blanchet, "Tidal effects in the gravitational-wave phase evolution of compact binary systems to next-to-next-to-leading post-Newtonian order," Phys. Rev. D **102**, no.4, 044033 (2020) [arXiv:2005.13367 [gr-qc]];

Q. Henry, G. Faye and L. Blanchet, "Hamiltonian for tidal interactions in compact binary systems to next-to-next-to-leading post-Newtonian order," [arXiv:2009.12332 [gr-qc]].

[26] D. Bini, T. Damour and A. Geralico, "Scattering of tidally interacting bodies in post-Minkowskian gravity," Phys. Rev. D **101**, no.4, 044039 (2020);

C. Cheung and M. P. Solon, "Tidal Effects in the Post-Minkowskian Expansion," [arXiv:2006.06665 [hep-th]].;

C. Cheung, N. Shah and M. P. Solon, Phys. Rev. D **103** (2021) no.2, 024030 doi:10.1103/PhysRevD.103.024030 [arXiv:2010.08568 [hep-th]].

Chapter 2

Non-renormalization and operator mixing via on-shell methods

Using on-shell methods, we present a new perturbative non-renormalization theorem for operator mixing in massless four-dimensional quantum field theories. By examining how unitarity cuts of form factors encode anomalous dimensions we show that longer operators are often restricted from renormalizing shorter operators at the first order where there exist Feynman diagrams. The theorem applies quite generally and depends only on the field content of the operators involved. We apply our theorem to operators of dimension five through seven in the Standard Model Effective Field Theory, including examples of nontrivial zeros in the anomalous-dimension matrix at one through four loops. The zeros at two and higher loops go beyond those previously explained using helicity selection rules. We also include explicit sample calculations at two loops.

2.1 Introduction

A key challenge in particle physics is to identify physics beyond the Standard Model. Because current experimental data at colliders is well described by the Standard Model, it is unclear which theoretical direction will ultimately prove to be the one chosen by Nature. It is therefore important to quantify new physics beyond the Standard Model in a systematic, model-independent manner. The theoretical framework for doing so is via effective field theories that extend the Standard Model Lagrangian by adding higher-dimension operators [1, 2]:

$$\Delta\mathcal{L} = \sum_i c_i \mathcal{O}_i \,, \tag{2.1}$$

with coefficients c_i suppressed by powers of a high-energy scale Λ dictated by the dimension of $\mathcal{O}_i$. The resulting theory, known as the Standard Model Effective Field Theory (SMEFT), is reviewed in Ref. [3].

As for all quantum field theories, renormalization induces mixing of these operators. This can be parametrized by the renormalization group equation,

$$16\pi^2 \frac{\partial c_i}{\partial \log \mu} = \gamma_{ij}^{\mathrm{UV}} c_j \,, \tag{2.2}$$

where $\gamma_{ij}^{\mathrm{UV}}$ is the anomalous-dimension matrix and μ is the renormalization scale. Usually, $\gamma_{ij}^{\mathrm{UV}}$ is calculated perturbatively in the marginal couplings of the Standard Model Lagrangian, which we will denote collectively as g. The complete one-loop anomalous-dimension matrix for operators up to dimension six has been computed in Refs. [4, 5]. These calculations reveal a number of vanishing entries related to supersymmetry [6], which seem surprising at first because there are valid diagrams that can be written down. These zeros have been elegantly explained [7] using tree-level helicity selection rules [8], which set certain classes of tree-level amplitudes to zero. The tree-level vanishings imply through unitarity that certain logarithms and their associated anomalous dimensions are not present. Although these selection rules

are reminiscent of supersymmetric ones, they hold for generic massless quantum field theories in four dimensions.

Might it be possible that beyond one loop there are new nontrivial zeros? At first sight, this seems rather unlikely because the helicity selection rules fail to hold at loop level. In this Letter, we show that, contrary to expectations, there are, in fact, additional nontrivial zeros in the higher-loop anomalous-dimension matrix. As in Ref. [7], our only assumption is that the theory does not contain any relevant couplings (e.g. masses). To state the new nonrenormalization theorem we define the length of an operator, $l(\mathcal{O})$, as the number of fundamental field insertions in $\mathcal{O}$. Then the statement of theorem is as follows:

Consider operators $\mathcal{O}_s$ and $\mathcal{O}_l$ such that $l(\mathcal{O}_l) > l(\mathcal{O}_s)$. $\mathcal{O}_l$ can renormalize $\mathcal{O}_s$ at L loops only if $L > l(\mathcal{O}_l) - l(\mathcal{O}_s)$.

At fixed loop order, sufficiently long operators cannot renormalize short operators because there would be too many legs to form a diagram with the right structure. Such zeros in the anomalous-dimension matrix are trivial. As written above the theorem applies non-trivially at $(l(\mathcal{O}_l) - l(\mathcal{O}_s))$-loops, i.e., the first loop order at which there could be renormalization because diagrams exist. However, in a general theory with multiple types of fields, the first renormalization can be delayed even further, depending on the precise field content of the two operators. We encapsulate this into the more general rule:

If at any given loop order, the only diagrams for a matrix element with the external particle content of $\mathcal{O}_s$ but an insertion of $\mathcal{O}_l$ involve scaleless bubble integrals, there is no renormalization of $\mathcal{O}_s$ by $\mathcal{O}_l$.

What makes them nontrivial is that Feynman diagrams exist that seem as if they should contribute to an anomalous dimension, but fail to do so because the diagrams do not generate the appropriate logarithms. The Feynman-diagram language can obscure this, because individual diagrams are not gauge invariant. While not difficult to disentangle at one loop,

at higher loops it becomes more advantageous to work in an on-shell formalism, which only takes gauge-invariant quantities as input. Indeed, modern unitarity methods [9] have clarified the structure of loop amplitudes resulting in significant computational advantages for a variety of problems, including the computation of form factors and associated anomalous dimensions [10].

2.2 Renormalization and Form Factors

Traditionally, the anomalous dimension corresponding to the renormalization of an operator $\mathcal{O}_i$ by an operator $\mathcal{O}_j$ is extracted from UV divergences. These can be found, for instance, in form factors,

$$F_j[p_1, ..., p_n; q; \mu] = \langle p_1, ..., p_n | \mathcal{O}_j(q) | 0 \rangle \,, \tag{2.3}$$

with an operator insertion $\mathcal{O}_j$ and external states $|p_1, ..., p_n\rangle$ that overlap with states created by $\mathcal{O}_i$. The divergences and associated anomalous dimensions can also be obtained from one-particle irreducible effective actions or from scattering amplitudes, $\mathcal{M}_{\mathcal{O}_j}$, corresponding to form factors with the operator momentum injection q set to zero.

Here we use the elegant on-shell approach developed by Caron-Huot and Wilhelm that extracts anomalous dimensions directly from renormalized quantities [11]. In this approach, the intuition that the renormalization properties of the theories are encoded in on-shell form factors through their logarithms is made precise by the following equation:

$$e^{-i\pi D} F^* = S \, F^* \,, \tag{2.4}$$

where F^* is the conjugate form factor with an insertion of an $\mathcal{O}_j$ operator. This relates the phase of the S-matrix, S, to the dilatation operator D which extracts anomalous dimensions. We point the interested reader to Ref. [11] for its derivation.

For simplicity we use dimensional regularization. In this case the dilatation operator D

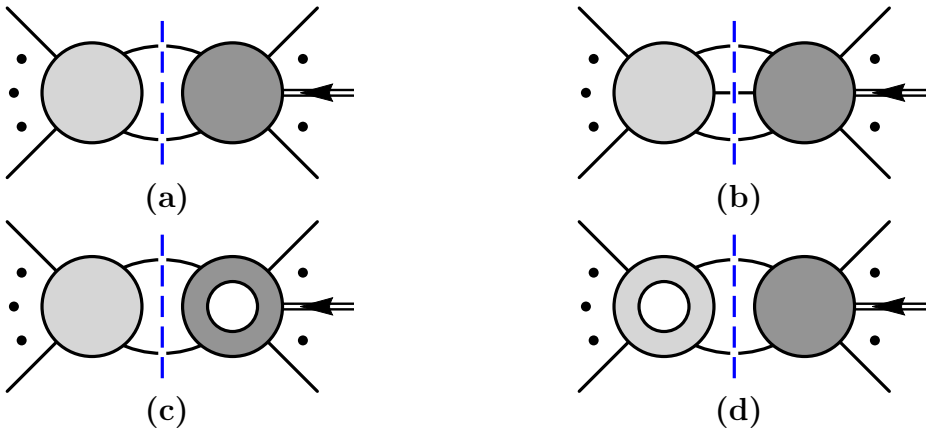

Figure 2.1: Unitarity cuts relevant for the extraction of anomalous dimensions from one- and two-loop form factors. The darker blobs indicate a higher-dimension operator insertion. The double-lined arrow indicates the insertion of additional off-shell momentum from the operator. The dashed line indicates the integral over phase space of the particles crossing the cut.

is related to the single renormalization scale $\mu = \mu_{\rm UV} = \mu_{\rm IR}$, as $D \simeq -\mu\partial_\mu$. Expanding Eq. (2.4) at one loop one obtains the following description of the renormalization of $\mathcal{O}_i$ by $\mathcal{O}_j$

$$\begin{aligned}\left(\gamma_{ij}^{\rm UV} - \gamma_{ij}^{\rm IR} + \beta(g)\partial_g\right)^{(1)} \langle p_1, ..., p_n|\mathcal{O}_i|0\rangle^{(0)} \\ = -\frac{1}{\pi}\langle p_1, ..., p_n|\mathcal{M}\otimes\mathcal{O}_j|0\rangle\,.\end{aligned} \tag{2.5}$$

On the left hand side we find the tree-level form factor of $\mathcal{O}_i$, the beta function $\beta(g)$ of the couplings g, the anomalous dimensions $\gamma_{\rm UV}$, which are the objects of interest, and the infrared anomalous dimensions $\gamma_{\rm IR}$, which arise from soft and/or collinear logarithms. The superscripts denote the perturbative order. The right hand side arises from the term $\mathcal{M}F^*$, where $\mathcal{M} = -i(S-1)$ is the scattering amplitude. The notation $\otimes$ here refers to an integration over the phase space of intermediate two-particle states in the product. This simply corresponds to a one-loop unitarity cut, as depicted in Figure 2.1(a). Schematically, Eq. (2.5) says that, up to terms coming from the β function, one-loop anomalous dimensions are eigenvalues of the S-matrix, with the form factors being the corresponding eigenvectors. More practically, this equation describes how to systematically extract the anomalous dimensions

from the coefficients of logarithms by taking discontinuities of the form factor.

The fact that dependence on the renormalization scale is related to discontinuities in kinematic variables is no surprise since the arguments of logarithms must balance kinematic variables against the renormalization scale to make them dimensionless. This observation has also been used to efficiently determine the renormalization-scale dependence of the two-loop counterterm in pure Einstein gravity from unitarity [12].

At higher-loop orders, other unitarity cuts, matching the order of the anomalous dimension, need to be considered. For instance at two loops, the three-particle cut is required, as well as the two-particle cut between the tree-level amplitude and the one-loop form factor and vice versa, as in Fig. 2.1(b–d).

2.3 Non-renormalization theorem

We would like to consider the renormalization of a shorter operator $\mathcal{O}_s$ by a longer operator $\mathcal{O}_l$. This could be, for example, the renormalization of $\phi^2 F^2$ by ϕ^6, where ϕ is a scalar and F is a vector field strength. For simplicity we will take $\mathcal{O}_s$ and $\mathcal{O}_l$ to be single operators, though in general they represent collections of operators with the same field content, but differing Lorentz contractions or color factors. Because our arguments rely only on the field content and basic structure of the unitarity cuts, our conclusions will apply just as well to the more general case.

The formalism reviewed above allows us to connect the anomalous dimensions to unitarity cuts of form factors, given knowledge of the β function of the leading couplings and the infrared anomalous dimensions. We now show that for the leading contributions, there is an even more direct connection between the ultraviolet anomalous dimensions and unitarity cuts.

The appearance of the β function in Eq. (2.5) is avoided simply by extracting the anomalous dimensions from the *minimal* form factor of $\mathcal{O}_s$, which is defined as the one with the

minimum number of legs needed to match the operator. We will denote this by a subscript on the state, $|p_1, ..., p_n\rangle_s$. Because of its defining property, the minimal tree-level form factor is local and does not depend on the couplings, g. Therefore the dependence of the higher-loop analog of Eq. (2.5) on the β function drops out.

Next, we would need knowledge of the infrared anomalous dimension $\gamma_{\rm IR}$. Infrared singularities are very well understood [13–16]. Our case is special, with a rather simple infrared structure. We are interested in the first loop order at which the higher-dimension operator could be renormalized. This would be the first loop order for which it is possible to write down valid diagrams. The lack of diagrams at lower-loop order means there cannot be any $\log(\mu_{\rm IR})$ terms or corresponding $\gamma_{\rm IR}$ at the given loop order under consideration. In addition, infrared singularities are diagonal for the operators with distinct fields, mixing only via color. Therefore at this order $\gamma_{\rm IR} = 0$. Various examples will be given in Ref. [17].

Thus, application of Eq. (2.4) is particularly simple for our case so that the relation between the first potentially nonvanishing anomalous dimension and unitarity cuts is direct:

$$\begin{aligned}(\gamma_{sl}^{\rm UV})^{(L)}\ {}_s\langle p_1, ..., p_n|\mathcal{O}_s|0\rangle^{(0)} \\ = -\frac{1}{\pi}{}_s\langle p_1, ..., p_n|\mathcal{M}\otimes\mathcal{O}_l|0\rangle\,.\end{aligned} \tag{2.6}$$

With this relation at hand, it is now straightforward to argue for new non-renormalization zeros by analyzing the allowed unitarity cuts. Eq. (2.6) gives $(\gamma_{sl}^{\rm UV})^{(L)}$ in terms of a sum over cuts of the form illustrated in Fig. 2.1. The left-hand side of any such k-particle cut is a $n_{\mathcal{M}}$-point amplitude, with the number of particles external to the cut equal to $n_{\mathcal{M}} - k$. Similarly the right-hand side is an n_F-point form factor, with $n_F - k$ particles external to the cut. Now, for the minimal form factor, the total number of external particles must match the length of $\mathcal{O}_s$, so we must have the relation,

$$n_{\mathcal{M}} + n_F - 2k = l(\mathcal{O}_s)\,. \tag{2.7}$$

The number of legs $n_{\mathcal{M}}$ and n_F are both bounded from below. For the unitarity cut to be non-zero, the scattering amplitude on the left must have at least two external particles, that is, $n_{\mathcal{M}} \geq k+2$. On the other side, n_F is restricted by the requirement that the form factor not include any scaleless bubbles. Since all legs of the form factor, including those crossing the cut, are on shell, any such scaleless bubbles would evaluate to zero. At one loop, for example, this implies $n_F \geq l(\mathcal{O}_l)$, which is the same as the tree level relation. At higher loops the particle count can be reduced depending on the number of loops in the form factor, which produces the relation

$$n_F \geq l(\mathcal{O}_l) - (L_F - 1) - \delta_{L_F,0}\,. \tag{2.8}$$

Here L_F is the number of loops contained in the form factor. $\delta_{L_F,0}$ is unity if the form factor is at tree level and zero otherwise, which accounts for the fact that there is no reduction in particle number between tree level and one loop. By considering the possible placings of the loops in the cut or on either side of the cut, we have $L_F \leq L - (k-1)$, implying $n_F \geq l(\mathcal{O}_l) - L + k - \delta_{L_F,0}$. Combining this with the condition on $n_{\mathcal{M}}$ and plugging in to equation (2.7), we obtain

$$l(\mathcal{O}_l) - L + 2 - \delta_{L_F,0} \leq l(\mathcal{O}_s)\,. \tag{2.9}$$

This inequality shows that the difference in length of the operators can preclude the renormalization unless

$$L > l(\mathcal{O}_l) - l(\mathcal{O}_s)\,, \tag{2.10}$$

and thus completes the proof of the first form of our theorem. In summary, we have shown that at loop orders less than or equal to $l(\mathcal{O}_l) - l(\mathcal{O}_s)$ there are no allowed unitarity cuts that can capture the coefficient of $\log(\mu^2)$, which in turn implies that $\gamma_{sl}^{\mathrm{UV}} = 0$. Eq. (2.9) also shows that the contributions to the anomalous dimension at loop order $L = l(\mathcal{O}_l) - l(\mathcal{O}_s) + 1$ are captured by cuts of the type in Figs. 2.1(a) and 2.1(b), that are given purely in terms of

tree-level matrix elements. Cuts of the type in Fig. 2.1(c) are directly ruled out by Eq. (2.9) and cuts of the type in Fig. 2.1(d) are ruled out because $l(O_l) - l(O_s) + 2$ legs need to be sewn across the cut to have a total of $l(O_s)$ external legs, so that all $l(O_l) - l(O_s) + 1$ loops are accounted for in the cut. This observation should help in their computation, for instance by allowing the use of four-dimensional helicity methods to evaluate the cut. It also implies that helicity selection rules can be active beyond one loop, contrary to expectations.

Depending on the particle contents of the two operators, it might happen that there are no allowed unitarity cuts even at a higher loop order than the one predicted by the first form of the theorem. Instead of analyzing the unitarity cuts, this can be explained in the more familiar diagrammatic language. Clearly, if the only diagrams that can be drawn involve scaleless bubbles, there will be no available cut where all loops are included in the cut. Thus, diagrams with fewer cut legs will force the form factor to include the scaleless bubble, and thus to evaluate to zero. Then the corresponding anomalous dimension must also be zero. This explains the more general rule presented in the introduction. As noted above this relies on the absence of infrared singularities whenever corresponding lower-loop form factors vanish.

Examples of zeros in the SMEFT at one loop are the renormalization of F^3 by $\phi^2 F^2$, and of $D^2\phi^4$, $F\phi\psi^2$, and $D\phi^2\psi^2$ by $\phi^3\psi^2$, which were already explained using the helicity selection rules [7], but also follow from the principles described here. In contrast to the helicity selection rules, however, our theorem can also apply at higher loops. The full set of zeros predicted by our rules for operators of dimensions five, six and seven includes examples at one through four loops and is described in Tables 2.1, 2.2, and 2.3 respectively. The tables also indicate the overlap between our theorem and the one-loop helicity selection rules of [7]. Note we have combined some of the categories of operators of [7], since our theorem does not need to distinguish operators based on their chirality.

2.4 Two-loop examples

Consider now two calculations that show explicit examples, from Table 2.2, of the nontrivial zeros in the anomalous-dimension matrix at two loops. The examples will also demonstrate the vanishing of $\gamma_{\rm IR}$. The first example is the renormalization of $\mathcal{O}_{\phi^2F^2}$ by $\mathcal{O}_{\phi^6}$, which is the entry (2,8) of Table 2.2.

The minimal two-loop form factor for $\mathcal{O}_{\phi^2F^2}$ includes two external scalars and two external gauge bosons. The product $\mathcal{M}F^*$ in Eq. (2.4) at two loops requires either a cut between a five-point amplitude and the tree-level form factor or a four-point amplitude and a one-loop form factor with an insertion of $\mathcal{O}_{\phi^6}$. However, the cut between the five-point amplitude and the tree-level form factor leaves five total external legs, and thus cannot match the minimal form factor for $\mathcal{O}_{\phi^2F^2}$. For the cut between the four-point amplitude and the one-loop form factor to match the minimal form factor for $\mathcal{O}_{\phi^2F^2}$, the one-loop form factor would have to involve a massless tadpole, which would evaluate to zero.

We can also directly check that the (single) diagram—Fig. 2.2(a)—for the $\mathcal{O}_{\phi^6} \to \mathcal{O}_{\phi^2F^2}$ renormalization evaluates to zero. By incorporating an IR regulator $\lambda_{\rm IR}$, we can evaluate the integral while keeping the UV and IR dependences separate and determine the behavior of the form factor in the limit $\lambda_{\rm IR} \to 0$. The integral for this diagram immediately factorizes, and each of the two loop integrals is of the form

$$\int \frac{d^D\ell_1}{(2\pi)^D} \frac{(2\ell_1 - k_1)\cdot\varepsilon_1}{(\ell_1^2 - \lambda_{\rm IR})((\ell_1 - k_1)^2 - \lambda_{\rm IR})}\,. \tag{2.11}$$

This integral vanishes by the on-shell condition $k_1 \cdot \varepsilon_1 = 0$ and Lorentz invariance, since k_1 is the only available momentum. Therefore $\mathcal{O}_{\phi^6}$ cannot renormalize $\mathcal{O}_{\phi^2F^2}$ at two loops.

For a slightly more complex example, consider the renormalization of $\mathcal{O}_{F^3}$ by $\mathcal{O}_{\psi^4}$ at two loops, corresponding to entry (1,6) of Table 2.2. Again, for this process the three-particle cut between the five-point amplitude and the tree-level form factor does not produce the

Table 2.1: Application of the non-renormalization theorem to dimension-five operators. The operators labeling the rows are renormalized by the operators labeling the columns. $\times_L$ indicates the theorem applies at L-loop order. (L) denotes that there are no diagrams before L-loops, but renormalization is possible at that order, since the required cuts can exist. Light-gray shading indicates a zero at one loop due to helicity selection rules, while dark-gray shading indicates the entry is a new zero predicted by our non-renormalization theorem.

	$F^2\phi$	$F\psi^2$	$\phi^2\psi^2$	ϕ^5
$F^2\phi$			(2)	$\times_2$
$F\psi^2$			$\times_1$	$\times_3$
$\phi^2\psi^2$				(2)
ϕ^5				

Table 2.2: Application of the non-renormalization theorem to dimension six. The notation is explained in Table I.

	F^3	ϕ^2F^2	$F\phi\psi^2$	$D^2\phi^4$	$D\phi^2\psi^2$	ψ^4	$\phi^3\psi^2$	ϕ^6
F^3		$\times_1$	(2)	$\times_2$	$\times_2$	$\times_2$	$\times_3$	$\times_3$
ϕ^2F^2							(2)	$\times_2$
$F\phi\psi^2$							$\times_1$	$\times_3$
$D^2\phi^4$							$\times_1$	$\times_2$
$D\phi^2\psi^2$							$\times_1$	(3)
ψ^4							(2)	(4)
$\phi^3\psi^2$								(2)
ϕ^6								

correct external-particle state corresponding to the field content of $\mathcal{O}_{F^3}$. The two-particle cut between the four-point amplitude and the one-loop form factor with an insertion of $\mathcal{O}_{\psi^4}$ is shown in Figure 2.2(b). By again adding an IR regulator, the result can be written as

$$\int d\text{LIPS}_{\ell_1} \frac{d^D\ell_2}{(2\pi)^D} \frac{\text{Tr}[X(\ell_1)\not{\ell}_2\not{\epsilon}_3(\not{\ell}_2 - \not{k}_3)]}{(\ell_2^2 - \lambda_{\text{IR}})((\ell_2 - k_3)^2 - \lambda_{\text{IR}})}\,, \tag{2.12}$$

where X receives contributions from the multiple possible diagrams of the four-point amplitude and includes the remaining propagators.

One can reduce the ℓ_2 tensor integrals using standard techniques to obtain the following result

Table 2.3: Application of the non-renormalization theorem to dimension seven. The notation is explained in Table I. The shortest and longest operators have been dropped from the list of columns and rows, respectively, since our theorem requires a reduction in length of the operators.

	ϕ^3F^2	$D^2\phi^5$	$D\phi^3\psi^2$	$\phi\psi^4$	$F\phi^2\psi^2$	$\phi^4\psi^2$	ϕ^7
$F^3\phi$	$\times_1$	$\times_2$	$\times_2$	$\times_2$	(2)	$\times_3$	$\times_3$
$DF\phi\psi^2$	(2)	$\times_2$	$\times_1$	$\times_1$	$\times_1$	$\times_2$	$\times_4$
$F^2\psi^2$	(2)	(3)	(2)	(2)	$\times_1$	$\times_2$	$\times_4$
$D^2\phi^2\psi^2$	(2)	(2)	$\times_1$	$\times_1$	$\times_1$	$\times_2$	(4)
$D\psi^4$	(3)	(3)	(2)	$\times_1$	(2)	(3)	(5)
ϕ^3F^2						(2)	$\times_2$
$D^2\phi^5$						$\times_1$	$\times_2$
$D\phi^3\psi^2$						$\times_1$	(3)
$\phi\psi^4$						(2)	(4)
$F\phi^2\psi^2$						$\times_1$	$\times_3$
$\phi^4\psi^2$							(2)

$$\int \frac{d^D\ell_2}{(2\pi)^D}\frac{\ell_2^\mu\ell_2^\nu}{(\ell_2^2-\lambda_{\rm IR})^2}\int d{\rm LIPS}_{\ell_1}\, Y_{\mu\nu}(\ell_1) \qquad (2.13)$$
$$= -\frac{i\Gamma(-1+\epsilon)}{2(4\pi)^{2-\epsilon}}(\lambda_{\rm IR})^{1-\epsilon}\int d{\rm LIPS}_{\ell_1}\, Y^\mu{}_\mu(\ell_1)\,,$$

where $\epsilon = (4-D)/2$, Y contains the rest of the trace in Eq. (2.12), and terms linear in ℓ_2 cancel. Since the phase-space integral can at worst result in a $\log(\lambda_{\rm IR})$ divergence, the factor $(\lambda_{\rm IR})^{1-\epsilon}$ ensures that the expression goes smoothly to zero as $\lambda_{\rm IR}$ approaches zero for all orders in ϵ. Therefore the cut vanishes, along with the UV anomalous dimension.

2.5 Conclusions

We have derived a new non-renormalization theorem that applies to higher-dimensional operators in quantum field theory. Since the theorem is dependent on only the number and type of fields in each operator, it applies to generic massless theories with no relevant operators.

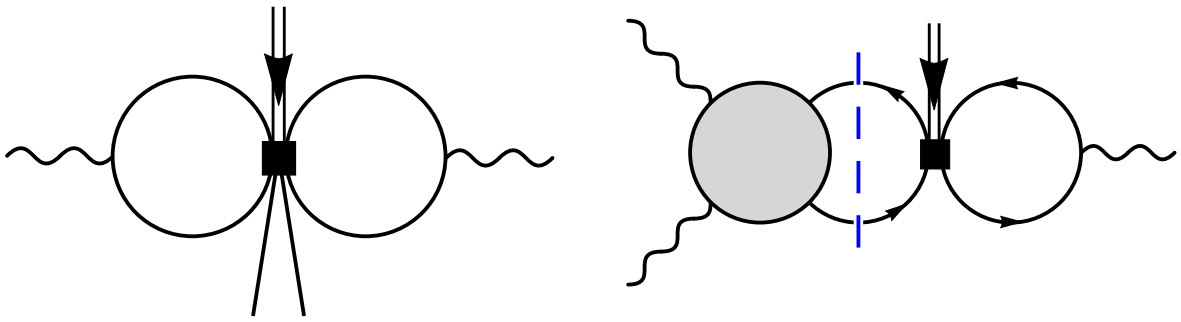

Figure 2.2: (a) Diagram showing the only possible two loop contribution to the renormalization of $\mathcal{O}_{\phi^2F^2}$ by $\mathcal{O}_{\phi^6}$. (b) Cut of a form factor showing that $\mathcal{O}_{\psi^4}$ cannot renormalize $\mathcal{O}_{F^3}$ at two loops. The solid square indicates the insertion of the ϕ^6 or ψ^4 operator, respectively.

Besides being helpful to find zeros of the anomalous-dimension matrix, the on-shell formalism of Ref. [11] is a good way to compute nonzero entries as well. Whenever an entry is excluded by our theorem, it should be much simpler to compute the entry at the next loop order compared to computing a generic entry at that loop order, because only tree-level quantities enter the cuts. In addition, helicity selection rules [7] might then apply, pushing the zero one loop further. For instance, it is straightforward to confirm that many of the nonzero entries in the tables above vanish in the absence of Yukawa couplings. It would also be interesting to combine our results with those of Ref. [18], where dimensional-analysis counting rules are used to constrain coupling-constant dependence, and more generally to find the full set constraints in the multiloop anomalous-dimension matrix of the SMEFT. On-shell methods [9] are also a good way to compute amplitudes including higher-dimension operators. Using these we have computed four-point one-loop massless amplitudes and associated anomalous dimensions of the SMEFT dimension-six operators, which will be described elsewhere [17].

Bibliography

[1] W. Buchmuller and D. Wyler, "Effective Lagrangian Analysis of New Interactions and Flavor Conservation," Nucl. Phys. B **268**, 621 (1986).

[2] B. Grzadkowski, M. Iskrzynski, M. Misiak and J. Rosiek, "Dimension-Six Terms in the Standard Model Lagrangian," JHEP **1010**, 085 (2010) [arXiv:1008.4884 [hep-ph]].

[3] I. Brivio and M. Trott, "The Standard Model as an Effective Field Theory," Phys. Rept. **793**, 1 (2019) [arXiv:1706.08945 [hep-ph]].

[4] C. Grojean, E. E. Jenkins, A. V. Manohar and M. Trott, "Renormalization Group Scaling of Higgs Operators and $\Gamma(h \to \gamma\gamma)$," JHEP **1304**, 016 (2013) [arXiv:1301.2588 [hep-ph]];
J. Elias-Miró, J. R. Espinosa, E. Masso and A. Pomarol, "Renormalization of dimension-six operators relevant for the Higgs decays $h \to \gamma\gamma, \gamma Z$," JHEP **1308**, 033 (2013) doi:10.1007/JHEP08(2013)033 [arXiv:1302.5661 [hep-ph]];
J. Elias-Miró, J. R. Espinosa, E. Masso and A. Pomarol, "Higgs windows to new physics through d=6 operators: constraints and one-loop anomalous dimensions," JHEP **1311**, 066 (2013) [arXiv:1308.1879 [hep-ph]].

[5] E. E. Jenkins, A. V. Manohar and M. Trott, "Renormalization Group Evolution of the Standard Model Dimension Six Operators I: Formalism and lambda Dependence," JHEP **1310**, 087 (2013) [arXiv:1308.2627 [hep-ph]];

E. E. Jenkins, A. V. Manohar and M. Trott, "Renormalization Group Evolution of the Standard Model Dimension Six Operators II: Yukawa Dependence," JHEP **1401**, 035 (2014) [arXiv:1310.4838 [hep-ph]];

R. Alonso, E. E. Jenkins, A. V. Manohar and M. Trott, "Renormalization Group Evolution of the Standard Model Dimension Six Operators III: Gauge Coupling Dependence and Phenomenology," JHEP **1404**, 159 (2014) [arXiv:1312.2014 [hep-ph]].

[6] R. Alonso, E. E. Jenkins and A. V. Manohar, "Holomorphy without Supersymmetry in the Standard Model Effective Field Theory," Phys. Lett. B **739**, 95 (2014) [arXiv:1409.0868 [hep-ph]];

J. Elias-Miró, J. R. Espinosa and A. Pomarol, "One-loop non-renormalization results in EFTs," Phys. Lett. B **747**, 272 (2015) [arXiv:1412.7151 [hep-ph]].

[7] C. Cheung and C. H. Shen, "Nonrenormalization Theorems without Supersymmetry," Phys. Rev. Lett. **115**, no. 7, 071601 (2015) [arXiv:1505.01844 [hep-ph]].

[8] M. L. Mangano and S. J. Parke, "Multiparton Amplitudes in Gauge Theories," Phys. Rept. **200**, 301 (1991) [hep-th/0509223].

[9] Z. Bern, L. J. Dixon, D. C. Dunbar and D. A. Kosower, "One Loop n Point Gauge Theory Amplitudes, Unitarity and Collinear Limits," Nucl. Phys. B **425**, 217 (1994) [hep-ph/9403226];

Z. Bern, L. J. Dixon, D. C. Dunbar and D. A. Kosower, "Fusing Gauge Theory Tree Amplitudes into Loop Amplitudes," Nucl. Phys. B **435**, 59 (1995) [hep-ph/9409265];

Z. Bern and A. G. Morgan, "Massive loop amplitudes from unitarity," Nucl. Phys. B **467**, 479 (1996) [hep-ph/9511336].

Z. Bern, L. J. Dixon and D. A. Kosower, "One loop amplitudes for e^+e^- to four partons," Nucl. Phys. B **513**, 3 (1998) [hep-ph/9708239].

R. Britto, F. Cachazo and B. Feng, "Generalized unitarity and one-loop amplitudes in

N=4 super-Yang-Mills," Nucl. Phys. B **725**, 275 (2005) [hep-th/0412103].

[10] A. Brandhuber, M. Kostacinska, B. Penante, G. Travaglini and D. Young, "The SU(2—3) dynamic two-loop form factors," JHEP **1608**, 134 (2016) [arXiv:1606.08682 [hep-th]];

A. Brandhuber, M. Kostacinska, B. Penante and G. Travaglini, "Higgs amplitudes from $\mathcal{N} = 4$ super Yang-Mills theory," Phys. Rev. Lett. **119**, no. 16, 161601 (2017) [arXiv:1707.09897 [hep-th]];

A. Brandhuber, M. Kostacinska, B. Penante and G. Travaglini, "Tr(F^3) supersymmetric form factors and maximal transcendentality Part I: $\mathcal{N} = 4$ super Yang-Mills," JHEP **1812**, 076 (2018) [arXiv:1804.05703 [hep-th]];

A. Brandhuber, M. Kostacinska, B. Penante and G. Travaglini, "Tr(F^3) supersymmetric form factors and maximal transcendentality Part II: $0 < \mathcal{N} < 4$ super Yang-Mills," JHEP **1812**, 077 (2018) [arXiv:1804.05828 [hep-th]].

[11] S. Caron-Huot and M. Wilhelm, "Renormalization Group Coefficients and the S-matrix," JHEP **1612**, 010 (2016) [arXiv:1607.06448 [hep-th]].

[12] Z. Bern, C. Cheung, H. H. Chi, S. Davies, L. Dixon and J. Nohle, "Evanescent Effects Can Alter Ultraviolet Divergences in Quantum Gravity without Physical Consequences," Phys. Rev. Lett. **115**, no. 21, 211301 (2015) [arXiv:1507.06118 [hep-th]];

Z. Bern, H. H. Chi, L. Dixon and A. Edison, Phys. Rev. D **95**, no. 4, 046013 (2017) [arXiv:1701.02422 [hep-th]].

[13] G. F. Sterman, "Mass Divergences in Annihilation Processes. 1. Origin and Nature of Divergences in Cut Vacuum Polarization Diagrams," Phys. Rev. D **17**, 2773 (1978);

G. F. Sterman, "Mass Divergences in Annihilation Processes. 2. Cancellation of Divergences in Cut Vacuum Polarization Diagrams," Phys. Rev. D **17**, 2789 (1978).

[14] L. Magnea and G. F. Sterman, "Analytic Continuation of the Sudakov Form-Factor in QCD," Phys. Rev. D **42**, 4222 (1990);

W. T. Giele and E. W. N. Glover, "Higher Order Corrections To Jet Cross-Sections in e^+e^- Annihilation," Phys. Rev. D **46**, 1980 (1992);

Z. Kunszt, A. Signer and Z. Trocsanyi, "Singular Terms of Helicity Amplitudes at One Loop in QCD and the Soft Limit Of The Cross-Sections of Multiparton Processes," Nucl. Phys. B **420**, 550 (1994) [hep-ph/9401294];

S. Catani, "The Singular Behavior of QCD Amplitudes at Two Loop Order," Phys. Lett. B **427**, 161 (1998) [hep-ph/9802439].

[15] G. F. Sterman, *An Introduction to Quantum Field Theory,* Cambridge University Press (1993).

[16] J.-y. Chiu, A. Fuhrer, R. Kelley and A. V. Manohar, "Factorization Structure of Gauge Theory Amplitudes and Application to Hard Scattering Processes at the LHC," Phys. Rev. D **80**, 094013 (2009) [arXiv:0909.0012 [hep-ph]].

[17] Z. Bern, J. Parra-Martinez and E. Sawyer, "Structure of two-loop SMEFT anomalous dimensions via on-shell methods," JHEP **2020.10** (2020): 1-60. arXiv:2005.12917 [hep-ph]

[18] E. E. Jenkins, A. V. Manohar and M. Trott, "Naive Dimensional Analysis Counting of Gauge Theory Amplitudes and Anomalous Dimensions," Phys. Lett. B **726**, 697 (2013) [arXiv:1309.0819 [hep-ph]].

Chapter 3

Structure of two-loop SMEFT anomalous dimensions via on-shell methods

We describe on-shell methods for computing one- and two-loop anomalous dimensions in the context of effective field theories containing higher-dimension operators. We also summarize methods for computing one-loop amplitudes, which are used as inputs to the computation of two-loop anomalous dimensions, and we explain how the structure of rational terms and judicious renormalization scheme choices can lead to additional vanishing terms in the anomalous dimension matrix at two loops. We describe the two-loop implications for the Standard Model Effective Field Theory (SMEFT). As a by-product of this analysis we verify a variety of one-loop SMEFT anomalous dimensions computed by Alonso, Jenkins, Manohar and Trott.

3.1 Introduction

Effective Field Theory (EFT) approaches have risen to prominence in recent years as a systematic means for quantifying new physics beyond the Standard Model. The Standard Model Effective Field Theory (SMEFT) incorporates the effects of new physics via higher-dimension operators built from Standard Model fields [1, 2]. The operators are organized according to their dimension, which gives a measure of their importance at low-energy scales. The SMEFT allows exploration of the effects of new physics without requiring a complete understanding of the more fundamental high-energy theory. While systematic, the SMEFT involves a large number of operators and free coefficients [3], making it useful to develop improved techniques for computing quantities of physical interest and for understanding their structure. One such quantity is the anomalous dimension matrix of the higher-dimension operators. The appearance of anomalous dimensions implies that the Wilson coefficients of operators at scales accessible by collider experiments differ from those at the high-energy matching scale to the more fundamental unknown theory. These also control operator mixing, providing important information on how experimental constraints from one operator affect the coefficients of other operators. This makes evaluating the anomalous dimension matrix a crucial aspect of interpreting results within the SMEFT. Towards this goal, here we apply on-shell methods that greatly streamline the computation of anomalous dimensions at one and two loops and expose hidden structure.

A systematic and complete computation of the one-loop anomalous dimension matrix for dimension-six operators in the SMEFT is found in the landmark calculations of Refs. [4]. Besides their importance for interpreting experimental data, these calculations reveal a remarkable structure with the appearance of nontrivial zeros in the anomalous dimension matrix [5]. These one-loop zeros have been understood as stemming from selection rules that arise from supersymmetry embeddings [6], helicity [7], operator lengths [8], and angular momentum [9]. Perhaps even more surprisingly, nontrivial zeros in the anomalous dimension

matrix of the SMEFT appear at any loop order and for operators of any dimension [8]. In addition, a surprising number of the associated one-loop scattering amplitudes vanish as well [9, 10], suggesting additional zeros may appear in the anomalous dimensions at two loops. Here we apply on-shell methods to identify a new set of vanishing terms in the two-loop anomalous dimension matrix of the SMEFT. As a by product of our two-loop study, we also confirm many one-loop anomalous dimensions computed in Refs. [4], via both the generalized unitarity method [11] and an elegant new unitarity-based method due to Caron-Huot and Wilhelm for directly extracting anomalous dimensions from cuts [12], which builds on insight developed in earlier work on $\mathcal{N} = 4$ super-Yang-Mills theory [13].

On-shell methods have proven to be quite useful in a variety of other settings, including collider physics (see e.g. Refs. [14]), ultraviolet properties of (super)gravity (see e.g. Refs. [15–18]), theoretical explorations of supersymmetric gauge and gravity theories (see e.g. Refs. [19, 20]), cosmological observables (see e.g. Refs. [21, 22]), and gravitational-wave physics (see e.g. Refs. [23]). They have also been used as a convenient means for classifying interactions in EFTs such as the SMEFT [24]. In addition, general properties of the S-matrix, such as unitarity, causality and analyticity have been used to constrain Wilson coefficients of EFTs [25], including the SMEFT [26].

In the context of anomalous dimensions and renormalization-group analyses, unitarity cuts give us direct access to renormalization-scale dependence. After subtracting infrared singularities, the renormalization-scale dependence can be read off from remaining dimensional imbalances in the arguments of logarithms [16]. The direct link between anomalous dimensions at any loop order and unitarity cuts is made explicit in the formulation of Caron-Huot and Wilhelm [12]. In carrying out our two-loop analysis we make extensive use of their formulation. Very recently the same formalism and general set of ideas was applied in Refs. [27, 28] to compute certain SMEFT anomalous dimensions.

In general, two-loop unitarity cuts include both three-particle cuts between two tree-level objects, as well as two-particle cuts between tree-level and one-loop objects. Consequently,

our exploration of two-loop anomalous dimensions will require computing one-loop matrix elements first. On-shell methods, in particular generalized unitary [11, 29, 30], are especially well suited for this task. Because we feed one-loop matrix elements into higher-loop calculations, we find it convenient to use D-dimensional techniques which account for rational terms. To carry out the integration, we decompose the integrands into gauge-invariant tensors along the lines of Refs. [31, 32]. In this form, the integrands can be straightforwardly reduced to a basis of scalar integrals using integration by parts technology (as implemented, e.g., in FIRE [33]). These one-loop amplitudes are among the building blocks that feed into the two-loop anomalous dimension calculation.

Using the unitarity-based formalism, we indeed find that many potential contributions to the two-loop anomalous dimension matrix vanish for a variety of reasons, including the appearance of only scaleless integrals [8], color selection rules, vanishing rational terms at one loop, as well as appropriate renormalization scheme choices at one loop. These vanishing contributions go beyond those identified in our previous paper [8]. Of the new vanishings, perhaps the most surprising is the finding that additional zeros can be induced at two loops by slightly adjusting the $\overline{\text{MS}}$ renormalization scheme at one loop. This is tied to the fact that two-loop anomalous dimensions and local rational contributions to one-loop amplitudes are scheme dependent, and can therefore be set to zero by appropriate finite shifts of operator coefficients, or, equivalently, by a finite renormalization of the operators, or the addition of finite local counterterms.

For simplicity, we use a non-chiral version of the Standard Model, with zero quark and Higgs masses, zero Yukawa couplings, and without an Abelian sector, but point out overlap with the SMEFT in Section 3.5. We note that although we only utilize Dirac fermions here, on-shell methods are well suited for dealing with chiral fermions as well (see e.g. Refs. [14, 29]). In any case, this model is a close enough cousin of the SMEFT that we can directly verify a variety of one-loop SMEFT anomalous dimensions calculated in Refs. [4], finding full agreement, and make some predictions about the structure of the two-loop anomalous

dimension matrix.

The paper is organized as follows. In Section 3.2, we explain our conventions, list the higher-dimensional operators in our simplified version of the SMEFT, and summarize the on-shell methods that we use to obtain anomalous dimensions. In Section 3.3 we explain the use of generalized unitarity in constructing full one-loop amplitudes, and we discuss the appearance of numerous zeros in the rational terms of the amplitudes. We also explain how finite counterterms can produce additional zeros in the rational terms of many of the one-loop amplitudes. Examples of additional vanishing contributions to the two-loop anomalous dimension matrix are presented in Section 3.4, including those that arise from finite counterterms at one-loop. In Section 3.5 we discuss the overlap between our simplified model and the full SMEFT in the basis of operators used in Refs. [4], and discus the implications of our results for the latter theory. We give our conclusions in Section 3.6. Appendix 3.A explains the projection method used for integration in detail and lists the gauge invariant basis tensors. The explicit D-dimensional forms of the full one-loop amplitudes, as well as their four-dimensional finite remainders, are relegated to the ancillary files [34] and Appendix 3.B, respectively.

3.2 Setup and formalism

We now present our conventions and explain the on-shell formalisms that we use for obtaining the anomalous dimensions. One procedure for doing so is to extract them from ultraviolet divergences in amplitudes. This procedure follows the generalized unitarity method for assembling scattering amplitudes from their unitarity cuts [11, 11, 14, 29]. While we describe the procedure for obtaining the anomalous dimensions in the current section, we leave a more detailed discussion of the generalized unitarity method for Section 3.3, where it will be used to construct full amplitudes.

As a second method, we apply the recent formalism of Caron-Huot and Wilhelm [12],

which directly expresses the anomalous dimensions in terms of unitarity cuts. This method is particularly effective for computing anomalous dimensions, and is our preferred method beyond one loop. We show how this method helps clarify the structure of the anomalous dimension matrix at two loops and exposes new nontrivial zeros.

3.2.1 Conventions and basic setup

To illustrate our methods we will consider a model with dimension-four Lagrangian given by

$$\mathcal{L}^{(4)} = -\frac{1}{4}F^a_{\mu\nu}F^{a\mu\nu} + D_\mu\varphi\, D^\mu\overline{\varphi} - \lambda\,(\varphi\overline{\varphi})^2 + i\sum_{m=1}^{N_f}\bar{\psi}_m \not{D}\psi_m\,, \tag{3.1}$$

where the gauge field strength, $F^a_{\mu\nu}$, is in the adjoint representation of $SU(N)$, while ψ_m and φ are fundamental representation Dirac fermions and scalars, respectively. The index m on the fermions denotes the flavor; for simplicity we take a single flavor of scalars. The covariant derivative is given by

$$(D_\mu\psi_m)_i = \Big(\delta_{ij}\partial_\mu + ig\frac{1}{\sqrt{2}}T^a_{ij}A^a_\mu\Big)(\psi_m)_j\,, \tag{3.2}$$

where T^a_{ij} is the $SU(N)$ generator. We normalize the generator in the standard amplitudes convention by $\mathrm{Tr}[T^aT^b] = \delta^{ab}$ which differs from the usual textbook one, and we define $f^{abc} = -i\,\mathrm{Tr}[[T^a,T^b]T^c]$ and $d^{abc} = \mathrm{Tr}[\{T^a,T^b\}T^c]$ for later use.[1]

This model theory has the general structure of the Standard Model, but with all masses and Yukawa couplings set to zero, and with only one gauge group. Here we also use Dirac instead of chiral fermions; the basic methods apply just as well to cases which include chiral fermions in the context of Standard Model calculations, as in Ref. [29].

To mimic the SMEFT we modify this Lagrangian by adding dimension-six operators

[1]Note that our structure constants, f^{abc}, carry an extra factor of $\sqrt{2}$ relative to standard textbook conventions [35].

supressed by a high-energy scale Λ:

$$\mathcal{L} = \mathcal{L}^{(4)} + \frac{1}{\Lambda^2} \sum_k c_i^{(6)} \mathcal{O}_i^{(6)} \,, \tag{3.3}$$

where the list of the operators that we consider here is given in Table 3.1[2]. Note that our simplified model contains representatives from all of the operator classes of the basis used in Refs. [4], other than the classes $\psi^2 F\varphi$ and $\psi^2\varphi^3$ ($\psi^2 XH$ and $\psi^2 H^3$ in the notation of Refs. [4]), since operators in these classes must always have one uncharged fermion. We defer a comparison to the full SMEFT to Section 3.5.

At first order in c_i/Λ^2, renormalization induces mixing of the dimension-six operators, as parametrized by

$$\dot{c}_i \equiv \frac{\partial c_i}{\partial \log \mu} = c_j \gamma_{ji} \,. \tag{3.4}$$

If the coefficient of operator $\mathcal{O}_j$ appears on the right-hand side of the RG equation for the coefficient of operator $\mathcal{O}_i$, as above, we say that $\mathcal{O}_j$ renormalizes $\mathcal{O}_i$, or that they mix under renormalization. Sometimes we write the corresponding anomalous dimension as $\gamma_{i\leftarrow j}$. In all tables which describe anomalous dimensions we will display $\gamma'_{ij} = \gamma_{ij}^{\mathrm{T}}$ to facilitate comparison with Refs. [4]. The anomalous dimension matrix γ_{ij} depends on the dimension-four couplings g and λ, in the combinations

$$\tilde{g}^2 = \frac{g^2}{(4\pi)^2} \,, \qquad\qquad \tilde{\lambda} = \frac{\lambda}{(4\pi)^2} \,, \tag{3.5}$$

which we sometimes refer to collectively as $g^{(4)}$.

We extract anomalous dimensions from both amplitudes and form factors. We define a form factor with an operator insertion as

$$F_i(1^{h_1}, ..., n^{h_n}; q) = \langle k_1^{h_1}, ..., k_n^{h_n} | \mathcal{O}_i(q) | 0 \rangle \,, \tag{3.6}$$

[2]We note that $\mathcal{O}_{\varphi^6}$ has no nonzero four-point amplitudes through two-loops, and therefore cannot renormalize any of the other operators [8]. We still include it here for completeness.

Label	Operator
$\mathcal{O}_{F^3}$	$\frac{1}{3} f^{abc} F^a_{\mu\nu} F^a_{\nu\rho} F^a_{\rho\mu}$
$\mathcal{O}_{(\varphi^2 F^2)_1}$	$(\varphi^\dagger \varphi) F^a_{\mu\nu} F^a_{\mu\nu}$
$\mathcal{O}_{(\varphi^2 F^2)_2}$	$d^{abc} (\varphi^\dagger T^a \varphi) F^b_{\mu\nu} F^c_{\mu\nu}$
$\mathcal{O}_{(D^2\varphi^4)_1}$	$(\varphi^\dagger D^\mu \varphi)^* (\varphi^\dagger D_\mu \varphi)$
$\mathcal{O}_{(D^2\varphi^4)_2}$	$(\varphi^\dagger \varphi) \Box (\varphi^\dagger \varphi)$
$\mathcal{O}_{\varphi^6}$	$(\varphi^\dagger \varphi)^3$
$\mathcal{O}^{pr}_{(D\varphi^2\psi^2)_1}$	$i(\varphi^\dagger (D_\mu - \overleftarrow{D}_\mu) \varphi)(\bar{\psi}_p \gamma^\mu \psi_r)$
$\mathcal{O}^{pr}_{(D\varphi^2\psi^2)_2}$	$i(\varphi^\dagger (T^a D_\mu - \overleftarrow{D}_\mu T^a) \varphi)(\bar{\psi}_p T^a \gamma^\mu \psi_r)$
$\mathcal{O}^{mnpr}_{(\psi^4)_1}$	$(\bar{\psi}_m \gamma^\mu \psi_n)(\bar{\psi}_p \gamma_\mu \psi_r)$
$\mathcal{O}^{mnpr}_{(\psi^4)_2}$	$(\bar{\psi}_m \gamma^\mu T^a \psi_n)(\bar{\psi}_p \gamma_\mu T^a \psi_r)$

Table 3.1: List of dimension-six operators considered here. For simplicity, we take the fermions to be Dirac. The labels *mnpr* are flavor indices and *abc* color indices. Note the operator $\mathcal{O}_{F^3}$ is normalized slightly differently than in Refs. [4], as are the color matrices T^a in the operators $\mathcal{O}_{(D\varphi^2\psi^2)_2}$ and $\mathcal{O}_{(\psi^4)_2}$. We will occasionally drop the $(\ )_1$ and $(\ )_2$ subscripts to refer to pairs of operators collectively.

which are matrix elements between an on-shell state $\langle k_1, ..., k_n|$, with particles of momenta $\{k_1 ... k_n\}$ and helicities $\{h_1 ... h_n\}$, and an operator $\mathcal{O}_i$ that injects additional off-shell momentum q. The states might also be dependent on the color and flavor of the particles, but we leave this dependence implicit for the moment. Form factors are especially useful when dealing with on-shell states with fewer than four particles, where kinematics would otherwise require the amplitude (with real momenta) to be zero. From the perspective of form factors, we can think of an amplitude with an operator insertion as a form factor, but where the higher-dimension operator injects zero momentum, $q = 0$,

$$A_i(1^{h_1}, ..., n^{h_n}) = \langle k_1^{h_1}, ..., k_n^{h_n} | \mathcal{O}_i(0) | 0 \rangle \,. \tag{3.7}$$

When the inserted operator is the identity, we recover the usual scattering amplitude, which

depends only on the dimension-four couplings. We denote such an amplitude as

$$A(1^{h_1},...,n^{h_n}) = \langle k_1^{h_1},...,k_n^{h_n}|0\rangle = \langle k_1^{h_1},...,k_i^{h_i}|\mathcal{M}| - k_{i+1}^{-h_{i+1}},\ldots,-k_n^{-h_n}\rangle\,. \tag{3.8}$$

Unless otherwise stated, we use an all outgoing convention where all the particles are crossed to the final state. When crossing fermions there are additional signs on the right-hand side of Eq. (3.8) that we leave implicit here. In general we can write the form factors (and amplitudes) as color-space vectors,

$$F_i(1,\ldots,n) = \sum_j \mathcal{C}^{[j]} F_{i\,[j]}(1,\ldots,n)\,, \tag{3.9}$$

where the $\mathcal{C}^{[i]}$ are a set of independent color factors. In the context of amplitudes, these correspond to *color-ordered* [36] or, more generally, *primitive* [37] amplitudes. The color factors $\mathcal{C}^{[i]}$ depend on which particles of the amplitude are in the adjoint or fundamental representation of $SU(N)$. Here, we only need the decomposition into a basis of color factors without using special properties of the coefficients. For the various processes we consider, the tree and one-loop amplitudes are listed in Appendix 3.B.

We use the conventional dimensional regularization and $\overline{\text{MS}}$-like schemes throughout, in which the amplitudes and form factors, F_i satisfy the renormalization-group equations

$$\left[(\mu\partial_\mu + \beta\,\partial)\,\delta_{ij} + \left(\gamma^{\text{UV}} - \gamma^{\text{IR}}\right)_{ij}\right] F_j = 0, \tag{3.10}$$

where $\partial_\mu := \partial/\partial\mu$, $\partial := \partial/\partial g^{(4)}$, $\beta := \beta(g^{(4)})$ is the β-function of the collection of marginal couplings, γ_{ij}^{UV} are the anomalous dimensions of the higher-dimension operators, and γ_{ij}^{IR} are the IR anomalous dimensions, arising from soft and/or collinear divergences[3]. For later

[3]The relative sign between UV and IR anomalous dimensions is merely a convention.

convenience, we introduce the shorthand

$$\Delta\gamma = \gamma^{\rm UV} - \gamma^{\rm IR}\,. \tag{3.11}$$

The appearance of both kinds of anomalous dimensions stems from the fact that there is a single dimensional-regularization parameter, $\epsilon = \epsilon_{\rm UV} = \epsilon_{\rm IR}$, and single scale, $\mu = \mu_{\rm UV} = \mu_{\rm IR}$, for both the UV and IR divergences. As usual we take $\epsilon = (4-D)/2$.

The perturbative expansion of the different quantities we consider is denoted by

$$\begin{aligned} F_i &= F_i^{(0)} + F_i^{(1)} + F_i^{(2)} + \cdots\,, \\ A_i &= A_i^{(0)} + A_i^{(1)} + A_i^{(2)} + \cdots\,, \\ \gamma_{ij} &= \gamma_{ij}^{(1)} + \gamma_{ij}^{(2)} + \cdots\,, \\ \beta &= \beta^{(1)} + \beta^{(2)} + \cdots\,, \end{aligned} \tag{3.12}$$

where each order in the expansion includes an additional power of the dimension-four couplings, $g^{(4)}$, as defined in Eq. (3.5), compared to the previous order. Since the operators we consider here have a least four fields, except for the F^3 case, any of the generated four-point tree amplitudes are local, and directly correspond to the operator. The amplitudes generated by the F^3 operator also contain a vertex obtained from the dimension-four operators. Thus, the four-point tree amplitudes have no powers of $g^{(4)}$, with the exception of the four-point amplitudes generated from the F^3 operator.

3.2.2 Anomalous dimensions from UV divergences

Anomalous dimensions are traditionally extracted from countertems associated to UV divergences. For instance, in Refs. [4] the full one-loop anomalous dimension matrix of the SMEFT was calculated by extracting the $1/\epsilon$ divergences of the one-particle irreducible (1PI) diagrams that generate the one-loop effective action in the background field method. Alter-

natively, one might extract the anomalous dimensions from on-shell amplitudes. Here, we use the full one-loop amplitudes to calculate the one-loop anomalous dimension matrix of our model, and thereby verify a representative set of the anomalous dimensions calculated in Refs. [4].

An efficient way of determining UV divergences at one loop was presented for the β-function in Ref. [38]. Here we adopt this method to calculate one-loop anomalous dimensions. In general, the renormalization of $\mathcal{O}_i$ by $\mathcal{O}_j$ at one loop is determined by calculating the matrix element with external particles corresponding to $\mathcal{O}_i$, but with an insertion of $\mathcal{O}_j$. In general, one-loop matrix elements can be expressed in terms of a basis of scalar integrals

$$A_i^{(1)} = \sum_s a^s_{4,\,i}\, I_{4,s} + \sum_s a^s_{3,\,i} I_{3,s} + \sum_s a^s_{2,\,i} I_{2,s}\,, \tag{3.13}$$

comprised of boxes $I_{4,s}$, triangles, $I_{3,s}$, and bubbles, $I_{2,s}$, where the corresponding coefficients, a_i^s, b_i^s and c_i are gauge invariant and generically depend on color and the dimensional regularization parameter ϵ. The integrals can then be expanded in ϵ, producing both UV and IR poles in ϵ. Only the scalar bubble integrals contain UV divergences, so we write a formula for the anomalous dimensions in terms of the bubble coefficients $a^s_{2,\,i}$, whose ϵ dependence can be ignored for this purpose. However, some care is required because of cancellations between UV and IR divergences. We delay a detailed discussion of the infrared structure of the amplitudes to Section 3.3. For the moment, we just recall that the $1/\epsilon$ pole in the bubble integrals in Eq. (3.13) does not contain the full UV divergence of the amplitude. The reason for this is that there is an additional $1/\epsilon$ pole which originates in bubble-on-external-leg diagrams, which are scaleless and set to zero in dimensional regularization because of a cancellation of UV and IR poles,

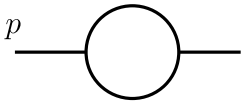

$$\Big|_{p^2=0} \quad \propto \frac{1}{\epsilon_{UV}} - \frac{1}{\epsilon_{IR}} + \log\frac{\mu^2_{UV}}{\mu^2_{IR}}\,. \tag{3.14}$$

Hence the bubbles on external legs give an additional UV contribution,

$$-\frac{1}{2\epsilon}\gamma_{\rm c}^{\rm IR\,(1)}A_i^{(0)} := -\frac{1}{2\epsilon}\sum_p \gamma_{{\rm c},\,p}^{\rm IR}A_i^{(0)}\,, \tag{3.15}$$

where γ_p^c is the so-called collinear anomalous dimension of particle p, and the sum is over all external states of the tree amplitude. For the vectors, fermions and scalars in our theory the collinear anomalous dimensions are given by [39]

$$\gamma_{{\rm c},\,v}^{\rm IR\,(1)} = -\tilde{g}^2 b_0\,, \quad \gamma_{{\rm c},\,f}^{\rm IR\,(1)} = -\tilde{g}^2 3C_F\,, \quad \gamma_{{\rm c},\,s}^{\rm IR\,(1)} = -\tilde{g}^2 4C_F\,, \tag{3.16}$$

where $b_0 = (11N - 2N_f - N_s/2)/3$ is the coefficient in the one-loop β-function of g, and $C_F = (N^2-1)/2N$ is the Casimir of the fundamental representation. While we only consider one flavor of scalar in our model, we include the parameter N_s in the β-function and elsewhere to track contributions from scalar loops.

In addition, there are contributions to the $1/\epsilon$ UV pole proportional to the one-loop β-function of the dimension-four couplings, related to the renormalization of such couplings

$$\frac{1}{2\epsilon}(n - L_i)\tilde{\beta}^{(1)}A_i^{(0)}\,, \tag{3.17}$$

where $\tilde{\beta}^{(1)} = \beta^{(1)}/g^{(4)}$, n is the number of external states and L_i is the length of the operator $\mathcal{O}_i$, i.e., the number of fields it contains. We therefore conclude that the sum over bubble coefficients is related to the UV anomalous dimensions by

$$\frac{1}{(4\pi)^2}\sum_s a_{2\,,i}^s = -\frac{1}{2}\big[\gamma_{ij}^{UV} - \gamma_{\rm c}^{\rm IR}\delta_{ij} + (n - L_i)\tilde{\beta}^{(1)}\delta_{ij}\big]A_j^{(0)}\,. \tag{3.18}$$

Similar formulas have recently been used in Ref. [28]. There are multiple methods by which one might calculate these coefficients. We do so by using generalized unitarity. For the purposes of extracting the UV divergences, it suffices to evaluate four-dimensional cuts [7, 38].

However, we are interested in obtaining the full amplitudes, including rational terms, as a stepping stone towards calculating two-loop anomalous dimensions, so we use D-dimensional unitarity cuts as described in Section 3.3.

The approach we outlined is very powerful at one loop, but at higher loops becomes more difficult to use, because it requires two-loop integration. In particular, at higher loops simple decompositions of integrals along the lines of Eq. (3.13) do not exist. One might still construct the amplitudes using unitarity methods, and then extract their UV divergences by carrying out the loop integration, but one would like a simpler technique that avoids much of the technical complexity. Furthermore, to calculate two-loop divergences, one must also keep track of evanescent one-loop subdivergences, which contaminate the result. By an evanescent subdivergence we mean a subdivergence whose corresponding counterterm vanishes in strictly four dimensions, but which cannot be ignored in dimensional regularization (see e.g. Ref. [40, 41]). While not physical, these evanescent subdivergences greatly complicate higher-loop calculations, and it is better to use a method that avoids them, whenever possible. Ref. [16] gives a nontrivial two-loop example for Einstein gravity showing how on-shell methods can efficiently bypass evanescent effects [15] to determine renormalization-scale dependence.

3.2.3 Anomalous dimensions directly from unitarity cuts

A much more direct way to obtain anomalous dimensions is to focus on the renormalization-scale dependence encoded in the logarithms, and not on the divergences. The logarithms are detectable in four-dimensional unitarity cuts. Any dimensional imbalance in the kinematic arguments of the logarithms must be balanced by renormalization-scale dependence, so one can directly determine the renormalization-scale dependence and any anomalous dimensions by collecting the contributions from unitarity cuts. For example, this strategy has been used to greatly simplify the extraction of the two-loop renormalization-scale dependence in Einstein gravity [16].

The formalism of Caron-Huot and Wilhelm [12] gives a rather neat way to carry out this strategy , allowing us to extract the anomalous dimension at L-loops directly from phase-space integrals of lower-loop on-shell form factors and amplitudes. Among other useful features, this makes potential zeros in the anomalous dimension matrix much more transparent than with conventional methods [8].

By considering the analyticity of the form factors with respect to complex shifts in momenta, along with unitarity, Caron-Huot and Wilhelm derived the following compact equation:

$$e^{-i\pi D} F_i^* = S\, F_i^* \,, \tag{3.19}$$

which relates the phase of the S-matrix, S, to the dilatation operator, D (ignoring trivial overall engineering dimensions). The dilation operator acts on the conjugate form factor F_i^*. Writing $S = 1 + i\mathcal{M}$, Eq. (3.19) can be rewritten more practically as

$$(e^{-i\pi D} - 1) F_i^* = i\mathcal{M} F_i^* \,, \tag{3.20}$$

where the scattering amplitude, $\mathcal{M}$, acts as a matrix on the form-factor, yielding its imaginary part via the optical theorem[4]. The right-hand side of this equation is defined to be a unitarity cut. As we discuss below, this equation precisely captures the notion that the scale dependence of F_i is encoded in the coefficients of its logarithms. We note that the use of the complex conjugate form factor, F^*, only affects the imaginary part, which do not affect our calculations through two loops. Therefore, we drop the complex conjugation henceforth.

In dimensional regularization, the dilatation operator is related to the single renormalization scale, μ, as $D = -\mu\partial_\mu$, reflecting the fact that F_i can only depend on dimensionless ratios s_{ij}/μ (ignoring the overall engineering dimensions), and that logarithms in s_{ij} kinematic variables must be balanced either by μ or by each other. The dilatation operator then

[4]In our notation the optical theorem states, $2\mathrm{Im}F_i^* = \mathcal{M}F_i^*$ for form factors or $2\mathrm{Im}\mathcal{M} = \mathcal{M}\mathcal{M}$ for amplitudes.

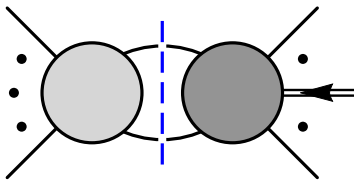

Figure 3.1: Unitarity cut relevant for the extraction of anomalous dimensions from one-loop form factors. The darker blobs indicate a higher-dimension operator insertion. The double-lined arrow indicates the insertion of additional off-shell momentum from the operator. The dashed line indicates the integral over phase space of the particles crossing the cut.

acts on the form factors as

$$DF_i = -\mu\partial_\mu F_i = \left[\Delta\gamma_{ij} + \delta_{ij}\beta\,\partial\right] F_j, \tag{3.21}$$

where we have used the renormalization-group equation (3.10). This, together with equation (3.19), gives us a powerful means to extract anomalous dimensions.

While Eqs. (3.19) and (3.21) are valid non-perturbatively, we can expand in perturbation theory to obtain order-by-order expressions for the anomalous dimensions. At one loop the expansion yields

$$\left[\Delta\gamma_{ij}^{(1)} + \delta_{ij}\beta^{(1)}\partial\right] F_j^{(0)} = -\frac{1}{\pi}(\mathcal{M}F_i)^{(1)}\,, \tag{3.22}$$

where the superscript denotes the order in perturbation theory. On the right-hand side $(\mathcal{M}F_i)^{(1)}$ indicates

$$(\mathcal{M}F_i)^{(1)} = \sum_{k=2}^{n}\sum_{c}(\mathcal{M}_{k\to 2}^{c})^{(0)} \otimes F_{n-k+2\,,i}^{(0)}\,, \tag{3.23}$$

where the sums are over all kinematic channels and the $\otimes$ denotes a sum over intermediate two-particle states in the product. For a given kinematic channel this is given by the Lorentz-

invariant phase-space integral

$$
\begin{aligned}
(\mathcal{M}^{1\cdots k}_{k\to 2})^{(0)} \otimes F^{(0)}_{n-k+2\,,i} &= \sum \int d\mathrm{LIPS}_2 \sum_{h_1,h_2} \langle 1\cdots k|\mathcal{M}|\ell_1^{h_1}\ell_2^{h_2}\rangle^{(0)} \langle \ell_1^{h_1}\ell_2^{h_2}\cdots n|\mathcal{O}_i|0\rangle^{(0)} \\
&= \sum \int d\mathrm{LIPS}_2 \sum_{h_1,h_2} A^{(0)}(1,\cdots,k,-\ell_1^{-h_1},-\ell_2^{-h_2}) F_i^{(0)}(\ell_1^{h_1},\ell_2^{h_2},\cdots,n)\,,
\end{aligned}
\tag{3.24}
$$

where the sum over helicities also includes a sum over different states crossing the cut. In summary, $(\mathcal{M}F_i)^{(1)}$ corresponds to a sum over all one-loop two-particle unitarity cuts, as depicted schematically in Figure 3.1.

After rewriting the expression in terms of four-dimensional spinors, the two-particle phase-space integrals can be easily evaluated following the discussion of Ref. [12],

$$
\begin{pmatrix} \lambda_1' \\ \lambda_2' \end{pmatrix} = \begin{pmatrix} \cos\theta & -\sin\theta\ e^{i\phi} \\ \sin\theta\ e^{-i\phi} & \cos\theta \end{pmatrix} \begin{pmatrix} \lambda_1 \\ \lambda_2 \end{pmatrix}, \tag{3.25}
$$

where the λ_i and $\tilde{\lambda}_i = \lambda_i^*$ spinors depend on the momenta of the external legs and the λ_i' and $\tilde{\lambda}_i' = \lambda_i'^*$ spinors on the momenta of the cut legs. With this parametrization the integration measure is simply,

$$
\int d\mathrm{LIPS}_2 \equiv \frac{1}{16\pi} \int_0^{2\pi} \frac{\mathrm{d}\phi}{2\pi} \int_0^{\frac{\pi}{2}} 2\cos\theta\sin\theta \mathrm{d}\theta\,. \tag{3.26}
$$

In the definition of the phase-space measure, here we have included an additional symmetry factor of 1/2, relative to the usual volume of two-particle phase space, i.e., 8π. This is generally convenient but requires some care when non-identical particles cross the cut, where we will need to multiply by two to cancel the symmetry factor.

Next consider two loops. Expanding Eq. (3.20) through this order, we obtain

$$
\begin{aligned}
&\left[\Delta\gamma_{ij}^{(1)} + \delta_{ij}\beta^{(1)}\partial\right] F_j^{(1)} + \left[\Delta\gamma_{ij}^{(2)} + \delta_{ij}\beta^{(2)}\partial\right] F_j^{(0)} \\
&\qquad - i\pi\,\frac{1}{2}\left[\Delta\gamma_{ik}^{(1)} + \delta_{ik}\beta^{(1)}\partial\right]\left[\Delta\gamma_{kj}^{(1)} + \delta_{kj}\beta^{(1)}\partial\right] F_j^{(0)} = -\frac{1}{\pi}(\mathcal{M}F_i)^{(2)}\,.
\end{aligned}
\tag{3.27}
$$

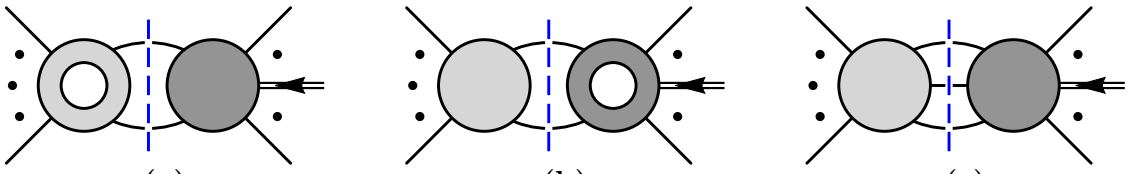

Figure 3.2: Unitarity cuts relevant for the extraction of anomalous dimensions from two-loop form factors, using the same notation as in Figure 3.1. The darker blobs indicate a higher-dimension operator insertion. The blobs with a hole indicate a one-loop form factor or amplitude.

On the right-hand side of this equation, $(\mathcal{M}F_i)^{(2)}$ denotes collectively the three two-loop unitarity cuts displayed in Figure 3.2,

$$(\mathcal{M}F_i)^{(2)} = \sum_{k=2}^{n} \sum_{c} \Big[(\mathcal{M}^c_{k\to 2})^{(1)} \otimes F^{(0)}_{n-k+2\,,i} + (\mathcal{M}^c_{k\to 2})^{(0)} \otimes F^{(1)}_{n-k+2\,,i} + (\mathcal{M}^c_{k\to 3})^{(0)} \otimes F^{(0)}_{n-k+3\,,i} \Big] . \tag{3.28}$$

In the first term we find two-particle cuts composed of the one-loop amplitude and the tree-level higher-dimension form factor depicted in Figure 3.2(a). These are

$$\begin{aligned} (\mathcal{M}^{1\cdots k}_{k\to 2})^{(1)} \otimes F^{(0)}_{n-k+2\,,i} &= \int d\mathrm{LIPS}_2 \sum_{h_1,h_2} \langle 1\cdots k|\mathcal{M}|\ell_1^{h_1}\ell_2^{h_2}\rangle^{(1)} \, \langle \ell_1^{h_1}\ell_2^{h_2}\cdots n|\mathcal{O}_i|0\rangle^{(0)} \\ &= \int d\mathrm{LIPS}_2 \sum_{h_1,h_2} A^{(1)}(1,\cdots,k,-\ell_1^{-h_1},-\ell_2^{-h_2})\, F_i^{(0)}(\ell_1^{h_1},\ell_2^{h_2},\cdots,n)\,. \end{aligned} \tag{3.29}$$

Similarly, the second term, shown in Figure 3.2(b), is a combination of cuts composed by the tree-level amplitude and the one-loop higher-dimension operator, which are

$$\begin{aligned} (\mathcal{M}^{1\cdots k}_{k\to 2})^{(0)} \otimes F^{(1)}_{n-k+2\,,i} &= \int d\mathrm{LIPS}_2 \sum_{h_1,h_2} \langle 1\cdots k|\mathcal{M}|\ell_1^{h_1}\ell_2^{h_2}\rangle^{(1)} \, \langle \ell_1^{h_1}\ell_2^{h_2}\cdots n|\mathcal{O}_i|0\rangle^{(0)} \\ &= \int d\mathrm{LIPS}_2 \sum_{h_1,h_2} A^{(0)}(1,\cdots,k,-\ell_1^{-h_1},-\ell_2^{-h_2})\, F_i^{(1)}(\ell_1^{h_1},\ell_2^{h_2},\cdots,n)\,. \end{aligned} \tag{3.30}$$

Finally, the third term is composed of three-particle cuts involving two tree-level objects, as

in Figure 3.2(c)

$$(\mathcal{M}^{1\cdots k}_{k\to 3})^{(0)} \otimes F^{(1)}_{n-k+3\,,i} = \int d\mathrm{LIPS}_3 \sum_{h_1,h_2,h_3} \langle 1\cdots k|\mathcal{M}|\ell_1^{h_1}\ell_2^{h_2}\ell_3^{h_3}\rangle^{(0)} \langle \ell_1^{h_1}\ell_2^{h_2}\ell_3^{h_3}\cdots n|\mathcal{O}_i|0\rangle^{(0)}$$
$$= \int d\mathrm{LIPS}_3 \sum_{h_1,h_2,h_3} A^{(0)}(1,\cdots,k,-\ell_1^{-h_1},-\ell_2^{-h_2},-\ell_3^{-h_3}) F_i^{(0)}(\ell_1^{h_1},\ell_2^{h_2},\ell_3^{h_3},\cdots,n)\,. \tag{3.31}$$

A parameterization analogous to (3.25) for the three-particle cut is given in Ref. [12]. We will not evaluate any three-particle cuts in the present work, so we refer the reader to this work for more details.

We can rearrange Eq. (3.27) to put it into a more convenient form for extracting two-loop anomalous dimensions. First, note that the imaginary part of Eq. (3.27)

$$-i\pi\,\frac{1}{2}\left[\Delta\gamma^{(1)}_{ik} + \delta_{ik}\beta^{(1)}\partial\right]\left[\Delta\gamma^{(1)}_{kj} + \delta_{kj}\beta^{(1)}\partial\right] F_j^{(0)} = -\frac{1}{\pi}\mathrm{Im}(\mathcal{M}F_i)^{(2)}\,, \tag{3.32}$$

does not feature the two-loop anomalous dimensions. Using the optical theorem again, we write its right-hand side in terms of unitarity cuts

$$\mathrm{Im}(\mathcal{M}F_i)^{(2)} = (\mathcal{M}\mathcal{M}F_i)^{(2)}\,, \tag{3.33}$$

where the relevant cuts are the iterated two-particle cuts in Fig. 3.3. For instance $(\mathcal{M}\mathcal{M}F_i)^{(2)}$ contains terms of the form

$$\int d\mathrm{LIPS}_2 d\mathrm{LIPS}'_2 \sum_{h_1,h_2}\sum_{h'_1,h'_2} \langle\cdots|\ell_1^{h_1}\ell_2^{h_2}\rangle^{(0)} \langle \ell_1^{h_1}\ell_2^{h_2}\cdots|\ell_{1'}^{h'_1}\ell_{2'}^{h'_2}\rangle^{(0)} \langle \ell_{1'}^{h'_1}\ell_{2'}^{h'_2}\cdots|\mathcal{O}_i|0\rangle^{(0)}\,, \tag{3.34}$$

which correspond to cuts of the type in Fig. 3.3(a). Note that Eq. (3.33) does not include a factor of 1/2 from the optical theorem because the imaginary part can arise from cutting either the one-loop amplitude or form factor, which give identical contributions.

Eq. (3.32) does not contain the two-loop anomalous dimensions but instead captures the

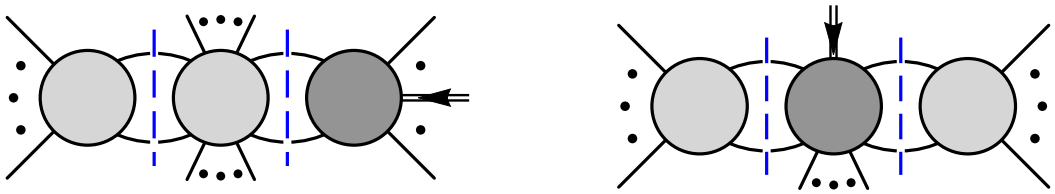

Figure 3.3: Iterated two-particle cuts that appear on the right-hand side of Eq. (3.33).

exponentiation of one-loop anomalous dimensions and the associated logarithms. Nonetheless (3.33) can be used to simplify the real part of Eq. (3.27), which yields

$$\begin{aligned}\left[\Delta\gamma_{ij}^{(1)}+\delta_{ij}\beta^{(1)}\partial\right]\mathrm{Re}F_j^{(1)}+\left[\Delta\gamma_{ij}^{(2)}+\delta_{ij}\beta^{(2)}\partial\right]F_j^{(0)} \\ =-\frac{1}{\pi}\mathrm{Re}(\mathcal{M}F_i)^{(2)}=-\frac{1}{\pi}(\mathcal{M}F_i-\mathcal{M}\mathcal{M}F_i)^{(2)}\,.\end{aligned} \tag{3.35}$$

Note that the right-hand side can be rewritten using

$$(\mathcal{M}F_i-\mathcal{M}\mathcal{M}F_i)^{(2)}=\left[\left(\mathcal{M}-\frac{1}{2}\mathcal{M}\mathcal{M}\right)\left(F_i-\frac{1}{2}\mathcal{M}F_i\right)\right]^{(2)}=[\mathrm{Re}(\mathcal{M})\mathrm{Re}(F_i)]^{(2)}\,, \tag{3.36}$$

and with this we arrive at

$$\left[\Delta\gamma_{ij}^{(1)}+\delta_{ij}\beta^{(1)}\partial\right]\mathrm{Re}F_j^{(1)}+\left[\Delta\gamma_{ij}^{(2)}+\delta_{ij}\beta^{(2)}\partial\right]F_j^{(0)}=-\frac{1}{\pi}\left[\mathrm{Re}(\mathcal{M})\mathrm{Re}(F_i)\right]^{(2)}\,. \tag{3.37}$$

We use this equation to extract two-loop anomalous dimensions. In practice Eq. (3.37) simply instructs us to drop the imaginary parts of the one-loop matrix elements when calculating the cuts in Figs. 3.2(a) and 3.2(b). On the left-hand side, we now see the appearance of one-loop anomalous dimensions and the β-function, as well as the one-loop form factor $F_i^{(1)}$. The two-loop UV anomalous dimension $\gamma_{ij}^{\mathrm{UV}(2)}$ contained in $\Delta\gamma_{ij}^{(2)}$ is the object of interest, but to extract it we first need to remove $\gamma_{ij}^{\mathrm{IR}(2)}$, which requires an understanding of the IR singularities, which we discuss below.

Simplifying strategies

A strategy that greatly simplifies the analysis is to choose an external state with the minimal number of external legs that is sensitive to the operator of interest, i.e. select the operator's minimal form factor. In this way we can avoid terms of the form $\beta^{(n)}\partial F_i^{(0)}$ in Eqs. (3.27) and (3.37), since, under this choice, $F_i^{(0)}$ is local, and thus does not depend on the dimension-four couplings, $g^{(4)}$. This strategy was used in Ref. [8] to prove nonrenormalization theorems at the first loop order where diagrams exist.

More generally, the β-function can no longer be eliminated by using minimal form factors whenever the one-loop form factor with an $\mathcal{O}_i$ insertion, $F_i^{(1)}$, produces a nonzero result with the chosen external states. In addition, the β-function acting on the one-loop anomalous-dimension matrix is nonzero if the matrix elements themselves are nonzero. For example, to determine the renormalization of $\mathcal{O}_{F^3}$ by itself at two loops, we would evaluate Eq. (3.37) with the external state $\langle 1^+2^+3^+|$. In this case the term $\beta^{(2)}\partial F_{F^3}^{(0)}$ would vanish, though the term $\beta^{(1)}\partial F_{F^3}^{(1)}$ would remain.

Unlike the β-function, the IR anomalous dimensions are non-trivial to eliminate. Ref. [12] removes them by subtracting, at the integrand level, form factors of global symmetry currents, such as the stress-tensor, which are UV finite but contain the same IR divergences. Alternatively, one can use the same on-shell methods to calculate them and subtract them after integration. At one loop, the structure of infrared divergences is well understood [42–44], and it is straightforward to subtract them after integration. We explain how to carry this out at the level of the amplitudes in the next section. Furthermore, whenever we are interested in a leading off-diagonal element of the anomalous dimension matrix, the IR anomalous dimensions does not appear, since the infrared divergences are diagonal in the operators (excluding color).

Finally, form factors are useful for operators with only two or three external fields, since they allow nonzero results when kinematics would otherwise set amplitudes with fewer than

four external particles to zero. Here we generally set the operator momentum insertion $q = 0$ and work in terms of amplitudes whenever possible, i.e. whenever there are four or more external states.

3.2.4 Comments on evanescent operators

When extracting anomalous dimensions from UV divergences in dimensional regularization one must carefully keep track of evanescent operators [40, 41]. These operators are non-trivial in D-dimensions, but whose matrix elements vanish for any choice of external four-dimensional states. In the context of the SMEFT an example of an evanescent operator would be the Lorentz–Fierz identities

$$\begin{aligned}\mathcal{O}_{\text{Fierz,L}} &= (\bar{\psi}_L^m \gamma^\mu \psi_L^n)(\bar{\psi}_L^p \gamma_\mu \psi_L^r) + (\bar{\psi}_L^p \gamma^\mu \psi_L^n)(\bar{\psi}_L^m \gamma_\mu \psi_L^r)\,, \\ \mathcal{O}_{\text{Fierz,R}} &= (\bar{\psi}_R^m \gamma^\mu \psi_R^n)(\bar{\psi}_R^p \gamma_\mu \psi_R^r) + (\bar{\psi}_R^p \gamma^\mu \psi_R^n)(\bar{\psi}_R^m \gamma_\mu \psi_R^r)\,,\end{aligned} \tag{3.38}$$

(where we raised the flavor indices for convenience) which are identically zero in four but not in arbitrary dimensions. More generally one can easily construct such operators by antisymmetrizing over five or more Lorentz indices. In the context of our model, an example of such an evanescent operator is

$$(\bar{\psi}\gamma_{[\alpha}\gamma_\mu\gamma_\nu\gamma_\sigma\gamma_{\rho]}\psi)(\bar{\psi}\gamma^{[\alpha}\gamma^\mu\gamma^\nu\gamma^\sigma\gamma^{\rho]}\psi)\,. \tag{3.39}$$

One-loop diagrams might contain a $1/\epsilon$ divergence proportional to the matrix element of an evanescent operator. While this does not affect one-loop anomalous dimensions because we can take the external states to be four-dimensional, when inserted in a higher-loop diagram in the context of dimensional regularization such evanescent operators are activated and can generate both UV divergent and finite contributions. In fact, they are needed to properly subtract subdivergences. These effects must be taken into account in order to

correctly extract two-loop UV divergences and their associated anomalous dimension. In practice we can deal with the effects of evanescent operators [40, 41], but the number of them grows with dimension and loop order (especially in the presence of fermions). For this reason it would be desirable to avoid them when possible, since they are a technical complication due to the use of dimensional regularization, and ultimately we would expect that they do not affect the physics [15].

We expect the on-shell methods presented above to completely sidestep the issue of evanescent operators when obtaining anomalous dimension, at least through two loops. Ref. [16] provides a nontrivial demonstration that complications from evanescent operators can be completely sidestepped using on-shell methods and by focusing on renormalization-scale dependence instead of divergences. In the two-loop formulas used here, anomalous dimensions and associated logarithms are given directly in terms of four-dimensional unitarity cuts of tree and one-loop objects. This automatically eliminates most of the evanescent dependence, except for finite shifts in one-loop matrix elements with evanescent operator insertions. We expect that any remaining evanescent dependence in the one-loop amplitudes or form factors to be eliminated by finite renormalizations [41]. Given the usual subtleties of dealing with evanescent operators, it would, of course, be important to explicitly verify that including or not including evanescent operators in the one- and two-loop anomalous dimension matrix amounts to a scheme choice.

3.2.5 Anomalous dimensions and non-interference

As noted in Ref. [45] helicity selection rules imply the non-interference of SMEFT tree-level matrix elements when constructing cross sections. This has important consequences in the context of the SMEFT, where the possibility of measuring the coefficient of higher-dimension operators at colliders can be impacted by the vanishings in the interference of the Standard-Model tree amplitudes and those of higher-dimension operators, when computing

cross sections. A connection between one-loop anomalous dimension and interference terms can be seen in Eq. (3.22), where, upon setting $q = 0$, the form factors become amplitudes and the right-hand side directly captures the interference of tree-level dimension-four and dimension-six amplitudes. Note that this holds even when the anomalous dimension is not zero, in which case this equation relates the interference terms to simpler objects, namely the one-loop anomalous dimensions and tree-level matrix elements. Of course, in a realistic cross-section calculation one would not integrate over the full phase space, due to experimental cuts.

At two loops the connection between zeros in the anomalous dimensions and non-interference is not as direct, since it requires cancellations between both sides of Eq. (3.27). Eq. (3.32) shows that, in general, the imaginary part of the interference term is given by the square of one-loop anomalous dimensions times tree-level matrix elements. Instead of non-interference, Eq. (3.35) shows that a vanishing two-loop anomalous dimension would imply that the real part of interference term is simply is related to the product of one-loop anomalous dimensions and one-loop matrix elements. It would be interesting to further investigate the consequences stemming from these observations, even in the presence of experimental cuts.

3.3 One-loop amplitudes and anomalous dimensions

In this section we describe our generalized unitarity calculation of the one-loop amplitudes with an insertion of a higher-dimensional operator in our simplified model. We then extract the one-loop anomalous dimension matrix of this theory. Finally, we comment on the structure of rational terms in the amplitudes and on the ability to set some of them to zero with a judicious scheme choice. The results in this section are building blocks needed for the two-loop analysis in the next section. In addition, they provide one-loop anomalous dimensions that can be cross-checked against those in Refs. [4].

3.3.1 One-loop amplitudes from generalized unitarity

The generalized unitarity method [11, 29, 30] for constructing one-loop amplitudes can be found in various reviews, for example see Ref. [46], but here we briefly review the procedure for the one-loop case. To construct the full one-loop amplitudes to all orders in the dimensional-regularization parameter ϵ, we begin with the D-dimensional four-point tree-level amplitudes with or without insertions of the dimension-6 operators (given in Appendix 3.B). By using D-dimensional tree amplitudes, we ensure that the cuts appropriately capture the coefficients of the D-dimensional box, triangle, and bubble scalar integrals that form a basis for the full one-loop amplitudes, as in Eq. (3.13). In general, the coefficients have ϵ dependence, and expanding in ϵ produces rational terms that would not automatically be included if a purely four-dimensional approach to the cuts were used [11]. Besides ϵ, the coefficients only depend on the Mandelstam invariants $s = (k_1 + k_2)^2$, $t = (k_2 + k_3)^2$ and $u = (k_1 + k_3)^2$.

We construct the cuts in the standard way. For example, the integrand-level s-channel cut with an $\mathcal{O}_n$ operator insertion is given by

$$\begin{aligned}
&\sum_i \mathcal{C}^{[i]} \left(\left[a^{st}_{4,n[i]} I_{4,st} + a^{su}_{4,n[i]} I_{4,su} + a^{s}_{3,n[i]} I_{3,s} + a^{s}_{2,n[i]} I_{2,s} \right] \Big|_{\ell^2=0} \right) \\
&\quad = \sum_{\text{states}} \sum_j \mathcal{C}^{[j]} A^{(0)}_n(1, 2, \ell_1^{h_1}, \ell_2^{h_2})_{[j]} \sum_k \mathcal{C}^{[k]} A^{(0)}(-\ell_2^{h_2}, -\ell_1^{h_1}, 3, 4)_{[k]} \\
&\qquad + \sum_{\text{states}} \sum_j \mathcal{C}^{[j]} A^{(0)}(1, 2, \ell_1^{h_1}, \ell_2^{h_2})_{[j]} \sum_k \mathcal{C}^{[k]} A^{(0)}_n(-\ell_2^{h_2}, -\ell_1^{h_1}, 3, 4)_{[k]} \,,
\end{aligned} \tag{3.40}$$

where the sum over states includes the helicity and the color, and, for this case, $\ell_2 = -(\ell_1 + k_1 + k_2)$. The $\mathcal{C}^{[i]}$ are the appropriate color factors for the associated amplitudes. Since the cut legs are on-shell, where $\ell_1^2 = \ell_2^2 = 0$. Often, the external particles will restrict $A^{(0)}_n$ to be nonzero only for certain cuts or placements within the cuts, depending on the field content of the operator inserted.

As an example, the cuts of the amplitude $A^{(1)}_{F^3}(1_\psi 2_{\bar{\psi}} 3\, 4)$, are shown in Figure 3.4, where

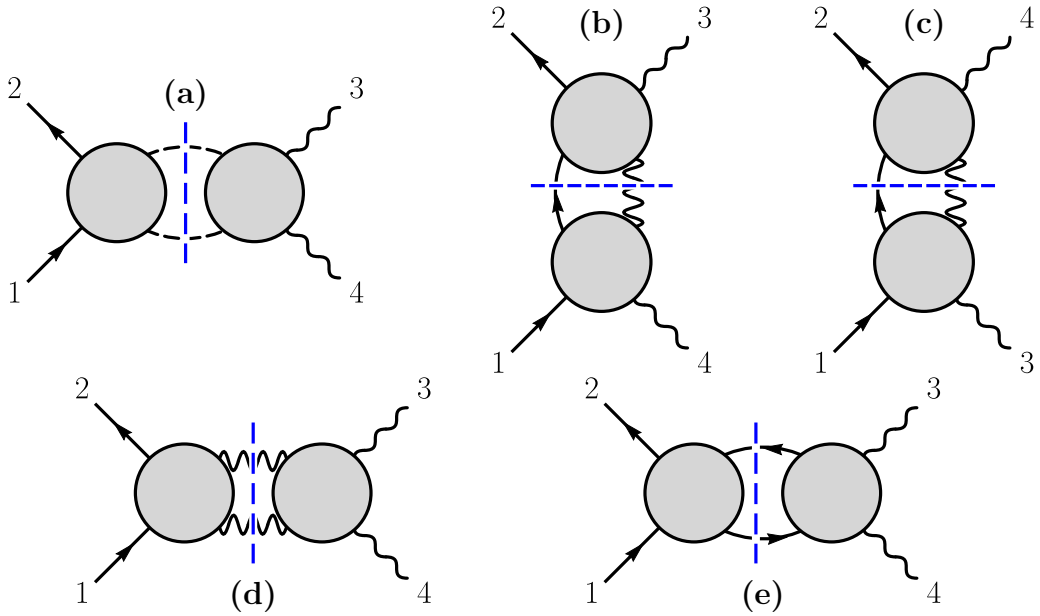

Figure 3.4: The necessary cuts for constructing a two-fermion, two-vector amplitude. For an amplitude with an insertion of a higher-dimension operator, one should insert the operator into either side of the diagrams when possible. The wavy lines are vector bosons, the lines with arrows fermions and the dashed lines scalars.

the operator $\mathcal{O}_{F^3}$ should be inserted on either side of the cuts, when the tree amplitudes exist. Other amplitudes with four-point operators require only the cuts corresponding to their correct external particles. The color factors $\mathcal{C}^{[j]}\mathcal{C}^{[k]}$ can be reduced to the appropriate color basis of the full amplitude, $\mathcal{C}^{[i]}$, based on the external particles. Doing so determines the contribution from each color-decomposed cut.

We evaluate the cuts using the D-dimensional state sum completeness relations,

$$\begin{aligned} \epsilon_i^{*\mu} \odot \epsilon_i^{\nu} &= \sum_{\text{states } h} \epsilon_i^{*(h)\mu} \epsilon_i^{(h)\nu} = -g^{\mu\nu} + \frac{q^\mu k_i^\nu + k_i^\mu q^\nu}{q \cdot k_i}\,, \\ \bar{u}_i \odot u_i &= \sum_{\text{states } h} \bar{u}_i^{(h)} u_i^{(h)} = \not{k}_i\,, \end{aligned} \tag{3.41}$$

where q is an arbitrary reference vector with $q^2 = 0$.

The next task is to merge the cuts and to integrate. One can merge the cuts at the level of the integrand to find a single integrand that has the correct cuts in all channels. However,

is it is generally simpler to merge the integrated results from each cut, treating each cut as an off-shell object, but dropping contributions that do not have a cut in the given channel. Integration is done by projecting each cut for a given process onto a basis of gauge-invariant tensors, as described in more detail in Appendix 3.A. Although the methods we use to extract anomalous dimensions do not require us to keep track of evanescent divergences, because the projection technique is fully D dimensional, we track them and confirm that they do not enter our calculations of various entries in the two-loop anomalous-dimension matrix. An alternative is to use spinor-helicity methods [47] which are much more powerful when the number of external legs increases. These have been successfully used for both chiral [29] and higher-loop calculations [48], but then additional care is needed to deal with subtleties that arise from using dimensional regularization.

After projection, the cut integrand is rewritten in terms of inverse propagators. We reduce the remaining integrals to the basis of scalar integrals in Eq. (3.13) using integration by parts relations as implemented in FIRE [33]. Cut merging is then straightforward, as the coefficients of integrals in the merged amplitude can be read directly off the results from each cut, summed over the possible particles crossing the cut. For example, the s-channel cut in Eq. (3.40) yields the coefficients of the s-channel bubble and triangle, as well as those of the (s,t) and (s,u) boxes in Eq. (3.13).

The full set of D-dimensional four-point one-loop amplitudes for the dimension-six operators in our model are given in the ancillary file [34]. These expressions are valid to all orders in ϵ, but to obtain the finite, renormalized expressions needed to feed into our calculation of two-loop anomalous dimensions, we need to subtract the UV poles.

The one-loop amplitudes are IR divergent. The IR singularities of gauge theories are well understood [39, 42–44], and can be expressed in terms of lower-loop amplitudes involving the same operator insertion and external particles. The explicit form of the one-loop infrared

singularity, for example, is given by

$$A_i^{(1)} = \boldsymbol{I}^{(1)} A_i^{(0)} \,, \tag{3.42}$$

where the IR operator $\boldsymbol{I}^{(1)}$ is given by [39, 42, 43][5]

$$\boldsymbol{I}^{(1)} = \frac{e^{\epsilon\gamma_E}}{\Gamma(1-\epsilon)} \sum_{p=1}^{n} \sum_{q\neq p} \frac{\boldsymbol{T}_p \cdot \boldsymbol{T}_q}{2} \left[\frac{\gamma_{\text{cusp}}^{\text{IR}\,(1)}}{\epsilon^2} - \frac{\gamma_{\text{c},\,p}^{\text{IR}\,(1)}}{\boldsymbol{T}_p^2} \frac{1}{\epsilon} \right] \left(\frac{-\mu^2}{2k_p \cdot k_q} \right)^{\epsilon} \,, \tag{3.43}$$

where the sums are over external particles. The color charge $\boldsymbol{T}_p = \{T_p^a\}$ is a vector with respect to the generator label a and a SU(N) matrix with respect to the outgoing particle p. The infrared divergence includes a $1/\epsilon^2$ pole, with coefficient given by the cusp anomalous dimension $\gamma_{\text{cusp}}^{\text{IR}\,(1)} = 4\tilde{g}^2$, and $1/\epsilon$ poles, with coefficient given by the collinear anomalous dimension of particle p given in Eq. (3.16). By obtaining the IR dependence of the one-loop amplitudes from Eq. (3.42), we can subtract it from the full one-loop amplitudes. As always, the definition of the IR-divergent parts carries with it some arbitrariness as to which finite pieces are included.[6]

The remaining poles in ϵ are UV poles, which we then match to the appropriate tree-level counterterm amplitude containing an insertion of the operator $\mathcal{O}_j$. A complication is that there can be multiple operators corresponding to the same external particle content, but with different color structures. Therefore, in these cases the coefficient of a single color factor in the loop amplitude is insufficient for the purpose of determining the anomalous dimensions, and in principle all the color factors for the given process and operator insertion must be considered simultaneously. For example, the one-loop amplitude with an insertion of the $\mathcal{O}_{(D\varphi^2\psi^2)_2}$ operator and four external scalars determines the renormalization of both the $\mathcal{O}_{(D^2\varphi^4)_1}$ and the $\mathcal{O}_{(D^2\varphi^4)_2}$ operators, where the operators are given in Table 3.1.

In some cases the IR structure is trivial, e.g. when the IR anomalous dimensions are zero

[5]The difference with the formulas in those references is due to our normalization of the $SU(N)$ generators.
[6]In physical quantities this arbitrariness cancels between real emission and virtual contributions.

simply because there are no lower-loop amplitudes for a given operator and given external state. Our examples in Section 3.4 follow this pattern. For instance, in the example of $\mathcal{O}_{(D^2\varphi^4)_1}$ renormalizing $\mathcal{O}_{(\psi^4)_1}$ at two loops, there is no tree level or one-loop amplitude with an insertion of $\mathcal{O}_{(D^2\varphi^4)_1}$ which has an external state of four fermions, simply due to the lack of Feynman diagrams. Since the full IR dependence is proportional to lower-loop amplitudes, this implies there cannot be an IR divergence at two loops. This same reasoning underpinned the non-renormalization theorem in Ref. [8]. More generally, one needs to account for the infrared singularities.

3.3.2 One-loop UV anomalous dimensions

After subtracting the IR singularities, the only remaining $1/\epsilon$ poles in the amplitudes correspond to the desired one-loop anomalous dimensions,

$$
\begin{aligned}
\dot{c}_{F^3} &= \tilde{g}^2(12N - 3b_0)c_{F^3}\,, \\
\dot{c}_{(\varphi^2F^2)_1} &= \tilde{g}^2\left(-5c_{F_3} - \frac{(3N^2-7)+2Nb_0}{N}c_{(\varphi^2F^2)_1} + \frac{N^2-4}{N^2}c_{(\varphi^2F^2)_2}\right) \\
&\quad + \tilde{\lambda}\,4(1+N)c_{(\varphi^2F^2)_1}\,, \\
\dot{c}_{(\varphi^2F^2)_2} &= \tilde{g}^2\left(-Nc_{F^3} + 2c_{(\varphi^2F^2)_1} + \frac{2N^2-5-2Nb_0}{N}c_{(\varphi^2F^2)_2}\right) + \tilde{\lambda}\,4c_{(\varphi^2F^2)_2}, \\
\dot{c}_{(D^2\varphi^4)_1} &= \tilde{g}^2\left(\frac{3(N+1)}{N}c_{(D^2\varphi^4)_1} + \frac{2(N-2)(N_s+9)}{3N}c_{(D^2\varphi^4)_2} + \frac{4}{3}\frac{N-2}{N}c^{ww}_{(D\varphi^2\psi^2)_2}\right) \\
&\quad + \lambda\,12c_{(D^2\varphi^4)_1}\,, \\
\dot{c}_{(D^2\varphi^4)_2} &= \tilde{g}^2\left(\frac{36NC_F-(2N-1)(N_s+9)}{3N}c_{(D^2\varphi^4)_2} + \frac{3(N-2)(N+1)}{2N}c_{(D^2\varphi^4)_1}\right. \\
&\quad \left. + \frac{2(2N-1)}{3N}c^{ww}_{(D\varphi^2\psi^2)_2}\right) + \tilde{\lambda}\,\left(2(N-2)c_{(D^2\varphi^4)_1} + 8(N+1)c_{(D^2\varphi^4)_2}\right), \\
\dot{c}^{pr}_{(D\varphi^2\psi^2)_1} &= 0\,, \\
\dot{c}^{pr}_{(D\varphi^2\psi^2)_2} &= \tilde{g}^2\left(\frac{1}{3}N_sc_{(D^2\varphi^4)_2}\delta_{pr} + \frac{1}{3}(-9N+N_s)c^{pr}_{(D\varphi^2\psi^2)_2} + \frac{4}{3}N_fc^{ww}_{(D\varphi^2\psi^2)_2}\delta_{pr}\right. \\
&\quad \left. - \frac{2}{3}N_fc^{pwwr}_{(\psi^4)_1} - \frac{2}{3}N_f\left(2c^{prww}_{(\psi^4)_2} - \frac{1}{N}c^{pwwr}_{(\psi^4)_2}\right)\right), \\
\dot{c}^{mnpr}_{(\psi^4)_1} &= \tilde{g}^2\frac{6\,(N^2-1)}{N^2}c^{mnpr}_{(\psi^4)_2}\,, \\
\dot{c}^{mnpr}_{(\psi^4)_2} &= \tilde{g}^2\left(-\frac{N_s}{3}(c^{mn}_{(D\varphi^2\psi^2)_2}\delta_{pr} + c^{pr}_{(D\varphi^2\psi^2)_2}\delta_{mn})\right. \\
&\quad + \frac{2}{3}N_f(\delta_{mn}c^{pwwr}_{(\psi^4)_1} + \delta_{pr}c^{mwwn}_{(\psi^4)_1}) + 6c^{mnpr}_{(\psi^4)_1} - \frac{3}{N}c^{mnpr}_{(\psi^4)_2} \\
&\quad \left. + \frac{2N_f}{3N}(2N(\delta_{pr}c^{mnww}_{(\psi^4)_2} + \delta_{mn}c^{prww}_{(\psi^4)_2}) - (\delta_{pr}c^{mwwn}_{(\psi^4)_2} + \delta_{mn}c^{pwwr}_{(\psi^4)_2}))\right)\,. \qquad (3.44)
\end{aligned}
$$

Here N_s is left as a parameter to track contributions from scalar loops. In our model it should be set to unity. These anomalous dimensions have been extracted directly from the

	F^3	$(\varphi^2F^2)_1$	$(\varphi^2F^2)_2$	$(D^2\varphi^4)_1$	$(D^2\varphi^4)_2$	$(D\varphi^2\psi^2)_1$	$(D\varphi^2\psi^2)_2$	$(\psi^4)_1$	$(\psi^4)_2$
F^3		0	0	$\emptyset$	$\emptyset$	$\emptyset$	$\emptyset$	$\emptyset$	$\emptyset$
$(\varphi^2F^2)_1$				0	0	0	0	$\emptyset$	$\emptyset$
$(\varphi^2F^2)_2$				0	0	0	0	$\emptyset$	$\emptyset$
$(D^2\varphi^4)_1$	0	0	0			0		$\emptyset$	$\emptyset$
$(D^2\varphi^4)_2$	0	0	0			0		$\emptyset$	$\emptyset$
$(D\varphi^2\psi^2)_1$	0	0	0	0	0	0	0	0	0
$(D\varphi^2\psi^2)_2$	0	0	0	0		0			
$(\psi^4)_1$	0	$\emptyset$	$\emptyset$	$\emptyset$	$\emptyset$	0	0	0	
$(\psi^4)_2$	0	$\emptyset$	$\emptyset$	$\emptyset$	$\emptyset$	0			

Table 3.2: Structure of the zeros in the one-loop anomalous dimension matrix. The $\emptyset$ entries indicate there are no contributing one-loop diagrams, whereas a 0 alone indicates that there are one-loop diagrams that could contribute, but actually give a vanishing result. The operators labeling the rows are renormalized by the operators labeling the columns.

scattering amplitudes, and, as a cross-check, we also used the unitarity cut method explained in the previous section [12] for computing directly the anomalous dimensions. The structure of the anomalous dimension matrix is summarized in Table 3.2. It is worth pointing out the simplicity in the renormalization and mixing of $(D\varphi^2\psi^2)_1$ and $(\psi^4)_1$, which is due to these operators being a product of global symmetry currents, which heavily constrains the kind of states they can overlap with. This is special in our model, which does not contain an Abelian gauge field. In the presence of the latter, the operators would be a product of gauge symmetry currents (just like $(D\varphi^2\psi^2)_2$ and $(\psi^4)_2$) which are renormalized [49], so the anomalous dimension matrix will receive contributions proportional to the Abelian gauge coupling.

We use these results to verify a representative set of the one-loop anomalous dimension calculated in Ref. [4], including entries from nearly all classes of operators. Additional details about this verification is given in Section 3.5. This provides a nontrivial check on our one-loop results, which we then feed into the two-loop anomalous dimension calculations.

3.3.3 Structure of one-loop amplitudes and rational terms

	$V^+V^+V^+V^+$	$V^+V^+V^+V^-$	$V^+V^+V^-V^-$	ϕV^+V^+	$\phi\phi V^+$	$\phi\phi\phi\phi$	$\psi^-\psi^+V^+V^+$	$\psi^-\psi^+V^+V^-$	$\psi^-\psi^+V^-V^-$	$\psi^+\psi^-V^+V^-$	$\psi^+\psi^-V^-V^-$	$\phi\phi\psi^+\psi^-$	$\psi^+\psi^-\psi^+\psi^-$	$\psi^+\psi^-\psi^+\psi^-$	$\psi^+\psi^-\psi^+\psi^-$
F^3	L	L	R	L	R	0	L	R	R	L	0	0	0	0
$(\varphi^2F^2)_1$	R	0	R	L	R	0	0	0	0	0	0	∅	∅	∅
$(\varphi^2F^2)_2$	R	0	R	L	L	0	0	0	0	0	0	∅	∅	∅
$(D^2\varphi^4)_1$	∅	∅	∅	0	0	L_0	∅	∅	∅	∅	0	∅	∅	∅
$(D^2\varphi^4)_2$	∅	∅	∅	R	0	L_0	∅	∅	∅	∅	L_0	∅	∅	∅
$(D\varphi^2\psi^2)_1$	∅	∅	∅	0	0	0	0	0	0	0	L_0	0	0	0
$(D\varphi^2\psi^2)_2$	∅	∅	∅	R	0	L_0	R	0	0	R	L_0	L_0	L_0	L_0
$(\psi^4)_1$	∅	∅	∅	∅	∅	∅	R	0	0	R	L_0	L	L	L
$(\psi^4)_2$	∅	∅	∅	∅	∅	∅	R	0	0	R	L_0	L	L	L

R: rational amplitude
L: amplitude with both logarithms and rational terms
∅: trivial zero, no contributing one-loop diagrams
0: zero explained by angular momentum selection rules [9]
0: zeros "accidental" to our model
0: zero from an appropriate local counterterm
L_0 zero rational term from an appropriate local counterterm, logarithmic terms remain.

Table 3.3: Structure of the zeros, rational terms, and logarithms in the full one-loop helicity amplitudes. In this table each entry indicates whether the operator of its row produces the amplitude with external state corresponding to its column. V denotes a vector boson, ψ a fermion and φ a scalar.

After subtracting the infrared singularities and renormalization, the amplitudes are finite. The full set of results for our renormalized and IR-subtracted amplitudes is given in Appendix 3.B. The renormalized helicity amplitudes include a large number of zeros, including those which would otherwise be rational contributions. A number of these zeros were pointed out in Ref. [10], and explained using angular-momentum selection rules in Ref. [9]. These

selection rules explain most of the observed zeros, leaving some "accidental" zeros, displayed as a blue 0 in Table 3.3. These zeros can be considered an accident of the simplicity of our model, and in a more general theory with an Abelian gauge field, we expect that such zeros should not occur. In each case, the entry directly below the blue zero shows that while the accident holds for that particular operator, another operator with identical particle content, but different color structure, produces a nonzero result in $\bar{\text{MS}}$. Intuitively, this is because only the first of each pair of operators is a product of global symmetry currents in our model (c.f. our discussion in Section 3.3.2). Alternatively, these "accidental" examples can be shown to follow from angular momentum selection rules combined with selection rules for gauge charges (i.e. color selection rules), as described in Ref. [9].

Perhaps more interesting is the surprisingly large number of amplitudes—with shaded (red) rectangles around 0 entries in Table 3.3—which do not evaluate to zero in the standard $\bar{\text{MS}}$ renormalization scheme, but which are proportional to a linear combination of the tree-level amplitudes of the dimension-six operators. These amplitudes can therefore be set to zero by an appropriate choice of finite counterterms. This corresponds to a scheme change, showing that these amplitudes are scheme dependent. Explicit examples of how these rational shifts are related to the scheme dependence of the two-loop anomalous dimensions is discussed at length in the next section.

Similarly, for a number of amplitudes (marked L_0 and in a shaded red rectangle in Table 3.3), all rational terms in the amplitude can be removed with an appropriate choice of finite counterterms, leaving behind logarithmic terms which cannot be subtracted in this way. These logarithmic terms do not appear to be of the right form to produce local results, so we may expect that they also do not produce contributions to the two-loop anomalous dimensions via Eq. (3.37). It would be interesting to investigate this, but we refrain from doing so here. Remarkably, only a small number of the one-loop amplitudes contain rational terms that cannot be removed via finite counterterms.

As expected, however, some amplitudes do contain non-local rational amplitudes, pro-

hibiting such a simple subtraction by a local counterterm. It is interesting to note that all the nonzero rational amplitudes of $(D^2\varphi^4)_2, (D\varphi^2\psi^2)_2, (\psi^4)_1$ and $(\psi^4)_2$ are non-local but can be individually set to zero by the introduction of an F^3 finite counterterm. This procedure, however, will always introduce new diagrams which make other $\emptyset$ entries in the same row nonzero. For example, since the F^3 tree contains nonzero four-vector tree amplitudes, entries in these columns will no longer be zero. Another interesting observation is that the UV divergence in the only nonzero amplitude of $(D\varphi^2\psi^2)_1$ cancels between terms, but the logarithms remain.

The vanishing one-loop amplitudes strongly suggests that many contributions to the two-loop anomalous dimension matrix should vanish, beyond those identified in Ref. [8]. For many of the two-loop anomalous dimensions, these zeros imply that the only contribution to the final result comes from the three-particle cut, making their evaluation much simpler than expected, since only four-dimensional tree-level objects are involved. In a number of cases, including multiple examples in Section 3.4, the three-particle cut also vanishes, thereby immediately implying that the corresponding two-loop anomalous dimension is zero. Of course, the amplitudes corresponding to the entries of Table 3.3 with shaded (red) rectangles are not zero when working strictly in $\bar{\text{MS}}$, so one would need to evaluate the two-particle cuts in order to determine the corresponding anomalous dimensions in this scheme.

Finally, the appearance of many zeros in Table 3.3 suggests that even more zeros in the two-loop anomalous dimension might be found by using the helicity selection rules of Ref. [7] or the angular momentum conservation rules of Ref. [9], given that the remaining three-particle cut only involves four-dimensional tree amplitudes, which are often restricted by these selection rules.

3.4 Two-loop zeros in the anomalous dimension matrix

In this section we use the results of the previous section and the tools in Section 3.2.3 to obtain two-loop anomalous dimensions in our simplified theory. These calculations will unveil a number of mechanisms that give rise to a wealth of new zeros in the two-loop anomalous dimension matrix. As mentioned in the previous section, two-loop anomalous dimensions are scheme dependent[7] This makes the question of whether a two-loop anomalous dimension is zero somewhat ill-defined. We will show explicit examples of anomalous dimensions that are nonzero in the $\bar{\text{MS}}$ scheme, but for which we can find a scheme in which they are zero. In addition, we demonstrate the cancellation of logarithms in the evaluation of Eq. (3.37) when they appear. For simplicitly, throughout this section, we assume the case of a single flavor of fermion, drop the flavor indices, and set $N_f = N_s = 1$. In all the cases we consider here, the one-loop amplitudes required for the two-loop computation are infrared finite, simplifying the discussion.

3.4.1 Zeros from length selection rules

First we summarize the results of our previous paper, which points out a set of nontrivial zeros in the two-loop anomalous dimension matrix of generic EFTs [8]: operators with longer length—those with more field insertions—are often restricted from renormalizing operators with shorter length, even if Feynman diagrams exist. Specifically, for operators $\mathcal{O}_l$ and $\mathcal{O}_s$, with lengths $l(\mathcal{O}_l)$ and $l(\mathcal{O}_s)$, $\mathcal{O}_l$ can renormalize $\mathcal{O}_s$ at L loops only if the inequality $L > l(\mathcal{O}_l) - l(\mathcal{O}_s)$ is satisfied. This implies, for example, that the operator $\mathcal{O}_{\varphi^6}$ cannot renormalize any of the other operators in our model (Table 3.1) at two loops. This is due to the fact that any two-loop diagram with an insertion of $\mathcal{O}_{\varphi^6}$ and four external particles must contain a scaleless integral, which evaluates to zero in dimensional regularization. This implies that the anomalous dimensions vanish, if there are no IR divergences. In this case

[7] This is in contrast to the β-function, which is scheme dependent starting at three loops [35, 50].

the lack of infrared singularities follows from the fact that they are proportional to the corresponding lower-loop amplitudes, which vanish due to the lack of diagrams when the bound is not satisfied.

In addition, as shown in Ref. [8], in a theory with multiple types of fields, such as the SMEFT, additional vanishing can occur at loop orders higher than indicated by the above bound. In general, whenever the only diagrams one can draw with an insertion of $\mathcal{O}_l$ and the external particles of $\mathcal{O}_s$ always involve scaleless integrals, then there will be no renormalization of $\mathcal{O}_s$ by $\mathcal{O}_l$. In the language of Section 3.2.3, this happens because there are no nonzero cuts on the right-hand side of Eq. (3.37) or the higher loop analog. Iteration pieces on the left-hand-side of Eq. (3.37)—terms other than $\gamma^{(L)}_{s\leftarrow l}F^{(0)}_s$—are also set to zero by the presence of scaleless integrals. Examples of this form of the rule in effect include the lack of two-loop renormalization of $\mathcal{O}_{F^3}$ by $\mathcal{O}_{D\varphi^2\psi^2}, \mathcal{O}_{D^2\varphi^4}$, or $\mathcal{O}_{\psi^4}$.

Another important consequence of the length selection rule is that, at loop order $L = l(\mathcal{O}_l) - l(\mathcal{O}_s) + 1$, only the $(L+1)$-particle cut can contribute [8]. For example, the three-particle cut depicted in Figure 3.8(a) is the only cut that can contribute to $\gamma^{\mathrm{UV}(2)}_{F^3\leftarrow(\varphi^2F^2)_1}$. The $(L+1)$-particle cut can then be evaluated using a four-dimensional tree-level amplitudes, making the calculation much simpler than that of a generic L-loop anomalous dimension matrix element. This observation, noted in Ref. [8], makes it straightforward to evaluate certain two-loop SMEFT anomalous dimensions solely from three-particle cuts [27].

3.4.2 Zeros from vanishing one-loop rational terms

Next, we show that the vanishing of many one-loop amplitudes and rational terms found in Section 3.3 yields additional zeros in the two-loop anomalous-dimension matrix of our theory. Somewhat surprisingly, this sometimes involves a cancelation between different contributions to the logarithms from one-loop terms in the cut. We will explain how this relates to the scheme dependence of two-loop anomalous dimensions.

$\mathcal{O}_{\psi^4} \leftarrow \mathcal{O}_{D^2\varphi^4}$

We begin by determining the renormalization of $\mathcal{O}_{(\psi^4)_1}$ and $\mathcal{O}_{(\psi^4)_2}$ by $\mathcal{O}_{(D^2\varphi^4)_1}$, which we denote by $\mathcal{O}_{(\psi^4)_1} \leftarrow \mathcal{O}_{(D^2\varphi^4)_1}$ and $\mathcal{O}_{(\psi^4)_2} \leftarrow \mathcal{O}_{(D^2\varphi^4)_1}$. To extract the anomalous dimensions, we examine cuts of amplitudes with four external quarks. We can readily prove that these anomalous dimension matrix elements are zero at two loops in our model. The contributing cuts would be

1. the three-particle cut between the five-point dimension-four tree amplitude and the five-point $(D^2\varphi^4)_1$ amplitude,

2. the two-particle cut between the four-point dimension-four one-loop amplitude and the four-point $(D^2\varphi^4)_1$ tree, and

3. the two-particle cut between the four-point dimension-four tree and the four-point $(D^2\varphi^4)_1$ one-loop amplitude.

In all cases the external particles must be four fermions to match the desired operator.

In case (1), the five point amplitude containing the operator $(D^2\varphi^4)_1$ must have two external fermions, but since the Yukawa couplings are set to zero in our simplified model, the $(D^2\varphi^4)_1$ tree must have at least four scalars, prohibiting the required three-scalar two-fermion amplitude. For case (2), the $(D^2\varphi^4)_1$ tree must again have two fermions, so that there are no valid diagram and the cut vanishes.

The vanishing of case (3) relies on our knowledge of the one-loop amplitudes with an operator insertion$(D^2\varphi^4)_1$, given in Appendix 3.B. In this case, the only $\mathcal{O}_{(D^2\varphi^4)_1}$ one-loop amplitude that can be inserted into the cut is the two-scalar two-fermion amplitude—as in Figure 3.5—which is zero for this operator. Therefore, all possible contributing cuts evaluate to zero. Since $\mathcal{O}_{(D^2\varphi^4)_1}$ does not renormalize $\mathcal{O}_{\varphi^2\psi^2 D}$ or $\mathcal{O}_{\psi^4}$ at one loop, which otherwise produce terms on the left-hand-side of Eq. (3.37), the vanishing of the three types of cuts implies that the two-loop anomalous-dimension matrix element is also zero.

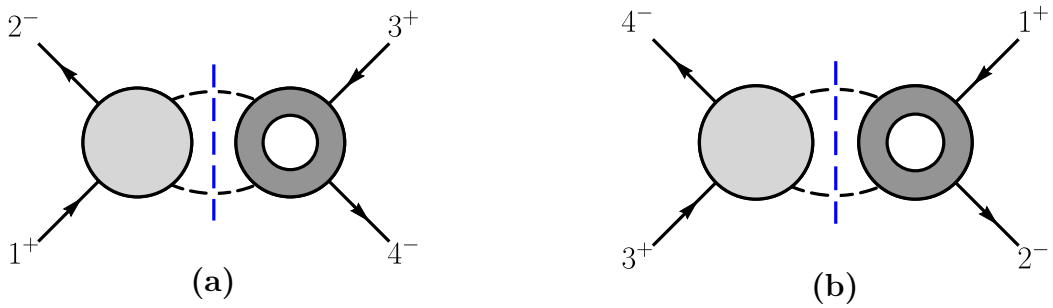

Figure 3.5: The (12)-channel (a) and (34)-channel (b) unitary cuts which determine the renormalization of $\mathcal{O}_{(\psi^4)_1}$ by $\mathcal{O}_{(D^2\varphi^4)_1}$ or $\mathcal{O}_{(D^2\varphi^4)_2}$. The (23)- and (14)-channel cuts are given by the exchange of legs 2 and 4. In each, the darker blobs indicate a higher-dimension operator insertion, and the vertical (blue) dashed line indicates the integral over phase space of the particles crossing the cut.

Next, consider the case $\mathcal{O}_{(\psi^4)_1} \leftarrow \mathcal{O}_{(D^2\varphi^4)_2}$, which we also show has a zero entry in the anomalous dimension matrix of our simplified model. We organize the calculation into the three types of cuts as in the previous case, with the only difference being that, in case (3), the one-loop amplitude with an insertion of $\mathcal{O}_{(D^2\varphi^4)_2}$, and with two scalars and two fermions as external particles is nonzero, and in fact has a UV divergence. While the presence of nonzero cuts, shown diagrammatically in Figure 3.5, might seem to imply that the two-loop anomalous dimension must be nonzero, we will show that it actually evaluates to zero as well.

Using the external state $\langle 1^+_\psi 2^-_{\overline{\psi}} 3^+_\psi 4^-_{\overline{\psi}} |$ and setting $\mathcal{O}_i = \mathcal{O}_{(D^2\varphi^4)_2}$, Eq. (3.37) reduces to

$$\begin{aligned} &\gamma^{\mathrm{UV}(2)}_{\psi^4 \leftarrow (D^2\varphi^4)_2} F^{(0)}_{\psi^4} + \gamma^{\mathrm{UV}(1)}_{(D\varphi^2\psi^2)_2 \leftarrow (D^2\varphi^4)_2} F^{(1)}_{(D\varphi^2\psi^2)_2} \\ &\qquad = -\frac{1}{\pi} (\mathcal{M}^{12}_{2\to 2} + \mathcal{M}^{14}_{2\to 2} + \mathcal{M}^{23}_{2\to 2} + \mathcal{M}^{34}_{2\to 2})^{(0)} \otimes \mathrm{Re} F^{(1)}_{(D^2\varphi^4)_2} \,, \end{aligned} \tag{3.45}$$

where on the right-hand side we only find cuts of the form in Figure 3.5 with an $\mathcal{O}_{(D^2\varphi^4)_2}$ insertion, and the (13) and (24) channels are not allowed. For instance the (12)-channel cut

is

$$
\begin{aligned}
&(\mathcal{M}^{12}_{2\to 2})^{(0)} \otimes \mathrm{Re}F^{(1)}_{(D^2\varphi^4)_2} \\
&\quad = 2\int d\mathrm{LIPS}_2\, \langle 1^+_\psi 2^-_{\overline{\psi}} |\mathcal{M}| \ell_{1\,\varphi} \ell_{2\,\overline{\varphi}} \rangle^{(0)}\, \mathrm{Re}\langle \ell_{1\,\varphi} \ell_{2\,\overline{\varphi}} 3^+_\psi 4^-_{\overline{\psi}} |\mathcal{O}_{(D^2\varphi^4)_2}|0\rangle^{(1)} \,.
\end{aligned}
\tag{3.46}
$$

The factor of 2 is required to cancel the symmetry factor of 1/2 in our definition of the phase-space measure. Other terms in Eq. (3.37) drop out because $\mathcal{O}_{(D^2\varphi^4)_2}$ does not have either a one-loop or tree-level form factor with a four-fermion external state, and does not renormalize $\mathcal{O}_{(D\varphi^2\psi^2)_1}$ or the $\mathcal{O}_{\psi^4}$ operators at one loop. In particular, the β-function also does not appear.

For simplicity, we set the off-shell momentum q to zero, and Eq. (3.45) then reduces to

$$
\begin{aligned}
&\gamma^{\mathrm{UV}(2)}_{\psi^4 \leftarrow (D^2\varphi^4)_2} A^{(0)}_{\psi^4}(1^+_\psi 2^-_{\overline{\psi}}\, 3^+_\psi 4^-_{\overline{\psi}}) + \gamma^{\mathrm{UV}(1)}_{(D\varphi^2\psi^2)_2 \leftarrow (D^2\varphi^4)_2} A^{(1)}_{(D\varphi^2\psi^2)_2}(1^+_\psi 2^-_{\overline{\psi}}\, 3^+_\psi 4^-_{\overline{\psi}}) \\
&\quad = -\frac{2}{\pi}\sum \int d\mathrm{LIPS}_2\, A^{(0)}(1^+_\psi 2^-_{\overline{\psi}}\, -\ell_{2\,\varphi}\, -\ell_{1\,\overline{\varphi}}) \mathrm{Re} A^{(1)}_{(D^2\varphi^4)_2}(\ell_{1\,\varphi} \ell_{2\,\overline{\varphi}}\, 3^+_\psi 4^-_{\overline{\psi}}) \,,
\end{aligned}
\tag{3.47}
$$

where the sum is over the available channels. The relevant tree and renormalized one-loop amplitudes needed to construct the cut are (including the color factors):

$$
A^{(0)}(1^+_\psi 2^-_{\overline{\psi}}\, 3_\varphi\, 4_{\overline{\varphi}}) = T^a_{i_2 i_1} T^a_{i_4 i_3}\, g^2 \frac{\langle 23\rangle [13]}{s} \,, \tag{3.48}
$$

$$
A^{(1)}_{(D^2\varphi^4)_2}(1^+_\psi 2^-_{\overline{\psi}}\, 3_\varphi\, 4_{\overline{\varphi}}) = T^a_{i_2 i_1} T^a_{i_4 i_3}\, \frac{\tilde{g}^2}{9} \langle 23\rangle [13] (3\log(-s/\mu^2) + 8) \,, \tag{3.49}
$$

where again the flavor indices have been dropped for simplicity. Note the form of Eq. (3.47) provides a nontrivial check on the phase space integral on the right-hand side: $A^{(1)}_{(D^2\varphi^4)_2}$ contains terms proportional to $\log(-s/\mu^2)$, which, after the phase-space integral, must cancel against terms in $A^{(1)}_{(D\varphi^2\psi^2)_2}$.

We can readily evaluate the cut by relabeling the amplitudes (3.48)–(3.49) and applying the spinor parametrization (3.25) to the scalars crossing the cut. This yields an integral

with no poles in $z = \mathrm{e}^{i\phi}$, other than the pole at zero. This can be seen by the fact that all spinor products in $A^{(0)}$ are either proportional to $\mathrm{e}^{\pm i\phi}$ or else have no ϕ dependence under our parametrization, whereas $A^{(1)}_{(D^2\varphi^4)_2}$ only has a pole in s. This makes the ϕ integral trivial to evaluate, resulting in:

$$\int_0^{\frac{\pi}{2}} d\theta\, \frac{\tilde{g}^4}{18}\langle 24\rangle[13]\sin^3(2\theta)(3\log(-s/\mu^2)+8)T^a_{i_2 i_1}T^a_{i_4 i_3} \\ = \frac{\tilde{g}^4}{27}\langle 24\rangle[13](3\log(-s/\mu^2)+8)T^a_{i_2 i_1}T^a_{i_4 i_3}\,, \tag{3.50}$$

for the (12)-channel cut. The (34)-channel cut gives the same result, while the other cuts yield the same result with legs two and four exchanged. Summing over the three other channels, we exactly match the second term on the left-hand side of Eq. (3.45), since $\gamma^{\mathrm{UV}(1)}_{(D\varphi^2\psi^2)_2\leftarrow(D^2\varphi^4)_2} = \tilde{g}^2/3$ and

$$A^{(1)}_{(D\varphi^2\psi^2)_2} = \frac{2\tilde{g}^2}{9}\langle 24\rangle[13](3\log(-s/\mu^2)+8)T^a_{i_2 i_1}T^a_{i_4 i_3} - (2\leftrightarrow 4)\,. \tag{3.51}$$

Therefore the cuts exactly cancel all terms on the left-hand side of Eq. (3.45) involving the one-loop anomalous dimensions and form-factors, leaving $\gamma^{\mathrm{UV}(2)}_{\psi^4\leftarrow(D^2\varphi^4)_2}F^{(0)}_{\psi^4} = 0$. Thus the two-loop anomalous dimension $\gamma^{\mathrm{UV}(2)}_{\psi^4\leftarrow(D^2\varphi^4)_2}$ is zero.

In fact, we could have come to this conclusion simply by examining the form of the one-loop amplitudes in Eqs. (3.49) and (3.51). First, note the two-loop anomalous dimension must be $\tilde{g}^4$ times a number (i.e., it does not have any kinematic dependence). Logarithmic terms resulting from the cut on the right-hand side of (3.45) must therefore cancel against logarithmic terms in $A^{(1)}_{(D\varphi^2\psi^2)_2}$. Since both one-loop form factors are proportional to the factor $(3\log(-s/\mu^2)+8)$, and since this term can be pulled out of the phase-space integral on the right-hand side of Eq. (3.45), the cancellation of the logarithmic terms implies cancellation of the rational term as well. Thus, even though there are nonzero cuts, there can be no remaining rational term that leads to a nonzero two-loop anomalous dimension.

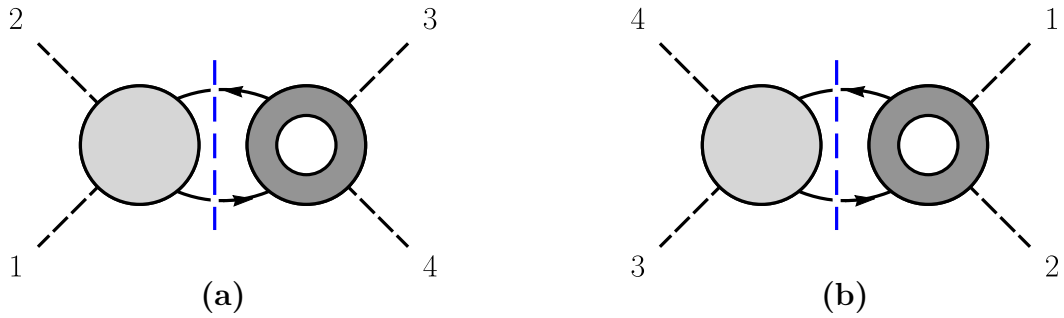

Figure 3.6: The (a) (12)-channel and (b) (34)-channel unitary cuts which determine the renormalization of $\mathcal{O}_{(D^2\varphi^4)_1}$ and $\mathcal{O}_{(D^2\varphi^4)_2}$ by $\mathcal{O}_{(\psi^4)_1}$ or $\mathcal{O}_{(\psi^4)_2}$. The (23)- and (14)-channel cuts are given by exchanging legs 2 and 4. In each, the darker blobs indicate a higher-dimension operator insertion, and the vertical (blue) dashed line indicates the integral over phase space of the particles crossing the cut.

At this point, the vanishing of the two-loop anomalous dimensions due to the cancellation of one-loop rational terms might seem accidental. However, one must remember that such *local* rational pieces are scheme dependent and can be adjusted by adding finite local counter-terms. As described in Section 3.3, the rational terms of both one-loop amplitudes in (3.49) and (3.51) can be set to zero by such finite counterterms, which would also result in $\gamma^{\text{UV}(2)}_{\psi^4 \leftarrow (D^2\varphi^4)_2} = 0$. For this particular example, it just so happened that the naive $\bar{\text{MS}}$ scheme has zero anomalous dimension, but next we will see that this is not always the case.

As a cross-check, we have verified that the Eq. (3.32) is also satisfied. The crucial substitution $\log(-s/\mu^2) \to \log(-s/\mu^2) - i\pi$, is required in the right-hand side of that equation, coming from the analytic continuation of the amplitude from the Euclidean region to the correct physical region, which must be carried out for use in Eqs. (3.29)–(3.31).

$\mathcal{O}_{D^2\varphi^4} \leftarrow \mathcal{O}_{(\psi^4)_1}$

This section will provide our first example of nonzero two-loop anomalous dimension matrix elements in $\bar{\text{MS}}$, while demonstrating how an appropriate choice of scheme, i.e. choice of finite local counterterms, can eliminate the two-loop anomalous dimensions of this example.

We will begin with the calculation in $\bar{\text{MS}}$. Again, there is no three-particle cut, due to the particle content of the two types of operators in question. Using the external state

$\langle 1_{\varphi}2_{\overline{\varphi}}3_{\varphi}4_{\overline{\varphi}}|$ and setting $\mathcal{O}_i \to \mathcal{O}_{(\psi^4)_1}$, Eq. (3.37) becomes

$$\begin{aligned}\gamma^{\mathrm{UV}(2)}_{(D^2\varphi^4)_1\leftarrow(\psi^4)_1} F^{(0)}_{(D^2\varphi^4)_1} + \gamma^{\mathrm{UV}(2)}_{(D^2\varphi^4)_2\leftarrow(\psi^4)_1} F^{(0)}_{(D^2\varphi^4)_2} + \gamma^{\mathrm{UV}(1)}_{(D\varphi^2\psi^2)_2\leftarrow(\psi^4)_1} F^{(1)}_{(D\varphi^2\psi^2)_2} \\ = -\frac{1}{\pi}(\mathcal{M}^{12}_{2\to2} + \mathcal{M}^{14}_{2\to2} + \mathcal{M}^{23}_{2\to2} + \mathcal{M}^{34}_{2\to2})^{(0)} \otimes \mathrm{Re}F^{(1)}_{(\psi^4)_1}\,.\end{aligned} \tag{3.52}$$

As for the previous example, the logarithmic terms in the cuts must cancel against terms in the amplitude $F^{(1)}_{(D\varphi^2\psi^2)_2}$ on the left-hand side of the equation. Since we are dealing with four-point matrix elements we will again set $q = 0$. Then the one-loop amplitudes required for this example are

$$A^{(1)}_{(\psi^4)_1}(1^+_{\psi}2^-_{\overline{\psi}}3_{\varphi}4_{\overline{\varphi}}) = \frac{2\tilde{g}^2}{9}\langle 23\rangle[13](3\log(-s/\mu^2) - 2)T^a_{i_2i_1}T^a_{i_4i_3}\,, \tag{3.53}$$

$$A^{(1)}_{(D\varphi^2\psi^2)_2}(1_{\varphi}2_{\overline{\varphi}}3_{\varphi}4_{\overline{\varphi}}) = \frac{2\tilde{g}^2}{9}(t-u)(3\log(-s/\mu^2) - 5)T^a_{i_2i_1}T^a_{i_4i_3} + (2\leftrightarrow 4)\,, \tag{3.54}$$

and the tree-level amplitudes needed are in Eq. (3.48) along with

$$A^{(0)}_{(D^2\varphi^4)_1}(1_{\varphi}2_{\overline{\varphi}}3_{\varphi}4_{\overline{\varphi}}) = t\delta_{i_2i_1}\delta_{i_4i_3} + s\delta_{i_4i_1}\delta_{i_2i_3}\,, \tag{3.55}$$

$$A^{(0)}_{(D^2\varphi^4)_2}(1_{\varphi}2_{\overline{\varphi}}3_{\varphi}4_{\overline{\varphi}}) = 2s\delta_{i_2i_1}\delta_{i_4i_3} + 2t\delta_{i_4i_1}\delta_{i_2i_3}\,, \tag{3.56}$$

which are shown in a slightly different basis of color factors than those shown in the appendix. The phase-space integral is evaluated in the same manner as the previous examples, with the result of the (12)-channel cut being

$$\begin{aligned}-\frac{1}{\pi}\int d\mathrm{LIPS}_2 \sum_{h_1,h_2} A^{(0)}(1_{\varphi}2_{\overline{\varphi}}-\ell_1{}^{h_1}_{\psi}-\ell_2{}^{h_2}_{\overline{\psi}})A^{(1)}_{(\psi^4)_1}(\ell_2{}^{h_2}_{\psi}\,\ell_1{}^{h_1}_{\overline{\psi}}\,3_{\varphi}4_{\overline{\varphi}}) \\ = -\frac{2}{27}\tilde{g}^4(t-u)(3\log(-s/\mu^2) - 2)T^a_{i_2i_1}T^a_{i_4i_3}\,.\end{aligned} \tag{3.57}$$

After summing over all channels and subtracting the contribution of $\gamma^{\mathrm{UV}(1)}_{(D\varphi^2\psi^2)_2\leftarrow(\psi^4)_1}F^{(1)}_{(D\varphi^2\psi^2)_2}$ in Eq. (3.52)—thus canceling the logarithmic terms—the two-loop anomalous dimensions

are given by

$$\begin{aligned}\gamma^{\mathrm{UV}(2)}_{(D^2\varphi^4)_1\leftarrow(\psi^4)_1}(t\delta_{i_2i_1}\delta_{i_4i_3}+s\delta_{41}\delta_{23})+\gamma^{\mathrm{UV}(2)}_{(D^2\varphi^4)_2\leftarrow(\psi^4)_1}(2s\delta_{i_2i_1}\delta_{i_4i_3}+2t\delta_{i_4i_1}\delta_{i_2i_3}) \\ =-\frac{4}{9}\tilde{g}^4(t-u)T^a_{i_2i_1}T^a_{i_4i_3}+(2\leftrightarrow 4)\,.\end{aligned} \tag{3.58}$$

Applying the color Fierz identity,

$$T^a_{ij}T^a_{kl}=\delta_{il}\delta_{kj}-\frac{1}{N}\delta_{ij}\delta_{kl}\,, \tag{3.59}$$

and solving for the two-loop anomalous dimensions, we find

$$\begin{aligned}\gamma^{\mathrm{UV}(2)}_{(D^2\varphi^4)_1\leftarrow(\psi^4)_1}=&-\frac{4\tilde{g}^4(N-2)}{9N}\,,\\ \gamma^{\mathrm{UV}(2)}_{(D^2\varphi^4)_2\leftarrow(\psi^4)_1}=&\frac{2\tilde{g}^4(2N-1)}{9N}\,,\end{aligned} \tag{3.60}$$

in the $\bar{\mathrm{M}}$S scheme. Although these anomalous dimension matrix elements are nonzero in the $\bar{\mathrm{M}}$S scheme, a simple rational shift of the coefficients $c_{(D^2\varphi^4)_1}$, $c_{(D^2\varphi^4)_2}$, and $c_{(D\varphi^2\psi^2)_2}$ can set them to zero. This is accomplished by the following shifts in the coefficients:

$$\begin{aligned}c_{(D^2\varphi^4)_1}\longrightarrow\tilde{c}_{(D^2\varphi^4)_1}&=c_{(D^2\varphi^4)_1}+\frac{10\tilde{g}^2(N-2)}{9N}c_{(D\varphi^2\psi^2)_2}\,,\\ c_{(D^2\varphi^4)_2}\longrightarrow\tilde{c}_{(D^2\varphi^4)_2}&=c_{(D^2\varphi^4)_2}+\frac{5\tilde{g}^2(2N-1)}{9N}c_{(D\varphi^2\psi^2)_2}\,,\\ c_{(D\varphi^2\psi^2)_2}\longrightarrow\tilde{c}_{(D\varphi^2\psi^2)_2}&=c_{(D\varphi^2\psi^2)_2}-\frac{2\tilde{g}^2}{9}c_{(\psi^4)_1}\,,\end{aligned} \tag{3.61}$$

which yields

$$\tilde{\gamma}^{\mathrm{UV}(2)}_{(D^2\varphi^4)_1\leftarrow(\psi^4)_1}=0\,,\qquad\qquad\tilde{\gamma}^{\mathrm{UV}(2)}_{(D^2\varphi^4)_2\leftarrow(\psi^4)_1}=0\,, \tag{3.62}$$

where the tilde indicates the modified scheme. The shifts above are equivalent to a finite renormalization of the operator at one loop. Generally this can be achieved by choosing

the rational terms in $\gamma^{\mathrm{UV}(1)}_{(D\varphi^2\psi^2)_2\leftarrow(\psi^4)_1} F^{(1)}_{(D\varphi^2\psi^2)_2}$ to match those of the cuts. In our particular example we set the rational terms of both (3.53) and (3.54) to zero. We briefly comment below on the consequences of this redefinition for the two-loop RG running of the operators involved.

While we do not present the analogous calculation for $\mathcal{O}_{(\psi^4)_2}$ here, by inspecting Table 3.3, we can deduce that the two-loop anomalous dimensions $\gamma^{\mathrm{UV}(2)}_{(D^2\varphi^4)_1\leftarrow(\psi^4)_2}$ and $\gamma^{\mathrm{UV}(2)}_{(D^2\varphi^4)_2\leftarrow(\psi^4)_2}$ can also be set to zero with the appropriate choice of finite counterterms.

General comments about scheme redefinition

As mentioned above, the scheme choice that sets some two-loop anomalous dimensions to zero is equivalent to a finite renormalization of the operators

$$\tilde{\mathcal{O}}_i = Z^{\mathrm{fin}}_{ij}\mathcal{O}_j\,, \quad \text{where} \quad Z^{\mathrm{fin}}_{ij} = \delta_{ij} + f_{ij}(g^{(4)})\,, \tag{3.63}$$

and the quantity f_{ij} is finite and has a perturbative expansion starting at one loop, $f_{ij}(g^{(4)}) = f^{(1)}_{ij} + \cdots$. As usual, the redefinition of the coefficients, $\tilde{c}_i = Z^{\mathrm{fin}\,(c)}_{ij} c_j$ is given by the inverse, $Z^{\mathrm{fin}\,(c)}_{ij} = (Z^{\mathrm{fin}}_{ij})^{-1}$. The effect of such a scheme redefinition can be easily analyzed using the unitarity-based formalism employed in this paper. Since the coupling dependence of f_{ij} starts at one loop we have that

$$\tilde{F}^{(0)}_i = F^{(0)}_i\,, \tag{3.64}$$

$$\tilde{F}^{(1)}_i = F^{(1)}_i + f^{(1)}_{ij} F^{(0)}_j\,, \tag{3.65}$$

where the tilde indicates a form factor of the redefined operator $\tilde{\mathcal{O}}_i$. From Eqs. (3.64) and (3.22) we conclude the one-loop anomalous dimensions are unaffected by the finite

renormalization, i.e., $\Delta\tilde{\gamma}_{ij}^{(1)} = \Delta\gamma_{ij}^{(1)}$. Similarly, writing Eq. (3.37) for the redefined operator

$$\left[\Delta\tilde{\gamma}_{ij}^{(1)} + \delta_{ij}\beta^{(1)}\partial\right] \mathrm{Re}\tilde{F}_j^{(1)} + \left[\Delta\tilde{\gamma}_{ij}^{(2)} + \delta_{ij}\beta^{(2)}\partial\right] \tilde{F}_j^{(0)} = -\frac{1}{\pi}\left[\mathrm{Re}(\mathcal{M})\mathrm{Re}(\tilde{F}_i)\right]^{(2)}. \tag{3.66}$$

and using Eqs. (3.64) and (3.65) together with Eqs. (3.22) and (3.37), while keeping in mind that the infrared anomalous dimensions are not changed by redefining the scheme, we find the relation between the two-loop anomalous dimensions in the two schemes,

$$\tilde{\gamma}_{ij}^{\mathrm{UV}(2)} = \gamma_{ij}^{\mathrm{UV}(2)} + f_{ik}^{(1)}\gamma_{kj}^{\mathrm{UV}(1)} - \gamma_{ik}^{\mathrm{UV}(1)} f_{kj}^{(1)} - \beta^{(1)}\partial f_{ij}^{(1)}\,. \tag{3.67}$$

In general, one would like to solve this equation for $f_{ik}^{(1)}$ to get as many vanishing entries as possible in $\tilde{\gamma}_{ij}^{\mathrm{UV}(2)}$.

We have explicitly verified Eq. (3.67) in the examples above, where we set the anomalous dimensions of the form $\tilde{\gamma}^{\mathrm{UV}(2)}_{D^2\varphi^4\leftarrow\psi^4}$ to zero by appropriately choosing $f^{(1)}_{D\varphi^2\psi^2\leftarrow\psi^4}$ and $f^{(1)}_{D^2\varphi^4\leftarrow D\varphi^2\psi^4}$. In addition, $f^{(1)}_{D^2\varphi^4\leftarrow\psi^4}$ vanished, which from Eq. (3.67) implies the the absence of a term induced by the β-function in the new two-loop anomalous dimension. On the other hand, it is clear from Eq. (3.67) that the finite renormalizations will induce some additional running in the two-loop anomalous dimensions $\tilde{\gamma}^{\mathrm{UV}(2)}_{D\varphi^2\psi^2\leftarrow\psi^4}$ and $\tilde{\gamma}^{\mathrm{UV}(2)}_{D^2\varphi^4\leftarrow D\varphi^2\psi^4}$, proportional to the one-loop beta function and $\partial f^{(1)}$. However, this additional running is harmless, since those operators already mix at one loop. Furthermore, the corresponding entries in the two-loop anomalous-dimension matrix receive contributions from both two- and three-particle cuts that have no a priori reason to vanish, so we expect them in any case to run. In summary, our scheme choice prevents certain operators from mixing at two loops at the expense of modifying the running of operators that, in any case, mix at one loop in the original scheme.

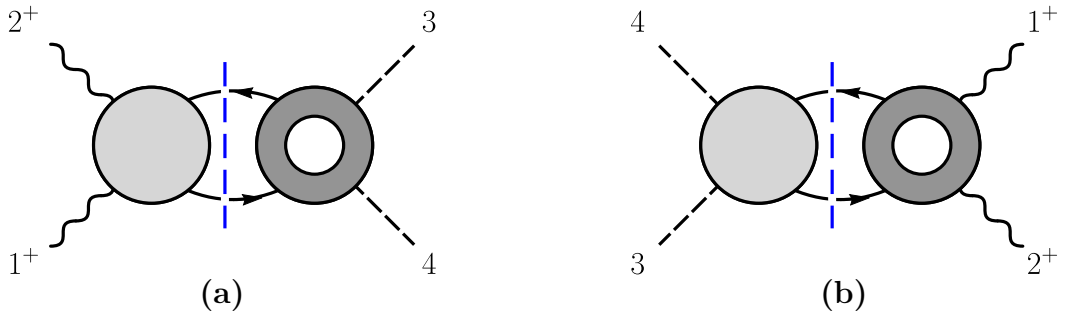

Figure 3.7: (12)-channel (a) and (34)-channel (b) unitary cuts which determine the renormalization of $\mathcal{O}_{(\varphi^2F^2)_1}$ and $\mathcal{O}_{(\varphi^2F^2)_2}$ by $\mathcal{O}_{(\psi^4)_1}$ or $\mathcal{O}_{(\psi^4)_2}$. There are no t-channel cuts for this process. In each diagram, the darker blobs indicate a higher-dimension operator insertion, and the dashed line indicates the integral over phase space of the particles crossing the cut.

3.4.3 Zeros from color selection rules

This section will provide an example of another type of selection rule, wherein a mismatch between the color of the cuts and the color of the target operators prevents renormalization at two loops.

$\mathcal{O}_{\varphi^2F^2} \leftarrow \mathcal{O}_{\psi^4}$

For this example we choose the external state to be $\langle 1_\varphi 2_{\overline{\varphi}} 3^+ 4^+|$, under which both $\mathcal{O}_{(\varphi^2F^2)_1}$ and $\mathcal{O}_{(\varphi^2F^2)_2}$ are nonzero. Using this state and setting $\mathcal{O}_i \to \mathcal{O}_{(\psi^4)_1}$, Eq. (3.37) reduces to

$$\begin{aligned}\gamma^{\mathrm{UV}(2)}_{(\varphi^2F^2)_1\leftarrow(\psi^4)_1} F^{(0)}_{(\varphi^2F^2)_1} + \gamma^{\mathrm{UV}(2)}_{(\varphi^2F^2)_2\leftarrow(\psi^4)_1} F^{(0)}_{(\varphi^2F^2)_2} + \gamma^{\mathrm{UV}(1)}_{(D\varphi^2\psi^2)_2\leftarrow(\psi^4)_1} F^{(1)}_{(D\varphi^2\psi^2)_2} \\ = -\frac{1}{\pi}\Big((\mathcal{M}^{12}_{2\to2})^{(0)} \otimes \mathrm{Re}F^{(1)}_{(\psi^4)_1} + (\mathcal{M}^{34}_{2\to2})^{(0)} \otimes \mathrm{Re}F^{(1)}_{(\psi^4)_1}\Big)\,.\end{aligned} \tag{3.68}$$

Naively there would be the additional term $\gamma^{\mathrm{UV}(2)}_{F^3\leftarrow(\psi^4)_1} F^{(0)}_{F^3}$ on the left-hand-side of the equation, since $\mathcal{O}_{F^3}$ produces a nonzero tree amplitude with the state $\langle 1_\varphi 2_{\overline{\varphi}} 3^+ 4^+|$. However, as was discussed in Section 3.4.1, the length and particle content of $\mathcal{O}_{(\psi^4)_1}$ requires

$\gamma^{\mathrm{UV}(2)}_{F^3\leftarrow(\psi^4)_1} = 0$. Setting $q = 0$, the (12)-channel cut of the above equation is

$$(\mathcal{M}^{12}_{2\to2})^{(0)} \otimes \mathrm{Re}F^{(1)}_{(\psi^4)_1} = \int d\mathrm{LIPS}_2 \sum_{h_1,h_2} A^{(0)}(1_\varphi 2_{\overline{\varphi}} - \ell_1{}_\psi^{h_1} - \ell_2{}_{\overline{\psi}}^{-h_2}) A^{(1)}_{(\psi^4)_1}(\ell_2{}_\psi^{h_2}\, \ell_1{}_{\overline{\psi}}^{h_1}\, 3^+4^+)\,, \tag{3.69}$$

and the (34)-channel cut is

$$(\mathcal{M}^{34}_{2\to2})^{(0)} \otimes \mathrm{Re}F^{(1)}_{(\psi^4)_1} = \int d\mathrm{LIPS}_2 \sum_{h_1,h_2} A^{(0)}(3^+4^+ - \ell_1{}_\psi^{h_1} - \ell_2{}_{\overline{\psi}}^{h_2}) A^{(1)}_{(\psi^4)_1}(\ell_2{}_\psi^{h_2}\, \ell_1{}_{\overline{\psi}}^{h_1}\, 1_\varphi 2_{\overline{\varphi}})\,. \tag{3.70}$$

The (34)-channel cut vanishes, because the amplitude $A^{(0)}(3^+4^+ - \ell_1{}_\psi - \ell_2{}_{\overline{\psi}})$ is zero for all helicities of the fermions crossing the cut. This vanishing is required for the consistency of the logarithmic terms: $A^{(1)}_{(\psi^4)_1}(\ell_2{}_\psi^{h_2}\, \ell_1{}_{\overline{\psi}}^{h_1}\, 1_\varphi 2_{\overline{\varphi}})$ includes a term proportional to $\log(-s/\mu^2)$, but there is no term on the left-hand side that can cancel it, since $F^{(1)}_{(D\varphi^2\psi^2)_2}(1_\varphi 2_{\overline{\varphi}}\, 3^+4^+)$ is purely rational. The one-loop amplitudes needed for this calculation are

$$A^{(1)}_{(\psi^4)_1}(1^+_\psi\, 2^-_{\overline{\psi}}\, 3^+4^+) = -\frac{\tilde{g}^2 s[14]\langle 24\rangle\, [T^{a_3}, T^{a_4}]_{i_2 i_1}}{3\langle 34\rangle^2}\,, \tag{3.71}$$

$$A^{(1)}_{(\psi^4)_1}(1^-_\psi\, 2^+_{\overline{\psi}}\, 3^+4^+) = -\frac{\tilde{g}^2 \langle 12\rangle[23][24]\, [T^{a_3}, T^{a_4}]_{i_2 i_1}}{3\langle 34\rangle}\,, \tag{3.72}$$

$$A^{(1)}_{(D\varphi^2\psi^2)_2}(1_\varphi 2_{\overline{\varphi}}\, 3^+4^+) = \frac{\tilde{g}^2 s(t-u)\, [T^{a_3}, T^{a_4}]_{i_2 i_1}}{3\langle 34\rangle^2}\,, \tag{3.73}$$

while the tree-level amplitudes needed for the cut calculation are (3.48) and its conjugate. The phase-space integrals are carried out in the same manner as the previous example, with the simplification that the functions are now entirely rational. The result of the phase-space

integral is

$$-\frac{1}{\pi}\int d\text{LIPS}_2 \sum_{h_1,h_2} A^{(0)}(1_{\varphi}2_{\overline{\varphi}}-\ell_1{}_{\psi}^{-h_1}-\ell_2{}_{\overline{\psi}}^{-h_2})A^{(1)}_{(\psi^4)_1}(\ell_2{}_{\psi}^{h_2}\,\ell_1{}_{\overline{\psi}}^{h_1}\,3^+4^+)$$
$$= -\frac{2\tilde{g}^4 s(t-u)\,[T^{a_3},T^{a_4}]_{i_2 i_1}}{9(\langle 34\rangle)^2} = \gamma^{\text{UV}(1)}_{(D\varphi^2\psi^2)_2\leftarrow(\psi^4)_1} A^{(1)}_{(D\varphi^2\psi^2)_2}\,. \tag{3.74}$$

Thus the phase-space integral exactly cancels against this term from the left-hand-side of Eq. (3.68), meaning the two-loop anomalous dimension is again zero.

Interestingly, this can also be seen without looking at the kinematic content of the cuts on the right-hand side of Eq. (3.68). Since the color of both $\mathcal{O}_{(\varphi^2F^2)_1}$ and $\mathcal{O}_{(\varphi^2F^2)_2}$ are symmetric in T^3 and T^4, no combination of the two can produce the color factor $[T^3,T^4]_{i_2i_1}$. Since this is the color of $A^{(1)}_{(D\varphi^2\psi^2)_2}(1_{\varphi}2_{\overline{\varphi}}3^+4^+)$, and the color of $A^{(1)}_{(\psi^4)_1}(1^{\pm}_{\psi}2^{\mp}_{\overline{\psi}}3^+4^+)$ is also anti-symmetric under the exchange of 3 and 4, we can see directly from the color that neither of these terms can contribute to the two-loop anomalous dimension, and therefore must cancel. As in the previous example, we can extend this argument trivially to the operator $\mathcal{O}_{(\psi^4)_2}$, since its two-fermion two-vector-boson amplitude is proportional to that of $\mathcal{O}_{(\psi^4)_1}$. In this case, the only difference on the left-hand side would being the value of $\gamma^{\text{UV}(1)}_{(D\varphi^2\psi^2)_2\leftarrow(\psi^4)_2}$ versus $\gamma^{\text{UV}(1)}_{(D\varphi^2\psi^2)_2\leftarrow(\psi^4)_1}$, but the color again ensures all terms must cancel, leaving

$$\begin{aligned}
\gamma^{\text{UV}(2)}_{(\varphi^2F^2)_1\leftarrow(\psi^4)_1} &= \gamma^{\text{UV}(2)}_{(\varphi^2F^2)_2\leftarrow(\psi^4)_1} = 0\,,\\
\gamma^{\text{UV}(2)}_{(\varphi^2F^2)_1\leftarrow(\psi^4)_2} &= \gamma^{\text{UV}(2)}_{(\varphi^2F^2)_2\leftarrow(\psi^4)_2} = 0\,.
\end{aligned} \tag{3.75}$$

Here we focused on a simple example in which the color can preclude renormalization. In more general cases, one can directly inspect the color of the amplitudes that compose the cuts contributing to a given anomalous dimension and determine whether a given operator can yield a nonzero contribution. Note that this is more efficient than studying the color of individual Feynman diagrams, since the color decomposed amplitudes have fewer color structures.

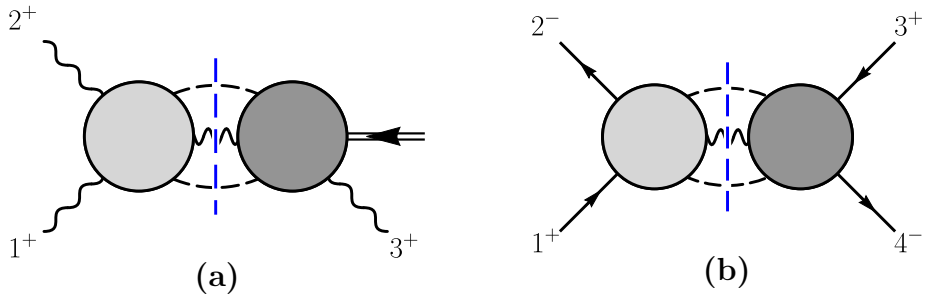

Figure 3.8: (a) Unitary cut which determines the renormalization of $\mathcal{O}_{F^3}$ by $\mathcal{O}_{(\varphi^2F^2)_1}$ or $\mathcal{O}_{(\varphi^2F^2)_2}$. Note this form factor requires $q \neq 0$, and the double-lined arrow indicates this insertion of additional off-shell momentum from the operator. (b) Unitarity cut which determines the renormalization of $\mathcal{O}_{(\psi^4)_1}$ and $\mathcal{O}_{(\psi^4)_2}$ by $\mathcal{O}_{(\varphi^2F^2)_1}$ or $\mathcal{O}_{(\varphi^2F^2)_2}$. In each, the darker blobs indicate a higher-dimension operator insertion, and the dashed line indicates the integral over phase space of the particles crossing the cut.

It is worth noting that, as mentioned in Section 3.3, the nonzero rational amplitudes (3.71)–(3.73) can be set to zero by introducing finite counterterms proportional to $c_{(\psi^4)_1}\mathcal{O}_{F^3}$ and $c_{(D\varphi^2\psi^2)_2}\mathcal{O}_{F^3}$, respectively. However, since these are non-local amplitudes, doing so introduces nonzero terms for other amplitudes, in particular any amplitudes where $\mathcal{O}_{F^3}$ produces a nonzero tree-level amplitude. This would introduce a great deal of confusion—for example, if we were to introduce a counterterm to cancel (3.71), we would then need to include additional cuts on the right-hand side of Eq. (3.68), including three-particle cuts and cuts with nontrivial IR dependence. Canceling either Eq. (3.71) or Eq. (3.73) with such a counterterm would also spoil the argument of Section 3.4.1, as the $\mathcal{O}_{F^3}$ self-renormalization would contribute in a nontrivial way. Therefore we would have to include the term $\gamma^{\text{UV}(2)}_{F^3\leftarrow(\psi^4)_1}F^{(0)}_{F^3}$ on the left-hand side of Eq. (3.68) as well. For all of the above reasons, we choose not to implement these finite shifts. It is interesting however, that even though the rational terms remain in this example, the structure of the color precludes renormalization at two loops.

3.4.4 Outlook on additional zeros

The previous sections have demonstrated numerous zeros in the two-loop anomalous dimension matrix, summarized in Table 3.4. However, the previous examples are by no means

	F^3	$(\varphi^2F^2)_1$	$(\varphi^2F^2)_2$	$(D^2\varphi^4)_1$	$(D^2\varphi^4)_2$	$(D\varphi^2\psi^2)_1$	$(D\varphi^2\psi^2)_2$	$(\psi^4)_1$	$(\psi^4)_2$	φ^6
F^3				0	0	0	0	0	0	$\emptyset$
$(\varphi^2F^2)_1$								0	0	0
$(\varphi^2F^2)_2$								0	0	0
$(D^2\varphi^4)_1$								0^*	0^*	0
$(D^2\varphi^4)_2$								0^*	0^*	0
$(D\varphi^2\psi^2)_1$										$\emptyset$
$(D\varphi^2\psi^2)_2$										$\emptyset$
$(\psi^4)_1$				0	0					$\emptyset$
$(\psi^4)_2$				0	0					$\emptyset$
φ^6										

$\emptyset$: trivial zero, no contributing two-loop diagrams

0 : zero predicted by the selection rules of Section 3.4

: only a three-particle cut is needed to evaluate $\gamma_{ij}^{\mathrm{UV}(2)}$

Table 3.4: Structure of the two-loop anomalous dimension matrix $\gamma_{ij}^{(2)}$ due to the collected rules outlined in this section. A $\emptyset$ indicates there are no contributing two-loop diagrams, whereas 0 alone indicates that there are one-loop diagrams that could contribute, but the anomalous dimension evaluates to zero. A 0^* indicates the result is nonzero in $\overline{\mathrm{MS}}$, but set to zero by introducing the appropriate finite counterterms. Shading indicates the entry depends only on the three-particle cut, due to either the length selection rules of Section 3.4.1 or the vanishing of the relevant one-loop amplitudes. As for Table 3.2, the operators labeling the rows are renormalized by the operators labeling the columns.

exhaustive, and more zeros may exist. The large number of zeros in the one-loop amplitudes (Table 3.3) implies that when calculating two-loop anomalous dimensions, the two-particle cut formed from the dimension-four tree and the dimension-six one-loop amplitude will not contribute. In some cases, the only contribution will come from the three-particle cut. Examples of this include the renormalization of $\mathcal{O}_{F^3}$ by $\mathcal{O}_{(\varphi^2F^2)_1}$ or $\mathcal{O}_{(\varphi^2F^2)_2}$, and the renormalization of $\mathcal{O}_{(\psi^4)_1}$ and $\mathcal{O}_{(\psi^4)_2}$ by $\mathcal{O}_{(\varphi^2F^2)_1}$ or $\mathcal{O}_{(\varphi^2F^2)_2}$. The cuts for these examples are depicted in Figure 3.8. While is may seem that there no reason to expect any given three-particle cut to evaluate to zero, it is possible that a detailed inspection may find that helicity

selection rules [7] or angular momentum selection rules [9] set certain cuts to zero. For a generic entry, the collection of these rules and the rules laid out in the sections above greatly simplify the calculation of the two-loop anomalous dimensions by eliminating one or more required unitary cuts, and one might expect that overlapping rules will conspire to eliminate all possible cuts and set additional entries in Table 3.4 to zero.

3.5 Implications for the SMEFT

The full SMEFT is more intricate than the simplified model adopted in this work, as it includes masses, multiple gauge groups and a number of additional operators. Still many of the results of our calculations provide nontrivial information about the structure of the anomalous dimension matrix of the SMEFT. In this section we describe the overlap of our theory with the SMEFT, and we explain how our results directly confirm a large number of the one-loop anomalous dimensions computed in Refs. [4]. We also comment on two-loop zeros and the coupling dependence of a subset of the two-loop anomalous-dimension matrix of the SMEFT.

3.5.1 Mapping our theory to the SMEFT

We now describe how the differences between our simplified model and SMEFT are taken into account to import the conclusions of our analysis to the SMEFT. First, the Standard Model spectrum contains massive particles, notably the Higgs, whose masses can affect the structure of the renomalization group running of both the Standard Model couplings and Wilson coefficients of the SMEFT. However, in this work we have focused on the mixing between dimension-six operators, which by dimensional analysis cannot depend on masses or other dimensionful parameters. In the presence of masses there can be additional mixing between operators of different dimensions, including modifications to the running of the Standard Model couplings, but these correspond to entries of the anomalous dimension matrix different

than those studied in this paper. The same holds for the finite renormalizations that were used to cancel certain one-loop matrix elements. Namely, in the presence of masses one might need to introduce finite renormalization of the Standard Model couplings to remove new local contributions to the one-loop matrix elements. Dimensional analysis ensures that this does not affect the structure of the two-loop dimension-six anomalous dimensions. In summary, the structure of the anomalous dimensions in our simplified model translates directly to the SMEFT, and our comparison and conclusions are unaffected by ignoring masses.

Compared to our simplified model the SMEFT also includes several gauge groups and additional higher-dimension operators. By keeping the gauge group to be a general $SU(N)$, and by leaving the identity of the fermions unspecified, we can still access many of the entries of the anomalous-dimension matrix in the full SMEFT basis of operators used by Refs. [4]. In particular, since the Higgs transforms under $SU(2)$, setting $N = 2$ and the number of scalars $N_s = 1$ allows us to map to anomalous dimensions or four-point amplitudes from representatives of any of the classes of operators in Ref. [4] other than the $\psi^2 F\varphi$ class ($\psi^2 XH$ in the notation of Ref. [4]). Since the scalar is in the fundamental representation that class necessarily involves both a left-handed fermion charged under $SU(2)$, as well as an uncharged right-handed fermion, which does not fit into our framework. By taking $N = 3$, parts of the anomalous dimensions in the SMEFT containing gluons can also be obtained. In principle, one can also compare anomalous dimensions for additional operators using more sophisticated embeddings of the Standard Model into $SU(N)$, including $U(1)$ charges (see e.g, Appendix IV of Ref. [51]), but we do not do so here.

By specifying the flavor of the fermions, we can map to a number of operators of the full basis used by Ref. [4] via different choices of gauge group and helicity. For example, by taking $N = 2$ and and left-handed helicity on the external states, we access the $SU(2)$ portions of the amplitudes involving the q and $\bar{q}$ quark doublets, and map onto the operators $(\bar{q}\gamma_\mu q)(\bar{q}\gamma^\mu q)$ and $(\bar{q}\gamma_\mu \tau^I q)(\bar{q}\gamma^\mu \tau^I q)$. One remaining difference in our approach compared to the full SMEFT is that we treat the fermions as Dirac instead of Weyl. This causes factor

of 2 differences in the N_f terms of the renormalization of $\mathcal{O}_{(D\varphi^2\psi^2)_2}$ and $\mathcal{O}_{(\psi^4)_2}$ compared to Ref. [4], which need to be taken into account when comparing. While our simplified model avoids having to deal with γ_5, the generalized unitarity method has been applied to such cases as well [29]. At one loop, the issue of Weyl versus Dirac fermions is reduced to a question of which helicities to take in the state sum in Eq. (3.24).

Setting aside the issue of Weyl versus Dirac fermions, mapping onto the four-fermion operators of Ref. [4], $(\bar{l}\gamma_\mu l)(\bar{l}\gamma^\mu l)$, $(\bar{u}\gamma_\mu u)(\bar{u}\gamma^\mu u)$, and $(\bar{d}\gamma_\mu d)(\bar{d}\gamma^\mu d)$ is possible as well, but requires some care, due to the presence of evanescent effects. In particular, for these cases the operator $\mathcal{O}_{(\psi^4)_2}$ is related to the operator $\mathcal{O}_{(\psi^4)_1}$ due to the $SU(N)$ Fierz identity (3.59)

$$(\bar{\psi}_m\gamma^\mu T^a\psi_n)(\bar{\psi}_p\gamma_\mu T^a\psi_r) = (\bar{\psi}_m\gamma^\mu\psi_n)(\bar{\psi}_p\gamma_\mu\psi_r)\left(\delta_{i_pi_n}\delta_{i_mi_r} - \frac{\delta_{i_mi_n}\delta_{i_pi_r}}{N}\right). \tag{3.76}$$

which, together with the Lorentz–Fierz relations for all left- or right-handed spinors

$$\begin{aligned}(\bar{\psi}^m_L\gamma^\mu\psi^n_L)(\bar{\psi}^p_L\gamma_\mu\psi^r_L) &= -(\bar{\psi}^p_L\gamma^\mu\psi^n_L)(\bar{\psi}^m_L\gamma_\mu\psi^r_L)\,,\\ (\bar{\psi}^m_R\gamma^\mu\psi^n_R)(\bar{\psi}^p_R\gamma_\mu\psi^r_R) &= -(\bar{\psi}^p_R\gamma^\mu\psi^n_R)(\bar{\psi}^m_R\gamma_\mu\psi^r_R)\,,\end{aligned} \tag{3.77}$$

(where we raised the flavor indices for convenience) can be applied to eliminate the need for the $\mathcal{O}_{(\psi^4)_2}$ operator in Table 3.1:

$$\mathcal{O}^{mnpr}_{(\psi^4)_2} = (\bar{\psi}_m\gamma^\mu T^a\psi_n)(\bar{\psi}_p\gamma_\mu T^a\psi_r) = \mathcal{O}^{mrpn}_{(\psi^4)_1} - \frac{1}{N}\mathcal{O}^{mnpr}_{(\psi^4)_1}\,, \tag{3.78}$$

when there are no additional group indices preventing the particle exchange (for example, the additional $SU(3)$ index prevents the reduction of $(\bar{q}\gamma^\mu\tau^I q)(\bar{q}\gamma_\mu\tau^I q)$ operator based on the $SU(2)$ Fierz identity). By choosing to implement Eq. (3.77) or not, we can map onto either the operators $(\bar{l}\gamma^\mu l)(\bar{l}\gamma_\mu l)$, $(\bar{u}\gamma^\mu u)(\bar{u}\gamma_\mu u)$, or $(\bar{d}\gamma^\mu d)(\bar{d}\gamma_\mu d)$, or onto the set of operators $(\bar{q}\gamma^\mu\tau^I q)(\bar{q}\gamma_\mu\tau^I q)$ and $(\bar{q}\gamma^\mu\tau^I q)(\bar{q}\gamma_\mu\tau^I q)$, respectively. Since we take all the fermions in our operators to be charged under the same gauge group, here we do not map onto the $(\bar{L}R)(\bar{L}R)$

	$\mathcal{O}_G$	$\mathcal{O}_W$	$\mathcal{O}_{HW}$	$\mathcal{O}_{H\Box}$ $\mathcal{O}_{HD}$	$\mathcal{O}_{Hl}^{(1)}$ $\mathcal{O}_{Hl}^{(3)}$	$\mathcal{O}_{Hq}^{(1)}$ $\mathcal{O}_{Hq}^{(3)}$	$\mathcal{O}_{ll}$	$\mathcal{O}_{qq}^{(1)}$ $\mathcal{O}_{qq}^{(3)}$	$\mathcal{O}_{uu}$ $\mathcal{O}_{dd}$
$\mathcal{O}_G$	✓$_3$	∅	∅	∅	∅	∅	∅	∅	∅
$\mathcal{O}_W$	∅	✓$_2$	✓$_2$	∅	∅	∅	∅	∅	∅
$\mathcal{O}_{HW}$	∅	✓$_2$	✓$_{2,\lambda}$	✓$_2$	✓$_2$	✓$_2$	∅	∅	∅
$\mathcal{O}_{H\Box}$, $\mathcal{O}_{HD}$	∅	✓$_2$	✓$_2$	✓$_{2,\lambda}$	✓$_2$	✓$_2$	∅	∅	∅
$\mathcal{O}_{Hl}^{(1)}$, $\mathcal{O}_{Hl}^{(3)}$	∅	✓$_2$	✓$_2$	✓$_2$	✓$_{2,\lambda}$	✓$_2$	✓$_2$	∅	∅
$\mathcal{O}_{Hq}^{(1)}$, $\mathcal{O}_{Hq}^{(3)}$	∅	✓$_2$	✓$_2$	✓$_2$	✓$_2$	✓$_{2,\lambda}$	∅	✓$_2$	∅
$\mathcal{O}_{ll}$	∅	✓$_2$	∅	∅	✓$_2$	∅	✓$_2$	∅	∅
$\mathcal{O}_{qq}^{(1)}$, $\mathcal{O}_{qq}^{(3)}$	✓$_3$	✓$_2$	∅	∅	∅	✓$_2$	∅	✓$_2$	∅
$\mathcal{O}_{uu}$, $\mathcal{O}_{dd}$	✓$_3$	∅	∅	∅	∅	∅	∅	∅	✓$_3$

Table 3.5: Checks on the one-loop anomalous dimensions calculated in Ref. [4] obtained from our calculations. The ∅ entries correspond to trivial cases were there are no contributing diagrams. The entries ✓$_3$ and ✓$_2$ are checked by setting the SU(N) group to SU(3) or SU(2), respectively. In both cases, only the pieces of the anomalous dimensions proportional to g_3^2 or g_2^2 are accessed by our amplitudes. The ✓$_{2,\lambda}$ cases indicates that both terms proportional to g_2^2 and λ are verified. Operators have been grouped according to whether the gauge dependence of the particle content is the same. As for the other tables, the operators labeling the rows are renormalized by the operators labeling the columns.

or $(\bar{L}R)(\bar{R}L)$ subsets of the four-fermion operators, which require the presence of multiple gauge groups.

It is worth noting, that there are some simplifications in the SMEFT relative to our model with general gauge group. The symmetric color tensor d^{abc} is zero in $SU(2)$, meaning that the operator $\mathcal{O}_{(\varphi^2F^2)_2}$ is identically zero. In addition, this implies the color factors for the two-vector, two-scalar or two-vector, two-fermion processes are related by $N\{T^{a_1}, T^{a_2}\}_{i_4 i_3} = 2\delta^{a_1 a_2}\delta_{i_4 i_3}$, meaning the number of color-ordered amplitudes is reduced for those processes in the case of $SU(2)$.

3.5.2 Verification of one-loop anomalous dimensions

From our one-loop calculations and the relations described above we have verified entries from numerous classes of operators in the SMEFT, as summarized in Table 3.5, following the notation of Ref. [4]. This includes examples proportional to g_3^2, g_2^2, and λ. In this sense our operators are a representative sample of the full SMEFT, despite the simplified nature of our dimension-four Lagrangian. The direct agreement with results of Ref. [4] displayed in Table 3.5 provides a highly non-trivial check of the validity and the effectiveness of the approach used here.

3.5.3 Two-loop implications

Next we briefly discuss the implications of the zeros in the two-loop anomalous dimensions of our simplifies model for the SMEFT. The selection rules of Section 3.4 set a number of entries strictly to zero, and restrict the coupling dependence of others. Our findings are summarized in Table 3.6. The full SMEFT anomalous dimensions include dependence on the Yukawa couplings, which are absent in our simplified theory, so some of the zeros uncovered above may be replaced by anomalous dimensions that depend on such couplings. Nevertheless, our results show that the coupling dependence of the anomalous dimensions is simpler than one might have expected, and that some of the entries are zero or do not have pure dependence on the gauge couplings. Though most of the strictly zero examples rely on the length selection rule, which does not depend on the gauge group or the presence of Yukawa couplings, the anomalous-dimension matrix element $\gamma^{(2)}_{HW\leftarrow qq}$ relies solely on the color selection rules. In this case, including Yukawa and U(1) couplings will not affect this zero, as the cuts still cannot match the color of the target operator.

In addition to the zeros, we find that many of the entries only receive contributions from either three- or two-particle cuts, which should greatly simplify their computation. One interesting example is the element $\gamma^{(2)}_{qq\leftarrow HW}$, which only has a three-particle cut due to the

vanishing of the one-loop amplitudes that would contribute to the two-particle cut. For this example, we have also checked the one-loop amplitudes with Yukawa and U(1) couplings do not contribute. As can also be seen in Table 3.6, many entries vanish when the Yukawa couplings are set to zero. Many of these zeros are trivial due to the particle content of the operators involved, but in some cases a closer examination of the diagrams is required to see that only diagrams with Yukawa couplings will produce nonvanishing results.

Note that the operators in Table 3.6 are merely a representative set, in that all of the operators of the SMEFT are restricted by one or more of our selection rules, either in terms of which operators they can renormalize, or vice versa. In particular, the length selection rules apply independently of the gauge group or the presence of Yukawa couplings, which allows us to include operators of the classes $\psi^2 F\varphi$ and $\psi^2\varphi^3$ in Table 3.6. We would also like to stress that our analysis of the structure of the two-loop anomalous dimensions is not an exhaustive study of the SMEFT anomalous dimensions. For this reason, we expect that there could be additional vanishings or structures that can be uncovered under closer scrutiny.

3.6 Conclusions

In this paper we applied on-shell methods to investigate the structure of the two-loop anomalous dimension matrix of dimension-six operators, in both a simplified model and in the SMEFT. At one loop, we used both the standard generalized unitarity method [11] and the recently developed approach for extracting anomalous dimensions directly from unitarity cuts [12]. At two loops, we find the latter method to be especially effective, with the former method providing one-loop amplitudes as inputs. As an initial step, we reorganized the basic equation for the two-loop anomalous dimension in the latter approach so as to simplify one-loop iterations. Using this equation, we revealed a number of vanishing contributions in the two-loop anomalous dimension matrix of the SMEFT. Our analysis was based on

a simplified model without U(1) or Yukawa interactions. Nevertheless, as summarized in Table 3.6, by analyzing the overlap of our simplified model with the SMEFT we found that a remarkable number of SMEFT two-loop anomalous dimensions either vanish or have a simpler dependence on the Standard Model couplings than naively expected.

The structure we uncovered has a number of origins, including length selection rules, color selection rules, and zeros in the one-loop amplitudes with dimension-six operator insertions. Additional zeros arise from the choice of an $\bar{\text{MS}}$-like scheme which includes additional finite renormalizations designed to set various rational terms in one-loop amplitudes to zero. This suggests that there exist interesting schemes that make the structure of the renormalization-group running beyond one loop more transparent. The full implications of choosing such schemes clearly deserve further study.

Since one-loop amplitudes are used as input for the two-loop calculation, we have computed the full set of four-point amplitudes with dimension-six operator insertions in our simplified version of the SMEFT. As a byproduct, these amplitudes have allowed us to verify a large subset of the one-loop anomalous dimensions calculated in Refs. [4].

The zeros that we found in the two-loop anomalous dimension matrix relied on choosing examples with trivial infrared dependence, as well as a lack of a three-particle cut. However, the methods can be applied just as well to any generic anomalous dimension matrix element at two or higher loops. It would be interesting to investigate whether there are additional zeros at two loops beyond those we identified. The large number of zeros in the one-loop amplitudes restrict the number of cuts that can contribute, suggesting that other mechanisms, such as helicity or angular-momentum selection rules, may set the remaining cuts to zero in some cases.

The presented methods are quite general, and should be applicable to general EFTs. In addition, while we have focused on ultraviolet anomalous dimensions here, this method could equally be applied to the evaluation of infrared anomalous dimensions, such as the soft anomalous dimension, by the use of ultraviolet protected operators such as the stress-tensor

or global symmetry currents. It would also be interesting to understand the implications, if any, of the vanishing of two-loop anomalous dimensions for the interference of Standard Model and higher-dimension operator matrix elements beyond tree level, in the presence of experimental cuts. Another obvious direction would be to include dimension seven and eight operators into the analysis [52].

The conclusions of the present work are unchanged by the presence of masses, as these only affect a different set of entries in the anomalous dimension matrix that relate operators of differing dimension. Studying such entries will require revisiting the proof of the length selection rules, since formerly scaleless integrals can have a UV divergence proportional to a mass, which generates running for operators of lower dimension. Additionally, masses allow additional logarithms of the form $\log(\mu/m)$, whose coefficient is not captured by traditional unitarity cuts. It would be interesting to study possible extensions of our formalism to capture these effects and explore the structure of that sector of the anomalous dimension matrix.

In summary, we have demonstrated that the on-shell methods applied here are well suited for computing anomalous dimensions and associated scattering amplitudes at one and two loops. We used these methods to expose new structures in the guise of vanishing terms in the anomalous matrix of the SMEFT beyond one loop. Our analysis here was not exhaustive, so it is likely that further vanishing contributions and new structures exist at two loops and beyond. Our results also suggest that a judicious choice of renormalization scheme can help expose such structures.

3.A Integral reduction via gauge-invariant tensors

In this appendix we summarize the projection technique that we use to perform tensor reduction of loop integrals in Section 3.3. The same technique has been previously used in Refs. [31, 32] and is a convenient method for decomposing D-dimensional tensor loop integrands (or cuts) into a basis of scalar master integrals, in a way that makes dimensional regularization, and any associated chiral and evanescent issues relatively straightforward. In particular this technique is well suited to deal with integrals with high-rank numerators, which naturally arise in loop amplitudes with insertions of higher-dimension operators.

We start by noting that scattering amplitudes amplitudes are gauge invariant and can therefore be decomposed into a basis of gauge-invariant tensors, T_m. For a given amplitude labeled by i we have,

$$A_i^{(L)} = \sum_m \mathcal{A}_{i,m}^{(L)}(k_j) T_m(k_j, \epsilon_j, u_j, \bar{u}_j)\,, \tag{3.79}$$

where the coefficients, $\mathcal{A}_{i,m}^{(L)}$, only depend on the external momenta, and all dependence on the polarization vectors or spinors is contained entirely within the basis tensors, T_m. The basis tensors for the various processes we consider in this paper are given below and in the supplementary material [34]. They are found by writing down the most general polynomials built from Lorentz invariant products of external polarizations, spinor and momenta and then demanding gauge invariance.

The desired coefficient of tensor T_j can be extracted using a projector

$$P_n = c_{nm} T_m^*\,, \tag{3.80}$$

where c_{nm} is the inverse of the matrix

$$m_{nm} = T_n^* \odot T_m\,. \tag{3.81}$$

Here the product $\odot$ corresponds to the state sum in Eq. (3.41), taken over all particles. The coefficient of the tensor is then simply given by

$$\mathcal{A}^{(L)}_{i,m} = P_m \odot A^{(L)}_i \,. \tag{3.82}$$

The projectors for all processes consider in this paper are given explicitly in an ancillary file [34].

Once projected, any gauge invariant quantity can be summarized as a list of the coefficients corresponding to each basis tensor. In the case of a loop integrand or cut thereof, each coefficient is a rational function of scalar propagators and inverse propagators (and irreducible numerators beyond one loop). The integrals corresponding to each term in the projected quantity are then in a form that can be reduced to a basis of master integrals using by integration by parts (IBP) relations. This can be done using by using IBP programs such as FIRE [33].

As described in Section 3.3, we can apply this procedure cut by cut to determine the coefficients of each gauge invariant tensor in the full amplitude.

Basis tensors

Basis tensors for the four-vector amplitudes are taken from [32], which we reproduce here. Beginning with the linearized field strength for each external particle:

$$F_{i\,\mu\nu} \equiv k_{i\,\mu}\varepsilon_{i\,\nu} - k_{i\,\nu}\varepsilon_{i\,\mu}\,, \tag{3.83}$$

one can construct the following combinations,

$$\begin{aligned} F^4_{st} &\equiv (F_1F_2F_3F_4)\,, & F^4_{tu} &\equiv (F_1F_4F_2F_3)\,, & F^4_{us} &\equiv (F_1F_3F_4F_2)\,, \\ (F^2_s)^2 &\equiv (F_1F_2)(F_3F_4)\,, & (F^2_t)^2 &\equiv (F_1F_4)(F_2F_3)\,, & (F^2_u)^2 &\equiv (F_1F_3)(F_4F_2)\,, \end{aligned} \tag{3.84}$$

where parentheses one the right-hand side of the above equations indicate taking the trace over adjacent Lorentz indices. The four-vector basis tensors are then given by

$$\begin{aligned}
T^{\text{tree}}_{vvvv} &= -\frac{1}{2}((F^2_s)^2 + (F^2_t)^2 + (F^2_u)^2) + 2\,(F^4_{st} + F^4_{tu} + F^4_{us})\,, \\
T^{++++}_{vvvv} &= -2\,F^4_{st} + \frac{1}{2}\,((F^2_s)^2 + (F^2_t)^2 + (F^2_u)^2)\,, \\
T^{-+++}_{vvvv} &= -T_{F^3} - (F^4_{tu} - F^4_{us})\,(s-t) + (F^4_{st} - \frac{1}{4}((F^2_s)^2 + (F^2_t)^2 + (F^2_u)^2))\,(s+t)\,, \\
T^{--++}_{vvvv} &= (F^2_s)^2 - (F^2_t)^2 + 2\,(F^4_{tu} - F^4_{us})\,, \\
T^{-+-+}_{vvvv} &= 2\,F^4_{st} - \frac{1}{2}((F^2_s)^2 + (F^2_t)^2 - (F^2_u)^2)\,, \\
T^{\text{ev1}}_{vvvv} &= -(2\,F^4_{st} + \frac{3}{2}\,((F^2_s)^2 + (F^2_t)^2 + (F^2_u)^2))\,(s+t) + 2\,(F^4_{us}\,(3\,s+t) + F^4_{tu}\,(s+3\,t))\,, \\
T^{\text{ev2}}_{vvvv} &= -(2\,F^4_{st} - \frac{1}{2}((F^2_s)^2 + (F^2_t)^2 + (F^2_u)^2))\,(s-t) + 2\,(F^4_{tu} - F^4_{us})\,(s+t)\,,
\end{aligned} \tag{3.85}$$

where the v labels signifies that a leg is a vector boson, and T_{F^3} is proportional to the F^3 amplitude [53]:

$$T_{F^3} = -istA^{(0)}_{F^3} = -istu\left(\frac{(F^2_s)^2}{4s^2} + \frac{(F^2_t)^2}{4t^2} + \frac{(F^2_u)^2}{4u^2} - \frac{g_1g_2g_3g_4}{(stu)^2}\right)\,, \tag{3.86}$$

where $g_i \equiv (k_{i+1}F_ik_{i-1})$. We note that we have written this expression in an explicitly gauge-invariant form at the expense of manifest locality. These tensors are nonzero only under the indicated (and parity conjugate) helicity configurations, along with cyclic permutations. T^{tree}_{vvvv} is nonzero for helicities $(1^-2^+3^-4^+)$, $(1^-2^-3^+4^+)$, and cyclic permutations. T^{ev1}_{vvvv} and T^{ev2}_{vvvv} are evanescent, i.e. zero for all helicity configurations in four dimensions. This can be made manifest by rewriting them as

$$\begin{aligned}
T^{\text{ev1}}_{vvvv} &= \frac{1}{2}k_4^{[\alpha}F_1^{\mu\nu}F_2^{\sigma\rho]}k_{2\alpha}F_{4\mu\nu}F_{3\sigma\rho} + \frac{1}{2}k_4^{[\alpha}F_3^{\mu\nu}F_2^{\sigma\rho]}k_{2\alpha}F_{4\mu\nu}F_{1\sigma\rho}\,, \\
T^{\text{ev2}}_{vvvv} &= \frac{1}{2}k_2^{[\alpha}F_1^{\mu\nu}F_3^{\sigma\rho]}k_{1\alpha}F_{2\mu\nu}F_{4\sigma\rho}\,,
\end{aligned} \tag{3.87}$$

where the anti-symmetrization does not include a symmetry factor.

The two-vector, two-scalar tensors are also nonzero under specific helicity combinations, and are given by

$$T^{+-}_{vvss} = 2(k_3 F_1 F_2 k_4) + 2(k_4 F_1 F_2 k_3) - (k_3 \cdot k_4)(F_1 F_2)\,, \quad T^{++}_{vvss} \quad = -(F_1 F_2)\,, \tag{3.88}$$

where the v and s labels specify the corresponding legs are vectors or scalars.

Similarly, the two-vector, two-fermion tensors are linear combinations of those in Ref. [31], chosen to again be nonzero only under specific helicities:

$$\begin{aligned}
T^{-+++}_{ffvv} &= -\frac{1}{2^4}(\bar{u}_2 \not{F}_4 \not{F}_3 \not{k}_2 u_1)\,, \qquad T^{-+-+}_{ffvv} = -\frac{1}{2^4}(\bar{u}_2 \not{F}_4 \not{k}_2 \not{F}_3 u_1)\,, \\
T^{-++-}_{ffvv} &= -\frac{1}{2^4}(\bar{u}_2 \not{F}_3 \not{k}_1 \not{F}_4 u_1)\,, \qquad T^{-+--}_{ffvv} = -\frac{1}{2^4}(\bar{u}_2 \not{k}_1 \not{F}_4 \not{F}_3 u_1)\,, \\
T^{\rm ev}_{ffvv} &= \frac{1}{2} k_1^{[\alpha} F_3^{\mu\nu} F_4^{\rho\sigma]} (\bar{u}_2 \gamma_\alpha \gamma_\mu \gamma_\nu \gamma_\rho \gamma_\sigma u_1)\,,
\end{aligned} \tag{3.89}$$

where f now indicates a leg as a fermion, $\not{F}_i = F_{i\,\mu\nu}\gamma^\mu\gamma^\nu$, and the antisymmetrization in $T^{\rm ev}$ includes a symmetry factor of 1/5!. As for the four-vector case, we encounter an evanescent tensor, $T^{\rm ev}_{ffvv}$ which vanishes for all four-dimensional helicities. For the two-fermion two-scalar case there is only a single basis tensor:

$$T_{ffss} = \bar{u}_2 \not{k}_3 u_1\,. \tag{3.90}$$

Finally, the four-fermion tensors are,

$$\begin{aligned}
T^1_{ffff} &= (\bar{u}_2 \gamma^\mu u_1)(\bar{u}_4 \gamma_\mu u_3)\,, \\
T^2_{ffff} &= (\bar{u}_2 \not{k}_4 u_1)(\bar{u}_4 \not{k}_2 u_3)\,, \\
T^3_{ffff} &= (\bar{u}_2 \gamma^\mu \gamma^\nu \gamma^\rho u_1)(\bar{u}_4 \gamma_\mu \gamma_\nu \gamma_\rho u_3) - 16(\bar{u}_2 \gamma^\mu u_1)(\bar{u}_4 \gamma_\mu u_3)\,, \\
T^4_{ffff} &= t\,(\bar{u}_2 \gamma^\mu \not{k}_4 \gamma^\rho u_1)(\bar{u}_4 \gamma_\mu \not{k}_2 \gamma_\rho u_3) - 4u(\bar{u}_2 \not{k}_4 u_1)(\bar{u}_4 \not{k}_2 u_3)\,,
\end{aligned} \tag{3.91}$$

plus those given by the exchange of legs 2 and 4. It should be noted, however, that in practice it is unnecessary to calculate the coefficients of the exchanged tensors, since they are fixed by the symmetry of the contributing diagrams. T^3_{ffff} and T^4_{ffff} are chosen to be zero for the helicity configuration $1^+_\psi 2^-_{\overline{\psi}} 3^+_\psi 4^-_{\overline{\psi}}$ and its conjugate, so that these tensors are evanescent if the spinors are Weyl of the same handedness.

3.B Tree-level and one-loop amplitudes

In this appendix we collect tree- and one-loop amplitudes. In addition to the spinor-helicity amplitudes given below, expressions that are valid to all orders in the dimensional regularization parameter ϵ are provided in a supplementary file [34]. While we do not require one-loop amplitudes without higher-dimension operators for our specific examples in Section 3.4, they would be required for the calculation of a generic two-loop anomalous dimension matrix element. These one-loop dimension-4 amplitudes can be found in various references; e.g. Refs. [54] gives the relevant amplitudes which exclude scalars.

The amplitudes and form factors can be written as vectors in color space,

$$A^{(L)}(\lambda_1\lambda_2\lambda_3\lambda_4) = S_{\lambda_1\lambda_2\lambda_3\lambda_4} \sum_i \mathcal{C}^{[i]}_{\lambda_1\lambda_2\lambda_3\lambda_4} A^{(L)}(\lambda_1\lambda_2\lambda_3\lambda_4)_{[i]}\,, \tag{3.92}$$

where $S_{\lambda_1\lambda_2\lambda_3\lambda_4}$ is a helicity-dependent factor which which depending on spinors when evaluated using four-dimensional spinor helicity. These factors are pure phases for the amplitudes with an even number of pairs of external fermions, and for the amplitudes with an odd number of fermions their square is a dimensionless ratio of s, t, or u and powers thereof. The full list of $S_{\lambda_1\lambda_2\lambda_3\lambda_4}$ for each process is listed below.

The IR dependence has been stripped from the amplitudes below, but can be recon-

structed, if desired, using the basic IR formulas given in the text, which we reproduce here:

$$A_i^{(1)} = \boldsymbol{I}^{(1)} A_i^{(0)} + A_i^{(1)\text{fin}}\,, \tag{3.93}$$

where the IR operator $\boldsymbol{I}^{(1)}$ is given by

$$\boldsymbol{I}^{(1)} = \frac{e^{\epsilon\gamma_E}}{\Gamma(1-\epsilon)} \sum_{p=1}^{n} \sum_{q\neq p} \frac{\boldsymbol{T}_p \cdot \boldsymbol{T}_q}{2} \left[\frac{\gamma_{\text{cusp}}^{\text{IR}\,(1)}}{\epsilon^2} - \frac{\gamma_{\text{c},\,p}^{\text{IR}\,(1)}}{\boldsymbol{T}_p^2} \frac{1}{\epsilon} \right] \left(\frac{-\mu^2}{2k_p \cdot k_q} \right)^{\epsilon}, \tag{3.94}$$

with

$$\gamma_{\text{cusp}}^{\text{IR}\,(1)} = \tilde{g}^2 4\,, \quad \gamma_{\text{c},\,v}^{\text{IR}\,(1)} = -\tilde{g}^2 b_0\,, \quad \gamma_{\text{c},\,f}^{\text{IR}\,(1)} = -\tilde{g}^2 3C_F\,, \quad \gamma_{\text{c},\,s}^{\text{IR}\,(1)} = -\tilde{g}^2 4C_F\,. \tag{3.95}$$

Explicit evaluations of $\boldsymbol{I}^{(1)}$ for various processes can be found, for example, in Refs. [31, 48]. All results below are reported in the Euclidean region and the $\bar{\text{MS}}$ scheme. As a shorthand, logarithms are given by:

$$\begin{gathered} X^2 = \log\left(\frac{s}{t}\right)^2 + \pi^2, \qquad Y^2 = \log\left(\frac{s}{u}\right)^2 + \pi^2, \qquad Z^2 = \log\left(\frac{u}{t}\right)^2 + \pi^2, \\ X_s = \log\left(\frac{\mu^2}{-s}\right), \qquad X_t = \log\left(\frac{\mu^2}{-t}\right), \qquad X_u = \log\left(\frac{\mu^2}{-u}\right). \end{gathered} \tag{3.96}$$

In general we drop the Wilson coefficients, for example c_{F^3} for amplitudes with an $\mathcal{O}_{F^3}$ insertion, since it is in this form that the amplitudes are used in Eq. (3.37). However we have contracted the Wilson coefficients with the amplitudes for operators which include fermions, since doing so simplifies the flavor information for these cases.

3.B.1 Four-vector amplitudes

The color factors for the four-vector amplitudes are

$$\begin{aligned}
\mathcal{C}^{[1]}_{vvvv} &= \mathrm{Tr}[T^1T^2T^3T^4]\,, \qquad \mathcal{C}^{[2]}_{vvvv} = \mathrm{Tr}[T^1T^3T^2T^4]\,,\\
\mathcal{C}^{[3]}_{vvvv} &= \mathrm{Tr}[T^1T^2T^4T^3]\,, \qquad \mathcal{C}^{[4]}_{vvvv} = \mathrm{Tr}[T^1T^4T^2T^3]\,,\\
\mathcal{C}^{[5]}_{vvvv} &= \mathrm{Tr}[T^1T^3T^4T^2]\,, \qquad \mathcal{C}^{[6]}_{vvvv} = \mathrm{Tr}[T^1T^4T^3T^2]\,,\\
\mathcal{C}^{[7]}_{vvvv} &= \mathrm{Tr}[T^1T^2]\,\mathrm{Tr}[T^3T^4]\,, \quad \mathcal{C}^{[8]}_{vvvv} = \mathrm{Tr}[T^1T^3]\,\mathrm{Tr}[T^2T^4]\,, \quad \mathcal{C}^{[9]}_{vvvv} = \mathrm{Tr}[T^1T^4]\,\mathrm{Tr}[T^2T^3]\,,
\end{aligned} \tag{3.97}$$

where only two partial amplitudes—one single-trace and one double-trace—are independent in general, and the rest are given by relabelings.

We remove dimensionless prefactors from the helicity amplitudes. These are all phases except for the amplitudes involving only one pair of fermions. For the four-vector amplitudes, the spinor prefactors are are given by

$$\begin{aligned}
S(1^+2^+3^+4^+) &= \frac{[12][34]}{\langle 12\rangle\langle 34\rangle}\,, \qquad S(1^-2^+3^+4^+) = \frac{\langle 12\rangle\langle 14\rangle[24]}{\langle 23\rangle\langle 24\rangle\langle 34\rangle}\,,\\
S(1^-2^-3^+4^+) &= \frac{\langle 12\rangle[34]}{\langle 34\rangle[12]}\,, \qquad S(1^-2^+3^-4^+) = \frac{\langle 13\rangle[24]}{\langle 24\rangle[13]}\,.
\end{aligned} \tag{3.98}$$

The tree-level D-dimensional amplitudes are given by

$$\begin{aligned}
A^{(0)}(1234)_{[1]} &= \frac{-g^2}{st}T^{\mathrm{tree}}_{vvvv}\,,\\
A^{(0)}(1234)_{[7]} &= 0\,,\\
A^{(0)}_{F^3}(1234)_{[1]} &= \frac{g}{2stu}\left(4stT^{++++}_{vvvv} - 2uT^{-+++}_{vvvv} + (s-t)T^{\mathrm{ev2}}_{vvvv}\right)\,,\\
A^{(0)}_{F^3}(1234)_{[7]} &= 0\,,
\end{aligned} \tag{3.99}$$

which have four-dimensional helicity values

$$
\begin{aligned}
&A^{(0)}(1^-2^+3^+4^+)_{[1]} = A^{(0)}(1^=2^+3^+4^+)_{[1]} = 0\,,\\
&A^{(0)}(1^-2^-3^+4^+)_{[1]} = -\frac{g^2 s}{t}\,,\\
&A^{(0)}(1^-2^+3^-4^+)_{[1]} = -\frac{g^2 u^2}{st}\,,\\
&A^{(0)}(1^\pm 2^\pm 3^\pm 4^\pm)_{[7]} = 0\,,
\end{aligned}
\tag{3.100}
$$

$$
\begin{aligned}
&A^{(0)}_{F^3}(1^+2^+3^+4^+)_{[1]} = 2gs\,,\\
&A^{(0)}_{F^3}(1^-2^+3^+4^+)_{[1]} = -gu\,,\\
&A^{(0)}_{F^3}(1^-2^-3^+4^+)_{[1]} = A^{(0)}_{F^3}(1^-2^+3^-4^+)_{[1]} = 0\,,\\
&A^{(0)}_{F^3}(1^\pm 2^\pm 3^\pm 4^\pm)_{[7]} = 0\,.
\end{aligned}
\tag{3.101}
$$

The one-loop amplitudes with one insertion of the F^3 operator are

$$
\begin{aligned}
A^{(1)\text{fin}}_{F^3}(1^+2^+3^+4^+)_{[1]} &= g\tilde{g}^2\big((4N(t-u)+2ub_0)X_s + (4N(s-u)+2ub_0)X_t\\
&\qquad - \frac{1}{2}(44N+2N_f-N_s)u\big)\,,\\
A^{(1)\text{fin}}_{F^3}(1^-2^+3^+4^+)_{[1]} &= g\tilde{g}^2\Big(N\frac{u^2-st}{u}X^2\\
&\qquad + (2N(t-u)+b_0u)X_s + (2N(s-u)+b_0u)X_t - 12u\Big)\,,\\
A^{(1)}_{F^3}(1^-2^+3^-4^+)_{[1]} &= 0\,,\\
A^{(1)}_{F^3}(1^-2^-3^+4^+)_{[1]} &= \frac{g\tilde{g}^2}{6}\left(4N(u-s)-(2N_f-N_s)(u-t)\right)\,,
\end{aligned}
\tag{3.102}
$$

where $\tilde{g}^2 = g^2/(4\pi)$ as defined in Eq.(3.5), and $b_0 = (11N - 2N_f - N_s/2)/3$. The double-trace amplitudes with an $\mathcal{O}_{F^3}$ insertion are given by the $U(1)$ decoupling identity

$$
A^{(1)}_{F^3}(1234)_{[7]} = \frac{1}{N}\left(A^{(1)}_{F^3}(1234)_{[1]} + A^{(1)}_{F^3}(1243)_{[1]} + A^{(1)}_{F^3}(1423)_{[1]}\right)\,. \tag{3.103}
$$

The amplitudes with one insertion of a $\varphi^2 F^2$ operators are

$$
\begin{aligned}
&A^{(1)}_{(\varphi^2F^2)_1}(1^{\pm}2^{\pm}3^{\pm}4^{\pm})_{[1]} = 0\,,\\
&A^{(1)}_{(\varphi^2F^2)_1}(1^{+}2^{+}3^{+}4^{+})_{[7]} = 4\tilde{g}^2N_s s\,,\\
&A^{(1)}_{(\varphi^2F^2)_1}(1^{-}2^{+}3^{+}4^{+})_{[7]} = A^{(1)}_{(\varphi^2F^2)_1}(1^{-}2^{+}3^{-}4^{+})_{[7]} = 0\,,\\
&A^{(1)}_{(\varphi^2F^2)_1}(1^{-}2^{-}3^{+}4^{+})_{[7]} = 4\tilde{g}^2N_s s\,,\\
&A^{(1)}_{(\varphi^2F^2)_2}(1^{+}2^{+}3^{+}4^{+})_{[1]} = -2\tilde{g}^2N_s u\,,\\
&A^{(1)}_{(\varphi^2F^2)_2}(1^{-}2^{+}3^{+}4^{+})_{[1]} = A^{(1)}_{(\varphi^2F^2)_2}(1^{-}2^{+}3^{-}4^{+})_{[1]} = 0\,,\\
&A^{(1)}_{(\varphi^2F^2)_2}(1^{-}2^{-}3^{+}4^{+})_{[1]} = 2\tilde{g}^2N_s s\,,\\
&A^{(1)}_{(\varphi^2F^2)_2}(1^{+}2^{+}3^{+}4^{+})_{[7]} = A^{(1)}_{(\varphi^2F^2)_2}(1^{-}2^{-}3^{+}4^{+})_{[7]} = -\frac{4\tilde{g}^2N_s s}{N}\,,\\
&A^{(1)}_{(\varphi^2F^2)_2}(1^{-}2^{+}3^{+}4^{+})_{[7]} = A^{(1)}_{(\varphi^2F^2)_2}(1^{-}2^{+}3^{-}4^{+})_{[7]} = 0\,.
\end{aligned}
\tag{3.104}
$$

3.B.2 Four-fermion amplitudes

The color structures for the four-fermion amplitudes are

$$
\mathcal{C}^{[1]}_{ffff} = T^a_{i_2 i_1}T^a_{i_4 i_3}\,, \qquad \mathcal{C}^{[2]}_{ffff} = T^a_{i_4 i_1}T^a_{i_2 i_3}\,. \tag{3.105}
$$

Note for any operator, due to the anti-symmetry of the amplitudes under exchange of (anti-)fermions:

$$
\begin{aligned}
&A^{(L)}_{\mathcal{O}}(1^{+}_{\psi_m}2^{-}_{\bar{\psi}_n}3^{+}_{\psi_p}4^{-}_{\bar{\psi}_r})_{[2]} = -A^{(L)}_{\mathcal{O}}(1^{+}_{\psi_m}2^{-}_{\bar{\psi}_r}3^{+}_{\psi_p}4^{-}_{\bar{\psi}_n})_{[1]}\ (s\leftrightarrow t)\,,\\
&A^{(L)}_{\mathcal{O}}(1^{+}_{\psi_m}2^{-}_{\bar{\psi}_n}3^{-}_{\psi_p}4^{+}_{\bar{\psi}_r})_{[2]} = -A^{(L)}_{\mathcal{O}}(1^{+}_{\psi_m}2^{+}_{\bar{\psi}_r}3^{-}_{\psi_p}4^{-}_{\bar{\psi}_n})_{[1]}\ (s\leftrightarrow t)\,,\\
&A^{(L)}_{\mathcal{O}}(1^{+}_{\psi_m}2^{+}_{\bar{\psi}_n}3^{-}_{\psi_p}4^{-}_{\bar{\psi}_r})_{[2]} = -A^{(L)}_{\mathcal{O}}(1^{+}_{\psi_m}2^{-}_{\bar{\psi}_r}3^{-}_{\psi_p}4^{+}_{\bar{\psi}_n})_{[1]}\ (s\leftrightarrow t)\,.
\end{aligned}
\tag{3.106}
$$

The overall spinor phases are

$$S(1^+_\psi 2^-_{\bar\psi}\, 3^+_\psi 4^-_{\bar\psi}) = \frac{\langle 24\rangle[12]}{\langle 34\rangle[24]}\,, \qquad S(1^+_\psi 2^-_{\bar\psi}\, 3^-_\psi 4^+_{\bar\psi}) = \frac{\langle 23\rangle[12]}{\langle 34\rangle[23]}\,,$$
$$S(1^+_\psi 2^+_{\bar\psi}\, 3^-_\psi 4^-_{\bar\psi}) = \frac{[12]}{[34]}\,. \tag{3.107}$$

The tree-level D-dimensional amplitudes are given by

$$\begin{aligned}
A^{(0)}(1_{\psi_m} 2_{\bar\psi_n} 3_{\psi_p} 4_{\bar\psi_r})_{[1]} &= g^2 \frac{u_2\gamma^\mu u_1\ \bar u_4\gamma_\mu u_3}{2s}\delta_{mn}\delta_{pr}\,,\\
A^{(0)}_{(\psi^4)_1}(1_{\psi_m} 2_{\bar\psi_n} 3_{\psi_p} 4_{\bar\psi_r})_{[1]} &= \frac{N}{N^2-1}(c^{nmrp}_{(\psi^4)_1} u_2\gamma^\mu u_1\ \bar u_4\gamma_\mu u_3 - c^{rmnp}_{(\psi^4)_1} N u_4\gamma^\mu u_1\ \bar u_2\gamma_\mu u_3)\,,\\
A^{(0)}_{(\psi^4)_2}(1_{\psi_m} 2_{\bar\psi_n} 3_{\psi_p} 4_{\bar\psi_r})_{[1]} &= c^{nmrp}_{(\psi^4)_2} u_2\gamma^\mu u_1\ \bar u_4\gamma_\mu u_3\,,
\end{aligned} \tag{3.108}$$

which have four-dimensional values

$$\begin{aligned}
A^{(0)}(1^+_{\psi_m} 2^-_{\bar\psi_n} 3^+_{\psi_p} 4^-_{\bar\psi_r})_{[1]} &= \frac{g^2 u}{s}\delta_{mn}\delta_{pr}\,,\\
A^{(0)}(1^+_{\psi_m} 2^-_{\bar\psi_n} 3^-_{\psi_p} 4^+_{\bar\psi_r})_{[1]} &= -\frac{g^2 t}{s}\delta_{mn}\delta_{pr}\,,\\
A^{(0)}(1^+_{\psi_m} 2^+_{\bar\psi_n} 3^-_{\psi_p} 4^-_{\bar\psi_r})_{[1]} &= 0\,,\\
A^{(0)}_{(\psi^4)_1}(1^+_{\psi_m} 2^-_{\bar\psi_n} 3^+_{\psi_p} 4^-_{\bar\psi_r})_{[1]} &= -\frac{2Nu(Nc^{rmnp}_{(\psi^4)_1} + c^{nmrp}_{(\psi^4)_1})}{N^2-1}\,,\\
A^{(0)}_{(\psi^4)_1}(1^+_{\psi_m} 2^-_{\bar\psi_n} 3^-_{\psi_p} 4^+_{\bar\psi_r})_{[1]} &= \frac{2Ntc^{nmrp}_{(\psi^4)_1}}{N^2-1}\,,\\
A^{(0)}_{(\psi^4)_1}(1^+_{\psi_m} 2^+_{\bar\psi_n} 3^-_{\psi_p} 4^-_{\bar\psi_r})_{[1]} &= \frac{2N^2 sc^{nmrp}_{(\psi^4)_1}}{N^2-1}\,,\\
A^{(0)}_{(\psi^4)_2}(1^+_{\psi_m} 2^-_{\bar\psi_n} 3^+_{\psi_p} 4^-_{\bar\psi_r})_{[1]} &= -2uc^{nmrp}_{(\psi^4)_2}\,,\\
A^{(0)}_{(\psi^4)_2}(1^+_{\psi_m} 2^-_{\bar\psi_n} 3^-_{\psi_p} 4^+_{\bar\psi_r})_{[1]} &= 2tc^{nmrp}_{(\psi^4)_2}\,,\\
A^{(0)}_{(\psi^4)_2}(1^+_{\psi_m} 2^+_{\bar\psi_n} 3^-_{\psi_p} 4^-_{\bar\psi_r})_{[1]} &= 0\,.
\end{aligned} \tag{3.109}$$

The amplitudes with one insertion of the F^3 operator are

$$
\begin{aligned}
A^{(1)}_{F^3}(1^+_{\psi_m}2^-_{\bar\psi_n}3^+_{\psi_p}4^-_{\bar\psi_r})_{[1]} &= \frac{1}{3}g\tilde g^2 u\delta_{mn}\delta_{pr}\,,\\
A^{(1)}_{F^3}(1^+_{\psi_m}2^-_{\bar\psi_n}3^-_{\psi_p}4^+_{\bar\psi_r})_{[1]} &= -\frac{1}{3}g\tilde g^2 t\delta_{mn}\delta_{pr}\,,\\
A^{(1)}_{F^3}(1^+_{\psi_m}2^+_{\bar\psi_n}3^-_{\psi_p}4^-_{\bar\psi_r})_{[1]} &= 0\,.
\end{aligned}
\tag{3.110}
$$

The amplitudes with one insertion of a $D\varphi^2\psi^2$ operator are

$$
\begin{aligned}
A^{(1)}_{(D\varphi^2\psi^2)_1}(1^\pm_{\psi_m}2^\pm_{\bar\psi_n}3^\pm_{\psi_p}4^\pm_{\bar\psi_r})_{[1]} &= 0\,,\\
A^{(1)}_{(D\varphi^2\psi^2)_2}(1^+_{\psi_m}2^-_{\bar\psi_n}3^+_{\psi_p}4^-_{\bar\psi_r})_{[1]} &= -\frac{1}{9}\tilde g^2 N_s(3X_s+8)u(c^{rp}_{(D\varphi^2\psi^2)_2}\delta_{mn}+c^{nm}_{(D\varphi^2\psi^2)_2}\delta_{pr})\,,\\
A^{(1)}_{(D\varphi^2\psi^2)_2}(1^+_{\psi_m}2^-_{\bar\psi_n}3^-_{\psi_p}4^+_{\bar\psi_r})_{[1]} &= \frac{1}{9}\tilde g^2 N_s(3X_s+8)t(c^{rp}_{(D\varphi^2\psi^2)_2}\delta_{mn}+c^{nm}_{(D\varphi^2\psi^2)_2}\delta_{pr})\,,\\
A^{(1)}_{(D\varphi^2\psi^2)_2}(1^+_{\psi_m}2^+_{\bar\psi_n}3^-_{\psi_p}4^-_{\bar\psi_r})_{[1]} &= 0\,.
\end{aligned}
\tag{3.111}
$$

The amplitudes with one insertion of a ψ^4 operator are

$$
\begin{aligned}
A^{(1)\text{fin}}_{(\psi^4)_1}(1^+_{\psi_m}2^-_{\bar\psi_n}3^+_{\psi_p}4^-_{\bar\psi_r})_{[1]} &= \frac{2\tilde g^2 u}{9t}\Big(t\big(72N c^{rmnp}_{(\psi^4)_1} \\
&\quad + N_f(3X_s+2)(\delta_{mn}c^{rwwp}_{(\psi^4)_1}+\delta_{pr}c^{nwwm}_{(\psi^4)_1})\big) \\
&\quad + 9(2s+t(3X_u+25))c^{nmrp}_{(\psi^4)_1}\Big)\,, \\
A^{(1)\text{fin}}_{(\psi^4)_1}(1^+_{\psi_m}2^-_{\bar\psi_n}3^-_{\psi_p}4^+_{\bar\psi_r})_{[1]} &= -\frac{2}{9}\tilde g^2(N_f t(3X_s+2)(\delta_{mn}c^{rwwp}_{(\psi^4)_1}+\delta_{pr}c^{nwwm}_{(\psi^4)_1}) \\
&\quad + 9(2s+t(5-3X_t))c^{nmrp}_{(\psi^4)_1})\,, \\
A^{(1)\text{fin}}_{(\psi^4)_1}(1^+_{\psi_m}2^+_{\bar\psi_n}3^-_{\psi_p}4^-_{\bar\psi_r})_{[1]} &= -16\tilde g^2 N s c^{rmnp}_{(\psi^4)_1}\,, \\
A^{(1)\text{fin}}_{(\psi^4)_2}(1^+_{\psi_m}2^-_{\bar\psi_n}3^+_{\psi_p}4^-_{\bar\psi_r})_{[1]} &= \frac{2\tilde g^2 u}{9Nst}\Big(9s\left(2\left(N^2-1\right)s+t\left(13N^2-3X_u-25\right)\right)c^{nmrp}_{(\psi^4)_2} \\
&\quad + t(N_f s(2N(3X_s+5)(\delta_{mn}c^{rpww}_{(\psi^4)_2}+\delta_{pr}c^{nmww}_{(\psi^4)_2}) \\
&\quad - (3X_s+2)(\delta_{mn}c^{rwwp}_{(\psi^4)_2}+\delta_{pr}c^{nwwm}_{(\psi^4)_2})) \\
&\quad + 9N(s(3X_u+17)+2t)c^{rmnp}_{(\psi^4)_2})\Big)\,, \\
A^{(1)\text{fin}}_{(\psi^4)_2}(1^+_{\psi_m}2^-_{\bar\psi_n}3^-_{\psi_p}4^+_{\bar\psi_r})_{[1]} &= -\frac{2\tilde g^2}{9N}\Big(9\left(2\left(N^2-1\right)s-t\left(3(N^2-1)X_t-3N^2+5\right)\right)c^{nmrp}_{(\psi^4)_2} \\
&\quad + N_f t(2N(3X_s+5)(\delta_{mn}c^{rpww}_{(\psi^4)_2}+\delta_{pr}c^{nmww}_{(\psi^4)_2}) \\
&\quad - (3X_s+2)(\delta_{mn}c^{rwwp}_{(\psi^4)_2}+\delta_{pr}c^{nwwm}_{(\psi^4)_2}))\Big)\,, \\
A^{(1)\text{fin}}_{(\psi^4)_2}(1^+_{\psi_m}2^+_{\bar\psi_n}3^-_{\psi_p}4^-_{\bar\psi_r})_{[1]} &= 2\tilde g^2(3s(X_s+1)-2t)c^{rmnp}_{(\psi^4)_2}\,.
\end{aligned}
\tag{3.112}
$$

3.B.3 Four-scalar amplitudes

The color structures for this process are identical to those of the four fermion case:

$$
\mathcal{C}^{[1]}_{ssss} = T^a_{i_2 i_1}T^a_{i_4 i_3}\,, \qquad \mathcal{C}^{[2]}_{ssss} = T^a_{i_4 i_1}T^a_{i_2 i_3}\,. \tag{3.113}
$$

There is no spinor phase in this case, as the scalars do not carry helicity weight. The tree-level amplitudes are

$$\begin{aligned} A^{(0)}(1_\varphi 2_{\bar\varphi} 3_\varphi 4_{\bar\varphi})_{[1]} &= -\frac{g^2(t-u)}{2s} - \frac{2\lambda N}{N-1}\,, \\ A^{(0)}_{(D^2\varphi^4)_1}(1_\varphi 2_{\bar\varphi} 3_\varphi 4_{\bar\varphi})_{[1]} &= \frac{N(Ns+t)}{N^2-1}\,, \\ A^{(0)}_{(D^2\varphi^4)_2}(1_\varphi 2_{\bar\varphi} 3_\varphi 4_{\bar\varphi})_{[1]} &= \frac{2N(Nt+s)}{N^2-1}\,. \end{aligned} \tag{3.114}$$

The one-loop amplitudes with an insertion of the F^3 operator are

$$A^{(1)}_{F^3}(1_\varphi 2_{\bar\varphi} 3_\varphi 4_{\bar\varphi})_{[1]} = -\frac{1}{6} g\tilde{g}^2 N(t-u)\,. \tag{3.115}$$

The one-loop amplitudes with an insertion of a $\varphi^2 F^2$ operator are

$$\begin{aligned} A^{(1)}_{(\varphi^2F^2)_1}(1_\varphi 2_{\bar\varphi} 3_\varphi 4_{\bar\varphi})_{[1]} &= 2\tilde{g}^2(Nt+s)\,, \\ A^{(1)}_{(\varphi^2F^2)_2}(1_\varphi 2_{\bar\varphi} 3_\varphi 4_{\bar\varphi})_{[1]} &= \frac{2\tilde{g}^2\,(N^2-4)\,s}{N}\,. \end{aligned} \tag{3.116}$$

The one-loop amplitudes with an insertion of a $D^2\varphi^4$ operator are

$$\begin{aligned} A^{(1)\text{fin}}_{(D^2\varphi^4)_1}(1_\varphi 2_{\bar\varphi} 3_\varphi 4_{\bar\varphi})_{[1]} &= \frac{\tilde{g}^2}{2}\Big(-4(4N+3)s - 2(3N+5)t \\ &\quad - 3(N-2)tX_t - 3sX_s + 3uX_u\Big) \\ &\quad + \frac{2\tilde{\lambda}}{N-1}\Big(2N((N-3)t-2s) - NsX_s \\ &\quad + (N-2)NtX_t + NuX_u\Big)\,, \\ A^{(1)\text{fin}}_{(D^2\varphi^4)_2}(1_\varphi 2_{\bar\varphi} 3_\varphi 4_{\bar\varphi})_{[1]} &= \frac{\tilde{g}^2}{9}\Big(-2(2t(9N+4N_s+27) + (4N_s+45)s) \\ &\quad + 27(2N-1)tX_t - 3X_s((N_s-18)s + 2N_st) + 27uX_u) \\ &\quad + \frac{4\tilde{\lambda}N}{N-1}(-4(Nt+s) + (1-2N)tX_t - sX_s + uX_u)\,. \end{aligned} \tag{3.117}$$

The one-loop amplitudes with an insertion of a $D\varphi^2\psi^2$ operator are

$$\begin{aligned} A^{(1)}_{(D\varphi^2\psi^2)_1}(1_\varphi 2_{\bar\varphi} 3_\varphi 4_{\bar\varphi})_{[1]} &= 0\,, \\ A^{(1)}_{(D\varphi^2\psi^2)_2}(1_\varphi 2_{\bar\varphi} 3_\varphi 4_{\bar\varphi})_{[1]} &= -\frac{2}{9} c^{ww}_{(D\varphi^2\psi^2)_2} \tilde{g}^2 (3X_s + 5)(t-u)\,. \end{aligned} \tag{3.118}$$

3.B.4 Two-fermion, two-vector amplitudes

The color factors for the two-fermion, two-vector amplitudes are

$$\mathcal{C}^{[1]}_{ffvv} = (T^3T^4)_{i_2 i_1}\,, \qquad \mathcal{C}^{[2]}_{ffvv} = (T^4T^3)_{i_2 i_1}\,, \qquad \mathcal{C}^{[3]}_{ffvv} = \mathrm{Tr}[T^3T^4]\delta_{i_2 i_1}\,. \tag{3.119}$$

In this case the spinor prefactors are not pure phases, but have magnitudes equal to ratios of s, t, and u:

$$\begin{aligned} S(1^-_{\psi_p} 2^+_{\bar\psi_r} 3^+ 4^+) &= \frac{\langle 13\rangle[34]}{\langle 23\rangle\langle 34\rangle}\,, & S(1^-_{\psi_p} 2^+_{\bar\psi_r} 3^- 4^+) &= \frac{\langle 13\rangle^3}{\langle 12\rangle\langle 34\rangle\langle 41\rangle}\,, \\ S(1^-_{\psi_p} 2^+_{\bar\psi_r} 3^+ 4^-) &= \frac{\langle 14\rangle^3}{\langle 12\rangle\langle 31\rangle\langle 43\rangle}\,, & S(1^-_{\psi_p} 2^+_{\bar\psi_r} 3^- 4^-) &= \frac{\langle 34\rangle^3}{\langle 23\rangle\langle 24\rangle[12]}\,. \end{aligned} \tag{3.120}$$

The tree-level amplitudes for this process are

$$\begin{aligned} A^{(0)}(1_{\psi_p} 2_{\bar\psi_r} 34)_{[1]} &= -\frac{g^2}{st}(2T^{-+-+}_{ffvv} - 2T^{-++-}_{ffvv} + T^{\mathrm{ev}}_{ffvv})\delta_{pr}\,, \\ A^{(0)}_{F^3}(1_{\psi_p} 2_{\bar\psi_r} 34)_{[1]} &= -\frac{2g}{s}(T^{-+++}_{ffvv} + T^{-+--}_{ffvv})\delta_{pr}\,, \end{aligned} \tag{3.121}$$

which evaluate in four dimensions as

$$
\begin{aligned}
A^{(0)}(1^-_{\psi_p}2^+_{\bar\psi_r}3^+4^+)_{[1]} &= 0\,,\\
A^{(0)}(1^-_{\psi_p}2^+_{\bar\psi_r}3^+4^-)_{[1]} &= g^2\delta_{pr}\,,\\
A^{(0)}(1^-_{\psi_p}2^+_{\bar\psi_r}3^-4^+)_{[1]} &= \frac{g^2 t}{u}\delta_{pr}\,,\\
A^{(0)}(1^-_{\psi_p}2^+_{\bar\psi_r}3^-4^-)_{[1]} &= 0\,,\\
A^{(0)}_{F^3}(1^-_{\psi_p}2^+_{\bar\psi_r}3^+4^+)_{[1]} &= -gt\delta_{pr}\,,\\
A^{(0)}_{F^3}(1^-_{\psi_p}2^+_{\bar\psi_r}3^+4^-)_{[1]} &= 0\,,\\
A^{(0)}_{F^3}(1^-_{\psi_p}2^+_{\bar\psi_r}3^-4^+)_{[1]} &= 0\,,\\
A^{(0)}_{F^3}(1^-_{\psi_p}2^+_{\bar\psi_r}3^-4^-)_{[1]} &= \frac{gtu}{s}\delta_{pr}\,.
\end{aligned}
\tag{3.122}
$$

The one-loop amplitudes with an insertion of a F^3 operator are

$$
\begin{aligned}
A^{(1)\text{fin}}_{F^3}(1^-_{\psi_p}2^+_{\bar\psi_r}3^+4^+)_{[1]} &= \frac{g\tilde g^2\delta_{pr}}{36Nu}\Big(2tu\big(34N^2+N(5N_f+2N_s)-18\big)\\
&\quad + 9Ntu((4N_f+N_s)X_s+2(N-b_0)X_t)\\
&\quad + 18N^2(t-u)tX^2\Big)\,,\\
A^{(1)\text{fin}}_{F^3}(1^-_{\psi_p}2^+_{\bar\psi_r}3^-4^+)_{[1]} &= 0\,,\\
A^{(1)}_{F^3}(1^-_{\psi_p}2^+_{\bar\psi_r}3^+4^-)_{[1]} &= g\tilde g^2\delta_{pr}N\frac{su}{t}\,,\\
A^{(1)\text{fin}}_{F^3}(1^-_{\psi_p}2^+_{\bar\psi_r}3^-4^-)_{[1]} &= -\frac{u}{s}A^{(1)\text{fin}}_{F^3}(1^-_{\psi_p}2^+_{\bar\psi_r}3^+4^+)_{[1]}\,,
\end{aligned}
\tag{3.123}
$$

$$
\begin{aligned}
A^{(1)\text{fin}}_{F^3}(1^-_{\psi_p}2^+_{\bar\psi_r}3^+4^+)_{[3]} &= g\tilde g^2\delta_{pr}\bigg(\frac{(3N+b_0)}{2N}t(X_u-X_t)\\
&\qquad +\frac{(t-u)}{2su}(stX^2+suY^2+utZ^2)\bigg)\,,\\
A^{(1)}_{F^3}(1^-_{\psi_p}2^+_{\bar\psi_r}3^-4^+)_{[3]} &= g\tilde g^2\delta_{pr}2\frac{st}{u}\,,\\
A^{(1)}_{F^3}(1^-_{\psi_p}2^+_{\bar\psi_r}3^+4^-)_{[3]} &= g\tilde g^2\delta_{pr}2\frac{su}{t}\,,\\
A^{(1)\text{fin}}_{F^3}(1^-_{\psi_p}2^+_{\bar\psi_r}3^-4^-)_{[3]} &= -\frac{u}{s}A^{(1)\text{fin}}_{F^3}(1^-_{\psi_p}2^+_{\bar\psi_r}3^+4^+)_{[3]}\,.
\end{aligned}
\tag{3.124}
$$

The one-loop amplitudes with an insertion of a φ^2F^2 operator all evaluate to zero:

$$
\begin{aligned}
A^{(1)}_{(\varphi^2F^2)_1}(1^\pm_{\psi_p}2^\pm_{\bar\psi_r}3^\pm4^\pm)_{[1]} &= A^{(1)}_{(\varphi^2F^2)_1}(1^\pm_{\psi_p}2^\pm_{\bar\psi_r}3^\pm4^\pm)_{[3]} = 0\,,\\
A^{(1)}_{(\varphi^2F^2)_2}(1^\pm_{\psi_p}2^\pm_{\bar\psi_r}3^\pm4^\pm)_{[1]} &= A^{(1)}_{(\varphi^2F^2)_2}(1^\pm_{\psi_p}2^\pm_{\bar\psi_r}3^\pm4^\pm)_{[3]} = 0\,.
\end{aligned}
\tag{3.125}
$$

The one-loop amplitudes with an insertion of a $D\varphi^2\psi^2$ operator are

$$
\begin{aligned}
A^{(1)}_{(D\varphi^2\psi^2)_1}(1^\pm_{\psi_p}2^\pm_{\bar\psi_r}3^\pm4^\pm)_{[1]} &= A^{(1)}_{(D\varphi^2\psi^2)_1}(1^\pm_{\psi_p}2^\pm_{\bar\psi_r}3^\pm4^\pm)_{[3]} = 0\,,\\
A^{(1)}_{(D\varphi^2\psi^2)_2}(1^-_{\psi_p}2^+_{\bar\psi_r}3^+4^+)_{[1]} &= \frac{1}{3}\tilde g^2c^{rp}_{(D\varphi^2\psi^2)_2}N_st\,,\\
A^{(1)}_{(D\varphi^2\psi^2)_2}(1^-_{\psi_p}2^+_{\bar\psi_r}3^+4^-)_{[1]} &= A^{(1)}_{(D\varphi^2\psi^2)_2}(1^-_{\psi_p}2^+_{\bar\psi_r}3^-4^+)_{[1]} = 0\,,\\
A^{(1)}_{(D\varphi^2\psi^2)_2}(1^-_{\psi_p}2^+_{\bar\psi_r}3^-4^-)_{[1]} &= -\frac{1}{3s}\tilde g^2c^{rp}_{(D\varphi^2\psi^2)_2}N_stu\,,\\
A^{(1)}_{(D\varphi^2\psi^2)_2}(1^\pm_{\psi_p}2^\pm_{\bar\psi_r}3^\pm4^\pm)_{[3]} &= 0\,.
\end{aligned}
\tag{3.126}
$$

The one-loop amplitudes with an insertion of a ψ^4 operator are

$$
\begin{aligned}
A^{(1)}_{(\psi^4)_1}(1^\pm_{\psi_p}2^\pm_{\bar\psi_r}3^\pm4^\pm)_{[1],[3]} &= \frac{N_f}{N_s}\frac{c^{rwwp}_{(\psi^4)_1}}{c^{rp}_{(D\varphi^2\psi^2)_2}}A^{(1)}_{(D\varphi^2\psi^2)_2}(1^\pm_{\psi_p}2^\pm_{\bar\psi_r}3^\pm4^\pm)_{[1],[3]}\,,\\
A^{(1)}_{(\psi^4)_2}(1^\pm_{\psi_p}2^\pm_{\bar\psi_r}3^\pm4^\pm)_{[1],[3]} &= \frac{2Nc^{rpww}_{(\psi^4)_2}-c^{rwwp}_{(\psi^4)_2}}{c^{rwwp}_{(\psi^4)_1}}A^{(1)}_{(\psi^4)_1}(1^\pm_{\psi_p}2^\pm_{\bar\psi_r}3^\pm4^\pm)_{[1],[3]}\,.
\end{aligned}
\tag{3.127}
$$

3.B.5 Two-scalar, two-vector amplitudes

The color basis for this process is analogous to the that of the previous:

$$\mathcal{C}^{[1]}_{vvss} = (T^1T^2)_{i_4 i_3}\,, \qquad \mathcal{C}^{[2]}_{vvss} = (T^2T^1)_{i_4 i_3}\,, \qquad \mathcal{C}^{[3]}_{vvss} = \mathrm{Tr}[T^1T^2]\delta_{i_4 i_3}\,. \tag{3.128}$$

The spinor factors are again pure phases:

$$S(1^+2^+3_\varphi 4_{\bar\varphi}) = \frac{[12]}{\langle 12\rangle}\,, \qquad S(1^+2^-3_\varphi 4_{\bar\varphi}) = \frac{\langle 23\rangle\langle 24\rangle[12][34]}{\langle 12\rangle\langle 34\rangle[23][24]}\,. \tag{3.129}$$

The D-dimensional tree-level expressions are given by

$$\begin{aligned}
A^{(1)}(123_\varphi 4_{\bar\varphi})_{[1]} &= -\frac{g^2}{st}T^{+-}_{vvss}\,,\\
A^{(1)}(123_\varphi 4_{\bar\varphi})_{[3]} &= 0\,,\\
A^{(1)}_{F^3}(123_\varphi 4_{\bar\varphi})_{[1]} &= \frac{g(t-u)}{2s}T^{++}_{vvss}\,,\\
A^{(1)}_{F^3}(123_\varphi 4_{\bar\varphi})_{[3]} &= 0\,,\\
A^{(1)}_{(\varphi^2F^2)_1}(123_\varphi 4_{\bar\varphi})_{[1]} &= 0\,,\\
A^{(1)}_{(\varphi^2F^2)_1}(123_\varphi 4_{\bar\varphi})_{[3]} &= -2T^{++}_{vvss}\,,\\
A^{(1)}_{(\varphi^2F^2)_2}(123_\varphi 4_{\bar\varphi})_{[1]} &= -2T^{++}_{vvss}\,,\\
A^{(1)}_{(\varphi^2F^2)_2}(123_\varphi 4_{\bar\varphi})_{[3]} &= -\frac{4}{N}T^{++}_{vvss}\,,
\end{aligned} \tag{3.130}$$

with four-dimensional helicity values

$$
\begin{aligned}
A^{(1)}(1^+2^+3_\varphi 4_{\bar\varphi})_{[1]} &= 0\,,\\
A^{(1)}(1^+2^-3_\varphi 4_{\bar\varphi})_{[1]} &= \frac{g^2 u}{s}\,,\\
A^{(1)}(1^\pm 2^\pm 3_\varphi 4_{\bar\varphi})_{[3]} &= 0\,,\\
A^{(1)}_{F^3}(1^+2^+3_\varphi 4_{\bar\varphi})_{[1]} &= \frac{1}{2} g(t-u)\,,\\
A^{(1)}_{F^3}(1^+2^-3_\varphi 4_{\bar\varphi})_{[1]} &= 0\,,\\
A^{(1)}_{F^3}(1^\pm 2^\pm 3_\varphi 4_{\bar\varphi})_{[3]} &= 0\,,\\
A^{(1)}_{(\varphi^2F^2)_1}(1^\pm 2^\pm 3_\varphi 4_{\bar\varphi})_{[1]} &= 0\,,\\
A^{(1)}_{(\varphi^2F^2)_1}(1^+2^+3_\varphi 4_{\bar\varphi})_{[3]} &= -2s\,,\\
A^{(1)}_{(\varphi^2F^2)_1}(1^+2^-3_\varphi 4_{\bar\varphi})_{[3]} &= 0\,,\\
A^{(1)}_{(\varphi^2F^2)_2}(1^+2^+3_\varphi 4_{\bar\varphi})_{[1]} &= -2s\,,\\
A^{(1)}_{(\varphi^2F^2)_2}(1^+2^-3_\varphi 4_{\bar\varphi})_{[1]} &= 0\,,\\
A^{(1)}_{(\varphi^2F^2)_2}(1^+2^+3_\varphi 4_{\bar\varphi})_{[3]} &= -\frac{4s}{N}\,,\\
A^{(1)}_{(\varphi^2F^2)_2}(1^+2^-3_\varphi 4_{\bar\varphi})_{[3]} &= 0\,.
\end{aligned}
\tag{3.131}
$$

The one-loop amplitudes with an insertion of the F^3 operator are

$$
\begin{aligned}
A^{(1)\text{fin}}_{F^3}(1^+2^+3_\varphi 4_{\bar\varphi})_{[1]} &= -\frac{g\tilde g^2}{72N}\Big(8((52N^2-18)s+(77N^2-36)t+N(t-u)(5N_f+2N_s)) \\
&\quad +18N((2N(5t-7u)-3b_0(t-u))X_t+X_s(2Ns+b_0(u-t))) \\
&\quad -72N^2tX^2\Big)\,, \\
A^{(1)}_{F_3}(1^+2^-3_\varphi 4_{\bar\varphi})_{[1]} &= \frac{1}{2}g\tilde g^2Nu\,, \\
A^{(1)\text{fin}}_{F^3}(1^+2^+3_\varphi 4_{\bar\varphi})_{[3]} &= \frac{g\tilde g^2}{4N}\Big((8Nt+b_0(t-u))X_t+(8Nu+b_0(u-t))X_u-4NsX_s \\
&\quad +\frac{1}{6s}(stX^2+suY^2+tuZ^2)\Big)\,, \\
A^{(1)}_{F_3}(1^+2^-3_\varphi 4_{\bar\varphi})_{[3]} &= -g\tilde g^2 s\,.
\end{aligned}
\tag{3.132}
$$

The one-loop amplitudes with an insertion of a φ^2F^2 operator are

$$
A^{(1)\text{fin}}_{(\varphi^2F^2)_1}(1^+2^+3_\varphi 4_{\bar\varphi})_{[1]} = -\frac{\tilde g^2 s}{N}((b_0-2N)X_t+b_0X_u)+4\tilde g^2 s\,, \tag{3.133}
$$

$$
\begin{aligned}
A^{(1)}_{(\varphi^2F^2)_1}(1^+2^-3_\varphi 4_{\bar\varphi})_{[1]} &= 2\tilde g^2(s+3t)\,, \\
A^{(1)\text{fin}}_{(\varphi^2F^2)_1}(1^+2^+3_\varphi 4_{\bar\varphi})_{[3]} &= \tilde g^2 s\,(4C_F-2(b_0+3C_F)X_s) \\
&\quad +4\tilde\lambda(N+1)s(X_s+2)\,, \\
A^{(1)}_{(\varphi^2F^2)_1}(1^+2^-3_\varphi 4_{\bar\varphi})_{[3]} &= 0\,, \\
A^{(1)\text{fin}}_{(\varphi^2F^2)_2}(1^+2^+3_\varphi 4_{\bar\varphi})_{[1]} &= \frac{\tilde g^2 s}{N^2}\Big(6N\left(2N^2-3\right)+N\left(3-Nb_0\right)X_s+2b_0X_u \\
&\quad +\left(2N(N^2-4)-b_0(N^2-2)\right)X_t\Big) \\
&\quad +4\tilde\lambda s(X_s+2)\,, \\
A^{(1)}_{(\varphi^2F^2)_2}(1^+2^-3_\varphi 4_{\bar\varphi})_{[1]} &= -\frac{2\tilde g^2}{N}\left(N^2u+4t\right)\,, \\
A^{(1)\text{fin}}_{(\varphi^2F^2)_2}(1^+2^+3_\varphi 4_{\bar\varphi})_{[3]} &= \frac{\tilde g^2 s}{N^2}\Big(2\left(b_0N-3\right)X_s+b_0N(X_t+X_u)-3\left(4N^2-1\right)\Big) \\
&\quad -\frac{8}{N}\tilde\lambda s(X_s+2)\,, \\
A^{(1)}_{(\varphi^2F^2)_2}(1^+2^-3_\varphi 4_{\bar\varphi})_{[3]} &= -4\tilde g^2 s\,.
\end{aligned}
\tag{3.134}
$$

The one-loop amplitudes with an insertion of a $D^2\varphi^4$ operator are

$$\begin{aligned}
&A^{(1)}_{(D^2\varphi^4)_1}(1^+2^+3_\varphi 4_{\bar\varphi})_{[1]} = -\frac{1}{2}\tilde g^2 N_s s\,,\\
&A^{(1)}_{(D^2\varphi^4)_1}(1^+2^-3_\varphi 4_{\bar\varphi})_{[1]} = 0\,,\\
&A^{(1)}_{(D^2\varphi^4)_1}(1^\pm2^\pm3_\varphi 4_{\bar\varphi})_{[3]} = -A^{(1)}_{(D^2\varphi^4)_1}(1^\pm2^\pm3_\varphi 4_{\bar\varphi})_{[1]}\,,\\
&A^{(1)}_{(D^2\varphi^4)_2}(1^+2^+3_\varphi 4_{\bar\varphi})_{[1]} = \frac{1}{3}\tilde g^2 N_s (s-t)\,,\\
&A^{(1)}_{(D^2\varphi^4)_2}(1^+2^-3_\varphi 4_{\bar\varphi})_{[1]} = 0\,,\\
&A^{(1)}_{(D^2\varphi^4)_2}(1^\pm2^\pm3_\varphi 4_{\bar\varphi})_{[3]} = 4A^{(1)}_{(D^2\varphi^4)_1}(1^\pm2^\pm3_\varphi 4_{\bar\varphi})_{[1]}\,.
\end{aligned} \tag{3.135}$$

The one-loop amplitudes with an insertion of a $D\varphi^2\psi^2$ operator are

$$\begin{aligned}
&A^{(1)}_{(D\varphi^2\psi^2)_1}(1^\pm2^\pm3_\varphi 4_{\bar\varphi})_{[1]} = A^{(1)}_{(D\varphi^2\psi^2)_1}(1^\pm2^\pm3_\varphi 4_{\bar\varphi})_{[3]} = 0\,,\\
&A^{(1)}_{(D\varphi^2\psi^2)_2}(1^+2^+3_\varphi 4_{\bar\varphi})_{[1]} = \frac{1}{3}\tilde g^2 c^{ww}_{(D\varphi^2\psi^2)_2} N_f (t-u)\,,\\
&A^{(1)}_{(D\varphi^2\psi^2)_2}(1^+2^-3_\varphi 4_{\bar\varphi})_{[1]} = A^{(1)}_{(D\varphi^2\psi^2)_2}(1^\pm2^\pm3_\varphi 4_{\bar\varphi})_{[3]} = 0\,.
\end{aligned} \tag{3.136}$$

3.B.6 Two-fermion, two-scalar amplitudes

The color structures for this process are identical to those of the four fermion case:

$$\mathcal{C}^{[1]}_{ffss} = T^a_{i_2 i_1} T^a_{i_4 i_3}\,, \qquad \mathcal{C}^{[2]}_{ffss} = T^a_{i_4 i_1} T^a_{i_2 i_3}\,. \tag{3.137}$$

There is only one independent spinor prefactor (which again is not a pure phase for this case):

$$S(1_\psi 2_{\bar\psi} 3_\varphi 4_{\bar\varphi}) = \frac{\langle 23\rangle[13]}{s}\,. \tag{3.138}$$

The tree-level amplitudes for this process are given by

$$
\begin{aligned}
A^{(0)}(1_{\psi_p}2_{\bar{\psi}_r}3_{\varphi}4_{\bar{\varphi}})_{[1]} &= g^2\frac{\bar{u}_2\not{k}_3u_1}{s}\delta_{pr}\,,\\
A^{(0)}(1_{\psi_p}2_{\bar{\psi}_r}3_{\varphi}4_{\bar{\varphi}})_{[2]} &= 0\,,\\
A^{(0)}_{(D\varphi^2\psi^2)_1}(1_{\psi_p}2_{\bar{\psi}_r}3_{\varphi}4_{\bar{\varphi}})_{[1]} &= -\frac{2c^{rp}_{(D\varphi^2\psi^2)_1}N(\bar{u}_2\not{k}_3u_1)}{N^2-1}\,,\\
A^{(0)}_{(D\varphi^2\psi^2)_1}(1_{\psi_p}2_{\bar{\psi}_r}3_{\varphi}4_{\bar{\varphi}})_{[2]} &= -\frac{2c^{rp}_{(D\varphi^2\psi^2)_1}N^2(\bar{u}_2\not{k}_3u_1)}{N^2-1}\,,\\
A^{(0)}_{(D\varphi^2\psi^2)_2}(1_{\psi_p}2_{\bar{\psi}_r}3_{\varphi}4_{\bar{\varphi}})_{[1]} &= -2c^{rp}_{(D\varphi^2\psi^2)_2}(\bar{u}_2\not{k}_3u_1)\,,\\
A^{(0)}_{(D\varphi^2\psi^2)_2}(1_{\psi_p}2_{\bar{\psi}_r}3_{\varphi}4_{\bar{\varphi}})_{[2]} &= 0\,,
\end{aligned}
\tag{3.139}
$$

with four-dimensional helicity values

$$
\begin{aligned}
A^{(0)}(1^+_{\psi_p}2^-_{\bar{\psi}_r}3_{\varphi}4_{\bar{\varphi}})_{[1]} &= g^2\delta_{pr}\,,\\
A^{(0)}(1^+_{\psi_p}2^-_{\bar{\psi}_r}3_{\varphi}4_{\bar{\varphi}})_{[2]} &= 0\,,\\
A^{(0)}_{(D\varphi^2\psi^2)_1}(1^+_{\psi_p}2^-_{\bar{\psi}_r}3_{\varphi}4_{\bar{\varphi}})_{[1]} &= -\frac{4c^{rp}_{(D\varphi^2\psi^2)_1}Ns}{N^2-1}\,,\\
A^{(0)}_{(D\varphi^2\psi^2)_1}(1^+_{\psi_p}2^-_{\bar{\psi}_r}3_{\varphi}4_{\bar{\varphi}})_{[2]} &= -\frac{4c^{rp}_{(D\varphi^2\psi^2)_1}N^2s}{N^2-1}\,,\\
A^{(0)}_{(D\varphi^2\psi^2)_2}(1^+_{\psi_p}2^-_{\bar{\psi}_r}3_{\varphi}4_{\bar{\varphi}})_{[1]} &= -4c^{rp}_{(D\varphi^2\psi^2)_2}s\,,\\
A^{(0)}_{(D\varphi^2\psi^2)_2}(1^+_{\psi_p}2^-_{\bar{\psi}_r}3_{\varphi}4_{\bar{\varphi}})_{[2]} &= 0\,.
\end{aligned}
\tag{3.140}
$$

The one-loop amplitudes with an insertion of the F^3 operator are

$$
\begin{aligned}
A^{(1)}_{F^3}(1^+_{\psi_p}2^-_{\bar{\psi}_r}3_{\varphi}4_{\bar{\varphi}})_{[1]} &= \frac{1}{6}g\tilde{g}^2Ns\delta_{pr}\,,\\
A^{(1)}_{F^3}(1^+_{\psi_p}2^-_{\bar{\psi}_r}3_{\varphi}4_{\bar{\varphi}})_{[2]} &= 0\,.
\end{aligned}
\tag{3.141}
$$

The one-loop amplitudes with an insertion of a $\varphi^2 F^2$ operator all evaluate to zero:

$$\begin{aligned}
&A^{(1)}_{(\varphi^2F^2)_1}(1^+_{\psi_p}2^-_{\bar\psi_r}3_\varphi 4_{\bar\varphi})_{[1]} = A^{(1)}_{(\varphi^2F^2)_1}(1^+_{\psi_p}2^-_{\bar\psi_r}3_\varphi 4_{\bar\varphi})_{[2]} = 0\,,\\
&A^{(1)}_{(\varphi^2F^2)_2}(1^+_{\psi_p}2^-_{\bar\psi_r}3_\varphi 4_{\bar\varphi})_{[1]} = A^{(1)}_{(\varphi^2F^2)_2}(1^+_{\psi_p}2^-_{\bar\psi_r}3_\varphi 4_{\bar\varphi})_{[2]} = 0\,.
\end{aligned} \tag{3.142}$$

The one-loop amplitudes with an insertion of a $D^2\varphi^4$ operator are

$$\begin{aligned}
&A^{(1)}_{(D^2\varphi^4)_1}(1^+_{\psi_p}2^-_{\bar\psi_r}3_\varphi 4_{\bar\varphi})_{[1]} = A^{(1)}_{(D^2\varphi^4)_1}(1^+_{\psi_p}2^-_{\bar\psi_r}3_\varphi 4_{\bar\varphi})_{[2]} = 0\,,\\
&A^{(1)}_{(D^2\varphi^4)_2}(1^+_{\psi_p}2^-_{\bar\psi_r}3_\varphi 4_{\bar\varphi})_{[1]} = \frac{1}{9}\tilde g^2 N_s s(3X_s+8)\delta_{pr}\,,\\
&A^{(1)}_{(D^2\varphi^4)_2}(1^+_{\psi_p}2^-_{\bar\psi_r}3_\varphi 4_{\bar\varphi})_{[2]} = 0\,.
\end{aligned} \tag{3.143}$$

The one-loop amplitudes with an insertion of a $D\psi^2\varphi^2$ operator are

$$\begin{aligned}
A^{(1)\text{fin}}_{(D\varphi^2\psi^2)_1}(1^+_{\psi_p}2^-_{\bar\psi_r}3_\varphi 4_{\bar\varphi})_{[1]} &= -\tilde g^2 s(3X_t-3X_u-16)c^{rp}_{(D\varphi^2\psi^2)_1}\,,\\
A^{(1)\text{fin}}_{(D\varphi^2\psi^2)_1}(1^+_{\psi_p}2^-_{\bar\psi_r}3_\varphi 4_{\bar\varphi})_{[2]} &= 16\tilde g^2 N s c^{rp}_{(D\varphi^2\psi^2)_1}\,,\\
A^{(1)\text{fin}}_{(D\varphi^2\psi^2)_2}(1^+_{\psi_p}2^-_{\bar\psi_r}3_\varphi 4_{\bar\varphi})_{[1]} &= \frac{\tilde g^2 s}{9N}c^{rp}_{(D\varphi^2\psi^2)_2}\Big(8\left(9N^2+NN_s-18\right)\\
&\qquad -27\left(N^2-1\right)X_t+3NN_sX_s-27X_u\Big)\\
&\quad +\frac{4}{9}\tilde g^2 N_f s(3X_s+5)c^{ww}_{(D\varphi^2\psi^2)_2}\delta_{pr}\,,\\
A^{(1)\text{fin}}_{(D\varphi^2\psi^2)_2}(1^+_{\psi_p}2^-_{\bar\psi_r}3_\varphi 4_{\bar\varphi})_{[2]} &= -3\tilde g^2 s(X_t-X_u)c^{rp}_{(D\varphi^2\psi^2)_2}\,.
\end{aligned} \tag{3.144}$$

The one-loop amplitudes with an insertion of a ψ^4 operator are

$$
\begin{aligned}
&A^{(1)}_{(\psi^4)_1}(1^+_{\psi_p}2^-_{\bar{\psi}_r}3_\varphi 4_{\bar{\varphi}})_{[1]} = -\frac{2}{9}\tilde{g}^2 N_f s(3X_s+2)c^{rwwp}_{(\psi^4)_1}\,,\\
&A^{(1)}_{(\psi^4)_1}(1^+_{\psi_p}2^-_{\bar{\psi}_r}3_\varphi 4_{\bar{\varphi}})_{[2]} = 0\,,\\
&A^{(1)}_{(\psi^4)_2}(1^+_{\psi_p}2^-_{\bar{\psi}_r}3_\varphi 4_{\bar{\varphi}})_{[1]} = \frac{2\tilde{g}^2 N_f s}{9N}((3X_s+2)c^{rwwp}_{(\psi^4)_2} - 2N(3X_s+5)c^{rpww}_{(\psi^4)_2})\,,\\
&A^{(1)}_{(\psi^4)_2}(1^+_{\psi_p}2^-_{\bar{\psi}_r}3_\varphi 4_{\bar{\varphi}})_{[2]} = 0\,.
\end{aligned}
\tag{3.145}
$$

	$\mathcal{O}_G$	$\mathcal{O}_W$	$\mathcal{O}_{HW}$	$\mathcal{O}_{uW}$	$\mathcal{O}_{H\Box}$ $\mathcal{O}_{HD}$	$\mathcal{O}_{Hq}^{(1)}$ $\mathcal{O}_{Hq}^{(3)}$	$\mathcal{O}_{qq}^{(1)}$ $\mathcal{O}_{qq}^{(3)}$	$\mathcal{O}_{uu}$	$\mathcal{O}_{uH}$	$\mathcal{O}_H$
$\mathcal{O}_G$		$\emptyset$	$\emptyset$	$\emptyset$	$\emptyset$	$\emptyset$	0	0	$\emptyset$	$\emptyset$
$\mathcal{O}_W$	$\emptyset$			0_y	0	0	0	$\emptyset$	$\emptyset$	$\emptyset$
$\mathcal{O}_{HW}$	$\emptyset$			0_y			0	$\emptyset$	0_y	0
$\mathcal{O}_{uW}$	0_y	0_y	0_y		0_y	0_y	0_y	0_y		$\emptyset$
$\mathcal{O}_{H\Box}$, $\mathcal{O}_{HD}$	$\emptyset$			0_y			$0_y(\not{g}_2^{4*})$	0_y	0_y	0
$\mathcal{O}_{Hq}^{(1)}$, $\mathcal{O}_{Hq}^{(3)}$				0_y				0_y	$0_y(\not{y}\not{\lambda})$	$\emptyset$
$\mathcal{O}_{qq}^{(1)}$, $\mathcal{O}_{qq}^{(3)}$				0_y	$0_y(\not{g}_2^4)$				$\emptyset$	$\emptyset$
$\mathcal{O}_{uu}$		$\emptyset$	$\emptyset$	0_y	0_y	0_y			$\emptyset$	$\emptyset$
$\mathcal{O}_{uH}$	0_y	0_y	0_y		0_y	0_y	0_y	0_y		0_y
$\mathcal{O}_H$	$\emptyset$			0_y					0_y	

$\emptyset$	: trivial zero, no contributing two-loop diagrams
0	: zero predicted by the selection rules of Section 3.4
	: only a three-particle cut is needed to evaluate $\gamma_{ij}^{\mathrm{UV}(2)}$
	: only two-particle cuts available for the relevant diagrams
$0(\not{y}\not{\lambda})$, etc.	: the selection rules of Section 3.4 forbid the stated coupling dependence
0_y	: $\gamma_{ij}^{\mathrm{UV}(2)}$ vanishes if Yukawa couplings are set to zero

Table 3.6: Predictions for the zeros and coupling dependences of a representative selection of the SMEFT two-loop anomalous-dimension matrix, $\gamma_{ij}^{\mathrm{UV}(2)}$. The notation for the operator labels follows that of [4]. The g_2^4 dependence of the entry labeled $0_y(\not{g}_2^{4*})$ vanishes using the appropriate counterterms at one loop. The operators labeling the rows are renormalized by the operators labeling the columns.

Bibliography

[1] W. Buchmuller and D. Wyler, "Effective Lagrangian Analysis of New Interactions and Flavor Conservation," Nucl. Phys. B **268**, 621 (1986).

[2] I. Brivio and M. Trott, "The Standard Model as an Effective Field Theory," Phys. Rept. **793**, 1 (2019) [arXiv:1706.08945 [hep-ph]].

[3] B. Grzadkowski, M. Iskrzynski, M. Misiak and J. Rosiek, "Dimension-Six Terms in the Standard Model Lagrangian," JHEP **1010**, 085 (2010) [arXiv:1008.4884 [hep-ph]].

[4] E. E. Jenkins, A. V. Manohar and M. Trott, "Renormalization Group Evolution of the Standard Model Dimension Six Operators I: Formalism and lambda Dependence," JHEP **1310**, 087 (2013) [arXiv:1308.2627 [hep-ph]];
E. E. Jenkins, A. V. Manohar and M. Trott, "Renormalization Group Evolution of the Standard Model Dimension Six Operators II: Yukawa Dependence," JHEP **1401**, 035 (2014) [arXiv:1310.4838 [hep-ph]];
R. Alonso, E. E. Jenkins, A. V. Manohar and M. Trott, "Renormalization Group Evolution of the Standard Model Dimension Six Operators III: Gauge Coupling Dependence and Phenomenology," JHEP **1404**, 159 (2014) [arXiv:1312.2014 [hep-ph]].

[5] R. Alonso, E. E. Jenkins, and A. V. Manohar "Holomorphy Without Supersymmetry in the Standard Model Effective Field Theory," Phys. Lett. B **739**, 95 (2014) [arXiv:1409.0868 [hep-ph]].

[6] J. Elias-Miro, J. R. Espinosa and A. Pomarol, "One-Loop Non-Renormalization Results in EFTs," Phys. Lett. B **747**, 272 (2015) [arXiv:1412.7151 [hep-ph]].

[7] C. Cheung and C. H. Shen, "Nonrenormalization Theorems without Supersymmetry," Phys. Rev. Lett. **115**, no. 7, 071601 (2015) [arXiv:1505.01844 [hep-ph]].

[8] Z. Bern, J. Parra-Martinez, and E. Sawyer "Nonrenormalization and Operator Mixing via On-Shell Methods," Phys. Rev. Lett. **124**, no. 5, 051601 (2020) [arXiv:1910.05831 [hep-th]].

[9] M. Jiang, J. Shu, M. Xiao and Y. Zheng, "New Selection Rules from Angular Momentum Conservation," [arXiv:2001.04481 [hep-ph]].

[10] N. Craig, M. Jiang, Y. Li and D. Sutherland, "Loops and Trees in Generic EFTs," [arXiv:2001.00017 [hep-ph]].

[11] Z. Bern, L. J. Dixon, D. C. Dunbar and D. A. Kosower, "One Loop n Point Gauge Theory Amplitudes, Unitarity and Collinear Limits," Nucl. Phys. B **425**, 217 (1994) [hep-ph/9403226];
Z. Bern, L. J. Dixon, D. C. Dunbar and D. A. Kosower, "Fusing Gauge Theory Tree Amplitudes into Loop Amplitudes," Nucl. Phys. B **435**, 59 (1995) [hep-ph/9409265];
Z. Bern and A. G. Morgan, "Massive Loop Amplitudes from Unitarity," Nucl. Phys. B **467**, 479 (1996) [hep-ph/9511336].

[12] S. Caron-Huot and M. Wilhelm, "Renormalization Group Coefficients and the S-matrix," JHEP **1612**, 010 (2016) [arXiv:1607.06448 [hep-th]].

[13] B. I. Zwiebel, "From Scattering Amplitudes to the Dilatation Generator in N=4 SYM," J. Phys. A **45**, 115401 (2012) [arXiv:1111.0083 [hep-th]];
M. Wilhelm, "Amplitudes, Form Factors and the Dilatation Operator in $\mathcal{N} = 4$ SYM Theory," JHEP **02**, 149 (2015) [arXiv:1410.6309 [hep-th]].

[14] C. Berger, Z. Bern, L. Dixon, F. Febres Cordero, D. Forde, H. Ita, D. Kosower and D. Maitre, "An Automated Implementation of On-Shell Methods for One-Loop Amplitudes," Phys. Rev. D **78**, 036003 (2008) [arXiv:0803.4180 [hep-ph]];
R. Ellis, K. Melnikov and G. Zanderighi, "W+3 Jet Production at the Tevatron," Phys. Rev. D **80**, 094002 (2009) [arXiv:0906.1445 [hep-ph]];
C. Berger, Z. Bern, L. J. Dixon, F. Febres Cordero, D. Forde, T. Gleisberg, H. Ita, D. Kosower and D. Maitre, "Precise Predictions for W + 4 Jet Production at the Large Hadron Collider," Phys. Rev. Lett. **106**, 092001 (2011) [arXiv:1009.2338 [hep-ph]].

[15] Z. Bern, C. Cheung, H. H. Chi, S. Davies, L. Dixon and J. Nohle, "Evanescent Effects Can Alter Ultraviolet Divergences in Quantum Gravity without Physical Consequences," Phys. Rev. Lett. **115**, no. 21, 211301 (2015) [arXiv:1507.06118 [hep-th]].

[16] Z. Bern, H. H. Chi, L. Dixon and A. Edison, "Two-Loop Renormalization of Quantum Gravity Simplified," Phys. Rev. D **95**, no. 4, 046013 (2017) [arXiv:1701.02422 [hep-th]].

[17] S. Abreu, F. Febres Cordero, H. Ita, M. Jaquier, B. Page, M. Ruf and V. Sotnikov, "The Two-Loop Four-Graviton Scattering Amplitudes," [arXiv:2002.12374 [hep-th]].

[18] Z. Bern, J. J. Carrasco, W. Chen, A. Edison, H. Johansson, J. Parra-Martinez, R. Roiban and M. Zeng, "Ultraviolet Properties of $\mathcal{N} = 8$ Supergravity at Five Loops," Phys. Rev. D **98**, no.8, 086021 (2018) [arXiv:1804.09311 [hep-th]].

[19] N. Arkani-Hamed and J. Trnka, "The Amplituhedron," JHEP **10**, 030 (2014) [arXiv:1312.2007 [hep-th]];
S. Caron-Huot, L. J. Dixon, F. Dulat, M. von Hippel, A. J. McLeod and G. Papathanasiou, "Six-Gluon Amplitudes in Planar $\mathcal{N} = 4$ Super-Yang-Mills Theory at Six and Seven Loops," JHEP **08**, 016 (2019) [arXiv:1903.10890 [hep-th]];
J. L. Bourjaily, E. Herrmann, C. Langer, A. J. McLeod and J. Trnka, "All-Multiplicity Non-Planar MHV Amplitudes in sYM at Two Loops," Phys. Rev. Lett. **124**, no.11,

111603 (2020) [arXiv:1911.09106 [hep-th]];

S. Caron-Huot, L. J. Dixon, J. M. Drummond, F. Dulat, J. Foster, Ö. Gürdoğan, M. von Hippel, A. J. McLeod and G. Papathanasiou, "The Steinmann Cluster Bootstrap for N=4 Super Yang-Mills Amplitudes," [arXiv:2005.06735 [hep-th]].

[20] Z. Bern, J. Carrasco, L. Dixon, H. Johansson and R. Roiban, "Simplifying Multiloop Integrands and Ultraviolet Divergences of Gauge Theory and Gravity Amplitudes," Phys. Rev. D **85**, 105014 (2012) [arXiv:1201.5366 [hep-th]];

Z. Bern, J. Parra-Martinez and R. Roiban, "Canceling the U(1) Anomaly in the S Matrix of N=4 Supergravity," Phys. Rev. Lett. **121**, no.10, 101604 (2018) [arXiv:1712.03928 [hep-th]];

Z. Bern, D. Kosower and J. Parra-Martinez, "Two-Loop n-Point Anomalous Amplitudes in $N = 4$ Supergravity," Proc. Roy. Soc. Lond. A **A476**, no.2235, 20190722 (2020) [arXiv:1905.05151 [hep-th]];

A. Edison, E. Herrmann, J. Parra-Martinez and J. Trnka, "Gravity Loop Integrands from the Ultraviolet," [arXiv:1909.02003 [hep-th]].

[21] N. Arkani-Hamed, P. Benincasa and A. Postnikov, "Cosmological Polytopes and the Wavefunction of the Universe," [arXiv:1709.02813 [hep-th]];

N. Arkani-Hamed and P. Benincasa, "On the Emergence of Lorentz Invariance and Unitarity from the Scattering Facet of Cosmological Polytopes," [arXiv:1811.01125 [hep-th]];

P. Benincasa, "From the flat-space S-matrix to the Wavefunction of the Universe," [arXiv:1811.02515 [hep-th]];

P. Benincasa, "Cosmological Polytopes and the Wavefuncton of the Universe for Light States," [arXiv:1909.02517 [hep-th]].

[22] N. Arkani-Hamed, D. Baumann, H. Lee and G. L. Pimentel, "The Cosmological Bootstrap: Inflationary Correlators from Symmetries and Singularities," JHEP **04**, 105

(2020) [arXiv:1811.00024 [hep-th]];

D. Baumann, C. Duaso Pueyo, A. Joyce, H. Lee and G. L. Pimentel, "The Cosmological Bootstrap: Weight-Shifting Operators and Scalar Seeds," [arXiv:1910.14051 [hep-th]];

D. Baumann, C. Duaso Pueyo, A. Joyce, H. Lee and G. L. Pimentel, "The Cosmological Bootstrap: Spinning Correlators from Symmetries and Factorization," [arXiv:2005.04234 [hep-th]].

[23] S. Caron-Huot and Z. Zahraee, "Integrability of Black Hole Orbits in Maximal Supergravity," JHEP **07**, 179 (2019) [arXiv:1810.04694 [hep-th]];

D. A. Kosower, B. Maybee and D. O'Connell, "Amplitudes, Observables, and Classical Scattering," JHEP **02**, 137 (2019) [arXiv:1811.10950 [hep-th]];

Z. Bern, C. Cheung, R. Roiban, C. Shen, M. P. Solon and M. Zeng, "Scattering Amplitudes and the Conservative Hamiltonian for Binary Systems at Third Post-Minkowskian Order," Phys. Rev. Lett. **122**, no.20, 201603 (2019) [arXiv:1901.04424 [hep-th]];

Z. Bern, C. Cheung, R. Roiban, C. Shen, M. P. Solon and M. Zeng, "Black Hole Binary Dynamics from the Double Copy and Effective Theory," JHEP **10**, 206 (2019) [arXiv:1908.01493 [hep-th]];

Z. Bern, H. Ita, J. Parra-Martinez and M. S. Ruf, "Universality in the Classical Limit of Massless Gravitational Scattering," [arXiv:2002.02459 [hep-th]];

Z. Bern, A. Luna, R. Roiban, C. H. Shen and M. Zeng, "Spinning Black Hole Binary Dynamics, Scattering Amplitudes and Effective Field Theory," [arXiv:2005.03071 [hep-th]];

J. Parra-Martinez, M. S. Ruf and M. Zeng, "Extremal black hole scattering at $\mathcal{O}(G^3)$: graviton dominance, eikonal exponentiation, and differential equations," [arXiv:2005.04236 [hep-th]].

[24] N. Arkani-Hamed, T. C. Huang and Y. t. Huang, "Scattering Amplitudes For All Masses and Spins," [arXiv:1709.04891 [hep-th]];

Y. Shadmi and Y. Weiss, "Effective Field Theory Amplitudes the On-Shell Way: Scalar and Vector Couplings to Gluons," JHEP **02**, 165 (2019) [arXiv:1809.09644 [hep-ph]];
T. Ma, J. Shu and M. L. Xiao, "Standard Model Effective Field Theory from On-shell Amplitudes," [arXiv:1902.06752 [hep-ph]];
G. Durieux, T. Kitahara, Y. Shadmi and Y. Weiss, "The Electroweak Effective Field Theory from On-Shell Amplitudes," JHEP **01**, 119 (2020) [arXiv:1909.10551 [hep-ph]];
B. Bachu and A. Yelleshpur, "On-Shell Electroweak Sector and the Higgs Mechanism," [arXiv:1912.04334 [hep-th]].

[25] A. Adams, N. Arkani-Hamed, S. Dubovsky, A. Nicolis and R. Rattazzi, "Causality, Analyticity and an IR Obstruction to UV Completion," JHEP **10**, 014 (2006) [arXiv:hep-th/0602178 [hep-th]].

[26] G. N. Remmen and N. L. Rodd, "Consistency of the Standard Model Effective Field Theory," JHEP **12**, 032 (2019) [arXiv:1908.09845 [hep-ph]];
G. N. Remmen and N. L. Rodd, "Flavor Constraints from Unitarity and Analyticity," [arXiv:2004.02885 [hep-ph]].

[27] J. Elias Miro, J. Ingoldby and M. Riembau, "EFT Anomalous Dimensions from the S-matrix," [arXiv:2005.06983 [hep-ph]].

[28] P. Baratella, C. Fernandez and A. Pomarol, "Renormalization of Higher-Dimensional Operators from On-shell Amplitudes," [arXiv:2005.07129 [hep-ph]];
M. Jiang, T. Ma and J. Shu, "Renormalization Group Evolution from On-shell SMEFT," [arXiv:2005.10261 [hep-ph]].

[29] Z. Bern, L. J. Dixon and D. A. Kosower, "One Loop Amplitudes for e^+e^- to Four Partons," Nucl. Phys. B **513**, 3 (1998) [hep-ph/9708239].

[30] R. Britto, F. Cachazo and B. Feng, "Generalized Unitarity and One-Loop Amplitudes in $N = 4$ Super-Yang-Mills," Nucl. Phys. B **725**, 275 (2005) [hep-th/0412103].

G. Ossola, C. G. Papadopoulos and R. Pittau, "Reducing Full One-Loop Amplitudes to Scalar Integrals at the Integrand Level," Nucl. Phys. B **763**, 147-169 (2007) [arXiv:hep-ph/0609007 [hep-ph]];

D. Forde, "Direct Extraction of One-Loop Integral Coefficients," Phys. Rev. D **75**, 125019 (2007) [arXiv:0704.1835 [hep-ph]];

[31] E. W. N. Glover and M. E. Tejeda-Yeomans, "Two Loop QCD Helicity Amplitudes for Massless Quark Massless Gauge Boson Scattering," JHEP **0306**, 033 (2003) [arXiv:0304169 [hep-ph]];

E. W. N. Glover "Two-loop QCD Helicity Amplitudes for Massless Quark-Quark Scattering," JHEP **0404**, 021 (2004) [arXiv:0401119 [hep-ph]].

[32] Z. Bern, A. Edison, D. Kosower and J. Parra-Martinez, "Curvature-Squared Multiplets, Evanescent Effects, and the U(1) Anomaly in $N = 4$ Supergravity," Phys. Rev. D **96**, no. 6, 066004 (2017) [arXiv:1706.01486 [hep-th]].

[33] A. Smirnov, "Algorithm FIRE – Feynman Integral REduction," JHEP **10**, 107 (2008) [arXiv:0807.3243 [hep-ph]];

A. V. Smirnov, "FIRE5: a C++ Implementation of Feynman Integral REduction," Comput. Phys. Commun. **189**, 182-191 (2015) [arXiv:1408.2372 [hep-ph]];

A. Smirnov and F. Chuharev, "FIRE6: Feynman Integral REduction with Modular Arithmetic," [arXiv:1901.07808 [hep-ph]].

[34] See the ancillary files of this manuscript.

[35] M. E. Peskin and D. V. Schroeder, "An Introduction to Quantum Field Theory," CRC Press, 2016

[36] L. J. Dixon, "Calculating Scattering Amplitudes Efficiently," [arXiv:hep-ph/9601359 [hep-ph]];

H. Elvang and Y. Huang, "Scattering Amplitudes," [arXiv:1308.1697 [hep-th]];
Z. Bern, J. J. Carrasco, M. Chiodaroli, H. Johansson and R. Roiban, "The Duality Between Color and Kinematics and its Applications," [arXiv:1909.01358 [hep-th]].

[37] Z. Bern, L. J. Dixon and D. A. Kosower, "One Loop Corrections to Two Quark Three Gluon Amplitudes," Nucl. Phys. B **437**, 259-304 (1995) [arXiv:hep-ph/9409393 [hep-ph]].

[38] L. Dixon, unpublished, (2002);
N. Arkani-Hamed, F. Cachazo and J. Kaplan, "What is the Simplest Quantum Field Theory?," JHEP **09**, 016 (2010) [arXiv:0808.1446 [hep-th]];
Y. Huang, D. A. McGady and C. Peng, "One-Loop Renormalization and the S-matrix," Phys. Rev. D **87**, no.8, 085028 (2013) [arXiv:1205.5606 [hep-th]].

[39] T. Becher and M. Neubert, "Infrared Singularities of Scattering Amplitudes in Perturbative QCD," Phys. Rev. Lett. **102**, 162001 (2009) [arXiv:0901.0722 [hep-ph]];
J. y. Chiu, A. Fuhrer, R. Kelley and A. V. Manohar, "Factorization Structure of Gauge Theory Amplitudes and Application to Hard Scattering Processes at the LHC," Phys. Rev. D **80**, 094013 (2009) [arXiv:0909.0012 [hep-ph]].

[40] A. J. Buras and P. H. Weisz, "QCD Nonleading Corrections to Weak Decays in Dimensional Regularization and 't Hooft-Veltman Schemes," Nucl. Phys. B **333**, 66-99 (1990)
I. Jack, D. Jones and K. Roberts, "Equivalence of Dimensional Reduction and Dimensional Regularization," Z. Phys. C **63**, 151-160 (1994) [arXiv:hep-ph/9401349 [hep-ph]];
S. Herrlich and U. Nierste, "Evanescent Operators, Scheme Dependences and Double Insertions," Nucl. Phys. B **455**, 39-58 (1995) [arXiv:hep-ph/9412375 [hep-ph]];
R. Harlander, P. Kant, L. Mihaila and M. Steinhauser, "Dimensional Reduction Applied to QCD at Three Loops," JHEP **09**, 053 (2006) [arXiv:hep-ph/0607240 [hep-ph]].

[41] M. J. Dugan and B. Grinstein, "On the Vanishing of Evanescent Operators," Phys. Lett. B **256**, 239-244 (1991)

[42] G. F. Sterman, "Mass Divergences in Annihilation Processes. 1. Origin and Nature of Divergences in Cut Vacuum Polarization Diagrams," Phys. Rev. D **17**, 2773 (1978);
G. F. Sterman, "Mass Divergences in Annihilation Processes. 2. Cancellation of Divergences in Cut Vacuum Polarization Diagrams," Phys. Rev. D **17**, 2789 (1978).

[43] L. Magnea and G. F. Sterman, "Analytic Continuation of the Sudakov Form-Factor in QCD," Phys. Rev. D **42**, 4222 (1990);
W. T. Giele and E. W. N. Glover, "Higher Order Corrections To Jet Cross-Sections in e^+e^- Annihilation," Phys. Rev. D **46**, 1980 (1992);
Z. Kunszt, A. Signer and Z. Trocsanyi, "Singular Terms of Helicity Amplitudes at One Loop in QCD and the Soft Limit Of The Cross-Sections of Multiparton Processes," Nucl. Phys. B **420**, 550 (1994) [hep-ph/9401294];
S. Catani, "The Singular Behavior of QCD Amplitudes at Two Loop Order," Phys. Lett. B **427**, 161 (1998) [hep-ph/9802439].

[44] G. F. Sterman, *An Introduction to Quantum Field Theory,* Cambridge University Press (1993).

[45] L. J. Dixon and Y. Shadmi, "Testing Gluon Self Interactions in Three Jet Events at Hadron Colliders," Nucl. Phys. B **423**, 3-32 (1994) [arXiv:hep-ph/9312363 [hep-ph]];
A. Azatov, R. Contino, C. S. Machado and F. Riva, "Helicity Selection Rules and Noninterference for BSM Amplitudes," Phys. Rev. D **95**, no.6, 065014 (2017) [arXiv:1607.05236 [hep-ph]];
A. Helset and M. Trott, "On Interference and Non-Interference in the SMEFT," JHEP **04**, 038 (2018) [arXiv:1711.07954 [hep-ph]].

[46] Z. Bern, L. J. Dixon and D. A. Kosower, "On-Shell Methods in Perturbative QCD,"

Annals Phys. **322**, 1587-1634 (2007) [arXiv:0704.2798 [hep-ph]];

Z. Bern and Y. Huang, "Basics of Generalized Unitarity," J. Phys. A **44**, 454003 (2011) [arXiv:1103.1869 [hep-th]];

H. Ita, "Susy Theories and QCD: Numerical Approaches," J. Phys. A **44**, 454005 (2011) [arXiv:1109.6527 [hep-th]];

L. J. Dixon, "A Brief Introduction to Modern Amplitude Methods," [arXiv:1310.5353 [hep-ph]].

[47] F. A. Berends, R. Kleiss, P. De Causmaecker, R. Gastmans and T. T. Wu, "Single Bremsstrahlung Processes in Gauge Theories," Phys. Lett. **103B**, 124 (1981);

F. A. Berends, R. Kleiss, P. De Causmaecker, R. Gastmans, W. Troost and T. T. Wu, "Multiple Bremsstrahlung in Gauge Theories at High-Energies. 2. Single Bremsstrahlung," Nucl. Phys. B **206**, 61 (1982);

Z. Xu, D. H. Zhang and L. Chang, "Helicity amplitudes for multiple bremsstrahlung in massless nonabelian gauge theories," Nucl. Phys. B **291** (1987) 392.

[48] Z. Bern, A. De Freitas and L. J. Dixon, "Two Loop Helicity Amplitudes for Gluon-Gluon Scattering in QCD and Supersymmetric Yang-Mills Theory," JHEP **03**, 018 (2002) [arXiv:hep-ph/0201161 [hep-ph]].

[49] J. C. Collins, A. V. Manohar and M. B. Wise, "Renormalization of the Vector Current in QED," Phys. Rev. D **73**, 105019 (2006) [arXiv:hep-th/0512187 [hep-th]].

[50] H. Politzer, "Asymptotic Freedom: An Approach to Strong Interactions," Phys. Rept. **14**, 129-180 (1974).

[51] Z. Bern, L. J. Dixon and D. A. Kosower, "One loop corrections to two quark three gluon amplitudes," Nucl. Phys. B **437**, 259-304 (1995) [arXiv:hep-ph/9409393 [hep-ph]].

[52] L. Lehman, "Extending the Standard Model Effective Field Theory with the Complete Set of Dimension-7 Operators," Phys. Rev. D **90**, no.12, 125023 (2014) [arXiv:1410.4193

[hep-ph]];

Y. Liao and X. D. Ma, "Renormalization Group Evolution of Dimension-seven Baryon- and Lepton-number-violating Operators," JHEP **11**, 043 (2016) [arXiv:1607.07309 [hep-ph]];

H. L. Li, Z. Ren, J. Shu, M. L. Xiao, J. H. Yu and Y. H. Zheng, "Complete Set of Dimension-8 Operators in the Standard Model Effective Field Theory," [arXiv:2005.00008 [hep-ph]];

C. W. Murphy, "Dimension-8 Operators in the Standard Model Effective Field Theory," [arXiv:2005.00059 [hep-ph]].

[53] Y. t. Huang, O. Schlotterer and C. Wen, "Universality in String Interactions," JHEP **09**, 155 (2016) [arXiv:1602.01674 [hep-th]].

[54] Z. Bern and D. A. Kosower, "The Computation of Loop Amplitudes in Gauge Theories," Nucl. Phys. B **379**, 451-561 (1992);

Z. Kunszt, A. Signer and Z. Trocsanyi, "One Loop Helicity Amplitudes for All $2 \to 2$ Processes in QCD and $N = 1$ Supersymmetric Yang-Mills Theory," Nucl. Phys. B **411**, 397-442 (1994) [arXiv:hep-ph/9305239 [hep-ph]].

Chapter 4

Leading Nonlinear Tidal Effects and Scattering Amplitudes

We present the two-body Hamiltonian and associated eikonal phase, to leading post-Minkowskian order, for infinitely many tidal deformations described by operators with arbitrary powers of the curvature tensor. Scattering amplitudes in momentum and position space provide systematic complementary approaches. For the tidal operators quadratic in curvature, which describe the linear response to an external gravitational field, we work out the leading post-Minkowskian contributions using a basis of operators with arbitrary numbers of derivatives which are in one-to-one correspondence with the worldline multipole operators. Explicit examples are used to show that the same techniques apply to both bodies interacting tidally with a spinning particle, for which we find the leading contributions from quadratic in curvature tidal operators with an arbitrary number of derivatives, and to effective field theory extensions of general relativity. We also note that the leading post-Minkowskian order contributions from higher-dimension operators manifest double-copy relations. Finally, we comment on the structure of higher-order corrections.

4.1 Introduction

The remarkable discovery of gravitational waves by the LIGO and Virgo collaborations [1] has ushered in a new era of exploration that promises major new discoveries on black holes, neutron stars and perhaps even new basic insights into fundamental physics. Theoretical tools of increased precision, matching that of gravitational-wave signals not only from current detectors but also from proposed gravitational-wave observatories [2], are required.

The evolution of a compact binary and the ensuing gravitational-wave emission can be divided in three distinct phases — inspiral, merger and ring down — according to their underlying properties. The inspiral part of binary mergers, which is the subject of this paper, is analyzed through models such as the effective one-body (EOB) formalism [3]. The weak gravitational field during this phase makes it suitable for a perturbative approach and these models import information from post-Newtonian (PN) gravity [4–7], as well as the self-force framework [8] and numerical relativity [9]. More recently, the post-Minkowskian (PM) expansion [10–16] has gained prominence due to its capture of the complete velocity dependence at fixed order in Newton's constant. By exposing the analytic structure of each order, this expansion also offers new insight into features of gravitational perturbation theory, exposes hereto unexpected structure in certain observables, and may open a path to the resummation of perturbation theory in the classical limit. The PN, PM and self-force expansions provide important nontrivial cross checks in their overlapping regions of validity [7, 13, 14, 17]. For recent reviews see Refs. [18].

Over the years a close link between classical physics and scattering amplitudes has been developed [11–13, 15, 19–21] and led to a robust and powerful means for obtaining two-body Hamiltonians [11] and observables in the post-Minkowskian expansion. It was obtained by combining modern techniques, such as generalized unitarity [22], which emphasize gauge-invariant building blocks at all stages and build higher-order contributions from lower-order ones with effective field theory methods. This framework proved its effectiveness through

the construction of the sought after two-body Hamiltonian at the third order in Newton's constant [12, 13] and the identification of surprising simplicity in physical observables of interacting spinning black holes [23]. The scattering angle is of particular importance, as it provides a direct link [20] with the EOB framework [3] used to predict gravitational wave emission from compact binaries.

In this paper we investigate the effects of tidal deformations [24] on the conservative two-body Hamiltonian during the inspiral phase, focusing on their structure in the post-Minkowskian expansion. The tidal deformations offer a window into the equation of state of neutrons stars [25] and test our understanding of black holes [21, 26–30] and of possible exotic physics [31]. While tidal effects are expected to vanish for black holes in general relativity [32], they are of crucial importance for understanding the equation of state of neutron stars. These corrections are formally equivalent to fifth-order post-Newtonian effects [5], highlighting the importance of precision perturbative calculations.

Properties of extended bodies that relate to their finite size can be encoded in local-operator deformations of a point-particle theory by integrating out their internal degrees of freedom. The set of all possible tidal operators is constrained only by the symmetry properties of the fundamental theory, such as parity. We introduce our organization of tidal operators in close analogy with the case of electromagnetic susceptibilities. Indeed, not only is there a formal similarity between gauge theory and gravity, but the integrand of gravitational scattering amplitudes can be obtained directly from gauge theory using the double copy [33, 34]. For the relatively simple case of the leading-PM order contribution of a given tidal operator to scattering amplitudes, these relations follow from the factorization of the point-particle energy-momentum tensor and from the fact that the linearized Riemann tensor is a product of two gauge-theory field strengths. Thus, in analogy with the case of electromagnetic interactions of extended bodies, tidal operators may contain arbitrarily-high number of Riemann curvature tensors with an arbitrary number of derivatives.

Curvature-squared tidal operators, describing the linear response of an extended body

to an external gravitational field, were recently classified in Ref. [30], where an expression for the two-body Hamiltonian and scattering angle at leading post-Minkowskian order was conjectured. Here we prove the conjecture for a basis of operators whose Wilson coefficients in the four-dimensional point-particle effective action are exactly the same as the worldline electric and magnetic tidal coefficients, related to the corresponding multipole Love numbers by factors of the typical scale of the body, see e.g. Ref. [5, 25, 28]. The lowest-order matrix elements of our tidal operators are, by construction, the same as the matrix elements of the worldline tidal operators. To establish the map beyond leading order it is necessary to compare physical quantities. At the next-to-leading order the contributions of low-derivative R^2 tidal operators to the two-body Hamiltonian and to the scattering angle were determined in Refs. [21, 29].

We also obtain the leading-order modifications of the two-body Hamiltonian and of the scattering angle due to tidal operators with arbitrarily-high number of Weyl tensors, which describe the nonlinear response of extended bodies to external gravitational field. As usual we organize the operators in terms of electric and magnetic-type components, E and B, of the Riemann (or Weyl) tensor. The finite rank of these tensors leads to nontrivial relations between different operators, allowing us to express the contributions of E^n and B^n-type operators for $n \geq 4$ in terms of those of products of simpler operators, thus reducing the number of independent structures.

While these relations appear mysterious for scattering amplitudes in momentum space, they are made manifest by Fourier-transforming the integral representation of the amplitude to position space. At any loop order, the transform decouples all integrals from each other. This observation allows us to write down closed-form expressions for amplitudes, two-body Hamiltonians and scattering angles generated by infinite families of operators. Beyond leading order the structure of tidally-deformed amplitudes is more complicated, but the momentum-space methods of Refs. [11–13, 21] can be applied systematically. Integration by parts methods [35] are especially powerful for the conservative two-body problem because in

the potential region of loop integrals all relevant integrals are of single-scale type [36].

The methods we use to describe tidal operators apply equally well to deformations of a point-particle theory by any operators, including e.g. those arising in effective field theory extensions of General Relativity [37–40]. We illustrate this point by working out the contributions of R^3 and R^4 and compare them with existing results. The two-body Hamiltonian and associated observables for a point-particle deformed by tidal operators interacting with a spinning particle can also be derived through similar methods. To leading PM order, only the single-graviton interaction of the spinning particle is relevant and it is captured by the stress tensors described in [23, 41, 42]. As an example, we find the leading spin-orbit contributions from E^2-type tidal operators with an arbitrary number of derivatives interacting with a spinning particle.

This paper organized as follows. In Section 4.2 we present a description of the operators encoding tidal deformations. In Section 4.3 we discuss the leading-order tidal contributions from R^2-type operators with an arbitrary number of derivatives. This section also demonstrate how to incorporate spin effects for the second body. We proceed to derive in Section 4.4 the leading contributions of various infinite classes of R^n-type tidal operators and also comment on their higher-order contributions. In Section 4.5 we discuss the application of our methods to the case of R^n extensions of General Relativity. We present our conclusions in Section 4.6. An appendix gives the explicit results for the contributions of a collection of high-order tidal operators to the two-body Hamiltonian and the associate scattering amplitudes.

Note added: While this project was ongoing we became aware of concurrent work by Cheung, Shah and Solon [43] based on using the geodesic equation and containing some overlap on leading contributions to the two-body Hamiltonian from the R^n tidal operators. In addition, the methods developed there determine the two-body Hamiltonian for a tidally-deformed test particle interacting with a Schwarzschild black hole, to all orders in

the Schwarzschild radius of the latter. We are grateful for interesting and helpful discussions and sharing drafts.

4.2 Effective actions for tidal effects

4.2.1 Effective actions for post-Minkowskian potentials

In this work we study tidal or finite-size effects in the gravitational interactions of two massive extended bodies. They are encoded in a classical two-body Hamiltonian of the form

$$H(\boldsymbol{p},\boldsymbol{r}) = \sqrt{\boldsymbol{p}^2+m_1^2}+\sqrt{\boldsymbol{p}^2+m_2^2}+V(\boldsymbol{p},\boldsymbol{r})\,, \tag{4.1}$$

and is extracted systematically, following the general approach introduced in [11], by matching QFT scattering amplitudes to a non-relativistic EFT. If the size of the two bodies is much smaller than their separation, non-analytic/long-distance classical potential has the form

$$V(\boldsymbol{p},\boldsymbol{r}) \sim c_i(\boldsymbol{p})\, m \left(\frac{Gm}{|\boldsymbol{r}|}\right)^i\,, \tag{4.2}$$

where m carries unit mass dimension and the momentum transfer $\boldsymbol{q}$, Fourier-conjugate to $\boldsymbol{r}$, is much smaller than the center of mass momentum $\boldsymbol{p}$. Such a conservative potential arises from integrating out gravitons with momenta ℓ in the potential region which has the scaling behavior

$$\ell = (\ell^0,\boldsymbol{\ell}) \sim (|\boldsymbol{q}||\boldsymbol{v}|,|\boldsymbol{q}|), \tag{4.3}$$

where $|\boldsymbol{v}| \sim \mathcal{O}\left(|\boldsymbol{p}|/m\right)$. Note that Gm is of the order of the effective Schwarzschild radius of the particles R_s, so the classical expansion[1] of the potential is an expansion in $R_s/|\boldsymbol{r}|$. If the separation of the two bodies can be of the same order as their typical size R, then the

[1]The amplitude also contains non-analytic terms which we will not study here, corresponding to quantum contributions to the potential of the form $(\ell_p^2/r^2)^n$, where ℓ_p is the Planck length.

classical potential takes the form

$$V(\boldsymbol{p},\boldsymbol{r}) \sim c_{i,k}(\boldsymbol{p})\, m \left(\frac{Gm}{|\boldsymbol{r}|}\right)^i \left(\frac{R}{|\boldsymbol{r}|}\right)^k . \tag{4.4}$$

For black holes $R \sim R_s$ so the size of terms with powers of R is comparable to higher PM orders. For other bodies $R > R_s$ so the contribution should be bigger. For reference, neutrons stars have $R/R_s \sim 10$, and the sun has $R/R_s \sim 10^5$. In practice, it is convenient to always use R_s/r as the expansion parameter so that the tidal effects just modify the coefficients in the usual PM potential, i.e. $c_{i,k} \sim \Delta c_{i+k}$.

From our point of view, the new scale R_s is introduced by integrating out the degrees of freedom that describe the tidal dynamics of an extended body to yield a point-particle effective theory. In such an effective theory the finite size effects are encoded as higher-dimension operators $\mathcal{O}_i$ which are suppressed by powers of $R_s|\boldsymbol{q}|$. Their Wilson coefficients can be determined either by matching to the complete theory that includes the tidal degrees of freedom, or by comparing to experiment. A side effect of choosing R_s instead of R as the scale characterizing finite-size effects is that for less compact bodies the Wilson coefficients are not necessarily $\mathcal{O}(1)$. This approach was pioneered in the context of a worldline PN formalism in Ref. [5], and recently adapted to the PM framework in Ref. [29]. In the QFT language this approach has been recently used in Refs. [21, 30]. In section we provide a systematic treatment of such effective actions and write a basis of operators which simplifies the translation between QFT and worldline formalisms and makes the relation to familiar *in-in* observables manifest.

The cases that we focus on in this paper correspond to leading contributions from tidal or other operators. Although these operators first contribute to loop amplitudes, the determination of their leading-order contribution to the two-body potential is straightforward and formally given by inverting the Born relation between the scattering amplitude and the

potential:

$$V_{\mathcal{O}}(\boldsymbol{p},\boldsymbol{r}) = -\frac{1}{4E_1E_2}\int \frac{d^{D-1}\boldsymbol{q}}{(2\pi)^{D-1}} e^{-i\boldsymbol{q}\cdot\boldsymbol{r}}\mathcal{M}_{\mathcal{O}}(\boldsymbol{p},\boldsymbol{q})\,. \tag{4.5}$$

Here $\mathcal{M}_{\mathcal{O}}$ is the leading-order four-scalar scattering amplitude with with a single insertion of $\mathcal{O}$, center of mass momentum $\boldsymbol{p}$, transferred momentum $\boldsymbol{q}$. In general the potential is gauge dependent and not unique. In the above equation we choose to expose the on-shell condition on $\boldsymbol{q}$ first such that $\boldsymbol{p}\cdot\boldsymbol{q} \simeq \mathcal{O}(\boldsymbol{q}^2) \sim 0$. This naturally gives the potential in the isotropic gauge.

Alternatively, the effective two-body Hamiltonian can be constructed by matching its conservative observables — such as the conservative scattering angle, or the impulse and spin kick — or the closely-related eikonal phase [44],

$$\delta_{\mathcal{O}}(\boldsymbol{p},\boldsymbol{b}) = \frac{1}{4m_1m_2\sqrt{\sigma^2-1}}\int \frac{d^{D-2}\boldsymbol{q}}{(2\pi)^{D-2}} e^{-i\boldsymbol{b}\cdot\boldsymbol{q}}\mathcal{M}_{\mathcal{O}}(\boldsymbol{p},\boldsymbol{q})\,, \tag{4.6}$$

with the corresponding quantities in the complete theory. Here we use $-p_i = -m_iu_i$ as the incoming momenta of particle 1 and 2 and

$$\sigma \equiv \frac{p_1\cdot p_2}{m_1m_2} = u_1\cdot u_2\,. \tag{4.7}$$

In either case, the matching is carried out order by order in Newton's constant G, that is order by order in the post-Minkowskian expansion. The relation between the eikonal and conservative observables holds also for the scattering of spinning particles. To leading nontrivial order, the effect of a composite operator $\mathcal{O}$ on the impulse and spin kick in the center-of-mass frame is

$$\Delta\boldsymbol{p} = -\nabla_{\boldsymbol{b}}\delta_{\mathcal{O}}(\boldsymbol{b}) + \dots\,, \qquad \Delta\boldsymbol{S}_i = -\{\boldsymbol{S}_i, \delta_{\mathcal{O}}(\boldsymbol{b})\} + \dots\,, \tag{4.8}$$

where the ellipsis stand for higher-order terms that depend on $\mathcal{O}$ and $\{\bullet,\bullet\}$ is the Poisson

bracket. We expect that the all-order relation between the eikonal phase and conservative observables put forth in Ref. [23] holds in the presence of deformations by tidal and other composite operators. At leading order, the semiclassical approximation implies that the eikonal phase coincides with the radial action integrated over the scattering trajectory. We discuss this further in Section 4.3.3. The latter allows us to make contact with Ref. [28] in which tidal effects were computed using a classical worldline formalism for a subset of tidal operators.

Alternatively the matching can be performed by directly computing a physically meaningful quantity such as the conservative scattering angle, corresponding to the scattering with radiation reaction turned off; or the closely related eikonal phase. In either case matching is performed order by order in perturbation theory in Newton's constant, G, that is order by order in the post-Minkowskian expansion.

$$\mathcal{M}_{\mathcal{O}}(\boldsymbol{q}) = |\boldsymbol{q}|^A \overline{\mathcal{M}}_{\mathcal{O}}\,, \tag{4.9}$$

$$V_{\mathcal{O}}(\boldsymbol{r}) = -\frac{1}{4E_1E_2}\frac{2^A\Gamma\left(\frac{1}{2}(D-1+A)\right)}{\pi^{(D-1)/2}\Gamma(-\frac{1}{2}A)}|\boldsymbol{r}|^{-A-(D-1)}\,\overline{\mathcal{M}}_{\mathcal{O}}\,, \tag{4.10}$$

$$\delta_{\mathcal{O}}(\boldsymbol{b}) = \frac{1}{4m_1m_2\sqrt{\sigma^2-1}}\frac{2^A\Gamma\left(\frac{1}{2}(D-2+A)\right)}{\pi^{(D-2)/2}\Gamma(-\frac{1}{2}A)}|\boldsymbol{b}|^{-A-(D-2)}\,\overline{\mathcal{M}}_{\mathcal{O}}\,, \tag{4.11}$$

where we have used the formula for the Fourier transform of a power

$$\int\frac{d^D\boldsymbol{q}}{(2\pi)^D}e^{-i\boldsymbol{x}\cdot\boldsymbol{q}}|\boldsymbol{q}|^A = \frac{2^A\Gamma\left(\frac{1}{2}(D+A)\right)}{\pi^{d/2}\Gamma(-\frac{1}{2}A)}|\boldsymbol{x}|^{-(A+D)}\,. \tag{4.12}$$

Here A is power of the soft q carried by the amplitude. For an operator with n power of Riemann or Weyl tensors with n_∂ derivatives acting on them, the leading contribution to the two-to-two scalar amplitude is

$$A = 3n + n_\partial - 3 - 2\epsilon(n-1), \tag{4.13}$$

where we use $D = 4 - 2\epsilon$. For example, for the electric and magnetic operators E^2 and B^2 we will introduce shortly, $n = 2$ and $n_\partial = 0$ so $A = 3 - 2\epsilon$, and every pair of derivatives acting of these increases n_∂ and A by two.

4.2.2 Effective actions for linear and non-linear tidal effects

We now explain how to parametrize the response of a general body to an external field and how this can be encoded in an effective action. We will discuss this in detail in the simpler case of electromagnetism, which will easily generalize to the gravitational case.

Tidal response in non-linear optics

The full non-linear response of a body to an external electric field E_i is described by the induced electric dipole moment density D_i. In the rest frame of the body, it has a formal expansion in powers of the electric field [45]:

$$D_{i_1}(t, \boldsymbol{x}) = \chi^{(1)}_{i_1 i_2}(t, \boldsymbol{x}) E_{i_2}(t, \boldsymbol{x}) + \chi^{(2)}_{i_1 i_2 i_3}(t, \boldsymbol{x}) E_{i_2}(t, \boldsymbol{x}) E_{i_3}(t, \boldsymbol{x}) + \cdots . \tag{4.14}$$

The first term is the familiar linear response function; the subsequent terms encode the properties of the body in the susceptibility tensors, $\chi^{(n)}$, which are symmetric in their indices. Similarly, in the presence of a magnetic field B_i, one can write magnetic susceptibilities, as well as general susceptibilities capturing the response under a general electromagnetic field.

It is convenient to transform Eq. (4.14) to Fourier space, where it takes the form

$$\begin{aligned} D_{i_1}(-\omega_1, -\boldsymbol{q}_1) = {} & \chi^{(1)}_{i_1 i_2}(\omega_1, \boldsymbol{q}_1; \omega_2, \boldsymbol{q}_2) E_{i_2}(\omega_2, \boldsymbol{q}_2) \\ & + \chi^{(2)}_{i_1 i_2 i_3}(\omega_1, \boldsymbol{q}_1; \omega_2, \boldsymbol{q}_2; \omega_3, \boldsymbol{q}_3) E_{i_2}(\omega_2, \boldsymbol{q}_2) E_{i_3}(\omega_3, \boldsymbol{q}_3) + \cdots . \end{aligned} \tag{4.15}$$

Here we have adopted a generalized summation convention where repeated frequencies and momenta are integrated over, and the Fourier susceptibilities include energy-momentum-

conservation delta functions

$$\chi^{(n-1)}_{i_1\cdots i_n} = \delta\left(\sum_i \omega_i\right)\delta\left(\sum_i \boldsymbol{q}_i\right)\tilde{\chi}^{(n-1)}_{i_1\cdots i_n}\,, \tag{4.16}$$

which account for the fact that the position-space product in Eq. (4.14) becomes a Fourier space convolution in Eq. (4.15).

The dipole density can be related to a generating function — or effective action — $S(E)$, via the usual response formula

$$D_{i_1}(-\omega_1, -\boldsymbol{q}_1) = \frac{\partial S(E)}{\partial E^{i_1}(\omega_1, \boldsymbol{q}_1)}\,. \tag{4.17}$$

The effective action, following from formally integrating Eq. (4.14), is given by

$$\begin{aligned} S(E) = &\frac{1}{2}\chi^{(1)}_{i_1 i_2}(\omega_1, \boldsymbol{q}_1; \omega_2, \boldsymbol{q}_2)E_{i_1}(\omega_1, \boldsymbol{q}_1)E_{i_2}(\omega_2, \boldsymbol{q}_2) \\ &+ \frac{1}{3}\chi^{(2)}_{i_1 i_2 i_3}(\omega_1, \boldsymbol{q}_1; \omega_2, \boldsymbol{q}_2; \omega_3, \boldsymbol{q}_3)E_{i_1}(\omega_1, \boldsymbol{q}_1)E_{i_2}(\omega_2, \boldsymbol{q}_2)E_{i_3}(\omega_3, \boldsymbol{q}_3) + \cdots\,. \end{aligned} \tag{4.18}$$

This makes clear that the momentum space susceptibilities are completely symmetric tensors, as well as symmetric functions of all their arguments. $S(E)$ could be put in a form closer to an action by series expanding the susceptibilities and rewriting the powers of frequency and three-momenta as derivatives. For instance one can rewrite some terms in the expansion as follows

$$\left(\frac{\partial \chi^{(1)}_{i_1 i_2}}{\partial \omega_1 \partial \boldsymbol{q}_2^j}(0)\,\omega_1 \boldsymbol{q}_2^j\right) E_{i_1}(\omega_1, \boldsymbol{q}_1)E_{i_2}(\omega_2, \boldsymbol{q}_2) \sim \left(\frac{\partial \chi^{(1)}_{i_1 i_2}}{\partial \omega_1 \partial \boldsymbol{q}_2^j}(0)\right)\partial_t E_{i_1}(t, \boldsymbol{x})\boldsymbol{\nabla}^j_{\boldsymbol{x}} E_{i_2}(t, \boldsymbol{x})\,. \tag{4.19}$$

Note that the expansion in the three momenta here simply corresponds to a multipole expansion of the electric fields.

So far we have been working in the rest frame of the object. The choice of a frame breaks manifest Lorentz invariance down to the rotations around the position of the object. We

would like to covariantize the expressions above so that is they are valid in an arbitrary reference frame, in which the body moves with velocity $\boldsymbol{v}$. This can be done by considering the four-velocity of the object $u^\mu = \gamma(1, \boldsymbol{v})$, where γ is the Lorentz factor. As is well known the electric field and magnetic fields in the rest frame of the body can be covariantly written as

$$E_\mu = F_{\mu\nu} u^\nu \,, \quad B_\mu = *F_{\mu\nu} u^\nu \,, \tag{4.20}$$

where $F_{\mu\nu}$ is the electromagnetic field strength, and $*F_{\mu\nu}$ its dual. Similarly, it is clear that any frequency and spatial momenta can be written as

$$\omega_i \to u \cdot q \equiv u^\mu q_\mu \,, \qquad \boldsymbol{q}_i \to (q^\perp)_\mu \equiv P_{\mu\nu} q^\nu \,, \tag{4.21}$$

where we have introduced the four momentum of the field, q_i^μ and a projector,

$$P^{\mu\nu} = \eta^{\mu\nu} - u^\mu u^\nu \,, \tag{4.22}$$

which makes indices purely spatial in the rest frame of the object. Naively this covariantization requires adding components to the polarizabilities so that $\chi^{(n-1)}_{i_1 \cdots i_n} \to \chi^{(n-1)}_{\mu_1 \cdots \mu_n}$, and we can write

$$\begin{aligned} S(E) = {} & \chi^{(1)}_{\mu_1\mu_2}(u \cdot q_1, q_1^\perp; u \cdot q_2, q_2^\perp) E_{\mu_1}(q_1) E_{\mu_2}(q_2) \\ & + \chi^{(2)}_{\mu_1\mu_2\mu_3}(u \cdot q_1, q_1^\perp; u \cdot q_2, q_2^\perp, u \cdot q_3, q_3^\perp) E_{\mu_1}(q_1) E_{\mu_2}(q_2) E_{\mu_3}(q_3) + \cdots \,, \end{aligned} \tag{4.23}$$

due to the fact that $u^\mu E_\mu = u^\mu B_\mu = 0$, which follows from the antisymmetry of the field strength.

The generating function written above describes the non-linear response of an arbitrary material, including those that violate rotational and Lorentz invariance. In the following we will be only interested in Lorentz-preserving effects, which impose addition constraints

on the susceptibility tensors. Firstly, Lorentz invariance constrains the index structure of the susceptibility, which can only be carried by Lorentz-covariant tensors. If we impose parity, the only such tensors are the metric itself and the graviton momenta, so the tensor susceptibility must decompose in a set of scalar susceptibilities as follows

$$\chi^{(1)}_{\mu_1\mu_2} = \chi^{(1)}_0\, g_{\mu_1\mu_2} + \chi^{(1)}_1\, q^{\perp}_{1\,\mu_1} q^{\perp}_{2\,\mu_2} \tag{4.24}$$

$$\chi^{(2)}_{\mu_1\mu_2\mu_3} = \chi^{(2)}_0 \left(g_{\mu_1\mu_2} q^{\perp}_{3\,\mu_3} + g_{\mu_2\mu_3} q^{\perp}_{1\,\mu_1} + g_{\mu_3\mu_1} q^{\perp}_{2\,\mu_2}\right), \tag{4.25}$$

$$\chi^{(3)}_{\mu_1\mu_2\mu_3\mu_4} = \chi^{(3)}_0\, g_{(\mu_1\mu_2} g_{\mu_3\mu_4)} + \chi^{(3)}_1 \left(g_{\mu_1\mu_2} q^{\perp}_{3\mu_3} q^{\perp}_{4\mu_4} + \text{perms}\right) + \chi^{(3)}_2\, q^{\perp}_{1\mu_1} q^{\perp}_{2\mu_2} q^{\perp}_{3\mu_3} q^{\perp}_{4\mu_4}\,, \tag{4.26}$$

where in general each tensor structure must be summed over permutations which respect the symmetry $(\mu_i \leftrightarrow \mu_j)$ while simultaneously swapping $q^{\perp}_i \leftrightarrow q^{\perp}_j$. Another consequence of Lorentz invariance is that the scalar susceptibilities only depend on Lorentz invariant combinations of momenta, so that

$$\chi^{(n-1)}_a(u\cdot q_i; q^{\perp}_i) \to \chi^{(n-1)}_a(u\cdot q_i; q^{\perp}_i \cdot q^{\perp}_j)\,. \tag{4.27}$$

Note that in the rest frame $q^{\perp}_i \cdot q^{\perp}_j = \boldsymbol{q}_i \cdot \boldsymbol{q}_j$.

Non-linear tidal response in gravity

It is now easy to generalize the tidal response for electromagnetism to its gravitational analog. In this case we start from the induced quadrupole moment, written in terms of the gravito-electric field

$$Q_{i_1 j_1}(t,\boldsymbol{x}) = \chi^{(1)}_{i_1 j_1 i_2 j_2}(t,\boldsymbol{x}) E_{i_2 j_2}(t,\boldsymbol{x}) + \chi^{(2)}_{i_1 j_1 i_2 j_2 i_3 j_3}(t,\boldsymbol{x}) E_{i_2 j_2}(t,\boldsymbol{x}) E_{i_3 j_3}(t,\boldsymbol{x}) + \cdots\,, \tag{4.28}$$

where now the gravitational susceptibilities are more general tensors symmetric in each pair of i and j indices

$$\chi_{\cdots ij\cdots} = \chi_{\cdots ji\cdots}\,, \qquad\qquad \chi_{\cdots i_a j_a \cdots i_b j_b \cdots} = \chi_{\cdots i_b j_b \cdots i_a j_a \cdots}\,. \tag{4.29}$$

In the rest frame of the object the electric field is related to the Weyl tensor as $E_{ij} = C_{0i0j}$. Similar expressions can be written for the response to a gravito-magnetic or to a mixed field.

All of these quantities can be covariantized by introducing

$$E_{\mu\nu} \equiv C_{\mu\alpha\nu\beta} u^\alpha u^\beta, \qquad B_{\mu\nu} \equiv (*C)_{\mu\alpha\nu\beta} u^\gamma u^\delta \equiv \frac{1}{2}\epsilon_{\alpha\beta\gamma\mu} C^{\alpha\beta}{}_{\delta\nu} u^\gamma u^\delta, \tag{4.30}$$

where all indices are curved and the Levi-Civita tensor is defined as $\epsilon^{0123} = +1$. As in the electromagnetic case the following relations hold

$$E_{\mu\nu} u^\nu = 0\,, \qquad B_{\mu\nu} u^\nu = 0\,, \tag{4.31}$$

as well as

$$E_\mu{}^\mu = 0\,, \qquad B_\mu{}^\mu = 0\,, \tag{4.32}$$

where the first equality is a consequence of the tracelessness of the Weyl tensor. The corresponding generating function for tidal response is then simply

$$\begin{aligned} S_{\rm grav}(E) = {} & \chi^{(1)}_{\mu_1\nu_1\mu_2\nu_2}(u\cdot q_1, Pq_1; u\cdot q_2, Pq_2)\phi(p') E^{\mu_1\nu_1}(q_1) E^{\mu_2\nu_2}(q_2)\phi(p) \\ & + \chi^{(2)}_{\mu_1\nu_2\mu_2\nu_2\mu_3\nu_3}(u\cdot q_1, Pq_1; u\cdot q_2, Pq_2, u\cdot q_3, Pq_3)\phi(p') E^{\mu_1\nu_1}(q_1) E^{\mu_2\nu_2}(q_2) E^{\mu_3\nu_3}(q_3)\phi(p) + \cdots \end{aligned} \tag{4.33}$$

where, as above, a convolution over all momenta is implicit, and the covariant susceptibilities are traceless in each pair of μ, ν indices $\eta^{\mu\nu}\chi_{\cdots\mu\nu\cdots} = 0$. Once again, Lorentz invariance will further constraint the form of the susceptibility tensors in a way analogous to Eqs. (4.24)-

(4.26).

From response to QFT effective actions

We now proceed to connect our discussion to a QFT effective action, focusing on the case of gravity; the electromagnetic case is completely analogous.

The connection can be easily made by interpreting the generating function, $S_{\rm grav}(E)$ as the expectation value in a background field of an operator in a one-particle state $|p\rangle$ with four momentum $p = mu$, and zero spin. In second-quantized language the one-particle state is created by a scalar field, ϕ, at infinity and

$$\begin{aligned} S_{\rm tidal} &= \chi^{(1)}_{\mu_1\mu_2}(u\cdot q_1, q_1^\perp; u\cdot q_2, q_2^\perp)\phi(p)E_{\mu_1}(q_1)E_{\mu_2}(q_2)\phi(p') \\ &\quad + \chi^{(2)}_{\mu_1\mu_2\mu_3}(u\cdot q_1, q_1^\perp; u\cdot q_2, q_2^\perp, u\cdot q_3, q_3^\perp)\phi(p)E_{\mu_1}(q_1)E_{\mu_2}(q_2)E_{\mu_3}(q_3)\phi(p') + \cdots\,, \end{aligned} \tag{4.34}$$

can be identified as the momentum-space effective action that encodes the response to the background field. Note that, in order to enforce momentum conservation, the Fourier-transformed susceptibilities must satisfy

$$\chi^{(n-1)}_{\mu_1\cdots\mu_n} = \delta\left(\sum_i q_i - q\right)\tilde{\chi}^{(n-1)}_{\mu_1\cdots\mu_n}\,, \tag{4.35}$$

where $q = -(p+p')$. Note that the susceptibilities are initially only defined for $q = 0$, so their covariantization requires an extension to $q \neq 0$. This does not affect the classical limit. As above, each term in the expansion of susceptibilities is encoded by a higher-dimension operator in the effective action, where now the factors of four-velocity u can be identified with derivatives acting on the scalar field. For instance,

$$\begin{aligned} &\partial_\omega^{2n}\chi^{(1)}_{\mu_1\nu_1\mu_2\nu_2}(0,0)[(u\cdot q_1)^{2n} + (u\cdot q_2)^{2n}]\phi(p')E^{\mu_1\nu_1}(q_1)E^{\mu_2\nu_2}(q_2)\phi(p) \\ &\quad\leftrightarrow \partial_\omega^{2n}\chi^{(1)}_{\mu_1\nu_1\mu_2\nu_2}(0,0)\int d^4x\sqrt{-g}\,\frac{1}{m^{2n}}\phi E^{\mu_1\nu_1}\nabla_{(\rho_1\cdots\rho_{2n})}E^{\mu_2\nu_2}\nabla^{(\rho_1\cdots\rho_{2n})}\phi\,. \end{aligned} \tag{4.36}$$

,

where the classical limit is implicit on the left-hand side. To write a generic operator appearing in this expansion it is convenient to introduce the combinations,

$$\begin{aligned}
\hat{E}_{\mu_1\mu_2\ldots\mu_n} &= \frac{i^2}{m^2}\mathrm{Sym}_{\mu_1\ldots\mu_n}[\nabla_{\nu_n}\ldots\nabla_{\nu_3}C_{\mu_1\alpha\mu_2\beta}\hat{P}^{\nu_n}_{\mu_n}\ldots\hat{P}^{\nu_3}_{\mu_3}\nabla^\alpha\nabla^\beta\,]\,,\\
\hat{B}_{\mu_1\mu_2\ldots\mu_n} &= \frac{i^2}{m^2}\mathrm{Sym}_{\mu_1\ldots\mu_n}[\nabla_{\nu_n}\ldots\nabla_{\nu_3}(*C)_{\mu_1\alpha\mu_2\beta}\hat{P}^{\nu_n}_{\mu_n}\ldots\hat{P}^{\nu_3}_{\mu_3}\nabla^\alpha\nabla^\beta\,]\,,\\
\hat{E}^{(l)}_{\mu_1\mu_2\ldots\mu_n} &= \frac{i^{m+2}}{m^{m+2}}\mathrm{Sym}_{\mu_1\ldots\mu_n}[\nabla_{\nu_n}\ldots\nabla_{\nu_3}\nabla^{\rho_1}\ldots\nabla^{\rho_l}C_{\mu_1\alpha\mu_2\beta}\hat{P}^{\nu_n}_{\mu_n}\ldots\hat{P}^{\nu_3}_{\mu_3}\nabla_{(\rho_1}\ldots\nabla_{\rho_l)}\nabla^\alpha\nabla^\beta\,]\,,\\
\hat{B}^{(l)}_{\mu_1\mu_2\ldots\mu_n} &= \frac{i^{m+2}}{m^{m+2}}\mathrm{Sym}_{\mu_1\ldots\mu_n}[\nabla_{\nu_n}\ldots\nabla_{\nu_3}\nabla^{\rho_1}\ldots\nabla^{\rho_l}(*C)_{\mu_1\alpha\mu_2\beta}\hat{P}^{\nu_n}_{\mu_n}\ldots\hat{P}^{\nu_3}_{\mu_3}\nabla_{(\rho_1}\ldots\nabla_{\rho_l)}\nabla^\alpha\nabla^\beta\,]\,,
\end{aligned} \tag{4.37}$$

where all the derivatives on the right of the Weyl tensor act on the scalar field, and the position-space projector is

$$\hat{P}^\nu_\mu = \frac{1}{m^2}(\partial_\mu\partial^\nu - \delta^\nu_\mu\partial^2)\,. \tag{4.38}$$

The terms in the expansion that encode the most general linear response are then

$$S^{\mathrm{QFT}}_{\mathrm{tidal}}\big|_{\mathrm{linear}} = m\int d^4x\sqrt{-g}\;\;\sum_{n=2}^{\infty}\sum_{l=0}^{\infty}(\mu^{(n,l)}\,\phi\hat{E}^{(l)}_{\mu_1\cdots\mu_n}\hat{E}^{(l)\,\mu_1\cdots\mu_n}\phi + \sigma^{(n,l)}\,\phi\hat{B}^{(l)}_{\mu_1\cdots\mu_n}\hat{B}^{(l)\,\mu_1\cdots\mu_n}\phi) \tag{4.39}$$

where the coefficients are related to the susceptibility as $\mu^{(n,l)} \sim (\partial_{\omega_2})^l(\partial_{q_1\cdot q_2})^l\chi^{(1)}_0(0;0)$, and the magnetic susceptibilities are related to $\sigma^{(n,l)}$ in a similar way. Operators like $\phi E^{(l_1)}_{\mu_1\mu_2}E^{(l_2)\mu_1\mu_2}\phi$ with $l_1 \neq l_2$ are related to operators with $l_1 = l_2$ by integration by parts and use of scalar field equations of motion. We therefore can ignore them at this order. Similarly, the effective action

$$S^{\mathrm{QFT}}_{\mathrm{tidal}}\big|_{\text{non-linear}} = m\int d^4x\sqrt{-g}\;\;\sum_{n=2}^{\infty}(\rho^{(n)}_e\,\phi\hat{E}_{\mu_1}{}^{\mu_2}\hat{E}_{\mu_2}{}^{\mu_3}\cdots\hat{E}_{\mu_n}{}^{\mu_1}\phi + \rho^{(n)}_m\,\phi\hat{B}_{\mu_1}{}^{\mu_2}\hat{B}_{\mu_2}{}^{\mu_3}\cdots\hat{B}_{\mu_n}{}^{\mu_1}\phi) + \cdots \tag{4.40}$$

encodes part of the lowest-multipole time-independent non-linear response,

It is not difficult to translate the different terms in the response functions into a first quantized framework. This leads to a one-to-one relation between the higher-dimension operators in the QFT effective action and worldline operators. The factors of u are identified with the four-velocity of the worldline $u^\mu = dx^\mu/d\tau$ and the factors of $(u\cdot\nabla)$ simply become derivatives with respect to the proper time τ. Thus, the analog of the operators in the effective worldline action are

$$\begin{aligned}
E_{\mu_1\mu_2\ldots\mu_n} &= \mathrm{Sym}_{\mu_1\mu_2\ldots\mu_n}\left[P^{\nu_3}_{\mu_3}\ldots P^{\nu_n}_{\mu_n}\nabla_{\nu_3}\ldots\nabla_{\nu_n}C_{\mu_1\alpha\mu_2\beta}\right]u^\alpha u^\beta\,,\\
B_{\mu_1\mu_2\ldots\mu_n} &= \mathrm{Sym}_{\mu_1\mu_2\ldots\mu_n}\left[P^{\nu_3}_{\mu_3}\ldots P^{\nu_n}_{\mu_n}\nabla_{\nu_3}\ldots\nabla_{\nu_n}(*C)_{\mu_1\alpha\mu_2\beta}\right]u^\alpha u^\beta\,,\\
E^{(m)}_{\mu_1\ldots\mu_n} &= (u^\alpha\nabla_\alpha)^m E_{\mu_1\ldots\mu_n} = (\partial_\tau)^m E_{\mu_1\ldots\mu_n}\,,\\
B^{(m)}_{\mu_1\ldots\mu_n} &= (u^\alpha\nabla_\alpha)^m B_{\mu_1\ldots\mu_n} = (\partial_\tau)^m B_{\mu_1\ldots\mu_n}\,,
\end{aligned} \tag{4.41}$$

where $P_{\mu\nu} = g_{\mu\nu} - u_\mu u_\nu$ is the u-orthogonal projector on the worldline. The effective action encoding the linear response are

$$S^{\text{worldline}}_{\text{tidal}}|_{\text{linear}} = \int d\tau \quad \sum_{n=2}^{\infty}\sum_{l=0}^{\infty}\mu^{(n,l)}\,(E^{(l)}_{\mu_1\cdots\mu_n}E^{(l)\,\mu_1\cdots\mu_n} + \sigma^{(n,l)}\,B^{(l)}_{\mu_1\cdots\mu_n}B^{(l)\,\mu_1\cdots\mu_n})\,. \tag{4.42}$$

Note that here we use a different normalization than Ref. [28], the relation between our coefficients is $\mu^{(n,l)}_{\text{BDG}} = 2l!\mu^{(n,l)}$ and $\sigma^{(n,l)}_{\text{BDG}} = 2(l+1)!\sigma^{(n,l)}$. The non-linear response is captured by

$$S^{\text{worldline}}_{\text{tidal}}\big|_{\text{non-linear}} = \int d\tau \quad \sum_{n=2}^{\infty}\rho^{(n)}_e\,E_{\mu_1}{}^{\mu_2}E_{\mu_2}{}^{\mu_3}\cdots E_{\mu_n}{}^{\mu_1} + \rho^{(n)}_m\,B_{\mu_1}{}^{\mu_2}B_{\mu_2}{}^{\mu_3}\cdots B_{\mu_n}{}^{\mu_1}) + \cdots\,. \tag{4.43}$$

Thus, for a particle of mass m_i described by the scalar field ϕ_i, the correspondence

between worldline operators and QFT Lagrangian operators is

$$\int d\tau E^{(l)}_{\mu_1\ldots\mu_n} E^{(l)\mu_1\ldots\mu_n} \longleftrightarrow m_i \int d^4x\sqrt{-g}\phi_i \hat{E}^{(l)}_{\mu_1\ldots\mu_n} \hat{E}^{(l)\mu_1\ldots\mu_n}\phi_i \,, \tag{4.44}$$

$$\int d\tau B^{(l)}_{\mu_1\ldots\mu_n} B^{(l)\mu_1\ldots\mu_n} \longleftrightarrow m_i \int d^4x\sqrt{-g}\phi_i \hat{B}^{(l)}_{\mu_1\ldots\mu_n} \hat{B}^{(l)\mu_1\ldots\mu_n}\phi_i \,. \tag{4.45}$$

The normalization of the QFT operators is fixed such that their four-point matrix elements in the classical limit reproduce the expectation value of the worldline operators, provided that the normalization of the asymptotic states is the same for both of them, i.e. it is a non-relativistic normalization for the QFT states. One may similarly construct a correspondence between worldline and QFT operators with more factors of the Riemann tensor. For more details about the correspondence between QFT amplitudes and worldline matrix elements see e.g. Ref. [46].

Four dimensional relations

In any fixed dimension, the operators described above satisfy relations stemming from their finite number of components[2]; thus they give an overcomplete description of the physics of extended bodies.

One class of relations follows from the the electric and magnetic fields being tensors of finite rank. Naively they have rank four, but because $E_{\mu\nu}u^\nu = B_{\mu\nu}u^\nu = 0$ their rank is lowered to three. This is not a surprise: it is a consequence of the fact that $E_{\mu\nu}$ and $B_{\mu\nu}$ are the covariant versions of the purely spatial E_{ij}, B_{ij} in the rest frame. The simplest relation following from the finiteness of the ranks of E and B is

$$E_{[\mu_1}{}^{\mu_2} E_{\mu_2}{}^{\mu_3} E_{\mu_3}{}^{\mu_4} E_{\mu_4]}{}^{\mu_1} = 0 \,, \tag{4.46}$$

which, together with the tracelessness of E, implies that $E^4 = 1/2(E^2)^2$. More generally,

[2]In a different context these relations are known as *evanescent operators* which are operators whose matrix elements vanish in four-dimensions but not in general dimension [47].

relations can be found which involve mixed powers of the electric and magnetic fields. For operators with no derivatives all such relations can be generated by evaluating the following determinant as a formal power series

$$\det[1 + t(E + rB)] = \sum_{i=2}^{\infty} \sum_{j=0}^{i} R_{i,j} t^i r^j \,. \tag{4.47}$$

The rank-three property of an arbitrary combination of E and B implies that $R_{i\geq 4,j} = 0$. A sample of such relations is

$$\begin{aligned}
2^3 R_{4,0} &= (E^2)^2 - 2(E^4) = 0\,, \\
2^2 R_{4,2} &= 2(EB)^2 + (B^2)(E^2) - 2(EBEB) - 4(E^2B^2) = 0\,, \\
5R_{5,0} &= (E^5) - \frac{5}{6}(E^2)(E^3) = 0\,, \\
6R_{5,2} &= 6(E^2BEB) + 6(E^3B^2) - (B^2)(E^3) - 3(E^2)(EB^2) = 0\,, \\
2R_{5,4} &= 2(EB^4) - (B^2)(EB^2) = 0\,,
\end{aligned} \tag{4.48}$$

as well as the ones that follow by interchanging E and B. Here the round parenthesis denote the matrix trace,

$$(\mathcal{O}) \equiv \mathrm{Tr}[\mathcal{O}]\,. \tag{4.49}$$

Recursively solving them implies that any operator of the form $(E^{n\geq 4})$ can be written as a polynomial in E^2 and E^3 as follows

$$(E^n) = n \sum_{2p+3q=n} \frac{1}{2^p 3^q} \frac{\Gamma(p+q)}{\Gamma(p+1)\Gamma(q+1)} (E^2)^p \, (E^3)^q \,. \tag{4.50}$$

A similar relation holds for (B^{2n}), while $(B^{2n+1}) = 0$ in a parity-invariant theory such as GR.

Another class of relations follows from the vanishing of the Gram determinants of any

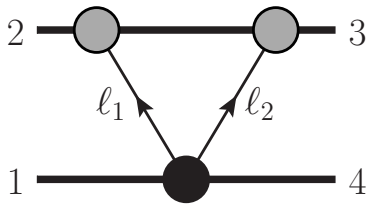

Figure 4.1: The generalized cut for leading-order contributions to E^2- or B^2-type tidal operators. Each blob is an on-shell amplitude, which in this case is local. Each exposed line is taken to be on shell and the blobs represent tree amplitudes. The dark blob contains an insertion of an E^2- or B^2-type higher-dimension operator with an arbitrary number of additional derivatives. The external momenta are all outgoing and the arrows indicated the direction of graviton momenta.

five or more four-momenta. They imply that certain terms in the power series expansion of susceptibilities are not linearly independent. For instance,

$$\det(v_i \cdot v_j) = 0 \quad \text{with} \quad v_i \subset \{p_1, p_2, q_1, q_2, q_3\}\,. \tag{4.51}$$

A final class of relations, which we will not detail any further, follows from the over-antisymmetrization of indices of both derivatives and E or B.

An exhaustive enumeration of the E^2- and B^2-type operators was carried out in Ref. [30], using Hilbert series techniques [48], which automatically eliminate the redundancies described here. In contrast, we will not make an attempt to eliminate all redundant operators, but rather use their relations as a check on our framework and calculations.

4.3 Leading order E^2 and B^2 tidal effects

In this section we discuss the leading-order contribution of the two-graviton tidal operators constructed in Section 4.2. The analysis parallels to some extent that of Ref. [30], with the main difference being the choice of operator basis. Our choice aligns with the worldline approach [5, 28] making it straightforward to compare Love numbers. We also evaluate all integrals providing a proof of the results with arbitrary numbers of derivatives. Here we work in an amplitudes-based approach following Refs. [11–13, 21].

4.3.1 Constructing integrands

The first task is to write down a scattering amplitude from which classical scattering angles and Hamiltonians can be extracted. To obtain the integrand we use the generalized unitarity method [22]. In this method, the integrand is constructed from the generalized unitarity cut which we define to be

$$\mathcal{C} \equiv \sum_{\text{states}} \mathcal{M}^{\text{tree}}_{(1)} \mathcal{M}^{\text{tree}}_{(2)} \mathcal{M}^{\text{tree}}_{(3)} \cdots \mathcal{M}^{\text{tree}}_{(m)} \,, \tag{4.52}$$

where the $\mathcal{M}^{\text{tree}}_{(i)}$ are tree amplitudes, some of which can have operator insertion. As a simple example, Fig. 4.1 displays the unitarity cut containing the leading-order effect of an R^2 tidal operator.

In general, the cuts that can contribute to the conservative classical Hamiltonian satisfy some simple rules. The first is that generalized unitarity cuts must separate the two matter lines to opposite sides of a cut, which follows from the fact we are interested only in long-range interactions. Another general rule is that every independent loop must have at least one cut matter line, so the energy is restricted to a matter residue. Any contribution with a graviton propagator attached to the same matter line also does not contribute to the conservative classical part. Further details are found in Ref. [13].

In constructing the amplitude integrand we may immediately expand in soft-graviton momenta, since each power of graviton momentum effectively carries an additional power of $\hbar$ and is quantum suppressed. This expansion can be carries out either on at the level of the input tree amplitudes or after assembling the cuts. The order to which a give term needs to be expanded is dictated by simple counting rules. Terms with too high a scaling in the graviton momenta are dropped. For example, at one-loop for the case without tidal or other higher-dimension operators this implies that any term in a diagram numerator with more than a single power of loop momentum in the numerators yields only quantum-mechanical contributions; some terms require fewer loop-momentum factors. In the presence of higher-dimension operators, the leading classical contributions can have higher powers of

loop momentum dictated simply by the number of extra derivatives in the operator compared to to the usual two derivative minimal coupling; the extra implicit powers of $\hbar$ are made up by the coefficient so the entire expression corresponds to a classical result.

In general to sew the trees together into generalized cuts one should use physical-state projectors which depend on null reference momenta

$$\mathbb{P}^{\mu\nu\rho\sigma} = \sum_{\text{states}} \varepsilon^{\mu\nu}(-p)\varepsilon^{\rho\sigma}(p) = \frac{1}{2}\Big(\mathbb{P}^{\mu\rho}\mathbb{P}^{\nu\sigma} + \mathbb{P}^{\mu\rho}\mathbb{P}^{\nu\sigma}\Big) - \frac{1}{D-2}\mathbb{P}^{\mu\nu}\mathbb{P}^{\rho\sigma}\,, \tag{4.53}$$

where $\mathbb{P}^{\mu\rho} = \eta^{\mu\rho} - (n^\mu p^\rho + n^\rho p^\mu)/(n\cdot p)$ and n^μ is the null reference momentum. However, the reference momenta will drop out if the seed amplitudes are manifestly transverse. In fact, one can always arrange for such terms to automatically drop out [49].

Alternatively, we can also use four-dimensional helicity states to sew gravitons across unitarity cuts. In general, some caution is required in the presence of infrared or ultraviolet singularites, although at least through third post-Minkowskian order helicity methods have been shown to correctly capture all contributions [13]. For cases without non-trivial infrared or ultraviolet divergences [3], we can straightforwardly apply four-dimensional methods. In our cases, the above D-dimensional sewing is simple enough so we will not use four-dimensional helicities here.

Finally, the information from multiple generalized cuts must be merged into a single expression. This can either be accomplished at the level of the integrand or after integration. For leading tidal coefficients, effectively only a single cut contributes, so merging information from the cuts is trivial.

[3]There are ultraviolet divergence at even loop orders that local in momentum transfer q, e.g. in the 3PM scattering [12, 13]. However, these are irrelevant for long-range dynamics because they can be absorbed by a contact interaction.

Simplifications from leading classical order

The on-shell amplitudes in the unitarity cut simplifies dramatically if we are only interested at leading classical order. Because there is no enhancement from iteration, any terms beyond the leading order in graviton momenta are quantum mechanical and can thus be ignored. For example, consider a three-point scalar-graviton-scalar amplitude at tree level

$$\mathcal{M}_3(\phi(p), h(\ell), \phi(p')) = -\kappa p^\mu p^\nu \varepsilon_{\mu\nu}(\ell)\,, \tag{4.54}$$

where κ is related to Newton's constant by $\kappa^2 = 32\pi G$. For any of the three-point amplitudes inserted in Figure 4.1, we can replace the scalar momenta p by the external momentum p_2 at leading classical order. Physically this implies that we ignore all back reaction on the particle 2, so all three-point amplitudes in Figure 4.1 are approximately the same.

For the amplitude with higher-dimension operator, it suffices to use linearized version of the curvature operators. Expanding the metric in the usual way, $g_{\mu\nu} = \eta_{\mu\nu} + \kappa h_{\mu\nu}$, we find the Weyl tensor to leading order is

$$C_{\mu\nu\rho\sigma} = -2\kappa \partial_{[\mu|}\partial_{[\rho} h_{\sigma]|\nu]} + \mathcal{O}(\kappa^2, \Box h)\,. \tag{4.55}$$

In deriving this expression we have also dropped terms proportional to the equations of motion for the graviton; this is because they do not contribute to the on-shell matrix elements necessary for the evaluation of the leading-order amplitude. The linearized Weyl tensor in momentum space then reads

$$C^{\text{lin}}_{\mu\nu\rho\sigma}(\ell) \equiv \frac{\kappa}{2}\left[\ell_\mu \ell_\rho\, \varepsilon(\ell)_{\nu\sigma} - \ell_\nu \ell_\rho\, \varepsilon(\ell)_{\mu\sigma} - \ell_\mu \ell_\sigma\, \varepsilon(\ell)_{\nu\rho} + \ell_\nu \ell_\sigma\, \varepsilon(\ell)_{\mu\rho}\right]. \tag{4.56}$$

The linearized Weyl tensor can be written a form that manifests the double copy in terms

of two gauge-theory field strengths

$$C^{\rm lin}_{\mu\nu\rho\sigma}(\ell) = \frac{\kappa}{2} F^{\rm lin}_{\mu\nu}(\ell) F^{\rm lin}_{\rho\sigma}(\ell)\,, \tag{4.57}$$

where

$$F^{\rm lin}_{\mu\nu\rho\sigma}(\ell) \equiv \ell_\mu \varepsilon(\ell)_\nu - \ell_\nu \varepsilon(\ell)_\mu\,, \tag{4.58}$$

and we identify the graviton polarization tensor as $\varepsilon(\ell)_{\nu\sigma} = \varepsilon(\ell)_\nu \varepsilon(\ell)_\sigma$. This simple example of a double-copy relation [33, 34], which is trivial at the linearized level, then implies that the leading-order amplitudes for tidal operators display double-copy relations. The gauge invariance is manifest.

To make the gravitational coupling manifest in all equations, we will extract all factors of κ from the building blocks of amplitudes. The linearized electric and magnetic components of the linearized Weyl tensor (4.56) follow from Eq. (4.30)

$$\mathcal{E}_{\mu_1\mu_2}(\ell,p) = \frac{1}{2m^2}\left[\ell_{\mu_1}\ell_{\mu_2}(p\cdot\varepsilon(\ell)\cdot p) - (p\cdot\ell)\left(\ell_{\mu_1}\varepsilon(\ell)_{\mu_2\rho}p^\rho + \ell_{\mu_2}\varepsilon(\ell)_{\mu_1\rho}p^\rho\right) + \varepsilon(\ell)_{\mu_1\mu_2}(p\cdot\ell)^2\right], \tag{4.59}$$

$$\mathcal{B}_{\mu_1\mu_2}(\ell,p) = \frac{1}{4m^2}\epsilon_{\alpha\beta\gamma\mu}\left[(p\cdot\ell)\left(\ell^\alpha\varepsilon(\ell)^\beta{}_{\mu_2} - \ell^\beta\varepsilon(\ell)^\alpha{}_{\mu_2}\right) + \ell^\beta\ell_{\mu_2}(p\cdot\varepsilon(\ell))^\alpha - \ell^\alpha\ell_{\mu_2}(p\cdot\varepsilon(\ell))^\beta\right], \tag{4.60}$$

where the particle momentum and its four-velocity are related in the usual way, $p_\mu = mu_\mu$. It is then straightforward to assemble the amplitude with insertions of a higher-dimension operator from above formulae.

In general to sew trees into generalized cuts one should use physical-state projectors which depend on null reference momenta. However, for the leading-order contributions that we will mostly be studying here, the terms containing dependence on the reference momentum automatically drop out because they are contracted into manifestly gauge-invariant (transverse)

quantities[4]. Effectively, we can use the numerator of the de Donder gauge propagator,

$$\mathbb{P}^{\mu\nu\rho\sigma} = \sum_{\text{states}} \varepsilon^{\mu\nu}(-p)\varepsilon^{\rho\sigma}(p) \to \frac{1}{2}\Big(\eta^{\mu\rho}\eta^{\nu\sigma} + \eta^{\mu\rho}\eta^{\nu\sigma}\Big) - \frac{1}{D-2}\eta^{\mu\nu}\eta^{\rho\sigma}\,, \tag{4.61}$$

to sew gravitons across cuts. Combining the projector with the three-point amplitude in Eq. (4.54) at leading classical order, effectively turns the graviton polarization tensors of the higher-dimension operator into

$$\varepsilon_{\mu\nu}(\ell) \to T_{\mu\nu}(p_2) = \left(p_{2,\mu}p_{2,\nu} - \frac{m_2^2}{D_s-2}\eta_{\mu\nu}\right)\,. \tag{4.62}$$

Crucially the result is independent of the loop momentum, implying that the sewing automatically imposes Bose symmetry for the gravitons of the higher-dimension operator. As we will outline in Sec. 4.4, this no longer holds beyond leading order where back-reaction becomes important. For example, at next-to-leading order pairs of the stress tensor in Eq. (4.54) can source a single graviton, acting as a sort of "impurity", which may be interpreted as the first correction to the gravitational field of a free particle towards that of a Schwarzschild black hole.

The discussion above can be extended to include the leading-order scattering of scalars deformed by higher-dimension operators off higher-spin particles described the Lagrangian in Ref. [23]. For a generic spinning body the stress tensor is

$$\mathcal{M}_3(\phi_s(p), h(\ell), \phi_s(p')) = -\kappa\, V_3^{\mu\nu}(\phi_s(p), h(\ell), \phi_s(p'))\varepsilon_{\mu\nu}(\ell)\,, \tag{4.63}$$

$$V_3^{\mu\nu}(\phi_s(p), h(\ell), \phi_s(p')) = p^\mu p^\nu \sum_{n=0}^{\infty} \frac{C_{ES^{2n}}}{(2n)!}\left(\frac{\ell\cdot S(p)}{m}\right)^{2n} - i\ell_\rho p^{(\mu} S(p)^{\nu)\rho} \sum_{n=0}^{\infty} \frac{C_{BS^{2n+1}}}{(2n+1)!}\left(\frac{\ell\cdot S(p)}{m}\right)^{2n},$$

where ℓ is the graviton momentum and $S(p)^\mu$ and $S(p)^{\mu\nu}$ are the covariant spin vector and

[4]In fact, one can always arrange for such terms to automatically drop out [49].

spin tensor, related by

$$S^{\mu\nu}(p) = -\frac{1}{m}\epsilon^{\mu\nu\gamma\delta}p_\gamma S_\delta(p)\,, \qquad\qquad S^{\mu}(p) = -\frac{1}{2m}\epsilon^{\mu\beta\gamma\delta}p_\beta S_{\gamma\delta}(p)\,, \tag{4.64}$$

and we recall that in the classical limit $\ell \cdot S(p)/m = \mathcal{O}(1)$.

For the Kerr black hole the stress tensor, originally found in Ref. [42] from different considerations, is obtained by setting $C_{ES^{2n}} = C_{BS^{2n}} = 1$ and has the closed-form expression

$$\mathcal{M}_3^{\rm Kerr}(\phi_s(p), h(\ell), \phi_s(p')) = -\kappa \exp(ia*\ell)^{(\mu}{}_\rho p^{\nu)} p^\rho \varepsilon_{\mu\nu}(\ell)\,, \tag{4.65}$$

where

$$a^\mu = \frac{1}{2p^2}\epsilon^\mu{}_{\nu\rho\sigma}p^\nu S^{\rho\sigma}(p)\,, \qquad\qquad (a*\ell)^\mu{}_\nu \equiv \epsilon^\mu{}_{\nu\rho\sigma}a^\rho \ell^\sigma\,. \tag{4.66}$$

Despite the more complicated dependence on the graviton momentum, the sewing of the spinning three-point amplitudes with the composite operator contact term can be carried by a replacement analogous to Eq. (4.62). For example, for a particle with the stress of a Kerr black hole, it is

$$\varepsilon_{\mu\nu}(\ell) \to T_{\mu\nu}^{\rm Kerr}(\ell, p_2) = \exp(ia*\ell)^{(\alpha}{}_\rho p^{\beta)} p^\rho \left(\delta^\mu_\alpha \delta^\nu_\beta - \eta_{\alpha\beta}\frac{\eta^{\mu\nu}}{D_s - 2}\right)\,. \tag{4.67}$$

We note that only the terms with an even number of spin vectors, in general governed by the coefficients $C_{ES^{2n}}$, contribute to the trace part of this replacement. To shorten the ensuing equations, in the following we will use the replacement

$$\epsilon^{\mu\nu}(\ell) \to T^{\mu\nu}_{\rm gen}(\ell, p_2) = \left(p_2^\mu p_2^\nu - \frac{m_2^2}{D_s - 2}\eta^{\mu\nu}\right) A(\ell) - \frac{i}{2}\ell_\rho (p_2^\mu S^{\nu\rho}(p_2) + p_2^\nu S^{\mu\rho}(p_2)) B(\ell)\,, \tag{4.68}$$

where $A(\ell)$ and $B(\ell)$ can be read off Eqs. (4.63) and (4.67).

4.3.2 Momentum-space analysis

Before discussing the leading-order effects of the most general tidal operators introduced in Sec. 4.2, we discuss here the simpler case of operators $E^{(m)}_{\mu_1\mu_2}$, corresponding to the multipoles of the gravitational field of the quadrupole operator $E_{\mu\nu}$.

The construction of the relevant four-point matrix element of the operator $\phi E^{(m)}_{\mu_1\mu_2} E^{(m)\mu_1\mu_2}\phi$, corresponding to the darker blob in Fig. 4.1, is straightforward. The matrix element is

$$\begin{aligned}\mathcal{M}_{\mathrm{E}^2_{l,2}}(h(\ell_1),h(\ell_2),\phi(p_1),\phi(p_4)) &= 2\kappa^2 m_1 \left(D_{\mathrm{E}^2_{l,2}}(p_1,\ell_1,p_4,\ell_2)+D_{\mathrm{E}^2_{l,2}}(p_1,\ell_2,p_4,\ell_1)\right),\\ D_{\mathrm{E}^2_{l,2}}(p_1,\ell_1,p_4,\ell_2) &= \left(\frac{i}{m_1}\right)^{2l}(p_1\cdot\ell_1)^l(p_1\cdot\ell_2)^l \mathcal{E}_{\mu_1\mu_2}(\ell_1,p_1)\mathcal{E}^{\mu_1\mu_2}(\ell_2,p_4)\,.\end{aligned} \tag{4.69}$$

As noted earlier, because tidal operators are gauge invariant and constructed out of Weyl tensors, this matrix element obeys the transversality conditions for the two gravitons. Thus, their contribution to generalized unitarity cut in Fig. 4.1 automatically accounts for the physical-state projection. The sewing is then simply given by the replacement in Eq. (4.62). To leading order in soft expansion we can also replace all $p_1\cdot\ell_2 = -p_1\cdot\ell_1 + \mathcal{O}(q)$.

The resulting amplitude is

$$\begin{aligned}\mathcal{M}_{\mathrm{E}^2_{l,2}}(\boldsymbol{p},\boldsymbol{q}) &= i\kappa^2\int\frac{d^D\ell_1}{(2\pi)^D}\frac{\mathcal{M}_{\mathrm{E}^2_{l,2}}(h(\ell_1),h(\ell_2),\phi(p_3),\phi(p_4))\big|_{\varepsilon_{\mu\nu}(\ell_i)\to T_{\mu\nu}(p_2)}}{\ell_1^2((\ell_1-p_2)^2-m_2^2)(q-\ell_1)^2}\\ &= 4i\,m_1\kappa^4\int\frac{d^D\ell_1}{(2\pi)^D}\frac{(u_1\cdot\ell_1)^{2l}\mathcal{E}_{\mu_1\mu_2}(\ell_1,p_1)\mathcal{E}^{\mu_1\mu_2}(\ell_2,p_1)\big|_{\varepsilon_{\mu\nu}(\ell_i)\to T_{\mu\nu}(p_2)}}{\ell_1^2((\ell_1-p_2)^2-m_2^2)(q-\ell_1)^2}\,,\end{aligned} \tag{4.70}$$

where the numerator is given more explicitly by

$$\begin{aligned}&\mathcal{E}_{\mu_1\mu_2}(\ell_1,p_1)\mathcal{E}^{\mu_1\mu_2}(\ell_2,p_1)\big|_{\varepsilon_{\mu\nu}(\ell_i)\to T_{\mu\nu}(p_2)} \\ &\quad=\frac{1}{8}m_2^4\left[(u_1\cdot\ell_1)^2((u_1\cdot\ell_1)^2+\frac{1}{2}q^2)-2\sigma^2q^2(u_1\cdot\ell_1)^2+\frac{1}{8}q^4(1-2\sigma^2)^2\right]+\mathcal{O}(q^6)\,.\end{aligned} \tag{4.71}$$

Further expanding the amplitude in the soft limit leads to

$$\mathcal{M}_{\mathrm{E}^2_{l,2}}(\boldsymbol{p},\boldsymbol{q})=64i\pi^2G^2|\boldsymbol{q}|^{3+2l}m_1m_2^3((1-2\sigma^2)^2I_{2l}+4(-1+4\sigma^2)I_{2(1+l)}+8I_{2(2+l)})\,,$$

where I_{2l} are triangle integrals

$$I_{2l}=\int\frac{d^D\ell}{(2\pi)^D}\frac{|\boldsymbol{q}|^{-2l+1}(\ell\cdot u_1)^{2l}}{\ell^2(-2\ell\cdot u_2)(\ell-q)^2}\,, \tag{4.72}$$

which must be evaluated in the potential region. The results of these integrals were conjectured in Ref. [30]. Here we present the proof, by going to the frame in which particle 2 is at rest

$$u_{1\mu}=-(\sigma,0,0,\sqrt{\sigma^2-1})\,,\qquad u_{2\mu}=-(1,0,0,0)\,,\qquad q_\mu=(0,\boldsymbol{q})=(0,q^x,q^y,q^z)\,, \tag{4.73}$$

under which $\ell_{i\mu}=(\ell_i^0,\boldsymbol{\ell}_i)=(\ell_i^0,\ell_i^x,\ell_i^y,\ell_i^z)$. Note that since $q^z=\boldsymbol{q}\cdot\hat{\boldsymbol{z}}=\mathcal{O}(q^2)$ by on shell conditions, we can treat $q^z\approx 0$ if we are only interested in the leading classical limit. We then have

$$I_{2l}=(\sigma^2-1)^l\int\frac{d^D\ell}{(2\pi)^D}\frac{|\boldsymbol{q}|^{-2l+1}(\ell^z)^{2l}}{(2\ell^0)\ell^2(\ell-q)^2}=\frac{i(\sigma^2-1)^l}{2^{2l+1}(4\pi)^{(D-1)/2}}\int\frac{d^{D-1}\boldsymbol{\ell}}{\pi^{(D-1)/2}}\frac{|\boldsymbol{q}|^{-2l+1}(2\ell^z)^{2l}}{\boldsymbol{\ell}^2(\boldsymbol{\ell}-\boldsymbol{q})^2}\,, \tag{4.74}$$

where in the second equality we have evaluated the residue of the energy pole with a symmetry factor 1/2 because the graviton propagators cannot be on shell in the potential region. The remaining integral is a Euclidean triangle with a linearized propagator and is given by

Smirnov in Ref. [50],

$$\int \frac{\mathrm{d}^{D-1}\boldsymbol{\ell}}{\pi^{(D-1)/2}} \frac{(\boldsymbol{q}^2)^{a+b+\frac{c}{2}-\frac{3}{2}}}{(\boldsymbol{\ell}^2-i0)^a[(\boldsymbol{\ell}-\boldsymbol{q})^2-i0]^b(2\ell^z-i0)^c} \tag{4.75}$$
$$= e^{\frac{i\pi c}{2}}|\boldsymbol{q}|^{-2\epsilon}\frac{\Gamma\left(\frac{c}{2}\right)\Gamma\left(\frac{3}{2}-a-\frac{c}{2}-\epsilon\right)\Gamma\left(\frac{3}{2}-b-\frac{c}{2}-\epsilon\right)\Gamma\left(a+b+\frac{c}{2}+\epsilon-\frac{3}{2}\right)}{2\Gamma(a)\Gamma(b)\Gamma(c)\Gamma(3-a-b-c-2\epsilon)},$$

for $\boldsymbol{q}\cdot\hat{\boldsymbol{z}}=0$ which is valid for leading order in the classical limit. The result is

$$I_{2l} = -\frac{i(\sigma^2-1)^l}{4^{l+2-\epsilon}(4\pi)^{1/2-\epsilon}}|\boldsymbol{q}|^{-2\epsilon}\frac{\Gamma\left(\frac{1}{2}-\epsilon\right)\Gamma\left(\frac{1}{2}+\epsilon\right)}{\Gamma\left(\frac{1}{2}-l\right)\Gamma\left(1-\epsilon+l\right)}. \tag{4.76}$$

Using the result for these integrals with $\epsilon=0$ the amplitude is

$$\mathcal{M}_{\mathrm{E}^2_{l,2}}(\boldsymbol{p},\boldsymbol{q}) = |\boldsymbol{q}|^{3+2l}\overline{\mathcal{M}}_{\mathrm{E}^2_{l,2}}(\boldsymbol{p}), \tag{4.77}$$

$$\overline{\mathcal{M}}_{\mathrm{E}^2_{l,2}}(\boldsymbol{p}) = G^2m_1m_2^3\,\frac{(-1)^l\pi^{3/2}\Gamma(\frac{1}{2}+l)}{2^{2(1+l)}\Gamma(3+l)} \tag{4.78}$$
$$\times(\sigma^2-1)^l(11+4l(3+l)-6(5+2l)\sigma^2+(5+2l)(7+2l)\sigma^4).$$

The corresponding potential and eikonal phase are

$$V_{\mathrm{E}^2_{l,2}}(\boldsymbol{p},\boldsymbol{r}) = \frac{-1}{4E_1E_2|\boldsymbol{r}|^{2l+6}}\,\frac{2^{3+2l}\Gamma(3+l)}{\pi^{3/2}\Gamma(-\frac{3}{2}-l)}\,\overline{\mathcal{M}}_{\mathrm{E}^2_{l,2}}(\boldsymbol{p}), \tag{4.79}$$

$$\delta_{\mathrm{E}^2_{l,2}}(\boldsymbol{p},\boldsymbol{b}) = \frac{1}{4m_1m_2\sqrt{\sigma^2-1}}\,\frac{1}{|\boldsymbol{b}|^{2l+5}}\,\frac{2^{3+2l}\Gamma(\frac{5}{2}+l)}{\pi\Gamma(-\frac{3}{2}-l)}\,\overline{\mathcal{M}}_{\mathrm{E}^2_{l,2}}(\boldsymbol{p}). \tag{4.80}$$

It is not difficult to see that, for $l=0$ and $l=1$, eq. (4.80) reproduces the expectation values of the operators E^2 and $(\dot{E})^2$ evaluated in Ref. [28].

The calculation above can be easily repeated for the operator $B^{(l)}_{\mu\nu}B^{\mu\nu(l)}$; it amounts to replacing in Eq. (4.70) $\mathcal{E}$ with $\mathcal{B}$ given in Eq. (4.60). The resulting amplitude, potential and

eikonal phase are:

$$\mathcal{M}_{\mathrm{B}^2_{l,2}}(\boldsymbol{p},\boldsymbol{q}) = |\boldsymbol{q}|^{3+2l}\overline{\mathcal{M}}_{\mathrm{B}^2_{l,2}}(\boldsymbol{p})\,, \tag{4.81}$$

$$\overline{\mathcal{M}}_{\mathrm{B}^2_{l,2}}(\boldsymbol{p}) = G^2 m_1 m_2^2 \frac{(-1)^l \pi^{3/2}\Gamma(\frac{1}{2}+l)}{2^{2(l+1)}\Gamma(3+l)}(5+2l)(\sigma^2-1)^{l+1}(1+2l+(7+2l)\sigma^2)\,, \tag{4.82}$$

$$V_{\mathrm{B}^2_{l,2}}(\boldsymbol{p},\boldsymbol{r}) = \frac{-1}{4E_1E_2|\boldsymbol{r}|^{2l+6}}\,\frac{2^{3+2l}\Gamma(3+l)}{\pi^{3/2}\Gamma(-\frac{3}{2}-l)}\,\overline{\mathcal{M}}_{\mathrm{B}^2_{l,2}}(\boldsymbol{p})\,, \tag{4.83}$$

$$\delta_{\mathrm{B}^2_{l,2}}(\boldsymbol{p},\boldsymbol{b}) = \frac{1}{4m_1m_2\sqrt{\sigma^2-1}}\,\frac{1}{|\boldsymbol{b}|^{2l+5}}\,\frac{2^{3+2l}\Gamma(\frac{5}{2}+l)}{\pi\Gamma(-\frac{3}{2}-l)}\,\overline{\mathcal{M}}_{\mathrm{B}^2_{l,2}}(\boldsymbol{p})\,. \tag{4.84}$$

Similarly to eq. (4.80), the eikonal phase above evaluated on $l=0$ and $l=1$ reproduces the expectation values of the operators B^2 and $(\dot{B})^2$ found in [28].

4.3.3 Position-space analysis

Alternatively, the calculation can be done in position space, more specifically in the rest frame of particle 2 as in Eq. (4.73). This approach will provide a simple way to generalize the analysis beyond one loop. There are two key observations here. First, the amplitude with C^2 operator insertion in Eq. (4.69) factorizes into a product of the multipole expansions of electric or magnetic tensors

$$\mathcal{M}_{\mathrm{E}^2_{l,2}}(h(\ell_1),h(\ell_2),\phi(p_1),\phi(p_4)) = 4m_1\kappa^2\left(\frac{i}{m_1}\right)^{2l}((p_1\cdot\ell_1)^l\mathcal{E}_{\mu_1\mu_2}(\ell_1,p_1))((p_1\cdot\ell_2)^l\mathcal{E}^{\mu_1\mu_2}(\ell_2,p_1)) + \mathcal{O}(q^{2l+4})\,, \tag{4.85}$$

where we have applied the classical limit $p_4 = -p_1 + \mathcal{O}(q)$ to Eq. (4.69). Second, in the potential region, we can integrated out graviton energy component by picking up residue from the matter propagator [11, 13]. This sets $\ell_1^0 = \ell_2^0 = 0$ and implies the graviton momenta ℓ_1, ℓ_2 are purely spatial. To exploit the factorization at the integrand level, we further Fourier

transform the spatial $\boldsymbol{q}$ in Eq. (4.70) to position space[5]

$$\begin{aligned}\mathcal{M}_{\mathrm{E}^2_{l,2}}(\boldsymbol{p},\boldsymbol{r}) &\equiv \int \frac{d^{D-1}\boldsymbol{q}}{(2\pi)^{D-1}} e^{-i\boldsymbol{r}\cdot\boldsymbol{q}}\, \widetilde{\mathcal{M}}_{\mathrm{E}^2_{l,2}}(\boldsymbol{p},\boldsymbol{q}) \\ &= \frac{\kappa^2}{4m_2}\prod_{i=1}^{2}\int \frac{d^{D-1}\boldsymbol{\ell}_i}{(2\pi)^{D-1}}\,\frac{e^{-i\boldsymbol{r}\cdot\boldsymbol{\ell}_i}}{\boldsymbol{\ell}_i^2}\,\mathcal{M}_{\mathrm{E}^2_{l,2}}(h(\ell_1),h(\ell_2),\phi(p_1),\phi(p_4))\big|_{\varepsilon_{\mu\nu}(\ell_i)\to T_{\mu\nu}(p_2)}.\end{aligned} \tag{4.86}$$

Crucially, the dependence on the two graviton momenta ℓ_1, ℓ_2 factorizes and each of them can be treated as an independent variable. Together with the factorization in Eq. (4.85), the Fourier transform acts on individual electric tensor $\mathcal{E}_{\mu_1\mu_2}(\ell_i, p_1)$. We define

$$\begin{aligned}\mathcal{E}_{\mu\nu}(\boldsymbol{r},p_1) \equiv& \int \frac{d^{D-1}\boldsymbol{\ell}_i}{(2\pi)^{D-1}}\frac{e^{-i\boldsymbol{r}\cdot\boldsymbol{\ell}_i}}{\boldsymbol{\ell}_i^2}\mathcal{E}_{\mu\nu}(\ell_i,p_1)\big|_{\varepsilon_{\rho\sigma}(\ell)\to T_{\rho\sigma}(p_2)} \\ =&\frac{-m_2^2}{16\pi|\boldsymbol{r}|^5}\Big[3\left(\boldsymbol{r}^2+2(\sigma^2-1)z^2\right)u_{2\mu}u_{2\nu}-3\sigma\boldsymbol{r}^2(u_{2\mu}u_{1\nu}+u_{2\mu}u_{1\nu})+2\boldsymbol{r}^2u_{1\mu}u_{1\nu} \\ &+3(2\sigma^2-1)r_\mu r_\nu-6\sigma\sqrt{\sigma^2-1}z\,(u_{2\mu}r_\nu+u_{2\mu}r_\nu)+3\sqrt{\sigma^2-1}z\,(u_{1\mu}r_\nu+u_{1\mu}r_\nu) \\ &+((3\sigma^2-2)\boldsymbol{r}^2-3(\sigma^2-1)z^2)\eta_{\mu\nu}\Big],\end{aligned} \tag{4.87}$$

where $r_\mu = (0,\boldsymbol{r}) = (0,x,y,z)$ in the frame of Eq. (4.73) as the electric field sourced by p_2 in position space. The Fourier transform of scalar-graviton amplitude (with the graviton propagators) is then

$$\begin{aligned}\mathcal{M}_{\mathrm{E}^2_{l,2}}(h_1,h_2,\phi(p_1),\phi(p_4)|\boldsymbol{r}) &\equiv \prod_{i=1}^{2}\int \frac{d^{D-1}\boldsymbol{\ell}_i}{(2\Pi)^{D-1}}\frac{e^{-i\boldsymbol{r}\cdot\boldsymbol{\ell}_i}}{\boldsymbol{\ell}_i^2}\mathcal{M}_{\mathrm{E}^2_{l,2}}(h(\ell_1),h(\ell_2),\phi(p_1),\phi(p_4)) \\ &= \mathcal{M}_{\mathrm{E}^2_{l,2}}(h(\ell_1),h(\ell_2),\phi(p_1),\phi(p_4)|\mathcal{E}_{\mu_1\mu_2}(\ell_j,p_1)\to\mathcal{E}_{\mu_1\mu_2}(\boldsymbol{r}_j,p_1),\ell_i\to i\nabla_j)\,\big|_{\boldsymbol{r}_j\to\boldsymbol{r}},\end{aligned} \tag{4.88}$$

where any loop momentum ℓ_j is replaced with the gradient on the position $\boldsymbol{r}_j$ of the electric field $\mathcal{E}_{\mu_1\mu_2}(\boldsymbol{r}_j,p_1)$ and all $\boldsymbol{r}_j$ are identified with $\boldsymbol{r}$. The two-scalar scattering amplitude in

[5]The Fourier transform acts on the amplitude with generic off-shell q, which is three dimensional. We use $\widetilde{\mathcal{M}}(\boldsymbol{p},\boldsymbol{q})$ to denote amplitude with off-shell $\boldsymbol{q}$.

position space then has a simple form

$$\begin{aligned}\mathcal{M}_{\mathrm{E}^2_{l,2}}(\boldsymbol{p},\boldsymbol{r}) &= \frac{\kappa^2}{4m_2}\,\mathcal{M}_{\mathrm{E}^2_{l,2}}\left(h_1,h_2,\phi(p_1),\phi(p_4)|\boldsymbol{r}\right)\\ &= \kappa^4\frac{m_1}{m_2}\left(\sigma^2-1\right)^l\left[(\hat{\boldsymbol{z}}\cdot\nabla)^l\,\mathcal{E}_{\mu_1\mu_2}(\boldsymbol{r},p_1)\right]^2\,,\end{aligned} \tag{4.89}$$

where in the second line we plug in the result in Eq. (4.85), apply the replacement in Eq. (4.88) and $\hat{\boldsymbol{z}}$ is the unit vector along z direction.

The position-space result is generally not isotropic; namely, it could depend on $\hat{\boldsymbol{z}}\cdot\boldsymbol{r}$. To make the result isotropic, we go back to momentum space and impose the on-shell condition $\hat{\boldsymbol{z}}\cdot\boldsymbol{q}=\mathcal{O}(\boldsymbol{q}^2)\simeq 0$,

$$\mathcal{M}_{\mathcal{O}}(\boldsymbol{p},\boldsymbol{q}) = \int d^{D-1}\boldsymbol{r}\,e^{+i\boldsymbol{r}\cdot\boldsymbol{q}}\,\mathcal{M}_{\mathcal{O}}(\boldsymbol{p},\boldsymbol{r})\big|_{\hat{\boldsymbol{z}}\cdot\boldsymbol{q}=0}\,. \tag{4.90}$$

Since the result only depends on the covariant variables σ and $q^2=-\boldsymbol{q}^2$, it can be promoted to any other frame. All Fourier-transforms that appear in this calculation are of the form

$$\int d^{D-1}\boldsymbol{r}\frac{e^{i\boldsymbol{r}\cdot\boldsymbol{q}}(\hat{\boldsymbol{z}}\cdot\boldsymbol{r})^s}{\boldsymbol{r}^h} = \frac{(-1)^{s/2}\pi^{D/2}}{2^{h-s-D+1}}\frac{|\boldsymbol{q}|^{h-s-D+1}}{\sin(\frac{1}{2}\pi(D-1-h))}\frac{\Gamma(\frac{1}{2}(1+s))}{\Gamma(\frac{1}{2}h)\Gamma(1+\frac{1}{2}(h-s-D+1))}\,, \tag{4.91}$$

for some exponents h and integer s. The isotropic potential then follows from Eq. (4.10).

From the position-space amplitude we can directly obtain the eikonal phase, although it can be calculated easily once we have the amplitude $\mathcal{M}_{\mathcal{O}}(\boldsymbol{p},\boldsymbol{b})$. To see this, we simply invert the amplitude in terms of Eq. (4.5) and plug it into Eq. (4.6)

$$\begin{aligned}\delta_{\mathcal{O}}(\boldsymbol{p},\boldsymbol{b}) &= \frac{1}{4m_1m_2\sqrt{\sigma^2-1}}\int\frac{d^{D-2}\boldsymbol{q}}{(2\pi)^{D-2}}e^{-i\boldsymbol{b}\cdot\boldsymbol{q}}\int d^{D-1}\boldsymbol{r}e^{i\boldsymbol{r}\cdot\boldsymbol{q}}\,\mathcal{M}_{\mathcal{O}}(\boldsymbol{p},\boldsymbol{r})\Big|_{\boldsymbol{q}=(q^x,q^y,0)}\\ &= \frac{1}{4m_1m_2\sqrt{\sigma^2-1}}\int_{-\infty}^{\infty}dz\,\mathcal{M}_{\mathcal{O}}(\boldsymbol{p},\boldsymbol{r}=(\boldsymbol{b},z)),\end{aligned} \tag{4.92}$$

where we use $\boldsymbol{b} = (b^x, b^y, 0)$ and $\boldsymbol{r} = (x, y, z)$. Since we are only interested in the leading order, the particle trajectory can be treated as a straight line. In the frame where particle 2 is rest at the origin, the position of particle 1 is $x_1^\mu = (t, \boldsymbol{r}) = b^\mu + u_1^\mu \tau = \tau(\sigma, b^x, b^y, \sqrt{\sigma^2 - 1})$. The above formula can be written as

$$\delta_{\mathcal{O}}(\boldsymbol{p}, \boldsymbol{b}) = \frac{1}{4m_1 m_2} \int_{-\infty}^{\infty} d\tau \, \mathcal{M}_{\mathcal{O}}(\boldsymbol{p}, \boldsymbol{r}(\tau)) \,. \tag{4.93}$$

So the eikonal phase can be obtained straightforwardly from $\mathcal{M}_{\mathcal{O}}(\boldsymbol{p}, \boldsymbol{r}(\tau))$. This is expected because the eikonal phase is proportional to the worldline action integrated over a straight line. Our approach here offers a derivation from purely scattering-amplitudes perspective.

The advantage of position-space approach is that it is very general. The discussion above applies to contribution of any tidal operator at its leading classical order. The only integrals needed, to any loop order, are in Eq. (4.91). We will discuss and illustrate this point in more detail in Sec. 4.4.

The discussion above can be generalized easily to the case with magnetic operators. The position-space magnetic component of the linearized Weyl tensor, contracted with a point-particle stress tensor, is

$$\mathcal{B}_{\mu\nu}(\boldsymbol{r}, p_1) \equiv \int \frac{d^{D-1}\boldsymbol{\ell}_i}{(2\pi)^{D-1}} \frac{e^{-i\boldsymbol{r}\cdot\boldsymbol{\ell}_i}}{\boldsymbol{\ell}_i^2} \mathcal{B}_{\mu\nu}(\ell_i, p_1)\big|_{\varepsilon_{\rho\sigma}(\ell) \to T_{\rho\sigma}(p_2)}. \tag{4.94}$$

We have the scalar-graviton amplitude in position space

$$\begin{aligned}
\mathcal{M}_{\mathrm{B}^2_{l,2}}(h(\ell_1), h(\ell_2), \phi(p_1), \phi(p_4)|\boldsymbol{r}) &\equiv \prod_{i=1}^{2} \int \frac{d^{D-1}\boldsymbol{\ell}_i}{(2\Pi)^{D-1}} \frac{e^{-i\boldsymbol{r}\cdot\boldsymbol{\ell}_i}}{\boldsymbol{\ell}_i^2} \mathcal{M}_{\mathrm{B}^2_{l,2}}(h(\ell_1), h(\ell_2), \phi(p_1), \phi(p_4)) \\
&= \mathcal{M}_{\mathrm{B}^2_{l,2}}(h(\ell_1), h(\ell_2), \phi(p_1), \phi(p_4)|\mathcal{B}_{\mu_1\mu_2}(\ell_j, p_1) \to \mathcal{B}_{\mu_1\mu_2}(\boldsymbol{r}_j, p_1), \ell_i \to i\nabla_j)\,\big|_{\boldsymbol{r}_j \to \boldsymbol{r}}.
\end{aligned} \tag{4.95}$$

Again we identify all $\boldsymbol{r}_j$ in the end with $\boldsymbol{r}$. The position-space amplitude is then

$$\mathcal{M}_{\mathrm{B}^2_{l,2}}(\boldsymbol{r}) = \frac{1}{m_2}\left(\frac{\kappa}{2}\right)^2 \mathcal{M}_{\mathrm{B}^2_{l,2}}\left(h_1, h_2, \phi(p_1), \phi(p_4)|\boldsymbol{r}\right). \tag{4.96}$$

Let us comment on an interesting relation between electric and magnetic operators. In position space we find

$$\mathcal{E}_{\mu\nu}(\boldsymbol{r}, p_1)\mathcal{E}^{\mu\nu}(\boldsymbol{r}, p_1) = \frac{3m_2^4}{128\pi|\boldsymbol{r}|^{10}}\left[3(\sigma^2-1)(\boldsymbol{r}^2-z^2)(\sigma^2\boldsymbol{r}^2-(\sigma^2-1)z^2)+\boldsymbol{r}^4\right], \tag{4.97}$$

$$\mathcal{B}_{\mu\nu}(\boldsymbol{r}, p_1)\mathcal{B}^{\mu\nu}(\boldsymbol{r}, p_1) = \frac{9m_2^4}{128\pi|\boldsymbol{r}|^{10}}(\sigma^2-1)(\boldsymbol{r}^2-z^2)(\sigma^2\boldsymbol{r}^2-(\sigma^2-1)z^2). \tag{4.98}$$

The two operators are almost identical. The difference between the two is independent of σ which is sub-sub-leading in the high-energy limit $\sigma \gg 1$. As explained in Ref. [28], this is expected because the difference is proportional to Weyl tensor squared which is independent of σ. This behavior has also been observed at the next-to-leading order in Ref. [29].

4.3.4 General multipole operators

Following the example discussed in detail in the previous sections, we proceed to evaluate the amplitudes and the corresponding eikonal phases with one insertion of the generic tidal operators $\phi E^{(l)}_{\mu_1\ldots\mu_n}E^{(l)\mu_1\ldots\mu_n}\phi$ and $\phi B^{(l)}_{\mu_1\ldots\mu_n}B^{(l)\mu_1\ldots\mu_n}\phi$. As already mentioned for operators with $n = 2$, we may choose without loss of generality, the two E and B factors to have equal upper index.

The calculations for the two operators are parallel. For this reason, in the common part we will collectively denote E or B by X, and specialize at them at the end. Thus, to leading

order in κ, the momentum space expressions of $\hat{E}^{(l)}$ and $\hat{B}^{(l)}$ defined in Eq. (4.37) are

$$X^{(l)}_{\mu_1\mu_2\ldots\mu_n} = i^{2l+(n-2)}\left(\frac{i}{m}\right)^l (p\cdot\ell)^l \mathrm{Sym}_{\mu_1\ldots\mu_n}[P^{\nu_3}_{\mu_3}(p)\ell_{\nu_3}\ldots P^{\nu_n}_{\mu_n}(p)\ell_{\nu_n}X(\ell,p)_{\mu_1\mu_2}] + \mathcal{O}(\kappa^2)\,, \tag{4.99}$$

where $P^{\nu_i}_{\mu_i}$ are the momentum space form of the projectors in Eq. (4.38) and $X_{\mu_1\mu_2}(\ell,p)$ being given by $\mathcal{E}_{\mu_1\mu_2}$ and $\mathcal{B}_{\mu_1\mu_2}$ in Eqs. (4.59)-(4.60) for the two operators, respectively. The symmetrization over the indices $\mu_1,\ldots,\mu_n$ includes division by the number of terms. In the expression above ℓ is the graviton momentum, p is the scalar momentum and $\varepsilon(\ell)$ in the explicit expressions of $\mathcal{E}_{\mu_1\mu_2}$ and $\mathcal{B}_{\mu_1\mu_2}$ is the graviton polarization tensor.

The product of two linearized $X^{(l)}_{\mu_1\ldots\mu_n}$ with different graviton momenta ℓ_1 and ℓ_2, and contracted as in Eqs. (4.44) and (4.45), contains three different structures: (1) all projectors are contracted with each other, (2) all but one projector are contracted with each other and (3) all but two projectors are contracted with each other. The four-point matrix element of the operator $\phi X^{(l)}_{\mu_1\ldots\mu_n}X^{(l)\mu_1\ldots\mu_n}\phi$ needed for the construction of the four-scalar amplitude is

$$\mathcal{M}_{\mathrm{X}^2_{l,n}}(h(\ell_1),h(\ell_2),\phi(p_1),\phi(p_4)) = 2\kappa^2 m_1\left(D_{\mathrm{X}^2_{l,n}}(p_1,\ell_1,p_4,\ell_2) + D_{\mathrm{X}^2_{l,n}}(p_1,\ell_2,p_4,\ell_1)\right), \tag{4.100}$$

where

$$\begin{aligned} D_{\mathrm{X}^2_{l,n}}(p_1,\ell_1,p_4,\ell_2) = i^{2(n-2)}i^{2l}(-1)^l\frac{2(n-2)!}{n!}(u_1\cdot\ell_1)^{2l}\Big[&(\ell_1\cdot P(p_1)\cdot P(p_4)\cdot\ell_2)^{n-2}\Pi^X_1(p_1,\ell_1,p_4,\ell_2) \\ &+ 2(n-2)(\ell_1\cdot P(p_1)\cdot P(p_4)\cdot\ell_2)^{n-3}\Pi^X_2(p_1,\ell_1,p_4,\ell_2) \\ &+ \frac{1}{2}(n-2)(n-3)(\ell_1\cdot P(p_1)\cdot P(p_4)\cdot\ell_2)^{n-4}\Pi^X_3(p_1,\ell_1,p_4,\ell_2)\Big]\,. \end{aligned} \tag{4.101}$$

The three factors $\Pi_1^X(p_1,\ell_1,p_4,\ell_2)$ are given by

$$\begin{aligned}
\Pi_1^X(p_1,\ell_1,p_4,\ell_2) &= X_{\mu_1\mu_2}(\ell_1,p_1)X^{\mu_1\mu_2}(\ell_2,p_4)\,, \\
\Pi_2^X(p_1,\ell_1,p_4,\ell_2) &= \ell_1\cdot P(p_1)\cdot X(\ell_2,p_4)\cdot X(\ell_1,p_1)\cdot P(p_4)\cdot\ell_2\,, \\
\Pi_3^X(p_1,\ell_1,p_4,\ell_2) &= \ell_1\cdot P(p_1)\cdot X(\ell_2,p_4)\cdot P(p_1)\cdot\ell_1\,\ell_2\cdot P(p_4)\cdot X(\ell_1,p_1)\cdot P(p_4)\cdot\ell_2\,.
\end{aligned} \tag{4.102}$$

To the order we are interested in we may freely replace $p_4 \to -p_1$, since the difference is of subleading order in the expansion in small transferred momentum. For $n=2$, the second and third line vanish and, for $X \equiv E$, we recover the four-point matrix element of the operator $\phi E^{(l)}_{\mu_1\mu_2}E^{(l)\mu_1\mu_2}\phi$ given in Eqs. (4.69).

Sewing this matrix element with two three-point scalar-graviton amplitudes in Eq. (4.54) using the rule (4.62) leads to

$$\begin{aligned}
\mathcal{M}_{\mathrm{X}^2_{l,n}}(\boldsymbol{p},\boldsymbol{q}) &= 8(8\pi G)^2 i^{2(n-2)} m_1 m_2^4\,\frac{2(n-2)!}{n!} \\
&\quad\times\left[\mathcal{M}_n^{(l)}(\Pi_1^X)+2(n-2)\mathcal{M}_n^{(l)}(\Pi_2^X)+\frac{1}{2}(n-2)(n-3)\mathcal{M}_n^{(l)}(\Pi_3^X)\right], \qquad (4.103)\\
\mathcal{M}_{l,n}(\Pi_k^X) &= \int\frac{d^D\ell}{(2\pi)^D}\frac{(u_1\cdot\ell)^{2l}((u_1\cdot\ell)^2+\frac{1}{2}q^2)^{n-2}}{\ell^2((\ell-p_2)^2-m_2^2)(\ell-q)^2}\left(\frac{q^2}{(u_1\cdot\ell)^2+\frac{1}{2}q^2}\right)^{k-1}\mathcal{M}(\Pi_k^X)\,, \qquad (4.104)
\end{aligned}$$

where $k=1,2,3$.

Both $\mathcal{M}(\Pi_k^{\mathcal{E}})$ and $\mathcal{M}(\Pi_k^{\mathcal{B}})$ have the same general structure:

$$\begin{aligned}
\mathcal{M}(\Pi_i^X) &= A_i^X(u_1\cdot\ell)^2((u_1\cdot\ell)^2+\tfrac{1}{2}q^2)+B_i^X q^2(u_1\cdot\ell)^2 \\
&\quad + C_i^X q^2((u_1\cdot\ell)^2+\tfrac{1}{2}q^2)+D_i^X q^4(1-2\sigma^2)^2\,.
\end{aligned} \tag{4.105}$$

The coefficients $A,\ldots,D$ for the amplitude with an insertion of an electric-type operator are

given by

$$
\begin{aligned}
&A_1^{\mathcal{E}} = 1\,, && B_1^{\mathcal{E}} = -2\sigma^2\,, && C_1^{\mathcal{E}} = 0\,, && D_1^{\mathcal{E}} = \frac{1}{8}\,,\\
&A_2^{\mathcal{E}} = \frac{1}{2}\,, && B_2^{\mathcal{E}} = \frac{1}{8}(1-8\sigma^2)\,, && C_2^{\mathcal{E}} = 0\,, && D_2^{\mathcal{E}} = \frac{1}{16}\,,\\
&A_3^{\mathcal{E}} = \frac{1}{2}\,, && B_3^{\mathcal{E}} = -\frac{1}{2}\sigma^2\,, && C_3^{\mathcal{E}} = 0 && D_3^{\mathcal{E}} = \frac{1}{32}\,,
\end{aligned}
\tag{4.106}
$$

while those for the amplitude with an insertion of the "magnetic" operator are

$$
\begin{aligned}
&A_1^{\mathcal{B}} = 4\,, && B_1^{\mathcal{B}} = (1-8\sigma^2)\,, && C_1^{\mathcal{B}} = -1\,, && D_1^{\mathcal{B}} = \frac{1}{2}\,,\\
&A_2^{\mathcal{B}} = 2\,, && B_2^{\mathcal{B}} = -4\sigma^2\,, && C_2^{\mathcal{B}} = -\frac{1}{2}\,, && D_2^{\mathcal{B}} = \frac{1}{4}\,,\\
&A_3^{\mathcal{B}} = 0 && B_3^{\mathcal{B}} = \frac{1}{4}(1-8\sigma^2)\,, && C_3^{\mathcal{B}} = -\frac{1}{4}\,, && D_3^{\mathcal{B}} = \frac{1}{8}\,.
\end{aligned}
\tag{4.107}
$$

In the soft limit, all integrals in the amplitude (4.103) are of the type

$$
I_{n,2l} = \int \frac{d^D\ell}{(2\pi)^D} \frac{|\boldsymbol{q}|^{1-2(n+l)}(u_1\cdot\ell)^{2l}((u_1\cdot\ell)^2+\frac{1}{2}q^2)^n}{\ell^2(-2u_2\cdot\ell)(\ell-q)^2}\,;
\tag{4.108}
$$

they can be evaluated in terms of the triangle integrals (4.72) found in Sec. 4.3.2:

$$
\begin{aligned}
I_{n,2l} &= \sum_{u=1}^{n} C_n^u \left(-\frac{1}{2}\right)^{n-u} I_{2(l+u)}\\
&= -\frac{i}{32}\frac{(-)^{n+l}}{2^{2l+n}}\frac{\Gamma(l+\frac{1}{2})}{\sqrt{\pi}\Gamma(l+1)}\,(\sigma^2-1)^m {}_2F_1\left(\tfrac{1}{2}+l,-n,1+l,\tfrac{1}{2}(1-\sigma^2)\right)\,,
\end{aligned}
\tag{4.109}
$$

where C_n^u are binomial coefficients. In terms of these integrals, the three terms $\mathcal{M}_n^{(l)}(\Pi_k^X)$ making up the complete amplitude are

$$
\mathcal{M}_{l,n}(\Pi_k^X) = A_k^X I_{n+1-k,2(l+1)} + B_k^X I_{n-k,2(l+1)} + q^2 C_k^X I_{n+1-k,2l} + (1-2\sigma^2) D_k^X I_{n-k,2l})\,,
\tag{4.110}
$$

with coefficients $A, \ldots, D$ given in (4.106) and (4.107). Using these building blocks it is then straightforward to assemble the amplitudes $\mathcal{M}_{\mathrm{E}^2_{l,n}}(\boldsymbol{p}, \boldsymbol{q})$ and $\mathcal{M}_{\mathrm{B}^2_{l,n}}(\boldsymbol{p}, \boldsymbol{q})$ in Eq. (4.103). The eikonal phases follows by Fourier-transforming them to impact parameter space and including the appropriate factors as in Eq. (4.80). Choosing $n = 2$ we recover the amplitudes in Eqs. (4.77) and (4.81). Last, the two-body potential and the eikonal phase are related to the leading-order amplitude in the usual way as in Eqs. (4.5) and (4.6).

The position-space analysis also works in this case. In fact. for this approach it is convenient to sidestep the encoding of the tidal effects in a particular basis of higher-dimensions operators and work directly with the susceptibility χ. From this perspective the matrix element of an arbitrary tidal operator quadratic in the electric field is

$$\mathcal{M}_{\chi\mathrm{EE}}(h(\ell_1), h(\ell_2), \phi(p_1), \phi(p_4)) = 2m_1\kappa^2 \chi_{\mu_1\nu_1\mu_2\nu_2}(u_1 \cdot \ell_1, \hat{\ell}_1; u_1 \cdot \ell_2, \hat{\ell}_2) \mathcal{E}_{\mu_1\nu_1}(\ell_1, p_1) \mathcal{E}^{\mu_2\nu_2}(\ell_2, p_1) + (p_1 \leftrightarrow p_4, u_1 \leftrightarrow u_4). \tag{4.111}$$

Bose symmetry guarantees that this is symmetric in the two gravitons, so the manipulations in the previous section can be repeated here. The Fourier transform of the one-loop integrand, after sewing the unitarity cut and evaluating the energy integral, is

$$\mathcal{M}_{\chi\mathrm{EE}}(\boldsymbol{p}, \boldsymbol{r}) = \frac{\kappa^2}{4m_2} \int \frac{d^{D-1}\boldsymbol{\ell}_1}{(2\pi)^{D-1}} \frac{e^{-i\boldsymbol{r}\cdot\boldsymbol{\ell}_1}}{\boldsymbol{\ell}_1^2} \int \frac{d^{D-1}\boldsymbol{\ell}_2}{(2\pi)^{D-1}} \frac{e^{-i\boldsymbol{r}\cdot\boldsymbol{\ell}_2}}{\boldsymbol{\ell}_2^2} \mathcal{M}_{\chi\mathrm{EE}}(h(\ell_1), h(\ell_2), \phi(p_1), \phi(p_4))\big|_{\varepsilon_{\mu\nu}(\ell)\to T_{\mu\nu}(p_2)} \tag{4.112}$$

$$= \frac{m_1\kappa^4}{2m_2} \left[\chi_{\mu_1\nu_1\mu_2\nu_2}(v\hat{\boldsymbol{z}} \cdot i\boldsymbol{\nabla}_1, \boldsymbol{\nabla}_1^\perp; v\hat{\boldsymbol{z}} \cdot i\boldsymbol{\nabla}_2, \boldsymbol{\nabla}_2^\perp) \mathcal{E}_{\mu_1\nu_1}(\boldsymbol{r}_1, p_1) \mathcal{E}_{\mu_2\nu_2}(\boldsymbol{r}_2, p_1)\right]_{\boldsymbol{r}_1=\boldsymbol{r}_2=\boldsymbol{r}} ,$$

where $v = \sqrt{\sigma^2 - 1}$, $\boldsymbol{\nabla}^\perp = \boldsymbol{\nabla} - v^2\, \hat{\boldsymbol{z}}\, (\hat{\boldsymbol{z}} \cdot \boldsymbol{\nabla})$, and we have introduced different positions, $\boldsymbol{r}_i$, for all the gravitons. They are to be set equal after the derivatives are evaluated. As before, we can obtain the isotropic potential by first generating the on-shell amplitude through Eq. (4.90) and Fourier transforming back to the position space. The eikonal phase can either be obtained from Eq. (4.6) or directly from $\mathcal{M}_{\chi\mathrm{EE}}(\boldsymbol{p}, \boldsymbol{r})$ via Eq. (4.93).

4.3.5 Adding spin

It is not difficult to formally the calculation in the previous sections to include spin degrees of freedom for the particle with momentum p_2. It amounts to changing $T_{\mu\nu}(p_2)$ in Eqs. (4.70), (4.86), (4.103) and (4.111) with $T^{\rm Kerr}_{\mu\nu}(p_2, l_i)$ in Eq. (4.67) or its general form defined from Eq. (4.63) and parametrized as in Eq. (4.68) and multiplying the resulting amplitude by the product of spin-S polarization tensors.

With this replacement, the contraction of two electric-type tensors $\mathcal{E}_{\mu_1\mu_2}(\ell_i, p_1)$ is

$$
\begin{aligned}
&\mathcal{E}_{\mu_1\mu_2}(\ell_1,p_1)\mathcal{E}^{\mu_1\mu_2}(\ell_2,p_1)\big|_{\varepsilon_{\mu\nu}(\ell_i)\to T^{\rm gen}_{\mu\nu}(p_2)} \qquad (4.113)\\
&\quad=\frac{1}{8}m_2^4A(\ell_1)A(\ell_2)(8(\ell\cdot u_1)^4+4(\ell\cdot u_1)^2q^2(1-4\sigma^2)+q^4(1-2\sigma^2)^2)\\
&\quad-\frac{i}{4}m_2^3A(\ell_1)B(\ell_2)q^2\sigma(-4(\ell\cdot u_1)^2+q^2(-1+2\sigma^2))\,S_2[u_1,q]\\
&\quad+\frac{i}{2}m_2^3(A(\ell_2)B(\ell_1)+A(\ell_1)B(\ell_2))\ell\cdot u_1\sigma(4(\ell\cdot u_1)^2+q^2(1-2\sigma^2))\,S_2[\ell,q]\\
&\quad-\frac{i}{4}m_2^3(A(\ell_2)B(\ell_1)-A(\ell_1)B(\ell_2))q^2\sigma(4(\ell\cdot u_1)^2+q^2(1-2\sigma^2))\,S_2[\ell,u_1]\\
&\quad+\frac{1}{2}m_2^2B(\ell_1)B(\ell_2)(\ell\cdot u_1)^2(-2(\ell\cdot u_1)^2+q^2\sigma^2)\,S_2[e^\mu,q]S_2[e_\mu,\ell]\\
&\quad+\frac{1}{2}m_2^2B(\ell_1)B(\ell_2)(\ell\cdot u_1)^2(2(\ell\cdot u_1)^2-q^2\sigma^2)\,S_2[e^\mu,\ell]S_2[e_\mu,\ell]\\
&\quad+m_2^2B(\ell_1)B(\ell_2)\ell\cdot u_1((\ell\cdot u_1)^2-q^2\sigma^2)\,S_2[\ell,q]S_2[u_1,q]\\
&\quad-\frac{1}{2}m_2^2B(\ell_1)B(\ell_2)q^2((\ell\cdot u_1)^2-q^2\sigma^2)\,S_2[\ell,p_1]S_2[u_1,q]\\
&\quad-m_2^2B(\ell_1)B(\ell_2)(\ell\cdot u_1)^2\sigma^2\,S_2[\ell,q]^2\\
&\quad+\frac{1}{2}m_2^2B(\ell_1)B(\ell_2)q^2(-(\ell\cdot u_1)^2+q^2\sigma^2)\,S_2[\ell,u_1]^2+\mathcal{O}(q^5)\,,
\end{aligned}
$$

where $\ell_1=\ell$, $\ell_2=q-\ell$ and

$$
S_2[a,b]\equiv S(p_2)^{\mu\nu}a_\mu b_\nu\,,\qquad S_2[e^\mu,a]S_2[e_\mu,b]\equiv\eta_{\mu\nu}S(p_2)^{\mu\rho}a_\rho S(p_2)^{\nu\sigma}b_\sigma\,. \qquad (4.114)
$$

For vanishing spin, $A(\ell_i)=1$ and $B(\ell_i)=0$, only the first line of Eq. (4.113) survives and we

recover Eq. (4.70). One may expand Eq. (4.113) to arbitrary order in spin. For example, to first nontrivial order, which corresponds to inclusion of the spin-orbit interaction for particle 2, we find

$$\begin{aligned}\mathcal{E}_{\mu_1\mu_2}(\ell_1,p_1)\mathcal{E}^{\mu_1\mu_2}(\ell_2,p_1)\big|_{\varepsilon_{\mu\nu}(\ell_i)\to T^{\rm gen}_{\mu\nu}(p_2)} &= \mathcal{E}_{\mu_1\mu_2}(\ell_1,p_1)\mathcal{E}^{\mu_1\mu_2}(\ell_2,p_1)\big|_{\varepsilon_{\mu\nu}(\ell_i)\to T_{\mu\nu}(p_2)} \\ &+ \frac{i}{4}C_{BS^1}m_2^3\,\sigma(4\ell\cdot u_1 S_2[\ell,q]+q^2\,S_2[u_1,q])(4(\ell\cdot u_1)^2+q^2(1-2\sigma^2))+\mathcal{O}((q\cdot S)^2)\,,\end{aligned} \tag{4.115}$$

where the first term on the right-hand side is given by Eq. (4.71).

It is straightforward, albeit tedious, to write out explicitly an integral representation of the amplitude by plugging in Eq. (4.113) in Eq. (4.70). We will refrain however from doing so, and rather only comment on its structure. In addition to the integrals in Eq. (4.72), the spin dependence introduces also tensor integrals:

$$I_l^{\mu_1\cdots\mu_s}=\int\frac{d^D\ell}{(2\pi)^D}\frac{|\boldsymbol{q}|^{-2l-s+1}\ell^{\mu_1}\ldots\ell^{\mu_s}(\ell\cdot u_1)^l}{\ell^2(-2\ell\cdot u_2)(\ell-q)^2}\,; \tag{4.116}$$

they may be parametrized as a scalar integral $I_l[w,s]$ by contracting the free indices with an arbitrary vector w, from which the desired tensor integral is extracted by taking s derivatives. Note that, unlike the triangle integrals in Eq. (4.72), here the exponent l is not constrained to be even. To leading order in spin only the vector integral is relevant. To this order, Eq. (4.115) becomes:

$$\begin{aligned}\mathcal{M}_{\mathrm{E}^2_{l,2},S(p_2)}(\boldsymbol{p},\boldsymbol{q}) &= \varepsilon_2\cdot\varepsilon_3\mathcal{M}_{\mathrm{E}^2_{l,2}}(\boldsymbol{p},\boldsymbol{q}) \\ &+ 128(-1)^l C_{BS^1}G^2\pi^2\sigma|\boldsymbol{q}|^{2l+3}\Big(S_2[u_1,q]\big((-1+2\sigma^2)I_{2l}+4I_{2+2l}\big) \\ &\quad + 4S_2[e_\mu,q]\big((1-2\sigma^2)I^\mu_{1+2l}-4I^\mu_{3+2l}\big)\Big)m_1m_2^3\varepsilon_2\cdot\varepsilon_3+\mathcal{O}((q\cdot S)^2)\,.\end{aligned} \tag{4.117}$$

It is not difficult to evaluate in the usual way the vector integrals, by writing them as a linear combination of u_1, u_2 and q and solving for the coefficients in terms of the scalar

triangle integrals in Eq. (4.72). Alternatively, one may re-evaluate the integrals in Eq. (4.72) by treating u_1, u_2 and q as uncorrelated vectors, differentiate s times with respect to u_1 and then impose $u_i^2 = 1, u_i \cdot q = 0$. For the vector integrals we find

$$I^{\mu}_{2l+1} = -\frac{u_1^{\mu} - u_2^{\mu} y}{y^2 - 1} I_{2l+2}\,. \tag{4.118}$$

Thus, the amplitude with the first spin-dependent term for particle 2 is

$$\begin{aligned}
&\mathcal{M}_{\mathrm{E}^2_{l,2},S(p_2)}(\phi(p_1),\phi(p_2),\phi(p_3),\phi(p_4)) = \varepsilon_2\cdot\varepsilon_3 \mathcal{M}_{\mathrm{E}^2_{l,2}}(\phi(p_1),\phi(p_2),\phi(p_3),\phi(p_4)) \qquad (4.119)\\
&- C_{BS^1} G^2 \pi^{3/2} \frac{\Gamma(\frac{1}{2}+l)}{2^{2l-5}\Gamma(3+l)} m_2^3 \sigma(-1+\sigma^2)^l(-3+(7+2l)\sigma^2)|\boldsymbol{q}|^{3+2l} S_2[p_1,(iq)]\varepsilon_2\cdot\varepsilon_3 + \mathcal{O}((q\cdot S)^2)\,.
\end{aligned}$$

To extract the two-body potential in terms of the rest-frame spin it is necessary to expand the product of polarization tensors to leading order in spin, as discussed in Ref. [23]. Using the relations

$$\begin{aligned}
\varepsilon_2\cdot\varepsilon_3 &= \left(1 - i\frac{\epsilon_{rsk} p_2^r p_3^s S^k}{m_2(m_2+E(\boldsymbol{p}_2))} + \mathcal{O}(\mathrm{S}^2\boldsymbol{q}^2)\right) + \mathcal{O}(q)\,,\\
\epsilon^{\mu\nu\rho\sigma} p_{1\mu} p_{2\nu} q_\rho S_{i\sigma} &= (E_1+E_2)\,(\boldsymbol{p}\times\boldsymbol{q})\cdot\boldsymbol{S}_i\,,
\end{aligned} \tag{4.120}$$

the amplitude becomes

$$\begin{aligned}
&\mathcal{M}_{\mathrm{E}^2_{l,2},S(p_2)}(\phi(p_1),\phi(p_2),\phi(p_3),\phi(p_4)) \qquad (4.121)\\
&= \overline{\mathcal{M}}_{\mathrm{E}^2_{l,2}}(\boldsymbol{p})|\boldsymbol{q}|^{2l+3} + \left(\frac{\overline{\mathcal{M}}_{\mathrm{E}^2_{l,2}}(\boldsymbol{p})}{m_2(E_2+m_2)} + (E_1+E_2)\overline{\mathcal{M}}_{\mathrm{E}^2_{l,2},1}(\boldsymbol{p})\right)|\boldsymbol{q}|^{2l+3}\, i(\boldsymbol{p}\times\boldsymbol{q})\cdot\boldsymbol{S}_2 + \mathcal{O}((q\cdot S)^2)\,,
\end{aligned}$$

where $\mathcal{M}_{\mathrm{E}^2_{l,2},1}$ is the coefficient of $S_2[p_1,(iq)]$ in Eq. (4.119) and, as before, the bar indicates that all $\boldsymbol{q}$ dependence has been extracted. The two-body potential and the eikonal phase are then extracted by three-dimensional and two-dimensional Fourier-transforms, in terms of their spinless counterparts and the coefficient of the spin-dependent structure in

the amplitude:

$$V_{\mathrm{E}^2_{l,2},S_2}(\boldsymbol{p},\boldsymbol{r}) = V_{\mathrm{E}^2_{l,2}}(\boldsymbol{p},\boldsymbol{r}) - \frac{(\boldsymbol{p}\times\boldsymbol{r})\cdot\boldsymbol{S}_2}{4E_1E_2|\boldsymbol{r}|^{2l+8}}\,\frac{2^{4+2l}\Gamma(4+l)}{\pi^{3/2}\Gamma(-\frac{3}{2}-l)} \times\left(\frac{\overline{\mathcal{M}}_{\mathrm{E}^2_{l,2}}(\boldsymbol{p})}{m_2(E_2+m_2)} + (E_1+E_2)\overline{\mathcal{M}}_{\mathrm{E}^2_{l,2},1}(\boldsymbol{p})\right) + \mathcal{O}((\boldsymbol{r}\boldsymbol{S})^2)\,, \quad (4.122)$$

$$\delta_{\mathrm{E}^2_{l,2},S_2}(\boldsymbol{p},\boldsymbol{b}) = \delta_{\mathrm{E}^2_{l,2}}(\boldsymbol{p},\boldsymbol{b}) + \frac{1}{4m_1m_2\sqrt{\sigma^2-1}}\,\frac{(\boldsymbol{p}\times\boldsymbol{b})\cdot\boldsymbol{S}_2}{|\boldsymbol{b}|^{2l+7}}\,\frac{2^{4+2l}\Gamma(\frac{7}{2}+l)}{\pi\Gamma(-\frac{3}{2}-l)} \times\left(\frac{\overline{\mathcal{M}}_{\mathrm{E}^2_{l,2}}(\boldsymbol{p})}{m_2(E_2+m_2)} + (E_1+E_2)\overline{\mathcal{M}}_{\mathrm{E}^2_{l,2},1}(\boldsymbol{p})\right) + \mathcal{O}((\boldsymbol{r}\boldsymbol{S})^2)\,. \quad (4.123)$$

The position-space analysis extended to include spin degrees of freedom is equally straightforward. It amounts to substituting in Eqs. (4.87) and (4.112) the stress tensor $T_{\mu\nu}(p_2)$ by the general spin-dependent one in Eq. (4.68) or, for the scattering off a Kerr black hole, with $T^{\mathrm{Kerr}}_{\mu\nu}(p_2)$ in Eq. (4.67). As already emphasized, $T^{\mathrm{gen}}_{\mu\nu}(\ell_i,p_2)$ depends on the graviton momentum ℓ_i which now makes a leading-order contribution because of the spin dependence. Nevertheless, the contribution of $T^{\mathrm{gen}}_{\mu\nu}(\ell_i,p_2)$ can be organized as a differential operator acting on the position-space three-dimensional scalar propagator:

$$\mathcal{E}_{\mu_1\mu_2}(\boldsymbol{r},p_1) = \mathcal{E}_{\mu_1\mu_2}(i\boldsymbol{\nabla},p_1)\big|_{\varepsilon_{\mu\nu}(\ell_i)\to T^{\mathrm{gen}}_{\mu\nu}(i\boldsymbol{\nabla},p_2)}\int\frac{d^{D-1}\boldsymbol{\ell}_i}{(2\pi)^{D-1}}\frac{e^{-i\boldsymbol{r}\cdot\boldsymbol{\ell}_i}}{\boldsymbol{\ell}_i^2}\,. \quad (4.124)$$

The structure of the stress tensor (4.67) implies that, for scattering off a Kerr black hole, the complete spin dependence is governed by the non-Abelian Fourier transform

$$\int\frac{d^{D-1}\boldsymbol{\ell}_i}{(2\pi)^{D-1}}\frac{e^{-i(\hat{\boldsymbol{r}}-\hat{\boldsymbol{a}})\cdot\boldsymbol{\ell}_i}}{\boldsymbol{\ell}_i^2}\,, \quad (4.125)$$

where $\hat{\boldsymbol{r}} = \boldsymbol{r}\,\mathbb{1}_4$ and $\hat{\boldsymbol{a}}$ is a vector of matrices, $(\hat{\boldsymbol{a}}_\sigma)^\mu{}_\nu = \epsilon^\mu{}_{\nu\rho\sigma}a^\rho$, with a defined in Eq. (4.66). One may evaluate it by formally expanding the integrand in $\hat{\boldsymbol{a}}$.

On general grounds, as discussed in Ref. [23], the impulse and spin kick is computed from the eikonal phase (4.123) through the relations (4.8) agree with those computed from

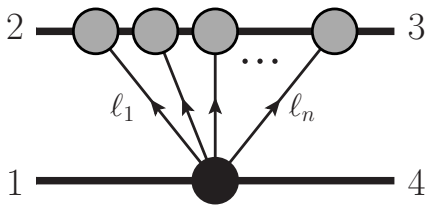

Figure 4.2: The generalized cut for leading order contributions to nonlinear tidal operators. Each blob is simply a (local) on-shell amplitude. The dark blob contains the X^n tidal operator. The direction of graviton momentum flow is indicated by the arrows.

Hamilton's equations of motion based on the two-body potential (4.122). The same holds for the magnetic analog of Eqs. (4.123) and (4.122).

4.4 Nonlinear tidal effects

The amplitude with nonlinear tidal effect, i.e. the scattering with an X^n operator insertion, where X stands for E or B, can be constructed from the unitarity cut in Figure 4.2. We will mostly focus on leading contribution for such an operator in this section. In this case, the simplifications described in Section 4.3.1 are all applicable. Namely, the amplitude with X^n tidal operator is still comprised of linearized electric and magnetic Weyl tensor in Eqs. (4.59) and (4.60); and the sewing of three-point amplitudes with the amplitude with X^n tidal operator is effectively replacing the polarization $\varepsilon_{\mu\nu}(\ell_i) \to T_{\mu\nu}(p_2)$ for each graviton. Start from the the unitarity cut in Figure 4.2. After sewing we find

$$\begin{aligned}\mathcal{M}_{\mathrm{X}^n}(\boldsymbol{p},\boldsymbol{q}) =& \frac{\kappa^n}{m_2^{n-1}} \int \mathcal{M}_{\mathrm{X}^n}(h(\ell_1),\ldots,h(\ell_n),\phi(p_1),\phi(p_4))\big|_{\varepsilon_{\mu\nu}(\ell_i)\to T_{\mu\nu}(p_2)} \\ &\times \frac{1}{\ell_1^2\ell_2^2\cdots\ell_n^2}\left[\frac{i}{(-2u_2\cdot\ell_1)}\frac{i}{(-2u_2\cdot\ell_{12})}\cdots\frac{i}{(-2u_2\cdot\sum_{j=1}^{n-1}\ell_j)}\right], \end{aligned} \tag{4.126}$$

where we integrate over ℓ_i with $i = 1,\ldots,n-1$ and $\sum_{i=1}^{n} l_i = q$.

As discussed in the previous section, we can include spin degrees of freedom for the field without the tidal deformation by simply replacing in Eq (4.126) the point-particle stress

tensor $T_{\mu\nu}$ with that of the general spinning particle $T^{\rm gen}_{\mu\nu}$, cf. Eq. (4.68), or with that of a Kerr black hole, cf. (4.67).

The calculations from position space and momentum space also follow similarly as before. We discuss them in turn.

4.4.1 Leading order position-space analysis

Start with Eq. (4.126). Again we consider the rest frame of particle 2 in which we have Eq. (4.73). The first step is to integrate out energy in potential region. Using the identity [51]

$$\delta\left(\sum_{i=1}^{n}\ell_i^0\right)\left[\frac{i}{(-2u_2\cdot\ell_1+i0)}\frac{i}{(-2u_2\cdot\ell_{12}+i0)}\cdots\frac{i}{(-2u_2\cdot\sum_{j=1}^{n-1}\ell_j+i0)}+\text{perm}\right]=\pi^{n-1}\prod_{i=1}^{n}\delta(\ell_i^0)\,, \tag{4.127}$$

where perm is the rest of $n!$ permutations of $\ell_{1,\ldots,n}$. Since the integrand is invariant under permutations, this localizes all $\ell_i^0=0$ with a $1/n!$ prefactor

$$\begin{aligned}\mathcal{M}_{\mathrm{X}^n}(\boldsymbol{p},\boldsymbol{q}) =&\frac{(-\kappa)^n}{(2m_2)^{n-1}\,n!}\int\left[\prod_{i=1}^{n}\frac{d^{D-1}\boldsymbol{\ell}_i}{(2\pi)^{D-1}}\,\frac{1}{\boldsymbol{\ell}_i^2}\right]\,\delta\left(\boldsymbol{q}-\sum_{i=1}^{n}\boldsymbol{\ell}_i\right)\\ &\times\mathcal{M}_{\mathrm{X}^n}(h(\ell_1),\ldots,h(\ell_n),\phi(p_1),\phi(p_4))\big|_{\varepsilon_{\mu\nu}(\ell_i)\to T_{\mu\nu}(p_2)},\end{aligned} \tag{4.128}$$

To evaluate this integral, we use the same manipulations as at one loop. First consider the Fourier transform to position space

$$\begin{aligned}\mathcal{M}_{\mathrm{X}^n}(\boldsymbol{p},\boldsymbol{r}) &= \int\frac{d^{D-1}\boldsymbol{q}}{(2\pi)^{D-1}}e^{-i\boldsymbol{r}\cdot\boldsymbol{q}}\widetilde{\mathcal{M}}_{\mathrm{X}^n}(\boldsymbol{p},\boldsymbol{q})\\ &=\frac{(-\kappa)^n}{(2m_2)^{n-1}\,n!}\prod_{i=1}^{n}\int\frac{d^{D-1}\boldsymbol{\ell}_i}{(2\pi)^{D-1}}\frac{e^{-i\boldsymbol{r}\cdot\boldsymbol{\ell}_i}}{\boldsymbol{\ell}_i^2}\,\mathcal{M}_{\mathrm{X}^n}(h(\ell_1),\ldots,h(\ell_n),\phi(p_1),\phi(p_4))\big|_{\varepsilon_{\mu\nu}(\ell_i)\to T_{\mu\nu}(p_2)}\\ &=\frac{(-\kappa)^n}{(2m_2)^{n-1}\,n!}\,\mathcal{M}_{\mathrm{X}^n}(h_1,\ldots,h_n,\phi(p_1),\phi(p_4)|\boldsymbol{r}),\end{aligned} \tag{4.129}$$

where we use Eq. (4.87) to define

$$\begin{aligned}
&\mathcal{M}_{\mathrm{X}^n}(h_1,\ldots,h_n,\phi(p_1),\phi(p_4)|\boldsymbol{r}) \qquad (4.130)\\
&\quad\equiv\prod_{i=1}^{n}\int\frac{d^{D-1}\boldsymbol{\ell}_i}{(2\pi)^{D-1}}\frac{e^{-i\boldsymbol{r}\cdot\boldsymbol{\ell}_i}}{\boldsymbol{\ell}_i^2}\,\mathcal{M}_{\mathrm{X}^n}(h(\ell_1),\ldots,h(\ell_n),\phi(p_1),\phi(p_4))\big|_{\varepsilon_{\mu\nu}(\ell_i)\to T_{\mu\nu}(p_2)}\\
&\quad=\mathcal{M}_{\mathrm{X}^n}(h(\ell_1),\ldots,h(\ell_n),\phi(p_1),\phi(p_4)|X_{\mu_1\mu_2}(\ell_j,p_1)\to X_{\mu_1\mu_2}(\boldsymbol{r}_j,p_1),\boldsymbol{\ell}_j\to i\nabla_j)\Big|_{\boldsymbol{r}_j\to\boldsymbol{r}}.
\end{aligned}$$

As before all the coordinates $\boldsymbol{r}_j$ are identified as $\boldsymbol{r}$ in the end. The above formula is very general and applies to higher multipole operators or general susceptibilities similar to Eq. (4.112). Recall that $\mathcal{M}_{\mathrm{X}^n}(h(\ell_1),\ldots,h(\ell_n),\phi(p_1),\phi(p_4))$ is only a function of $\mathcal{E}_{\mu_1\mu_2}(\ell_i,p_2)$, $\mathcal{B}_{\mu_1\mu_2}(\ell_i,p_2)$, and Mandelstam invariants. The Fourier transform simply replaces them with their corresponding in position-space expressions defined in Eqs. (4.87) and (4.94). As before, the result of $\mathcal{M}_{\mathrm{X}^n}(\boldsymbol{p},\boldsymbol{r})$ is generally not isotropic, because any $u_1\cdot\ell$ in momentum space generates dependence on $\hat{\boldsymbol{z}}\cdot\boldsymbol{\ell}$. To bring it into the isotropic form, we Fourier transform back to momentum space, as in Eq. (4.90).

A simple example is the operator $E_\mu{}^\nu E_\nu{}^\rho E_\rho{}^\mu$, denoted as (E^3). With the contraction of three $\mathcal{E}$ tensors (4.87) given by

$$\mathcal{E}_\mu{}^\nu(\boldsymbol{r},p_1)\mathcal{E}_\nu{}^\rho(\boldsymbol{r},p_1)\mathcal{E}_\rho{}^\mu(\boldsymbol{r},p_1)=\frac{3m_2^6}{4096\pi^3|\boldsymbol{r}|^{13}}\left[9(\sigma^2-1)(\boldsymbol{r}^2-z^2)(\sigma^2\boldsymbol{r}^2-(\sigma^2-1)z^2)+2\boldsymbol{r}^2\right], \qquad (4.131)$$

the graviton-scalar amplitude is

$$\mathcal{M}_{(\mathrm{E}^3)}(h_1,h_2,h_3,\phi(p_1),\phi(p_4)|\boldsymbol{r})=12\kappa^3\,m_1\,\mathcal{E}_\mu{}^\nu(\boldsymbol{r},p_1)\mathcal{E}_\nu{}^\rho(\boldsymbol{r},p_1)\mathcal{E}_\rho{}^\mu(\boldsymbol{r},p_1)\,. \qquad (4.132)$$

Plugging into Eq. (4.129) then yields the four-scalar amplitude in position space

$$\mathcal{M}_{(\mathrm{E}^3)}(\boldsymbol{p},\boldsymbol{r})=-\frac{\kappa^6 m_1}{2m_2^2}\,\mathcal{E}_\mu{}^\nu(\boldsymbol{r},p_1)\mathcal{E}_\nu{}^\rho(\boldsymbol{r},p_1)\mathcal{E}_\rho{}^\mu(\boldsymbol{r},p_1). \qquad (4.133)$$

Using the Fourier transform formula in Eq. (4.91), we arrive the final result

$$\mathcal{M}_{(\mathrm{E}^3)}(\boldsymbol{p},\boldsymbol{q}) = \frac{-|\boldsymbol{q}|^{6-4\epsilon}}{2\epsilon}\,\overline{\mathcal{M}}_{(\mathrm{E}^3)}(\boldsymbol{p}) = \frac{18}{11!!}G^3 m_1 m_2^4 \pi\Big(\frac{7}{4} - 9\sigma^2 + 10\sigma^4\Big)\frac{|\boldsymbol{q}|^{6-4\epsilon}}{\epsilon}\,. \tag{4.134}$$

An important feature of the position-space scalar-graviton amplitude (4.130), which we already encountered in the one-loop analysis in Sec. 4.3.3, is that it factorizes into a product of position-space $\mathcal{E}$ tensor, defined in Eq. (4.87) and its magnetic counterpart, perhaps with additional derivatives. As explained in Section 4.2, the fact that these position-space tensors have rank 3 implies that such a product can be further expressed as a sum of products of traces of at most three factors. For example, Eq. (4.50) gives the decomposition of any power of a rank-3 matrix in terms of in terms of traces of two and three such matrices. It applies directly to the four-scalar amplitude with an insertion of (E^n) and expresses it as a sum of four-scalar amplitudes with an insertion of $(E^2)^{n_2}(E^3)^{n_3}$ with $n = 2n_2 + 3n_3$. It also applies directly to amplitudes with an insertion of (B^n). While the resulting amplitude vanishes of n is odd, it also further simplifies if n is even. The parity-odd nature of $\mathcal{B}_{\mu,\nu}(\boldsymbol{r},\boldsymbol{p})$ and position-space factorization imply that, to leading order, $(B^3) = 0$ because there are insufficient vectors to saturate the Levi-Civita tensor. Therefore, to leading order, the analog of Eq. (4.50) for the magnetic operators reduces to,

$$(B^{n=2k}) = \frac{1}{2^{k-1}}(B^2)^k\,. \tag{4.135}$$

The amplitudes collected in the Appendix 4.A verify these formulas for up to $n = 8$.

The momentum-space four-scalar amplitude is related to the position-space four-scalar amplitude by single $(D-1)$-dimensional Fourier transform. The structure of the position-space amplitude is essential. This observation allows us to evaluate amplitudes and the corresponding two-body potentials to leading order for arbitrary operators.

Since the position-space scalar-graviton amplitudes with one insertion of either one of

(E^2), (B^2) or (E^3) have a similar structure, we will discuss them simultaneously, referring to these operators as $(\mathcal{O})$. They have the form,

$$\widetilde{\mathcal{M}}_{(\mathcal{O})} = \mathcal{N}_{(\mathcal{O})} \frac{1}{\boldsymbol{r}^h} \Big(a_{(\mathcal{O})} + b_{(\mathcal{O})} \frac{(\boldsymbol{r}\cdot\boldsymbol{u}_1)^2}{\boldsymbol{r}^2} + c_{(\mathcal{O})} \frac{(\boldsymbol{r}\cdot\boldsymbol{u}_1)^4}{\boldsymbol{r}^4} \Big) , \tag{4.136}$$

where $\mathcal{N}_{(\mathcal{O})}$ is an operator-dependent normalization factor. For the three operators it is,

$$\mathcal{N}_{(\mathrm{E}^2)} = \mathcal{N}_{(\mathrm{B}^2)} = 2^4 G^2 \pi^2 m_1 m_2^3 , \qquad \mathcal{N}_{(\mathrm{E}^3)} = 2^5 G^3 \pi^3 m_1 m_2^4 , \tag{4.137}$$

and the coefficients are

$$\begin{aligned}
a_{(\mathrm{E}^2)} &= \frac{3(1-3\sigma^2+3\sigma^4)}{2\pi^2} , & b_{(\mathrm{E}^2)} &= \frac{9(1-2\sigma^2)}{2\pi^2} , & c_{(\mathrm{E}^2)} &= \frac{9}{2\pi^2} , \\
a_{(\mathrm{B}^2)} &= \frac{9\sigma^2(\sigma^2-1)}{2\pi^2} , & b_{(\mathrm{B}^2)} &= \frac{9(1-2\sigma^2)}{2\pi^2} , & c_{(\mathrm{B}^2)} &= \frac{9}{2\pi^2} , \\
a_{(\mathrm{E}^3)} &= -\frac{3(2-9\sigma^2+9\sigma^4)}{8\pi^3} , & b_{(\mathrm{E}^3)} &= -\frac{27(1-2\sigma^2)}{8\pi^3} , & c_{(\mathrm{E}^3)} &= -\frac{27}{8\pi^3} .
\end{aligned} \tag{4.138}$$

The exponent of the overall $\boldsymbol{r}$ factor is $h = 6$ for $(\mathcal{O}) = (E^2)$ and $(\mathcal{O}) = (B^2)$ and $h = 9$ for $(\mathcal{O}) = (E^3)$.

The position- space amplitude with an insertion of an operator made up of n such traces is simply given by raising (4.136) to the nth power and adjusting the normalization factor,

$$\widetilde{\mathcal{M}}_{(\mathcal{O})^n} = \mathcal{N}_{(\mathcal{O})^n} \Big[\frac{1}{\boldsymbol{r}^h} \Big(a_{(\mathcal{O})} + b_{(\mathcal{O})} \frac{(\boldsymbol{r}\cdot\boldsymbol{u}_1)^2}{\boldsymbol{r}^2} + c_{(\mathcal{O})} \frac{(\boldsymbol{r}\cdot\boldsymbol{u}_1)^4}{\boldsymbol{r}^4} \Big) \Big]^n . \tag{4.139}$$

The change in normalization factor is related to the normalization of the tree-level amplitude with one insertion of the composite operator. We find

$$\mathcal{N}_{(\mathrm{E}^2)^\mathrm{n}} = \mathcal{N}_{(\mathrm{B}^2)^\mathrm{n}} = 2^{2n+2} G^{2n} \pi^{2n} m_1 m_2^{2n+1} , \qquad \mathcal{N}_{(\mathrm{E}^3)^\mathrm{n}} = 2^{3n+2} G^{3n} \pi^{3n} m_1 m_2^{3n+1} . \tag{4.140}$$

To obtained the momentum-space scattering amplitude with an insertion of an arbitrary

operator $(\mathcal{O})^n$ we first use twice the binomial expansion and put the position-space amplitude in the form

$$\widetilde{\mathcal{M}}_{(\mathcal{O})^n} = \frac{\mathcal{N}_{(\mathcal{O})^n}}{\boldsymbol{r}^{nh}} \sum_{k=0}^{n} \sum_{l=0}^{k} \binom{n}{k} \binom{k}{l} a_{\mathcal{O}}^{n-k}\, b_{\mathcal{O}}^{l}\, c_{\mathcal{O}}^{k-l} \left(\frac{(\boldsymbol{r}\cdot\boldsymbol{u}_1)^2}{\boldsymbol{r}^2} \right)^{2k-l} . \tag{4.141}$$

Using then the general tensor Fourier-transform relation (4.91) which enforces $\boldsymbol{q}\cdot\boldsymbol{u}_1 = \boldsymbol{q}^2/2 \to 0$ leads to the desired result:

$$\begin{aligned} \mathcal{M}_{(\mathcal{O})^n}(\boldsymbol{p},\boldsymbol{q}) = \frac{\mathcal{N}_{(\mathcal{O})^n}}{|\boldsymbol{q}|^{D-nh-1}} \sum_{k=0}^{n} \sum_{l=0}^{k} \binom{n}{k} \binom{k}{l} a_{\mathcal{O}}^{n-k}\, b_{\mathcal{O}}^{l}\, c_{\mathcal{O}}^{k-l} \\ \times \frac{2^{D-hn-1}\pi^{D/2}(\sigma^2-1)^{2k-l}\Gamma(\frac{1}{2}+2k-l)}{\sin(\frac{\pi}{2}(D-hn-1))\Gamma(\frac{1}{2}(3+hn-D))\Gamma(2k-l+\frac{1}{2}hn)} , \end{aligned} \tag{4.142}$$

where $D = 4-2\epsilon$. The two-body potential and the eikonal phase follow then straightforwardly via Eqs. (4.9)-(4.12):

$$V_{(\mathcal{O})^n}(\boldsymbol{p},\boldsymbol{r}) = -\frac{\mathcal{N}_{(\mathcal{O})^n}}{4E_1E_2\,|\boldsymbol{r}|^{nh}} \sum_{k=0}^{n} \sum_{l=0}^{k} \binom{n}{k} \binom{k}{l} a_{\mathcal{O}}^{n-k}\, b_{\mathcal{O}}^{l}\, c_{\mathcal{O}}^{k-l}\, (\sigma^2-1)^{2k-l} \frac{\Gamma(\frac{1}{2}+2k-l)\Gamma(\frac{1}{2}hn)}{\sqrt{\pi}\Gamma(2k-l+\frac{1}{2}hn)} , \tag{4.143}$$

$$\delta_{(\mathcal{O})^n}(\boldsymbol{p},\boldsymbol{b}) = \frac{\mathcal{N}_{(\mathcal{O})^n}}{4m_1m_2\,|\boldsymbol{b}|^{nh-1}} \sum_{k=0}^{n} \sum_{l=0}^{k} \binom{n}{k} \binom{k}{l} a_{\mathcal{O}}^{n-k}\, b_{\mathcal{O}}^{l}\, c_{\mathcal{O}}^{k-l}\, (\sigma^2-1)^{2k-l-1/2} \frac{\Gamma(\frac{1}{2}+2k-l)\Gamma(\frac{1}{2}(hn-1))}{\Gamma(2k-l+\frac{1}{2}hn)} .$$

As discussed earlier, parity and factorization of the position-space amplitude implies that, to leading order in the classical limit, amplitudes with an insertion of an operator which has at least one parity-odd factor vanish identically even if the operator is overall parity-even. Thus, Eq. (4.50) with $E \to B$ implies that the approach described here yields the two-body potential for all nonlinear tidal operators of the type (B^{2n}).

The discussion above can be easily extended to cover amplitudes with one insertion of (E^n). Eq. (4.50) expresses it as a linear combination of amplitudes with one insertion of $(E^2)^{n_2}(E^3)^{n_3}$ with $2n_2+3n_3 = n$. The position space form of the latter involves a product of

two factors analogous to the right-hand side of Eq. (4.139). Each of them can be binomially expanded (with a slight simplification based on the equality $b_{(E^2)}/b_{(E^3)} = c_{(E^2)}/c_{(E^3)}$ visible in Eq. (4.138)) and put in a form analogous to the right-hand side of Eq. (4.141). Fourier-transforming using Eq. (4.91) and putting together all terms leads to the momentum-space amplitude with one insertion of (E^n).

The general formulas above show explicitly that the difference $E^{2n} - B^{2n}$ is subleading in the high-energy limit. This extends the observations of Refs. [28, 29] beyond the linear order.

4.4.2 Order by order momentum-space analysis

The above position-space evaluation is a very effective means for evaluating leading contributions to any given tidal operator. Momentum-space methods for evaluating the loop integrals instead offer a straightforward way to systematically extend the results to higher orders following the methods presented in Refs. [11–13]. Indeed following these methods, next to leading order contributions to E^2 and B^2 tidal operators were evaluated in Ref. [21]. A related approach for tidal operators based on world lines has been recently given in Ref. [29] where additional E^2 operators were evaluated.

Here we first re-evaluate the amplitudes in momentum space through C^4 and then discuss the extension to higher orders. The starting point is again the generalized cut shown in Figure 4.2. We evaluate the expressions in D-dimensions. Here we do not make use of the special real-space factorization of the integrals discussed in the previous section, but rather simply carry out the evaluation of the cut and then reduce the result to a basis of independent momentum products. We can simplify the resulting expressions considerably by applying the cut conditions and expanding in small momentum transfer q. Specifically, we can choose a basis of momentum invariants which does not contain any of the products $(p_2 \cdot \ell_k)$, since

the cut conditions give

$$\left(-p_2+\sum_{i=1}^{k}\ell_i\right)^2-m_2^2=0\;\rightarrow\;(p_2\cdot\ell_k)=\sum_{i=2}^{k}\sum_{j=1}^{i-1}(\ell_i\cdot\ell_j)-\sum_{i=1}^{k-1}(p_2\cdot\ell_i)\,, \tag{4.144}$$

where the final term can be eliminated inductively starting with $p_2\cdot\ell_1=0$. Products of the form $(p_3\cdot\ell_k)$ can then be eliminated using momentum conservation $p_3=-p_2-q=-p_2-\sum\ell_i$. Since the cut graviton momenta scale as $\mathcal{O}(q)$, the cut conditions thus ensure that the scaling of $(p_2\cdot\ell_k)$ or $(p_3\cdot\ell_k)$, which naively would be $\mathcal{O}(q)$, instead scale as $\mathcal{O}(q^2)$. This greatly aids in the simplification of the integrand after expanding in small q.

Unlike in the position-space analysis, the integrals do not decouple into a product, and in general, the momentum-space integrals can be challenging to evaluate. To do so, we use FIRE6 [52] which uses integration by parts methods [35] to reduce the integrals a single master integral, which can then be evaluated either by direct integration or by differential equations [53]. Evaluating the integrals is the most significant bottleneck for this method, but the task is significantly aided by the use of special variables as described in [36],

$$p_1=-(\bar{p}_1-q/2)\,,\qquad p_4=\bar{p}_1+q/2\,,\qquad p_2=-(\bar{p}_2+q/2)\,,\qquad p_3=\bar{p}_2-q/2\,. \tag{4.145}$$

The $\bar{p}_i$ are orthogonal to q by construction: $\bar{p}_i\cdot q=0$. As described in more detail in Ref. [36], with these variables the matter propagators reduce to

$$\frac{1}{(p_2+\ell_{1\cdots i})^2-m_2^2}=\frac{1}{2\bar{p}_2\cdot\ell_{1\cdots i}}+\mathcal{O}(q^0)\,, \tag{4.146}$$

so the matter propagators are linear in the loop momenta. In addition, we can define normalized external momenta, $\bar{u}_i^\mu=\bar{p}_i^\mu/\sqrt{m_i^2-q^2/4}$, such that $\bar{u}_i^2=1$ The net effect is that the q^2 dependence is scaled out of the integral so that it is only a function of a single-scale $\bar{u}_1\cdot\bar{u}_2=\sigma+\mathcal{O}(q^2)$. Using these variables integral encountered at any order of perturbation

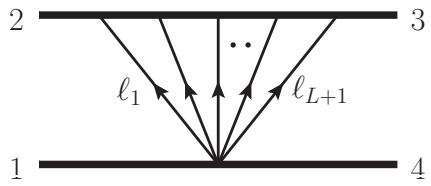

Figure 4.3: The L-loop fan integral.

theory can then be converted to a single scale integral. Such integrals are quite amenable to integration-by-parts methods, greatly speeding the evaluation.

The restriction to the potential region precludes pinching any propagators and the existence of irreducible scalar products. Thus, the result of IBP reduction is a single master integral, with a coefficient given by powers of $\boldsymbol{q}$ dictated by dimensional analysis, as well as a polynomial in σ. The master integral is the scalar *fan* integral in Fig. 4.3, which can be easily evaluated by factorizing the loops by going to position space and Fourier transforming back, with the result

$$\begin{aligned} I^{(L)}_{\text{fan}} &= \int \left(\prod_{i=1}^{L+1} \frac{d^D\ell}{(2\pi)^D} \frac{1}{\ell_i^2} \right) \frac{|\boldsymbol{q}|^{2-L}\delta(\sum_i \ell_i - q)}{(-2u_2\cdot\ell_1 + i0)(-2u_2\cdot\ell_{12} + i0)\cdots(-2u_2\cdot\ell_{1\cdots n-1} + i0)} \\ &= \frac{i^{L+2}}{2^{L(4-2\epsilon)}\pi^{L\left(\frac{3}{2}-\epsilon\right)}} \frac{\Gamma\left(\frac{1}{2}-\epsilon\right)^{L+1}\Gamma\left((\epsilon-\frac{1}{2})L+1\right)}{\Gamma(L+2)\Gamma\left((\frac{1}{2}-\epsilon)(L+1)\right)} |\boldsymbol{q}|^{-2\epsilon L}\,. \end{aligned} \tag{4.147}$$

At one loop this agrees with Eq. (4.76) with $l = 0$, and at two and three loops it yields

$$I^{(2)}_{\text{fan}} = \frac{1}{768\pi^2}\frac{(\boldsymbol{q}^2)^{-2\epsilon}}{2\epsilon} + \mathcal{O}(\epsilon^0)\,, \qquad I^{(3)}_{\text{fan}} = -\frac{i}{49152\pi^2} + \mathcal{O}(\epsilon)\,. \tag{4.148}$$

The results of the IBP reduction at two loops gives the amplitudes with a single insertion

of the tidal operators in terms of a single master integral:

$$\begin{aligned}
\mathcal{M}_{(\mathrm{E}^3)} &= \frac{1024}{385}\pi^3 G^3 m_1 m_2^4 |\boldsymbol{q}|^6 \left(\frac{7}{4} - 9\sigma^2 + 10\sigma^4\right) I^{(2)}_{\text{fan}}\,, \\
\mathcal{M}_{(\mathrm{EB}^2)} &= \frac{1024}{1155}\pi^3 G^3 m_1 m_2^4 |\boldsymbol{q}|^6 \left(\sigma^2 - 1\right)\left(1 + 10\sigma^2\right) I^{(2)}_{\text{fan}}\,, \\
\mathcal{M}_{(\mathrm{B}^3)} &= \mathcal{M}_{\mathrm{E}^2\mathrm{B}} = 0\,.
\end{aligned} \tag{4.149}$$

As expected, the parity odd operators E^2B and B^3 operator do not contribute.

At three loops, by reducing the integrand to the sole master integral we find the following for the amplitudes with an insertion of the single trace operators,

$$\begin{aligned}
\mathcal{M}_{(\mathrm{E}^4)} &= -i\frac{983}{9031680}\pi^4 G^4 m_1 m_2^5 |\boldsymbol{q}|^9 (1231 - 7304\sigma^2 + 18590\sigma^4 - 22880\sigma^6 + 12155\sigma^8) I^{(3)}_{\text{fan}}\,, \\
\mathcal{M}_{(\mathrm{B}^4)} &= -i\frac{140569}{9031680}\pi^4 G^4 m_1 m_2^5 |\boldsymbol{q}|^9 (\sigma^2 - 1)^2 (1 + 10\sigma^2 + 85\sigma^4) I^{(3)}_{\text{fan}}\,, \\
\mathcal{M}_{(\mathrm{EEBB})} &= -i\frac{10813}{27095040}\pi^4 G^4 m_1 m_2^5 |\boldsymbol{q}|^9 (\sigma^2 - 1)(41 + 689\sigma^2 - 2925\sigma^4 + 3315\sigma^6) I^{(3)}_{\text{fan}}\,, \\
\mathcal{M}_{(\mathrm{EBEB})} &= i\frac{10813}{27095040}\pi^4 G^4 m_1 m_2^5 |\boldsymbol{q}|^9 (\sigma^2 - 1)(25 + 481\sigma^2 - 2925\sigma^4 + 3315\sigma^6) I^{(3)}_{\text{fan}}\,.
\end{aligned} \tag{4.150}$$

Similarly, the amplitudes with double trace insertions evaluate to,

$$\begin{aligned}
\mathcal{M}_{(\mathrm{E}^2)^2} &= -i\frac{983}{4515840}\pi^4 G^4 m_1 m_2^5 |\boldsymbol{q}|^9 (1231 - 7304\sigma^2 + 18590\sigma^4 - 22880\sigma^6 + 12155\sigma^8) I^{(3)}_{\text{fan}}\,, \\
\mathcal{M}_{(\mathrm{B}^2)^2} &= -i\frac{140569}{4515840}\pi^4 G^4 m_1 m_2^5 |\boldsymbol{q}|^9 (\sigma^2 - 1)^2 (1 + 10\sigma^2 + 85\sigma^4) I^{(3)}_{\text{fan}}\,, \\
\mathcal{M}_{(\mathrm{E}^2)(\mathrm{B}^2)} &= -i\frac{10813}{4515840}\pi^4 G^4 m_1 m_2^5 |\boldsymbol{q}|^9 (\sigma^2 - 1)(19 + 299\sigma^2 - 975\sigma^4 + 1105\sigma^6) I^{(3)}_{\text{fan}}\,, \\
\mathcal{M}_{(\mathrm{EB})^2} &= 0\,,
\end{aligned} \tag{4.151}$$

It is not difficult to check that these results satisfy the four-dimensional relations described in Section 4.2. In addition, they agree with the results obtained in the previous section for tidal operators with arbitrary numbers of Es and Bs and collected in the Appendix for a variety of operators up to E^8 and B^8.

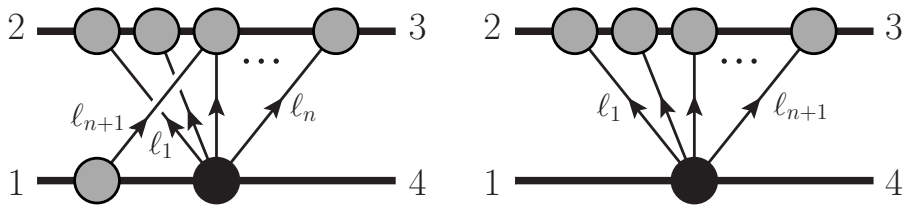

Figure 4.4: The generalized cuts that need to be evaluated at next to leading order for an R^n type tidal operator.

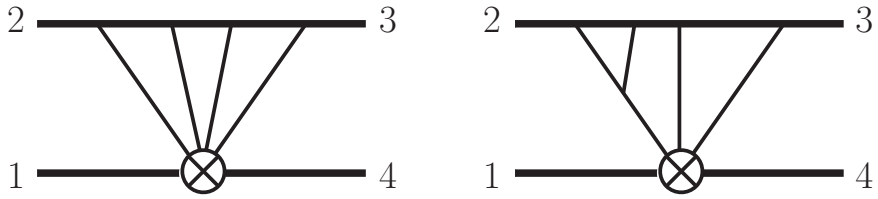

Figure 4.5: Sample diagrams for next-to-leading-order contributions for the R^3 tidal operators which are simple to evaluate.

An important aspect of the momentum-space approach is that it gives a systematic means for obtaining corrections higher order in Newton's constant for any operator insertion. For example Fig. 4.4 shows the generalized cuts that would need to be evaluated to obtain the next-to-leading order corrections from an C^3 tidal operator. In the first of these cuts the four-point amplitude can appear at any location on the top matter line. The mapping of the integrands resulting from these cuts onto a integral basis generates a number of diagrams. For example, in Fig. 4.5 we show a sample of the diagrams that that are quite easy to evaluate for an R^3 tidal operator, as we can again evaluate the integral using the real-space technique presented in the previous section. More complicated diagrams that involve

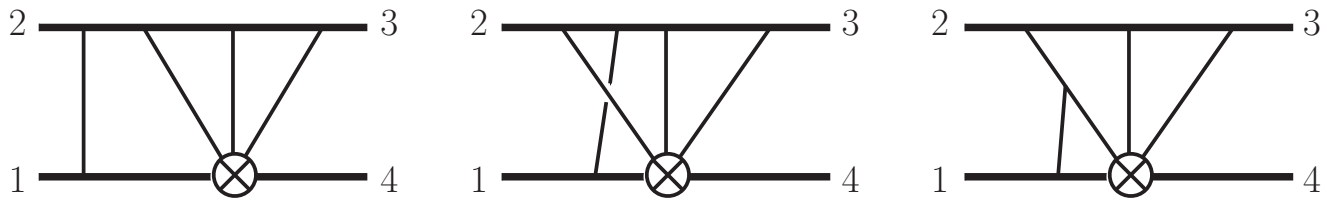

Figure 4.6: Sample diagrams next-to-leading order contributions for the R^3 tidal operators that involve iteration contributions or nontrivial integrals.

iteration contributions or non-trivial integrations are shown in Fig. 4.6. In these cases, the integrals do not factorize, but the momentum-space approach of evaluating cuts and reducing to a basis of master integrals will still be quite feasible. As noted in Refs. [15, 21] the probe limit simplifies the evaluation of the contributions. In any case, it is clear that amplitude methods can be applied beyond leading order to understand the systematics of higher-dimension operators. We leave this to future studies.

4.5 Effective field theory extensions of GR

The same methods apply just as well to any operator, not just the tidal ones. For example, we can consider the R^n operators arising from unknown short distance physics. Here we will not classify such operators, but pick illustrative examples. The effect of operators up to R^4 has already been discussed in some detail in Refs. [38–40]. In order to be concrete here we discuss an effective action of the form

$$S = \frac{1}{16\pi G}\int d^D x\sqrt{-g}\,(-R + c_K K_{\mu_1\ldots\rho_n} R^{\mu_1\nu_1\sigma_1\rho_1} R^{\mu_2\nu_2\sigma_2\rho_2}\cdots R^{\mu_n\nu_n\sigma_n\rho_n})\ , \tag{4.152}$$

where the first term is the usual Einstein-Hilbert action, and $K_{\mu_1\ldots\rho_n}$ merely gives the contraction between the Riemann tensors. Each independent contraction carries an independent Wilson coefficient c_K.

We construct the integrands for pure R^n modifications of gravity in a similar manner as for those of the tidal operators. The leading contribution to the potential due to R^n operators is captured by the cuts in Fig. 4.7. The diagrams in general are a product of two fan diagrams, where all graviton legs, as well as the matter lines between the three point vertices, are on shell, the exception being the case where $(n-1)$ on-shell gravitons attach to one of the matter lines, while one graviton which we take to be off shell attaches to the other matter line. In this case, it is convenient to include the matter line to which the single

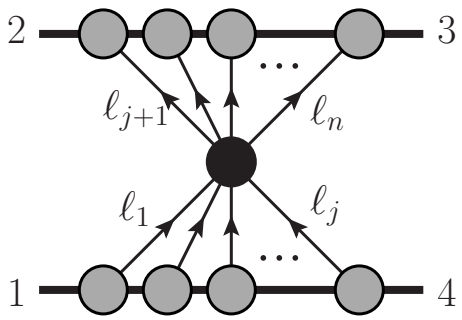

Figure 4.7: Cut for a general R^n type operator. In the case $j = 1$, it is convenient to take the single graviton attaching to the bottom matter line as off shell and part of a tree amplitude including the lower massive scalar line. All other gravitons and exposed matter lines are taken on shell. The direction of graviton momentum flow is indicated by the arrows.

graviton propagator is attached as part of a single tree amplitude.

To evaluate the cuts in Fig. 4.7 we use the replacement derived above (see Eq. (4.62)). This simplifies the form of the Riemann tensor:

$$R^{\mu\nu\rho\sigma}(\ell_i)\big|_{\varepsilon_{\mu\nu}(\ell_i)\to T_{\mu\nu}(p_a)} = -\frac{1}{2}\left(\ell_i^\mu \ell_i^\rho \left(p_a^\nu p_a^\sigma - \frac{1}{2}\eta^{\nu\sigma} m_a^2\right) - (\sigma \leftrightarrow \rho)\right) + ((\mu,\rho) \leftrightarrow (\nu,\sigma)) + \mathcal{O}(q^3)\,, \tag{4.153}$$

where p_a and m_a are the momentum and mass of the matter line the graviton attaches to. When contracted in sequence with other gravitons attaching to the same matter line, products involving the matter momenta in the above expression must reduce to $p_a \cdot p_a = m_a^2$, or the q scaling will become sub-leading, as shown in the previous section.

The cut corresponding to Figure 4.7 is simply a product of two fans,

$$\mathcal{C}_{R^n} = K_{\mu_1 \ldots \rho_n} \mathcal{O}^{\mu_1 \cdots \rho_j}(\ell_1, ..., \ell_j; p_1) \mathcal{O}^{\mu_{j+1} \cdots \rho_n}(\ell_{j+1}, ..., \ell_n; p_2)\,, \tag{4.154}$$

where, for instance,

$$\mathcal{O}^{\mu_1 \cdots \rho_j}(\ell_1, ..., \ell_j; p_1) = R_1^{\mu_1\nu_1\sigma_1\rho_1} \cdots R_j^{\mu_j\nu_j\sigma_j\rho_j}\big|_{\varepsilon_{\mu\nu}(\ell_i)\to T_{\mu\nu}(p_1)}\,. \tag{4.155}$$

As in previous sections, the integrands obtained after restoring the cut propagators are also

well suited for applying position-space techniques. In this case, we must introduce a fictitious momentum transfer $\boldsymbol{q}'$ such that the integrand decouples in two parts, corresponding to the two terms in Eq. (4.154) decouple, and the corresponding propagators attached to one matter line or the other. The energy integrations can be carried out as in the previous sections with the result

$$\mathcal{M}_{R^n}(\boldsymbol{p},\boldsymbol{q}) = K_{\mu_1\ldots\rho_n}\int d^{D-1}\boldsymbol{q}'\,\delta(\boldsymbol{q}+\boldsymbol{q}')\int\left(\prod_{a=1}^{j}\frac{d^{D-1}\boldsymbol{\ell}_a}{(2\pi)^{D-1}}\right)\frac{\delta(\sum_{a=1}^{j}\boldsymbol{\ell}_a+\boldsymbol{q}')\mathcal{O}^{\mu_1\ldots\rho_j}(\boldsymbol{\ell}_1,...,\boldsymbol{\ell}_j;p_1)}{\boldsymbol{\ell}_1^2\cdots\boldsymbol{\ell}_j^2}$$
$$\times\int\left(\prod_{a=j+1}^{n}\frac{d^{D-1}\boldsymbol{\ell}_a}{(2\pi)^{D-1}}\right)\frac{\delta(\sum_{a=j+1}^{n}\boldsymbol{\ell}_a-\boldsymbol{q})\mathcal{O}^{\mu_{j+1}\ldots\rho_n}(\boldsymbol{\ell}_{j+1},...,\boldsymbol{\ell}_n;p_2)}{\boldsymbol{\ell}_{j+1}^2\cdots\boldsymbol{\ell}_n^2}\,. \tag{4.156}$$

Writing

$$\delta(\boldsymbol{q}+\boldsymbol{q}') = \int\frac{d^{D-1}\boldsymbol{x}}{(2\pi)^{D-1}}e^{i(\boldsymbol{q}+\boldsymbol{q}')\cdot\boldsymbol{x}} \tag{4.157}$$

and taking the Fourier transform of the amplitude we find

$$\begin{aligned}\mathcal{M}_{R^n}(\boldsymbol{p},\boldsymbol{r}) &= \int\frac{d^{D-1}\boldsymbol{q}}{(2\pi)^{D-1}}e^{-i\boldsymbol{q}\cdot\boldsymbol{r}}\mathcal{M}_{R^n}(\boldsymbol{p},\boldsymbol{q})\\ &= K_{\mu_1\ldots\rho_n}\int d^{D-1}\boldsymbol{x}\int\left(\prod_{a=1}^{j}\frac{d^{D-1}\boldsymbol{\ell}_a}{(2\pi)^{D-1}}\frac{e^{-i\boldsymbol{\ell}_a\cdot\boldsymbol{x}}}{\boldsymbol{\ell}_a^2}\right)\mathcal{O}^{\mu_1\ldots\rho_j}(\boldsymbol{\ell}_1,...,\boldsymbol{\ell}_j;p_1)\\ &\quad\times\int\left(\prod_{a=j+1}^{n}\frac{d^{D-1}\boldsymbol{\ell}_a}{(2\pi)^{D-1}}\frac{e^{-i\boldsymbol{\ell}_a\cdot(\boldsymbol{r}-\boldsymbol{x})}}{\boldsymbol{\ell}_a^2}\right)\mathcal{O}^{\mu_{j+1}\ldots\rho_n}(\boldsymbol{\ell}_{j+1},...,\boldsymbol{\ell}_n;p_2)\\ &= K_{\mu_1\ldots\rho_n}\int d^{D-1}\boldsymbol{x}\,\mathcal{O}^{\mu_1\ldots\rho_j}(\boldsymbol{x};p_1)\mathcal{O}^{\mu_{j+1}\ldots\rho_n}(\boldsymbol{r}-\boldsymbol{x};p_2)\,.\end{aligned} \tag{4.158}$$

The product in momentum space has become a convolution in position space over $\boldsymbol{x}$, which can be viewed as the position in the bulk, i.e. away from the massive particle trajectories, at which the R^n operator is inserted. Note however that this formula does not have a natural interpretation in position space, given that the energy integrals in each factor were performed by going to the rest frame of different particles. In practice, as in previous

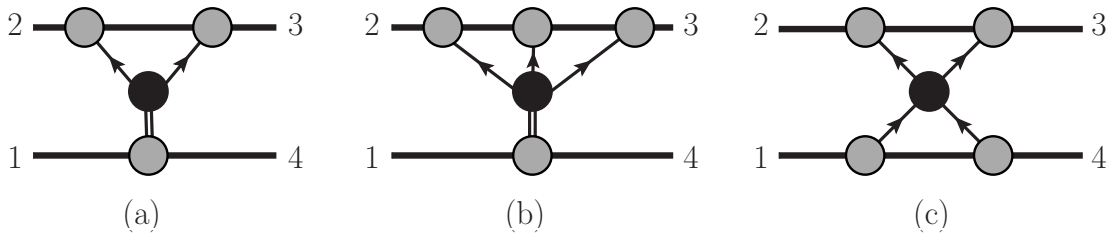

Figure 4.8: The corrections from (a) R^3 and (b,c) R^4 operators that appear in EFT extensions of GR. The double-line notation indicates that we have not used on-shell conditions on that line.

sections, this formula can be used by transforming one last time to momentum space, so that the convolution is trivialized and each factor can be written in isotropic coordinates.

The inclusion of derivatives, $\nabla^{2m}R^n$, or of spin on the matter lines poses no obstruction to applying this method. In the former case one must organize the additional powers of loop momentum in the integrand into either factor in analogy with Eq. (4.154). The factorization argument carries over and the additional loop momenta become derivatives in position space acting on either factor of Eq. (4.158). For the case of spin, the only difference is that the Fourier transforms in Eq. (4.158) become non-Abelian Fourier transforms defined in Eq. (4.125).

As simple examples, consider the cases of $\mathcal{O}_{R^3} = R^{\mu_1\nu_1}{}_{\mu_2\nu_2}R^{\mu_2\nu_2}{}_{\mu_3\nu_3}R^{\mu_3\nu_3}{}_{\mu_1\nu_1}$ and $\mathcal{O}_{(R^2)^2} = (R^{\mu_1\nu_1}{}_{\mu_2\nu_2}R^{\mu_2\nu_2}{}_{\mu_1\nu_1})^2$. The contributing generalized unitarity cut for the R^3 operator are shown in Fig. 4.8(a) while the two potentially contributing cuts for the the R^4 operator are shown in Fig. 4.8(b,c). In the diagrams the double-line notation indicates that we have not used on-shell conditions on that line, but consider the two connected blobs as part of a single tree amplitude.[6]

After carrying out the integration, the R^3 and R^4 amplitudes are

$$\begin{aligned}\mathcal{M}_{R^3} &= -6c_{R^3}G^2\pi^2 m_1^2 m_2^2(m_1+m_2)|\boldsymbol{q}|^3(\sigma^2-1)\,,\\ \mathcal{M}_{(R^2)^2} &= -\frac{2^7}{315}c_{(R^2)^2}G^3\pi m_1^2 m_2^2(m_1^2+m_2^2)\frac{(\boldsymbol{q}^2)^{3-2\epsilon}}{2\epsilon}(3\sigma^2-1)\,,\end{aligned} \tag{4.159}$$

[6]Whether on-shell conditions are used on the intermediate leg corresponds to shifting the coefficient of $\phi R^n\phi$ operators.

where we took the operators to have coefficient c_R^3 and $c_{(R^2)^2}$ respectively. Taking the Fourier transform (4.12) to position space gives the potentials

$$V_{R^3} = \frac{18}{E_1 E_2} c_{R^3} G^2 m_1^2 m_2^2 (m_1 + m_2)(\sigma^2 - 1) \frac{1}{r^6} ,$$
$$V_{(R^2)^2} = \frac{2^8}{E_1 E_2} c_{(R^2)^2} G^3 m_1^2 m_2^2 (m_1^2 + m_2^2)(3\sigma^2 - 1) \frac{1}{r^9} . \tag{4.160}$$

The $\mathcal{O}_{R^3}$ amplitude and potential was obtained previously in Refs. [39, 40] and we find agreement. In Ref. [39] the authors also evaluate the effect of an additional R^3 operator,

$$G_3 = \mathcal{O}_{R^3} - R^{\mu\nu\alpha}{}_{\beta} R^{\beta\gamma}{}_{\nu\sigma} R^{\sigma}{}_{\mu\gamma\alpha} ; \tag{4.161}$$

this is related to tidal operators via a field redefinition up to operators that vanish in four dimensions. This can be seen by evaluating its four-dimensional four-point amplitude, which feeds into the two-graviton cut, using spinor-helicity methods [39]:

$$\mathcal{M}_{G^3}(\phi(p_1), h^{++}(k_2), h^{++}(k_3), \phi(p_4)) \propto [23]^4 (-q^2 + 2m_1^2) . \tag{4.162}$$

Since this is a local contribution, it is already captured by tidal operators of the form E^2, B^2. Interestingly, though, if this operator were present with a sufficiently large coefficient, it would produce a result equivalent to the leading tidal Love numbers, even if these are set identically to zero for black holes in Einstein gravity [32].

The leading PN contribution from the R^4 operator ($\mathcal{O}_{(R^2)^2}$) was calculated in Ref. [38], with which we find agreement. We can also easily determine that the other operators considered in Ref. [38] give no contribution to the leading conservative potential. The contribution from $\mathcal{O}_{(R^2)(R\tilde{R})} = (R^{\mu_1\nu_1}{}_{\alpha\beta} \epsilon^{\alpha\beta}{}_{\mu_2\nu_2} R^{\mu_2\nu_2}{}_{\mu_1\nu_1})(R^{\mu_3\nu_3}{}_{\mu_4\nu_4} R^{\mu_4\nu_4}{}_{\mu_3\nu_3})$ is zero simply because it is parity odd. The operator $\mathcal{O}_{(R\tilde{R})^2} = (R^{\mu_1\nu_1}{}_{\alpha\beta} \epsilon^{\alpha\beta}{}_{\mu_2\nu_2} R^{\mu_2\nu_2}{}_{\mu_1\nu_1})^2$, while being parity even, contributes zero at leading order, in analogy to the tidal operator $\mathcal{O}_{(EB)^2}$. In both cases, the

factorization of the integrand in real space forces the separate parity-odd factors to evaluate to zero, as discussed in Section 4.4.1

Here we refrain from evaluating the amplitudes for the R^5 and higher operators. However, in these cases, there is an additional link between the R^n extensions of Einstein gravity and the tidal operators. After carrying out the soft expansion of the integrand for the R^n operators, one encounters ultraviolet divergences that renormalize tidal operators [5]. For example, in principle the R^5 operator, which produces a diagram with three gravitons attached to one matter line and two attached to the other, could produce a UV subdivergence and thereby renormalize E^2 or B^2 tidal operators (with additional derivatives). It would be an interesting problem to systematically study this interplay for infinite sequences of R^n operators.

4.6 Conclusions

In this paper we evaluated the leading-PM order contributions to the two-body Hamiltonian from infinite classes of tidal operators using momentum space and position space scattering amplitude and effective field theory methods. The same principles yield leading-PM order Hamiltonian terms from tidal deformations probed by a spinning particle and also from effective field theory modifications of general relativity. Our results offer a new perspective on the general structure of linear and nonlinear tidal effects in the relativistic two-body problem while also being of potential phenomenological interest.

Our analysis of E^2 and B^2 tidal operators arbitrary number of derivatives is similar to that of Ref. [30], except that we use a basis of operators which aligns with the more standard worldline tidal operators [5, 28]. Their Wilson coefficients are the same (up to an overall normalization that we provide) with the worldline electric and magnetic tidal coefficients which in turn are proportional to the corresponding multipole Love numbers. By directly evaluating all relevant integrals we obtain explicit expressions for the two-body

Hamiltonian and the amplitude's eikonal phase, from which both scattering and closed-orbit observables can be found straightforwardly. We illustrated the inclusion of spin by working out the leading-order tidal contributions from E^2-type operators with arbitrary number of derivatives for one object interacting with the spin of the other.

For tidal operators with arbitrary numbers of electric or magnetic components of the Weyl tensor, the integrand for the leading-order contributions are not difficult to construct because their building blocks are tree-level leading order on-shell matrix elements of the point-particle energy-momentum tensor and of the tidal operator. The simple loop-momentum dependence and the permutation symmetry of the three-point amplitude factors makes the integrals simple to evaluate. Indeed, Fourier-transforming all graviton propagators decouples all integrals from each other, making it straightforward to write down explicit results for infinite classes of tidal operators. We have verified that the results obtained this way thought direct momentum space integration. While position space methods make leading-order calculations straightforward, momentum-space methods can be applied systematically, to arbitrary PM order.

An interesting feature of gravitational tidal operators, which we exploited in their description, is their close similarity with gauge theory operators describing the interaction of extended charge distributions with electromagnetic fields. This formal connection extends to dynamical level double-copy relations. For leading-order contributions this is a straightforward consequence of the factorization of the linearized Riemann tensor into two gauge-theory field strengths and of the factorization of the energy-momentum tensor into two gauge theory currents. Such double-copy factorizations also hold for the energy-momentum tensor [23]. It would be very interesting to investigate double-copy relations beyond the leading PM order.

In summary, in this paper we took some steps towards systematically evaluating contributions to the two-body Hamiltonian from infinite families of tidal operators. The leading order in G results are remarkably simple, suggesting that much more progress will be forthcoming.

4.A Appendix: Summary of Explicit Results

In this appendix we collect explicit results for scattering amplitudes with a tidal operator insertion. Using Eq. (4.5), this immediately gives us the potential. Here we consider the amplitudes with operator insertions of the type $E^{n-2m}B^{2m}$. We express the amplitude in terms of the variable $\sigma = p_1 \cdot p_2/m_1 m_2$. The general formulae for $(E^2)^n$, $(B^2)^n$ and $(E^3)^n$ are given from Eq. (4.141) to Eq. (4.143) with the coefficients in Eq. (4.138). Here we give explicit results corresponding up to 7 loops in the amplitudes approach. As noted in the text, the amplitudes with an odd B-field insertions vanish by parity so we do not include those. We also do not explicitly list cases where a trace contains an odd number of Bs since these also vanish.

To list the amplitudes we scale out the powers of $|\boldsymbol{q}|$ from the scattering amplitudes, following Eq. (4.9),

$$\mathcal{M}_{\mathrm{X}^{2n}} = |\boldsymbol{q}|^{3(2n-1)}\overline{\mathcal{M}}_{\mathrm{X}^{2n}} = |\boldsymbol{q}|^{3(2n-1)}\mathrm{C}_{\mathrm{X}^{2n}}\,, \tag{4.163}$$

for a tidal operator which we build from a total of $2n$ Es or Bs, independent of the trace structure. For operators where total number of Es and B is odd the rescaling is bit difference because of the appearance of a divergence

$$\mathcal{M}_{\mathrm{X}^{2n+1}} = |\boldsymbol{q}|^{6n-4n\epsilon}\overline{\mathcal{M}}_{\mathrm{X}^{2\mathrm{n}}} = -\frac{1}{2n}\frac{1}{\epsilon}|\boldsymbol{q}|^{6n-4n\epsilon}\,\mathrm{C}_{\mathrm{X}^{2\mathrm{n}+1}}\,, \tag{4.164}$$

The long-range classical contribution comes from the $\log \boldsymbol{q}^2$ term that arises from expanding in ϵ.

As discussed in Section 4.2, the potential is given in the two-body Hamiltonian is given by a Fourier transform (4.5) and the eikonal phase is also given by Eq. (4.6). Carrying out

the Fourier transform we have from Eq. (4.10) and Eq. (4.11)

$$V_{\mathrm{X}^{2n}} = -\frac{1}{4E_1E_2}\frac{8^{2n-1}\,\Gamma(3n)}{\pi^{3/2}\Gamma(\frac{3}{2}-3n)}\frac{\mathrm{C}_{\mathrm{X}^{2n}}}{|\boldsymbol{r}|^{6n}}\,, \tag{4.165}$$

$$\delta_{\mathrm{X}^{2n}} = \frac{1}{4m_1m_2\sqrt{\sigma^2-1}}\frac{8^{2n-1}\,\Gamma(3n-\frac{1}{2})}{\pi\Gamma(\frac{3}{2}-3n)}\frac{\mathrm{C}_{\mathrm{X}^{2n}}}{|\boldsymbol{b}|^{6n-1}}\,, \tag{4.166}$$

where we only keep the finite term in ϵ. Similarly, for the odd powers

$$V_{\mathrm{X}^{2n+1}} = \frac{1}{4E_1E_2}\frac{(-1)^n\,\Gamma(6n+2)}{2\pi}\frac{\mathrm{C}_{\mathrm{X}^{2n+1}}}{|\boldsymbol{r}|^{6n+3}}\,, \tag{4.167}$$

$$\delta_{\mathrm{X}^{2n+1}} = \frac{1}{4m_1m_2\sqrt{\sigma^2-1}}\frac{(-1)^{n-1}8^{2n}\,\Gamma(3n+1)^2}{\pi}\frac{\mathrm{C}_{\mathrm{X}^{2n+1}}}{|\boldsymbol{b}|^{6n+2}}\,. \tag{4.168}$$

For X^2 we have,

$$\begin{aligned}\mathrm{C}_{(\mathrm{E}^2)} &= \frac{5}{2^3}G^2m_1m_2^3\pi^2\Big(\frac{11}{5}-6\sigma^2+7\sigma^4\Big)\,,\\ \mathrm{C}_{(\mathrm{B}^2)} &= \frac{5}{2^3}G^2m_1m_2^3\pi^2(\sigma^2-1)\Big(1+7\sigma^2\Big)\,,\end{aligned} \tag{4.169}$$

where the parenthesis on the operator denote the matrix trace, as defined in Eq. (4.49)

For X^3:

$$\begin{aligned}\mathrm{C}_{(\mathrm{E}^3)} &= -\frac{2^2\,3^2}{11!!}G^3m_1m_2^4\pi\Big(\frac{7}{4}-9\sigma^2+10\sigma^4\Big)\,,\\ \mathrm{C}_{(\mathrm{EB}^2)} &= -\frac{2^2\,3}{11!!}G^3m_1m_2^4\pi(\sigma^2-1)\Big(1+10\sigma^2\Big)\,.\end{aligned} \tag{4.170}$$

For X^4:

$$
\begin{aligned}
\mathrm{C}_{(\mathrm{E}^4)} &= -\frac{11\cdot 13}{2^{12}\,(7!!)^2} G^4 m_1 m_2^5 \pi^2 \Big(\frac{1231}{143} - \frac{664}{13}\sigma^2 + 130\sigma^4 - 160\sigma^6 + 85\sigma^8\Big)\,, \\
\mathrm{C}_{(\mathrm{B}^4)} &= -\frac{11\cdot 13}{2^{12}\,(7!!)^2} G^4 m_1 m_2^5 \pi^2 (\sigma^2-1)^2 \Big(1 + 10\sigma^2 + 85\sigma^4\Big)\,, \\
\mathrm{C}_{(\mathrm{EEBB})} &= -\frac{11\cdot 13}{2^{12}\,(7!!)^2} G^4 m_1 m_2^5 \pi^2 (\sigma^2-1) \Big(\frac{41}{39} + \frac{53}{3}\sigma^2 - 75\sigma^4 + 85\sigma^6\Big)\,, \\
\mathrm{C}_{(\mathrm{EBEB})} &= \frac{11\cdot 13}{2^{12}\,(7!!)^2} G^4 m_1 m_2^5 \pi^2 (\sigma^2-1) \Big(\frac{25}{39} + \frac{37}{3}\sigma^2 - 75\sigma^4 + 85\sigma^6\Big)\,, \\
\mathrm{C}_{(\mathrm{E}^2)^2} &= 2\mathrm{C}_{(\mathrm{E}^4)}\,, \\
\mathrm{C}_{(\mathrm{B}^2)^2} &= 2\mathrm{C}_{(\mathrm{B}^4)}\,, \\
\mathrm{C}_{(\mathrm{E}^2)(\mathrm{B}^2)} &= -\frac{11\cdot 13}{2^{11}\,(7!!)^2} G^4 m_1 m_2^5 \pi^2 (\sigma^2-1) \Big(\frac{19}{13} + 23\sigma^2 - 75\sigma^4 + 85\sigma^6\Big)\,.
\end{aligned}
\tag{4.171}
$$

For X^5:

$$
\begin{aligned}
\mathrm{C}_{(\mathrm{E}^5)} &= \frac{1}{2^6\,(19!!)} G^5 m_1 m_2^6 \pi \Big(1094 - 8535\sigma^2 + 24608\sigma^4 - 32832\sigma^6 + 17280\sigma^8\Big)\,, \\
\mathrm{C}_{(\mathrm{E}^3\mathrm{B}^2)} &= \frac{1}{2^6\,5\,(19!!)} G^5 m_1 m_2^6 \pi (\sigma^2-1) \Big(499 + 10144\sigma^2 - 46656\sigma^4 + 51840\sigma^6\Big)\,, \\
\mathrm{C}_{(\mathrm{EBEBE})} &= -\frac{1}{2^5\,5\,(19!!)} G^5 m_1 m_2^6 \pi (\sigma^2-1) \Big(61 + 1336\sigma^2 - 7776\sigma^4 + 8640\sigma^6\Big)\,, \\
\mathrm{C}_{(\mathrm{EB}^4)} &= \frac{3^2}{2^2\,5\,(19!!)} G^5 m_1 m_2^6 \pi (\sigma^2-1)^2 \Big(1 + 12\sigma^2 + 120\sigma^4\Big)\,, \\
\mathrm{C}_{(\mathrm{E}^3)(\mathrm{B}^2)} &= \frac{3}{2^4\,5\,(19!!)} G^5 m_1 m_2^6 \pi (\sigma^2-1) \Big(61 + 1336\sigma^2 - 7776\sigma^4 + 8640\sigma^6\Big)\,, \\
\mathrm{C}_{(\mathrm{E}^2)(\mathrm{EB}^2)} &= \frac{3}{2^5\,5\,(19!!)} G^5 m_1 m_2^6 \pi (\sigma^2-1) \Big(85 + 1600\sigma^2 - 5184\sigma^4 + 5760\sigma^6\Big)\,, \\
\mathrm{C}_{(\mathrm{B}^2)(\mathrm{EB}^2)} &= 2\mathrm{C}_{\mathrm{EB}^4}\,.
\end{aligned}
\tag{4.172}
$$

For X^6, X^7, X^8:

$$
\begin{aligned}
\mathrm{C}_{(\mathrm{E}^6)} &= \frac{17\cdot 19\cdot 3^5}{2^{21}\,5^2\,(13!!)^2} G^6 m_1 m_2^7 \pi^2 \Big(\frac{5558245}{26163} - \frac{328930}{171}\sigma^2 + \frac{609305}{81}\sigma^4 - \frac{144980}{9}\sigma^6 \\
&\qquad + \frac{183425}{9}\sigma^8 - 14950\sigma^{10} + 5175\sigma^{12} \Big) , \\
\mathrm{C}_{(\mathrm{B}^6)} &= \frac{17\cdot 19\cdot 3^5}{2^{21}\,5^2\,(13!!)^2} G^6 m_1 m_2^7 \pi^2 (\sigma^2-1)^3 \Big(5 + 69\sigma^2 + 575\sigma^4 + 5175\sigma^6 \Big) , \\
\mathrm{C}_{(\mathrm{E}^7)} &= -\frac{3}{2^{12}\,(31!!)} G^7 m_1 m_2^8 \pi \Big(1496063 - 15991430\sigma^2 + 71940660\sigma^4 \\
&\qquad - 177188000\sigma^6 + 253373120\sigma^8 - 200648448\sigma^{10} + 69189120\sigma^{12} \Big) , \qquad (4.173) \\
\mathrm{C}_{(\mathrm{E}^8)} &= -\frac{23\cdot 29\cdot 3^7\cdot 5}{2^{31}\,7^2\,(19!!)^2} G^8 m_1 m_2^9 \pi^2 \Big(\frac{57426585223}{7293645} - \frac{10076129056}{105705}\sigma^2 + \frac{32319394660}{63423}\sigma^4 \\
&\qquad - \frac{1227512720}{783}\sigma^6 + \frac{82520830}{27}\sigma^8 - 3916416\sigma^{10} + 3294060\sigma^{12} \\
&\qquad - 1718640\sigma^{14} + 441595\sigma^{16} \Big) , \\
\mathrm{C}_{(\mathrm{B}^8)} &= -\frac{23\cdot 29\cdot 3^7\cdot 5}{2^{31}\,7^2\,(19!!)^2} G^8 m_1 m_2^9 \pi^2 (\sigma^2-1)^4 \Big(35 + 620\sigma^2 + 6138\sigma^4 + 47740\sigma^6 + 441595\sigma^8 \Big) .
\end{aligned}
$$

As noted in Section 4.4, in the high-energy limit, where σ is large, simple relations are visible between amplitudes with E^2 and B^2 operators inserted [28, 29].

Bibliography

[1] B. P. Abbott *et al.* [LIGO Scientific and Virgo Collaborations], "Observation of gravitational waves from a binary black hole merger," Phys. Rev. Lett. **116**, no. 6, 061102 (2016) [arXiv:1602.03837 [gr-qc]];

B. P. Abbott *et al.* [LIGO Scientific and Virgo Collaborations], "GW170817: Observation of gravitational waves from a binary neutron star inspiral," Phys. Rev. Lett. **119**, no. 16, 161101 (2017) [arXiv:1710.05832 [gr-qc]].

[2] M. Punturo *et al.,* "The Einstein Telescope: A third-generation gravitational wave observatory," Class. Quant. Grav. 27 (2010) 194002;

S. Dwyer, D. Sigg, S. W. Ballmer, L. Barsotti, N. Mavalvala and M. Evans, "Gravitational wave detector with cosmological reach," Phys. Rev. D **91**, no.8, 082001 (2015) [arXiv:1410.0612 [astro-ph.IM]];

P. Amaro-Seoane *et al.* [LISA], "Laser Interferometer Space Antenna," [arXiv:1702.00786 [astro-ph.IM]].

[3] A. Buonanno and T. Damour, "Effective one-body approach to general relativistic two-body dynamics," Phys. Rev. D **59**, 084006 (1999) [gr-qc/9811091];

A. Buonanno and T. Damour, "Transition from inspiral to plunge in binary black hole coalescences," Phys. Rev. D **62**, 064015 (2000) [gr-qc/0001013].

[4] J. Droste. "The field of n moving centres in Einstein's theory of gravitation," Proc. Acad. Sci. Amst. 19:447–455 (1916);

H. A. Lorentz and J. Droste, "De beweging van een stelsel lichamen onder de theorie van Einstein I,II" Koninklijke Akademie Van Wetenschappen te Amsterdam 26 392, 649 (1917). English translation in "Lorentz Collected papers," P. Zeeman and A. D. Fokker editors, Vol 5, 330 (1934-1939), The Hague: Nijhof;

A. Einstein, L. Infeld and B. Hoffmann, "The Gravitational equations and the problem of motion," Annals Math. **39**, 65 (1938);

T. Ohta, H. Okamura, T. Kimura and K. Hiida, "Physically acceptable solution of einstein's equation for many-body system," Prog. Theor. Phys. **50**, 492 (1973);

P. Jaranowski and G. Schäfer, "Third post-Newtonian higher order ADM Hamilton dynamics for two-body point mass systems," Phys. Rev. D **57**, 7274 (1998) Erratum: [Phys. Rev. D **63**, 029902 (2000)] [gr-qc/9712075];

T. Damour, P. Jaranowski and G. Schäfer, "Dynamical invariants for general relativistic two-body systems at the third post-Newtonian approximation," Phys. Rev. D **62**, 044024 (2000) [gr-qc/9912092];

L. Blanchet and G. Faye, "Equations of motion of point particle binaries at the third post-Newtonian order," Phys. Lett. A **271**, 58 (2000) [gr-qc/0004009];

T. Damour, P. Jaranowski and G. Schäfer, "Dimensional regularization of the gravitational interaction of point masses," Phys. Lett. B **513**, 147 (2001) [gr-qc/0105038];

T. Damour, P. Jaranowski and G. Schäfer, "Nonlocal-in-time action for the fourth post-Newtonian conservative dynamics of two-body systems," Phys. Rev. D **89**, no. 6, 064058 (2014) [arXiv:1401.4548 [gr-qc]];

P. Jaranowski and G. Schäfer, "Derivation of local-in-time fourth post-Newtonian ADM Hamiltonian for spinless compact binaries," Phys. Rev. D **92**, no. 12, 124043 (2015) [arXiv:1508.01016 [gr-qc]];

L. Bernard, L. Blanchet, A. Bohé, G. Faye and S. Marsat, "Fokker action of nonspinning compact binaries at the fourth post-Newtonian approximation," Phys. Rev. D **93**, no.8, 084037 (2016) [arXiv:1512.02876 [gr-qc]];

L. Bernard, L. Blanchet, A. Bohé, G. Faye and S. Marsat, "Energy and periastron advance of compact binaries on circular orbits at the fourth post-Newtonian order," Phys. Rev. D **95**, no.4, 044026 (2017) [arXiv:1610.07934 [gr-qc]];
D. Bini and T. Damour, "Gravitational scattering of two black holes at the fourth post-Newtonian approximation," Phys. Rev. D **96**, no.6, 064021 (2017) [arXiv:1706.06877 [gr-qc]];
L. Bernard, L. Blanchet, A. Bohé, G. Faye and S. Marsat, "Dimensional regularization of the IR divergences in the Fokker action of point-particle binaries at the fourth post-Newtonian order," Phys. Rev. D **96**, no.10, 104043 (2017) [arXiv:1706.08480 [gr-qc]];
T. Marchand, L. Bernard, L. Blanchet and G. Faye, "Ambiguity-Free Completion of the Equations of Motion of Compact Binary Systems at the Fourth Post-Newtonian Order," Phys. Rev. D **97**, no.4, 044023 (2018) [arXiv:1707.09289 [gr-qc]];
L. Bernard, L. Blanchet, G. Faye and T. Marchand, "Center-of-Mass Equations of Motion and Conserved Integrals of Compact Binary Systems at the Fourth Post-Newtonian Order," Phys. Rev. D **97**, no.4, 044037 (2018) [arXiv:1711.00283 [gr-qc]].

[5] W. D. Goldberger and I. Z. Rothstein, "An effective field theory of gravity for extended objects," Phys. Rev. D **73**, 104029 (2006) [hep-th/0409156].

[6] B. Kol and M. Smolkin, "Classical effective field theory and caged black holes," Phys. Rev. D **77**, 064033 (2008) [arXiv:0712.2822 [hep-th]];
B. Kol and M. Smolkin, "Non-Relativistic gravitation: from Newton to Einstein and back," Class. Quant. Grav. **25**, 145011 (2008) [arXiv:0712.4116 [hep-th]];
J. B. Gilmore and A. Ross, "Effective field theory calculation of second post-Newtonian binary dynamics," Phys. Rev. D **78**, 124021 (2008) [arXiv:0810.1328 [gr-qc]];
S. Foffa and R. Sturani, "Effective field theory calculation of conservative binary dynamics at third post-Newtonian order," Phys. Rev. D **84**, 044031 (2011) [arXiv:1104.1122 [gr-qc]];

S. Foffa, P. Mastrolia, R. Sturani and C. Sturm, "Effective field theory approach to the gravitational two-body dynamics, at fourth post-Newtonian order and quintic in the Newton co nstant," Phys. Rev. D **95**, no. 10, 104009 (2017) [arXiv:1612.00482 [gr-qc]];
R. A. Porto and I. Z. Rothstein, "Apparent ambiguities in the post-Newtonian expansion for binary systems," Phys. Rev. D **96**, no. 2, 024062 (2017) [arXiv:1703.06433 [gr-qc]];
S. Foffa, P. Mastrolia, R. Sturani, C. Sturm and W. J. Torres Bobadilla, "Static two-body potential at fifth post-Newtonian order," Phys. Rev. Lett. **122**, no. 24, 241605 (2019) [arXiv:1902.10571 [gr-qc]];
J. Blümlein, A. Maier and P. Marquard, "Five-Loop static contribution to the gravitational interaction potential of two point masses," Phys. Lett. B **800**, 135100 (2020) [arXiv:1902.11180 [gr-qc]];
S. Foffa and R. Sturani, "Conservative dynamics of binary systems to fourth Post-Newtonian order in the EFT approach I: Regularized Lagrangian," Phys. Rev. D **100**, no. 2, 024047 (2019) [arXiv:1903.05113 [gr-qc]];
S. Foffa, R. A. Porto, I. Rothstein and R. Sturani, "Conservative dynamics of binary systems to fourth Post-Newtonian order in the EFT approach II: Renormalized Lagrangian," Phys. Rev. D **100**, no. 2, 024048 (2019) [arXiv:1903.05118 [gr-qc]];
J. Blümlein, A. Maier and P. Marquard, "Five-Loop Static Contribution to the Gravitational Interaction Potential of Two Point Masses," Phys. Lett. B **800**, 135100 (2020) [arXiv:1902.11180 [gr-qc]];
J. Blümlein, A. Maier, P. Marquard and G. Schäfer, "Fourth post-Newtonian Hamiltonian dynamics of two-body systems from an effective field theory approach," arXiv:2003.01692 [gr-qc].

[7] J. Blümlein, A. Maier, P. Marquard and G. Schäfer, "Testing binary dynamics in gravity at the sixth post-Newtonian level," arXiv:2003.07145 [gr-qc];

D. Bini, T. Damour and A. Geralico, "Binary dynamics at the fifth and fifth-and-a-half post-Newtonian orders," [arXiv:2003.11891 [gr-qc]];

D. Bini, T. Damour and A. Geralico, "Sixth post-Newtonian local-in-time dynamics of binary systems," [arXiv:2004.05407 [gr-qc]].

[8] Y. Mino, M. Sasaki and T. Tanaka, "Gravitational radiation reaction to a particle motion," Phys. Rev. D **55**, 3457 (1997) doi:10.1103/PhysRevD.55.3457 [gr-qc/9606018];

T. C. Quinn and R. M. Wald, "An Axiomatic approach to electromagnetic and gravitational radiation reaction of particles in curved space-time," Phys. Rev. D **56**, 3381 (1997) doi:10.1103/PhysRevD.56.3381 [gr-qc/9610053].

[9] F. Pretorius, "Evolution of binary black hole spacetimes," Phys. Rev. Lett. **95**, 121101 (2005) [gr-qc/0507014];

M. Campanelli, C. O. Lousto, P. Marronetti and Y. Zlochower, "Accurate evolutions of orbiting black-hole binaries without excision," Phys. Rev. Lett. **96**, 111101 (2006) [gr-qc/0511048];

J. G. Baker, J. Centrella, D. I. Choi, M. Koppitz and J. van Meter, "Gravitational wave extraction from an inspiraling configuration of merging black holes," Phys. Rev. Lett. **96**, 111102 (2006) [gr-qc/0511103].

[10] B. Bertotti, "On gravitational motion", Nuovo Cimento **4**:898-906 (1956) doi:10.1007/BF02746175;

R. P. Kerr, "The Lorentz-covariant approximation method in general relativity", I. Nuovo Cimento **13**:469-491 (1959);

B. Bertotti, J. F. Plebański, "Theory of gravitational perturbations in the fast motion approximation", Ann, Phys, **11**:169-200 (1960);

M. Portilla, "Momentum and angular momentum of two gravitating particles," J. Phys. A **12**, 1075 (1979);

K. Westpfahl and M. Goller, "Gravitational scattering of two relativistic particles in

postlinear approximation," Lett. Nuovo Cim. **26**, 573 (1979) M. Portilla, "Scattering of two gravitating particles: classical approach," J. Phys. A **13**, 3677 (1980) L. Bel, T. Damour, N. Deruelle, J. Ibanez and J. Martin, "Poincaré-invariant gravitational field and equations of motion of two pointlike objects: The postlinear approximation of general relativity," Gen. Rel. Grav. **13**, 963 (1981) doi:10.1007/BF00756073;
K. Westpfahl, "High-speed scattering of charged and uncharged particles in general relativity", Fortschr. Phys., **33**, 417 (1985);
T. Ledvinka, G. Schaefer and J. Bicak, "Relativistic closed-form Hamiltonian for many-body gravitating systems in the post-Minkowskian approximation," Phys. Rev. Lett. **100**, 251101 (2008) doi:10.1103/PhysRevLett.100.251101 [arXiv:0807.0214 [gr-qc]].

[11] C. Cheung, I. Z. Rothstein and M. P. Solon, "From scattering amplitudes to classical potentials in the post-Minkowskian expansion," Phys. Rev. Lett. **121**, no. 25, 251101 (2018) [arXiv:1808.02489 [hep-th]].

[12] Z. Bern, C. Cheung, R. Roiban, C. H. Shen, M. P. Solon and M. Zeng, "Scattering amplitudes and the conservative Hamiltonian for binary systems at third post-Minkowskian order," Phys. Rev. Lett. **122**, no. 20, 201603 (2019) doi:10.1103/PhysRevLett.122.201603 [arXiv:1901.04424 [hep-th]].

[13] Z. Bern, C. Cheung, R. Roiban, C. H. Shen, M. P. Solon and M. Zeng, "Black hole binary dynamics from the double copy and effective theory," JHEP **10** (2019), 206 [arXiv:1908.01493 [hep-th]].

[14] A. Antonelli, A. Buonanno, J. Steinhoff, M. van de Meent and J. Vines, "Energetics of two-body Hamiltonians in post-Minkowskian gravity," Phys. Rev. D **99**, no. 10, 104004 (2019) doi:10.1103/PhysRevD.99.104004 [arXiv:1901.07102 [gr-qc]].

[15] C. Cheung and M. P. Solon, "Classical gravitational scattering at $\mathcal{O}(G^3)$ from Feynman diagrams," arXiv:2003.08351 [hep-th].

[16] G. Kälin, Z. Liu and R. A. Porto, "Conservative Dynamics of Binary Systems to Third Post-Minkowskian Order from the Effective Field Theory Approach," [arXiv:2007.04977 [hep-th]].

[17] D. Bini, T. Damour and A. Geralico, "Novel approach to binary dynamics: application to the fifth post-Newtonian level," Phys. Rev. Lett. **123**, no. 23, 231104 (2019) [arXiv:1909.02375 [gr-qc]];

N. Siemonsen and J. Vines, "Test black holes, scattering amplitudes and perturbations of Kerr spacetime," arXiv:1909.07361 [gr-qc];

A. Antonelli, C. Kavanagh, M. Khalil, J. Steinhoff and J. Vines, "Gravitational spin-orbit coupling through third-subleading post-Newtonian order: from first-order self-force to arbitrary mass ratios," [arXiv:2003.11391 [gr-qc]].

[18] L. Blanchet, "Gravitational radiation from post-Newtonian sources and inspiralling compact binaries," Living Rev. Rel. **17**, 2 (2014) [arXiv:1310.1528 [gr-qc]];

R. A. Porto, "The effective field theorist's approach to gravitational dynamics," Phys. Rept. **633**, 1 (2016) [arXiv:1601.04914 [hep-th]];

G. Schäfer and P. Jaranowski, "Hamiltonian formulation of general relativity and post-Newtonian dynamics of compact binaries," Living Rev. Rel. **21**, no. 1, 7 (2018) [arXiv:1805.07240 [gr-qc]];

L. Barack and A. Pound, "Self-force and radiation reaction in general relativity," Rept. Prog. Phys. **82**, no. 1, 016904 (2019) [arXiv:1805.10385 [gr-qc]];

L. Barack *et al.*, "Black holes, gravitational waves and fundamental physics: a roadmap," Class. Quant. Grav. **36**, no. 14, 143001 (2019) [arXiv:1806.05195 [gr-qc]];

M. Levi, "Effective field theories of post-Newtonian gravity: A comprehensive review," arXiv:1807.01699 [hep-th].

[19] Y. Iwasaki, "Quantum theory of gravitation vs. classical theory—fourth-order potential," Prog. Theor. Phys. **46**, 1587 (1971);

Y. Iwasaki, "Fourth-order gravitational potential based on quantum field theory," Lett. Nuovo Cim. **1S2**, 783 (1971) [Lett. Nuovo Cim. **1**, 783 (1971)];

S. N. Gupta and S. F. Radford, "Improved gravitational coupling of scalar fields," Phys. Rev. D **19**, 1065 (1979);

B. R. Holstein and J. F. Donoghue, "Classical physics and quantum loops," Phys. Rev. Lett. **93**, 201602 (2004) [hep-th/0405239];

D. Neill and I. Z. Rothstein, "Classical space-times from the S matrix," Nucl. Phys. B **877**, 177 (2013) [arXiv:1304.7263 [hep-th]];

N. E. J. Bjerrum-Bohr, J. F. Donoghue and P. Vanhove, "On-shell techniques and universal results in quantum gravity," JHEP **1402**, 111 (2014) [arXiv:1309.0804 [hep-th]];

N. E. J. Bjerrum-Bohr, P. H. Damgaard, G. Festuccia, L. Planté and P. Vanhove, "General relativity from scattering amplitudes," Phys. Rev. Lett. **121**, no. 17, 171601 (2018) [arXiv:1806.04920 [hep-th]];

T. Damour, "Gravitational scattering, post-Minkowskian approximation and effective one-body theory," Phys. Rev. D **94**, no. 10, 104015 (2016) [arXiv:1609.00354 [gr-qc]];

F. Cachazo and A. Guevara, "Leading singularities and classical gravitational scattering," JHEP **2002**, 181 (2020) [arXiv:1705.10262 [hep-th]];

A. Cristofoli, N. E. J. Bjerrum-Bohr, P. H. Damgaard and P. Vanhove, "On post-Minkowskian Hamiltonians in general relativity," arXiv:1906.01579 [hep-th];

D. A. Kosower, B. Maybee and D. O'Connell, "Amplitudes, observables, and classical scattering," JHEP **1902**, 137 (2019) [arXiv:1811.10950 [hep-th]];

G. Kälin and R. A. Porto, "From Boundary Data to Bound States," JHEP **01**, 072 (2020) doi:10.1007/JHEP01(2020)072 [arXiv:1910.03008 [hep-th]];

N. E. J. Bjerrum-Bohr, A. Cristofoli and P. H. Damgaard, "Post-Minkowskian Scattering Angle in Einstein Gravity," JHEP **08**, 038 (2020) doi:10.1007/JHEP08(2020)038 [arXiv:1910.09366 [hep-th]];

G. Kälin and R. A. Porto, "From boundary data to bound states. Part II.

Scattering angle to dynamical invariants (with twist)," JHEP **02**, 120 (2020) doi:10.1007/JHEP02(2020)120 [arXiv:1911.09130 [hep-th]].

[20] T. Damour, "High-energy gravitational scattering and the general relativistic two-body problem," Phys. Rev. D **97**, no.4, 044038 (2018) [arXiv:1710.10599 [gr-qc]].

[21] C. Cheung and M. P. Solon, "Tidal Effects in the Post-Minkowskian Expansion," [arXiv:2006.06665 [hep-th]].

[22] Z. Bern, L. J. Dixon, D. C. Dunbar and D. A. Kosower, "One loop n-point gauge-theory amplitudes, unitarity and collinear limits," Nucl. Phys. B **425**, 217 (1994) [hep-ph/9403226];

Z. Bern, L. J. Dixon, D. C. Dunbar and D. A. Kosower, "Fusing gauge-theory tree amplitudes into loop amplitudes," Nucl. Phys. B **435**, 59 (1995) [hep-ph/9409265];

Z. Bern and A. G. Morgan, "Massive loop amplitudes from unitarity," Nucl. Phys. B **467**, 479 (1996) [hep-ph/9511336];

Z. Bern, L. J. Dixon and D. A. Kosower, "One loop amplitudes for e^+e^- to four partons," Nucl. Phys. B **513**, 3 (1998) [hep-ph/9708239];

Z. Bern, L. J. Dixon, D. C. Dunbar, M. Perelstein and J. S. Rozowsky, "On the relationship between Yang-Mills theory and gravity and its implication for ultraviolet divergences," Nucl. Phys. B **530**, 401 (1998) [hep-th/9802162];

R. Britto, F. Cachazo and B. Feng, "Generalized unitarity and one-loop amplitudes in $N = 4$ super-Yang-Mills," Nucl. Phys. B **725**, 275 (2005) [hep-th/0412103];

Z. Bern, J. J. M. Carrasco, H. Johansson and D. A. Kosower, "Maximally supersymmetric planar Yang-Mills amplitudes at five loops," Phys. Rev. D **76**, 125020 (2007) [arXiv:0705.1864 [hep-th]];

C. F. Berger, Z. Bern, L. J. Dixon, F. Febres Cordero, D. Forde, H. Ita, D. A. Kosower and D. Maitre, "An Automated Implementation of On-Shell Methods for One-Loop Amplitudes," Phys. Rev. D **78**, 036003 (2008) [arXiv:0803.4180 [hep-ph]].

[23] Z. Bern, A. Luna, R. Roiban, C. H. Shen and M. Zeng, "Spinning Black Hole Binary Dynamics, Scattering Amplitudes and Effective Field Theory," [arXiv:2005.03071 [hep-th]].

[24] A. Buonanno and B. S. Sathyaprakash, "Sources of Gravitational Waves: Theory and Observations," [arXiv:1410.7832 [gr-qc]];
T. Dietrich, T. Hinderer and A. Samajdar, "Interpreting Binary Neutron Star Mergers: Describing the Binary Neutron Star Dynamics, Modelling Gravitational Waveforms, and Analyzing Detections," [arXiv:2004.02527 [gr-qc]];
K. Chatziioannou, "Neutron star tidal deformability and equation of state constraints," [arXiv:2006.03168 [gr-qc]].

[25] E. E. Flanagan and T. Hinderer, "Constraining neutron star tidal Love numbers with gravitational wave detectors," Phys. Rev. D **77**, 021502 (2008) [arXiv:0709.1915 [astro-ph]];
T. Damour and A. Nagar, "Relativistic tidal properties of neutron stars," Phys. Rev. D **80**, 084035 (2009) [arXiv:0906.0096 [gr-qc]];
M. F. Carney, L. E. Wade and B. S. Irwin, "Comparing two models for measuring the neutron star equation of state from gravitational-wave signals," Phys. Rev. D **98**, no.6, 063004 (2018) [arXiv:1805.11217 [gr-qc]];
B. P. Abbott *et al.* [LIGO Scientific and Virgo], "GW170817: Measurements of neutron star radii and equation of state," Phys. Rev. Lett. **121**, no.16, 161101 (2018) [arXiv:1805.11581 [gr-qc]].

[26] D. Bini and T. Damour, "Gravitational self-force corrections to two-body tidal interactions and the effective one-body formalism," Phys. Rev. D **90**, no.12, 124037 (2014) [arXiv:1409.6933 [gr-qc]];
J. Steinhoff, T. Hinderer, A. Buonanno and A. Taracchini, "Dynamical Tides in General

Relativity: Effective Action and Effective-One-Body Hamiltonian," Phys. Rev. D **94**, no.10, 104028 (2016) [arXiv:1608.01907 [gr-qc]].

[27] Q. Henry, G. Faye and L. Blanchet, "Tidal effects in the equations of motion of compact binary systems to next-to-next-to-leading post-Newtonian order," Phys. Rev. D **101**, no.6, 064047 (2020) [arXiv:1912.01920 [gr-qc]];
Q. Henry, G. Faye and L. Blanchet, "Tidal effects in the gravitational-wave phase evolution of compact binary systems to next-to-next-to-leading post-Newtonian order," Phys. Rev. D **102**, no.4, 044033 (2020) [arXiv:2005.13367 [gr-qc]];
Q. Henry, G. Faye and L. Blanchet, "Hamiltonian for tidal interactions in compact binary systems to next-to-next-to-leading post-Newtonian order," [arXiv:2009.12332 [gr-qc]].

[28] D. Bini, T. Damour and A. Geralico, "Scattering of tidally interacting bodies in post-Minkowskian gravity," Phys. Rev. D **101**, no.4, 044039 (2020) [arXiv:2001.00352 [gr-qc]].

[29] G. Kälin, Z. Liu and R. A. Porto, "Conservative Tidal Effects in Compact Binary Systems to Next-to-Leading Post-Minkowskian Order," [arXiv:2008.06047 [hep-th]].

[30] K. Haddad and A. Helset, "Gravitational tidal effects in quantum field theory," [arXiv:2008.04920 [hep-th]].

[31] V. Cardoso, E. Franzin, A. Maselli, P. Pani and G. Raposo, "Testing strong-field gravity with tidal Love numbers," Phys. Rev. D **95**, no.8, 084014 (2017) [arXiv:1701.01116 [gr-qc]];
N. Sennett, T. Hinderer, J. Steinhoff, A. Buonanno and S. Ossokine, "Distinguishing Boson Stars from Black Holes and Neutron Stars from Tidal Interactions in Inspiraling Binary Systems," Phys. Rev. D **96**, no.2, 024002 (2017) [arXiv:1704.08651 [gr-qc]];
A. Nelson, S. Reddy and D. Zhou, "Dark halos around neutron stars and gravitational waves," JCAP **07**, 012 (2019) [arXiv:1803.03266 [hep-ph]];

A. Addazi, A. Marciano and N. Yunes, "Can we probe Planckian corrections at the horizon scale with gravitational waves?," Phys. Rev. Lett. **122**, no.8, 081301 (2019) [arXiv:1810.10417 [gr-qc]];

A. Quddus, G. Panotopoulos, B. Kumar, S. Ahmad and S. K. Patra, "GW170817 constraints on the properties of a neutron star in the presence of WIMP dark matter," J. Phys. G **47**, no.9, 095202 (2020) [arXiv:1902.00929 [nucl-th]];

K. Chakravarti, S. Chakraborty, K. S. Phukon, S. Bose and S. SenGupta, "Constraining extra-spatial dimensions with observations of GW170817," Class. Quant. Grav. **37**, no.10, 105004 (2020) [arXiv:1903.10159 [gr-qc]];

R. Brustein and Y. Sherf, "Quantum Love," [arXiv:2008.02738 [gr-qc]].

[32] T. Binnington and E. Poisson, "Relativistic theory of tidal Love numbers," Phys. Rev. D **80**, 084018 (2009) [arXiv:0906.1366 [gr-qc]];

T. Damour and A. Nagar, "Relativistic tidal properties of neutron stars," Phys. Rev. D **80**, 084035 (2009) [arXiv:0906.0096 [gr-qc]];

B. Kol and M. Smolkin, "Black hole stereotyping: Induced gravito-static polarization," JHEP **02**, 010 (2012) [arXiv:1110.3764 [hep-th]];

N. Gürlebeck, "No-hair theorem for Black Holes in Astrophysical Environments," Phys. Rev. Lett. **114**, no.15, 151102 (2015) [arXiv:1503.03240 [gr-qc]];

L. Hui, A. Joyce, R. Penco, L. Santoni and A. R. Solomon, "Static response and Love numbers of Schwarzschild black holes," [arXiv:2010.00593 [hep-th]].

[33] H. Kawai, D. C. Lewellen and S. H. H. Tye, "A relation between tree amplitudes of closed and open strings," Nucl. Phys. B **269**, 1 (1986);

Z. Bern, L. J. Dixon, M. Perelstein and J. S. Rozowsky, "Multileg one loop gravity amplitudes from gauge theory," Nucl. Phys. B **546**, 423 (1999) [hep-th/9811140].

[34] Z. Bern, J. J. M. Carrasco and H. Johansson, "New relations for gauge-theory amplitudes," Phys. Rev. D **78**, 085011 (2008) [arXiv:0805.3993 [hep-ph]];

Z. Bern, J. J. M. Carrasco and H. Johansson, "Perturbative quantum gravity as a double copy of gauge theory," Phys. Rev. Lett. **105**, 061602 (2010) [arXiv:1004.0476 [hep-th]];
Z. Bern, J. J. Carrasco, M. Chiodaroli, H. Johansson and R. Roiban, "The duality between color and kinematics and its applications," arXiv:1909.01358 [hep-th].

[35] K.G. Chetyrkin and F.V. Tkachov, "Integration by parts: the algorithm to calculate beta functions in 4 loops," Nucl. Phys. B **192**, 159 (1981);
S. Laporta, "High precision calculation of multiloop Feynman integrals by difference equations," Int. J. Mod. Phys. A **15**, 5087-5159 (2000) [arXiv:hep-ph/0102033 [hep-ph]].

[36] J. Parra-Martinez, M. Ruf, and M. Zeng, "Extremal black hole scattering at $O(G^3)$: graviton dominance, eikonal exponentiation, and differential equations" [arXiv:2005.04236 [hep-th]].

[37] J. F. Donoghue, "General relativity as an effective field theory: The leading quantum corrections," Phys. Rev. D **50**, 3874-3888 (1994) [arXiv:gr-qc/9405057 [gr-qc]];
J. F. Donoghue, "Introduction to the effective field theory description of gravity," [arXiv:gr-qc/9512024 [gr-qc]];
S. Endlich, V. Gorbenko, J. Huang and L. Senatore, "An effective formalism for testing extensions to General Relativity with gravitational waves," JHEP **09**, 122 (2017) [arXiv:1704.01590 [gr-qc]].

[38] S. Endlich, V. Gorbenko, J. Huang and L. Senatore, "An effective formalism for testing extensions to General Relativity with gravitational waves," JHEP **09** (2017), 122 [arXiv:1704.01590 gr-qc]].

[39] A. Brandhuber and G. Travaglini, "On higher-derivative effects on the gravitational potential and particle bending," JHEP **01** (2020), 010 [arXiv:1905.05657 [hep-th]].

[40] W. T. Emond and N. Moynihan, "Scattering Amplitudes, Black Holes and Leading Singularities in Cubic Theories of Gravity," JHEP **12**, 019 (2019) [arXiv:1905.08213 [hep-th]];
A. Cristofoli, "Post-Minkowskian Hamiltonians in Modified Theories of Gravity," Phys. Lett. B **800**, 135095 (2020) [arXiv:1906.05209 [hep-th]];
S. Cai and K. D. Wang, "Non-vanishing of tidal Love numbers," [arXiv:1906.06850 [hep-th]].

[41] M. Levi and J. Steinhoff, "Spinning gravitating objects in the effective field theory in the post-Newtonian scheme," JHEP **1509**, 219 (2015) [arXiv:1501.04956 [gr-qc]].

[42] J. Vines, "Scattering of two spinning black holes in post-Minkowskian gravity, to all orders in spin, and effective-one-body mappings," Class. Quant. Grav. **35**, no.8, 084002 (2018) [arXiv:1709.06016 [gr-qc]].

[43] C. Cheung, N. N. Shah, M. Solon, to appear simultaneously.

[44] R. J. Glauber, "Lectures in theoretical physics", ed. by W. E. Brittin and L. G. Dunham, Interscience Publishers, Inc., New York, Volume I, page 315, (1959);
D. Amati, M. Ciafaloni and G. Veneziano, "Higher order gravitational deflection and soft bremsstrahlung in planckian energy superstring collisions," Nucl. Phys. B **347**, 550 (1990);
R. Akhoury, R. Saotome and G. Sterman, "High energy scattering in perturbative quantum gravity at next to leading power," arXiv:1308.5204 [hep-th];
Z. Bern, H. Ita, J. Parra-Martinez and M. S. Ruf, Phys. Rev. Lett. **125**, no.3, 031601 (2020) [arXiv:2002.02459 [hep-th]].

[45] Boyd, R.W. and Boyd, M.D., "Nonlinear Optics", Academic Press (1959).

[46] G. Mogull, J. Plefka and J. Steinhoff, "Classical black hole scattering from a worldline quantum field theory," [arXiv:2010.02865 [hep-th]].

[47] A. J. Buras and P. H. Weisz, "QCD Nonleading Corrections to Weak Decays in Dimensional Regularization and 't Hooft-Veltman Schemes," Nucl. Phys. B **333**, 66-99 (1990); M. J. Dugan and B. Grinstein, "On the vanishing of evanescent operators," Phys. Lett. B **256**, 239-244 (1991)

[48] S. Benvenuti, B. Feng, A. Hanany and Y. H. He, "Counting BPS Operators in Gauge Theories: Quivers, Syzygies and Plethystics," JHEP **11**, 050 (2007) [arXiv:hep-th/0608050 [hep-th]];
B. Feng, A. Hanany and Y. H. He, "Counting gauge invariants: The Plethystic program," JHEP **03**, 090 (2007) [arXiv:hep-th/0701063 [hep-th]];
A. Hanany, E. E. Jenkins, A. V. Manohar and G. Torri, "Hilbert Series for Flavor Invariants of the Standard Model," JHEP **03**, 096 (2011) [arXiv:1010.3161 [hep-ph]].

[49] D. Kosmopoulos, "Simplifying D-Dimensional Physical-State Sums in Gauge Theory and Gravity," [arXiv:2009.00141 [hep-th]].

[50] V. A. Smirnov, "Evaluating Feynman integrals," Springer Tracts Mod. Phys. **211**, 1 (2004).

[51] R. Saotome and R. Akhoury, "Relationship Between Gravity and Gauge Scattering in the High Energy Limit," JHEP **01**, 123 (2013) [arXiv:1210.8111 [hep-th]].

[52] A. V. Smirnov, "Algorithm FIRE – Feynman Integral REduction," JHEP **10**, 107 (2008) [arXiv:0807.3243 [hep-ph]];
A. V. Smirnov and F. S. Chuharev, "FIRE6: Feynman Integral REduction with Modular Arithmetic," [arXiv:1901.07808 [hep-ph]].

[53] A. V. Kotikov, "Differential equations method: New technique for massive Feynman diagrams calculation," Phys. Lett. B **254**, 158-164 (1991);
Z. Bern, L. J. Dixon and D. A. Kosower, "Dimensionally regulated pentagon integrals,"

Nucl. Phys. B **412**, 751-816 (1994) [arXiv:hep-ph/9306240 [hep-ph]];

E. Remiddi, "Differential equations for Feynman graph amplitudes," Nuovo Cim. A **110**, 1435-1452 (1997) [arXiv:hep-th/9711188 [hep-th]];

T. Gehrmann and E. Remiddi, "Differential equations for two loop four point functions," Nucl. Phys. B **580**, 485-518 (2000) [arXiv:hep-ph/9912329 [hep-ph]].